

# **An investigation of the pathogenesis of ochronosis in Alkaptonuria (AKU)**

**Thesis submitted in accordance with the requirements of the University of Liverpool for  
the degree of Doctor in Philosophy by Adam Michael Taylor**

**May 2011**

Alkaptonuria (AKU) is a rare autosomal recessive condition which is caused by deficiency of a single enzyme on the tyrosine metabolic pathway. The disorder results from the absence of homogentisate 1,2 dioxygenase (HGD), which breaks down homogentisic acid (HGA). This disorder was the first shown to be an inborn error of metabolism. The absence of HGD results in high circulating levels of HGA. The disorder shows a triad of clinical features, the first of these is excretion of gram quantities of HGA in the urine. Over time or on addition of alkali the urine darkens. The second feature is ochronosis, which results from long term exposure of collagenous tissues to HGA. The circulating HGA shows high affinity for collagenous tissues and undergoes polymerisation and deposition by a currently unknown mechanism to appear as a dark melanin like pigment in collagenous tissues, predominantly the load-bearing articular cartilages. The final clinical feature is ochronotic arthropathy which results from the ochronosis of the articular cartilages. There is currently no known treatment for this disease, the chromosomal location and structure of the missing enzyme is known and the gene has been cloned. The aim of this study was to gain an insight into the pathogenesis of the disorder.

Utilising the largest number of in a single study of AKU tissue samples, this study has been able to provide insights in to the effects and distribution of ochronosis in patient tissues. The most striking feature of the observations was the non-uniform distribution of ochronotic pigment in the patient tissues. Consistent with these observations ultrastructural analysis demonstrates that even in tissues which ochronosis appears in all regions macroscopically, ultrastructurally there are regions of tissue that demonstrate no association with ochronotic pigment. This study shows the earliest association of ochronotic pigment with collagen fibres in the matrix of patient tissues, furthermore this association shows a regular periodicity that is possibly associated with the periodic banding that is typical of the fibrillar collagens. Analysis of *in vitro* cultures demonstrates similar association of pigment with matrix fibres in culture of osteo and chondrosarcoma cells incubated in HGA.

This study, through meticulous examination by microscopical techniques a novel bone and cartilage phenotype has been seen in alkaptonuric joint samples. In the most severely ochronotic samples, there is absence of the subchondral bone and calcified cartilage plates. Alongside this observation the earliest detectable ochronosis associated with individual chondrocyte has been seen, demonstrating that ochronosis commences closest to the subchondral boundary before progressing to the articular surface. Alongside the observations of the cartilage phenotype, novel bone structures were observed in AKU specimens, and subsequently observed in osteoarthritis (being used as control) samples.

Through macroscopic and microscopic analysis of a murine model of AKU, this study demonstrates the first observations of ochronosis in a murine model of AKU. This model demonstrates the earliest signs of ochronosis observed around single chondrocytes in the cartilage matrix, identical to those observed in human joint tissues.

This thesis also describes novel observation of ochronosis in pathological tissues, both in the presence and absence of a collagenous matrix. This raises the question of the role of factors other than the presence of HGA in the deposition of ochronotic pigment in patient tissues.

In summary this study represents novel and significant advances in the understanding of the pathogenesis of ochronosis and also providing useful tools that can be used in advancing the understanding of the disease further but more importantly identifying and utilising therapeutic targets to tackle this rare condition.



### **Acknowledgements**

I would first like to offer thanks and appreciation to Professor Jim Gallagher for offering me the opportunity to undertake this PhD project in his lab and his support, guidance and endless opportunities to excel during the course of my studies. I must also offer my sincere thanks to Dr Lakshminarayan Ranganath, who has supported me throughout the course of my PhD and without his groundwork and clinical input this project would not have been possible. I would like to thank everyone in the Human Bone Cell Research Group, particularly Jane Dillon for the endless hours she has spent proof reading abstracts, draft manuscripts and ensuring a supply of tea was always on hand to maintain the quality of science (I am sure there is a positive correlation)! I would also like to thank Dr Peter Wilson for his help in the lab and his friendship. I am extremely grateful to Brenda Wlodarski who has taught me the ins and outs of maintaining high quality histology. Thank you to everyone else in the lab that has passed through during the course of my PhD, your friendship has been fantastic. Thank you to all who have proved worthy opponents on the 5 a-side field and apologies to all those who I have branded with a football imprint over the last 4 years! I am also grateful to all my collaborators and colleagues in the labs of Dr Melinda Duer (University of Cambridge - ssNMR), Prof. Markus Grompe (Oregon Health & Science University - mouse model) who made me feel welcome and offered their support and friendship for my time spent in their labs. Thank you also to all the surgeons and their teams for allowing me access to theatre(s) and being so co-operative in sample collections. I would like to offer special thanks to Professor Alan Boyde (QMUL), who gave me the opportunity to obtain the most striking and spectacular images of AKU specimens! Without question the best scientist in the world at imaging calcified tissues and whose SEM images form parts of the results of this thesis, I owe you numerous beers!

Thank you to Dr Nick Sireau and Mr Robert “Bob” Gregory who are instrumental in maintaining and founding the AKU Society, who funded my PhD. I must express my sincere thanks to all the AKU patients and their friends and families I have met over the last 4 years, without your generous tissue donations this thesis and research would not have been possible.

I would like to thank my family and friends who have offered the constant support during the course of my PhD. In particular I would like to thank my mum, who has always been supportive of what I have done and I hope you will be proud of this thesis, and my brother who has always been supportive. I would like to thank Anthony Garcia & Rachel Houten for their friendship and finally Professor Richard Dutton who convinced me that doing a PhD, this one in particular was a good idea.

Finally my greatest thanks of all must go to my fiancée Claire for her unwavering support of my work, her tolerance of the late nights, early mornings and the in depth descriptions of my work which I would share, usually over dinner, having spent the day in operating theatre. The hard work will pay off in the long run. Words cannot express my thanks and appreciation for having your support through the course of my PhD. Now the work is over we can look forward to the wedding and the rest of our lives together!

### **Abbreviations**

**2D:** 2 dimensional

**3D:** 3 dimensional

**ACC:** Articular calcified cartilage

**ACL:** Anterior cruciate ligament

**AKU:** Alkaptonuria

**ASC:** Ascorbic acid

**bp:** base pairs

**BQA:** Benzoquinone acetic acid

**Col:** Collagen

**ColI:** Collagen type I

**ColII:** Collagen type II

**CT:** Computer tomography

**dH<sub>2</sub>O:** Distilled water

**DMEM:** Dulbecco's modified eagles  
medium

**DOPA:** L-3,4-dihydroxyphenylalanine

**ECM:** Extracellular matrix

**EDTA:** Ethylenediaminetetraacetic acid

**FAA:** Fumarylacetoacetic acid

**FAH:** Fumarylacetoacetate hydrolase

**g:** grammes

**H&E:** Haemotoxylin & eosin

**HAC:** Hyaline articular cartilage

**HCl:** Hydrochloric acid

**HGA:** Homogentisic acid

**HGD:** Homogentisate 1,2-dioxygenase

**HPLC:** High performance liquid  
chromatography

**HPPD:** 4-Hydroxyphenylpyruvate  
dioxygenase

**HTT1:** Hereditary tyrosinaemia type 1

**ITM:** Interterritorial matrix

**LM:** Light microscopy

**MAA:** Maleylacetoacetic acid

**mg:** milligrammes

**mins:** minutes

**ml:** millilitres

**mM:** millimolar

**MW:** molecular weight

**MRI:** Magnetic resonance imaging

**NAC:** N-Acetylcysteine

**NFR:** Nuclear fast red

**NMR:** Nuclear magnetic resonance

<b>NTBC:</b> 2-(2-nitro-4-trifluoromethylbenzoyl)-1,3-cyclohexanedione	<b>SEM:</b> Scanning electron microscopy
<b>OA:</b> Osteoarthritis	<b>ssNMR:</b> Solid state nuclear magnetic resonance
<b>PBS:</b> Phosphate buffered saline	<b>TEM:</b> Transmission electron microscopy
<b>PBFS:</b> Phosphate buffered formol saline	<b>THR:</b> Total hip replacement
<b>PKU:</b> Phenylketonuria	<b>TKR:</b> Total knee replacement
<b>P/S:</b> Penicillin / Streptomycin	<b>TM:</b> Territorial matrix
<b>qBSE-SEM:</b> Quantitative back scattered electron-scanning electron microscopy	<b>µg:</b> micrograms
<b>REC:</b> Research ethics committee	<b>µl:</b> microlitres
<b>SCB:</b> Subchondral bone	<b>UK:</b> United Kingdom

## Table of Contents

<b>1.</b>	<b>Introduction</b>	<b>1</b>
<b>1.1.</b>	<b>Joint Tissues</b>	<b>2</b>
1.1.1.	Articular cartilage	2
1.1.2.	Structure, function and composition of articular cartilage	3
1.1.3.	Collagen	5
1.1.4.	Chondrocytes	6
<b>1.2.</b>	<b>Bone</b>	<b>7</b>
1.2.1.	Bone structure and function	7
1.2.2.	Cells within bone	8
1.2.3.	Bone turnover	8
1.2.4.	Subchondral bone	9
<b>1.3.</b>	<b>Synovial and soft tissues</b>	<b>10</b>
<b>1.4.</b>	<b>Metabolism</b>	<b>11</b>
1.4.1.	Tyrosine metabolism	12
<b>1.5.</b>	<b>Alkaptonuria</b>	<b>13</b>
1.5.1.	History	13
1.5.2.	Epidemiology	16
1.5.3.	Clinical presentations	17
1.5.4.	Therapeutic strategies	21
1.5.4.1.	Ascorbic acid	22
1.5.4.2.	Nitisinone (NTBC)	23
1.5.4.3.	Low protein diet	25
1.5.4.4.	Enzyme replacement therapy	26
<b>1.6.</b>	<b>Homogentisate 1,2 dioxygenase production, function and mutations</b>	<b>26</b>
<b>1.7.</b>	<b>Homogentisic acid</b>	<b>28</b>
<b>1.8.</b>	<b>AKU in other organisms</b>	<b>29</b>
<b>1.9.</b>	<b>AKU in animal models</b>	<b>30</b>
<b>1.10.</b>	<b>Fungal model</b>	<b>32</b>
<b>1.11.</b>	<b>Summary</b>	<b>33</b>
<b>1.12.</b>	<b>Aims of the study</b>	<b>34</b>
<b>2.</b>	<b>Materials and Methods</b>	<b>35</b>
<b>2.1.</b>	<b>Ethical Approval</b>	<b>36</b>
<b>2.2.</b>	<b>Cell Culture</b>	<b>36</b>
2.2.1.	Reagents	36
2.2.2.	Plasticware	36
2.2.3.	Culture of human osteosarcoma and chondrosarcoma cells	37
2.2.4.	Preparation of Homogentisic acid stock solution	37
2.2.5.	Preparation of HGA culture plates	37
2.2.6.	Preparation of ascorbic acid stock solution	38
2.2.7.	Addition of ascorbic acid to culture plates	38
2.2.8.	Preparation of Dexamethosone stock solution	39
2.2.9.	Addition of Dexamethosone to culture plates	39
<b>2.3.</b>	<b>Histology</b>	<b>39</b>
2.3.1.	Reagents	39

2.3.2.	Fixation	39
2.3.3.	Decalcification of mineralised tissues	40
2.3.4.	Processing of samples for embedding	40
2.3.5.	Subbing of glass slides	40
2.3.5.1.	Subbing solution	40
2.3.5.2.	Subbing procedure	40
2.3.6.	Sectioning of tissues	41
2.3.7.	Histological staining of slides	41
2.3.7.1.	H&E	42
2.3.7.2.	Schmorl's	42
2.3.7.3.	Method	43
<b>2.4.</b>	<b>Transmission electron microscopy</b>	<b>43</b>
2.4.1.	Reagents	43
2.4.1.1.	Preparation of lead citrate solution	43
2.4.2.	Preparation of specimens for transmission electron microscopy	44
2.4.2.1.	Dehydration at room temperature	44
2.4.2.2.	Resin infiltration	45
2.4.3.	Sectioning and post staining of tissues in resin blocks	45
<b>2.5.</b>	<b>Scanning electron microscopy</b>	<b>46</b>
2.5.1.	Reagents	46
2.5.2.	Sample processing	46
2.5.3.	Fluorescence light microscopy	46
<b>2.6.</b>	<b>Murine experiments</b>	<b>47</b>
2.6.1.	Reagents	47
2.6.2.	NTBC Stock solution preparation	47
2.6.3.	NTBC working solution preparation	47
2.6.4.	Mouse care	48
2.6.5.	C57/Bl6 FAH $-/-$ , HGD $+/-$ dissection	48
2.6.5.1.	Skin	48
2.6.5.2.	Abdomen	49
2.6.5.3.	Thorax	49
2.6.5.4.	Limbs	49
2.6.5.5.	Head and Trachea	49
<b>2.7.</b>	<b>ssNMR</b>	<b>50</b>
2.7.1.	Reagents	50
2.7.2.	Method	50
<b>2.8</b>	<b>Mechanical testing</b>	<b>51</b>
2.8.1	Mechanical testing protocol	51
2.8.2	Statistical analysis	51
<b>2.9.</b>	<b>Patient demographics and symptoms</b>	<b>52</b>
<b>3.</b>	<b>Macroscopic presentation of AKU joint samples</b>	<b>54</b>
<b>3.1.</b>	<b>Introduction</b>	<b>55</b>
<b>3.2.</b>	<b>Results</b>	<b>56</b>
3.2.1.	Ochronosis in hips	57
3.2.2.	Ochronosis in knees	65
3.2.3.	Arthroscopies	78
3.2.4.	Spine and revision surgeries	81
3.2.5.	Discussion	82

<b>4.</b>	<b>Ultrastructural analysis of ochronotic tissues</b>	<b>85</b>
<b>4.1.</b>	<b>Introduction</b>	<b>86</b>
<b>4.2.</b>	<b>Results</b>	<b>86</b>
4.2.1.	TEM of AKU Cartilage	86
4.2.2.	TEM of OA Cartilage	92
4.2.3.	TEM of AKU Bone	95
4.2.4.	TEM of AKU Capsule	97
4.2.5.	TEM of spinal ligament	107
4.2.6.	TEM of <i>in vitro</i> cultures	113
4.2.7.	TEM analysis of pure HGA polymer	126
4.2.8.	ssNMR of ochronotic cartilage	128
<b>4.3.</b>	<b>Discussion</b>	<b>130</b>
<b>5.</b>	<b>The role of calcified cartilage and subchondral bone in the initiation and progression of ochronotic arthropathy in alkaptonuria</b>	<b>138</b>
<b>5.1.</b>	<b>Introduction</b>	<b>139</b>
<b>5.2.</b>	<b>Results</b>	<b>141</b>
5.2.1.	Macroscopic	141
5.2.2.	Material Properties of cartilage samples	141
5.2.3.	Mechanical loading of cartilage	142
5.2.3.1.	Mechanical loading	142
5.2.4.	Enzymatic digestion of cartilage	144
5.2.5.	Histological observations	150
5.2.6.	Fluorescence microscopy	165
5.2.7.	SEM	171
<b>5.3.</b>	<b>Discussion</b>	<b>180</b>
<b>6.</b>	<b>Ochronosis in a murine model of alkaptonuria</b>	<b>187</b>
<b>6.1.</b>	<b>Introduction</b>	<b>188</b>
<b>6.2.</b>	<b>Results</b>	<b>191</b>
6.2.1.	Macroscopic observations of murine tissues	191
6.2.2.	Histology	195
6.2.2.1.	Heart	195
6.2.2.2.	Tracheal cartilages	196
6.2.2.3.	Kidneys	200
6.2.2.4.	Schmorl's staining of kidneys	204
6.2.2.5.	Knee Joints	209
<b>6.3.</b>	<b>Discussion</b>	<b>214</b>
<b>7.</b>	<b>Identification of trabecular excrescences, novel microanatomical structures, present in bone in osteoarthropathies</b>	<b>220</b>
<b>7.1.</b>	<b>Introduction</b>	<b>221</b>

<b>7.2.</b>	<b>Results</b>	<b>225</b>
7.2.1.	3D topographical SEM imaging of AKU Bone	225
7.2.2.	Histology of AKU bone	236
7.2.3.	qBSE - SEM imaging of AKU bone	241
7.2.4.	3D topographical SEM imaging of the osteoarthritic arthropathy samples	246
<b>7.3.</b>	<b>Discussion</b>	<b>252</b>
<b>8.</b>	<b>Investigation into the deposition of ochronotic pigment in submandibular tissues</b>	<b>257</b>
<b>8.1.</b>	<b>Introduction</b>	<b>258</b>
<b>8.2.</b>	<b>Case history</b>	<b>258</b>
<b>8.3.</b>	<b>Results</b>	<b>258</b>
8.3.1.	Macroscopic examination of submandibular tissues	258
8.3.2.	Microscopic examination of submandibular tissue	261
<b>8.4.</b>	<b>Discussion</b>	<b>263</b>
<b>9.</b>	<b>Ochronosis in a mediastinal mass</b>	<b>267</b>
<b>9.1.</b>	<b>Introduction</b>	<b>268</b>
<b>9.2.</b>	<b>Case history</b>	<b>268</b>
<b>9.3.</b>	<b>Results</b>	<b>269</b>
9.3.1.	Macroscopic examination of Mediastinal tissues	269
9.3.2.	Microscopic examination of Mediastinal tissues	270
<b>9.4</b>	<b>Discussion</b>	<b>273</b>
<b>10.</b>	<b>General discussion</b>	<b>277</b>
<b>References</b>		<b>289</b>
<b>Appendix A: Publications</b>		<b>311</b>



## Table of Figures

### Chapter 1:

Figure 1.1: A schematic of cartilage cells and matrix	5
Figure 1.2: Diagram of phenylalanine and tyrosine metabolism	13
Figure 1.3: Chemical structure of homogentisic acid	28
Figure 1.4: Diagram of metabolic pathway of ochronotic pigment production	29

### Chapter 2:

### Chapter 3:

Figure 3.1: Macroscopic image AKU3	58
Figure 3.2: Macroscopic image AKU3	59
Figure 3.3: Macroscopic images AKU13	60
Figure 3.4: Macroscopic image AKU16	61
Figure 3.5: Macroscopic image AKU16	62
Figure 3.6: Macroscopic image AKU16	62
Figure 3.7: Macroscopic image AKU18	64
Figure 3.8: Macroscopic image AKU18	64
Figure 3.9: Macroscopic image AKU9	66
Figure 3.10: Macroscopic image AKU9	66
Figure 3.11: Macroscopic image AKU9	67
Figure 3.12: Macroscopic image AKU10	68
Figure 3.13: Macroscopic image AKU12	70
Figure 3.14: Macroscopic image AKU12	70
Figure 3.15: Macroscopic image AKU12	71
Figure 3.16: Macroscopic image AKU15	73
Figure 3.17: Macroscopic image AKU19	74
Figure 3.18: Macroscopic image AKU21	75
Figure 3.19: Macroscopic image AKU21	77
Figure 3.20: Macroscopic image AKU8	79
Figure 3.21: Macroscopic image AKU11	80

### Chapter 4:

Figure 4.1: TEM ochronotic cartilage (x9,900)	87
Figure 4.2: TEM ochronotic cartilage (x20,500)	88
Figure 4.3: TEM ochronotic cartilage (x43,000)	89
Figure 4.4: TEM ochronotic cartilage (x87,000)	90
Figure 4.5: TEM ochronotic cartilage (x160,000)	91
Figure 4.6: TEM of OA cartilage (x8,200)	92
Figure 4.7: TEM of OA cartilage (x43,000)	93
Figure 4.8: TEM of OA cartilage (x160,000)	94
Figure 4.9: TEM ochronotic bone (x9,900)	95
Figure 4.10: TEM ochronotic bone (x26,500)	96
Figure 4.11: TEM ochronotic capsule (x87,000)	98
Figure 4.12: TEM ochronotic capsule (x160,000)	100

Figure 4.13: TEM ochronotic capsule (20,500)	102
Figure 4.14: TEM ochronotic capsule (x20,500), inset (x87,000)	103
Figure 4.15: TEM ochronotic capsule (x6,000)	104
Figure 4.16: TEM ochronotic capsule (x26,000), insets (x20,000 & x60,000)	106
Figure 4.17: TEM ochronotic ligament (9,900)	108
Figure 4.18: TEM ochronotic ligament (43,000)	109
Figure 4.19: TEM ochronotic ligament (43,000)	110
Figure 4.20: TEM ochronotic ligament (26,500)	111
Figure 4.21: TEM ochronotic ligament (x60,000)	112
Figure 4.22: TEM <i>in vitro</i> MG63 (x6,000)	114
Figure 4.23: TEM <i>in vitro</i> MG63 (x9,900)	115
Figure 4.24: TEM <i>in vitro</i> SaOS-2 (x16,500)	116
Figure 4.25: TEM <i>in vitro</i> C20 (x9,900)	117
Figure 4.26: TEM <i>in vitro</i> C20 (x43,000)	118
Figure 4.27: TEM <i>in vitro</i> MG63 (x60,000)	119
Figure 4.28: TEM <i>in vitro</i> MG63 (x105,000)	120
Figure 4.29: TEM <i>in vitro</i> C20 (x135,000)	121
Figure 4.30: TEM <i>in vitro</i> C20 (x160,000)	122
Figure 4.31: TEM <i>in vitro</i> SaOS-2 (x105,000)	123
Figure 4.32: TEM <i>in vitro</i> MG63 (x8,200)	124
Figure 4.33: TEM <i>in vitro</i> C20 (x6,000)	125
Figure 4.34: TEM <i>in vitro</i> HGA pigment (x1,250)	126
Figure 4.35: TEM <i>in vitro</i> HGA pigment (x2,550)	127
Figure 4.36: Solid state $^{13}\text{C}$ NMR spectra ochronotic vs non-ochronotic cartilage	129

## Chapter 5:

Figure 5.1: Young's modulus ochronotic cartilage	143
Figure 5.2: Graph of Young's modulus of ochronotic cartilage	144
Figure 5.3: Macroscopic cartilage digestion pre-treatment	145
Figure 5.4: Macroscopic cartilage digestion post-treatment	146
Figure 5.5: SEM ochronotic cartilage (x10)	147
Figure 5.6: SEM ochronotic cartilage (x20)	148
Figure 5.7: SEM ochronotic cartilage (x100)	149
Figure 5.8: Histology of initiation of ochronotic pigmentation	151
Figure 5.9: Histology of subchondral resorption	153
Figure 5.10: Histology of pigmented osteocytes liberated from matrix	154
Figure 5.11: Histology of pigmented osteoclasts	155
Figure 5.12: High power histology of Figure 5.11	156
Figure 5.13: Histology of multinuclear cells engulfing pigmented osteocytes	157
Figure 5.14: Histology of ochronotic cartilage embedded in synovium	158
Figure 5.15: High power of Figure 5.14	159
Figure 5.16: Histology of different types of pigment	160
Figure 5.17: Histology of pigmented mononuclear cells	161
Figure 5.18: Histology of pigmented mononuclear cells	162
Figure 5.19: Histology of pigmented adipocytes	163
Figure 5.20: Fluorescence microscopy of femoral condyle	165

Figure 5.21: Fluorescence microscopy of articular cartilage surface	166
Figure 5.22: Fluorescence microscopy of subchondral tissues	167
Figure 5.23: Unstained & Fluorescence histology of subchondral tissues	168
Figure 5.24: Fluorescence histology of marrow space	169
Figure 5.25: Fluorescence histology of marrow space	170
Figure 5.26: SEM image of subchondral interface	172
Figure 5.27: Topographical SEM with grayscale overlay of subchondral interface	173
Figure 5.28: Halogenated qBSE-SEM of subchondral interface	174
Figure 5.29: Macroscopic image of OA tissues used for SEM	176
Figure 5.30: 3D SEM of OA femoral condyle	177
Figure 5.31: 3D SEM of AKU femoral condyle	178
Figure 5.32: 3D SEM of AKU femoral head	179
Figure 5.33: 3D SEM of AKU femoral head	179
Figure 5.34: Schematic showing progression of ochronotic osteoarthropathy	185

#### Chapter 6:

Figure 6.1: Macroscopic image of M283 kidneys	192
Figure 6.2: Macroscopic image of M271 kidneys	192
Figure 6.3: Macroscopic image of M272 kidneys	193
Figure 6.4: Macroscopic image of M282 kidneys	193
Figure 6.5: Macroscopic image of M280 kidneys	193
Figure 6.6: Histology of M283 heart valves	195
Figure 6.7: High power histology of M283 heart valves	196
Figure 6.8: Histology of tracheal rings of M283	197
Figure 6.9: Histology of thyroid cartilage of M283	198
Figure 6.10: High power histology of thyroid cartilage of M283	199
Figure 6.11: Histology of M283 kidneys	201
Figure 6.12: High power histology of M283 kidneys	202
Figure 6.13: High power histology of M283 kidneys	203
Figure 6.14: High power histology of M272 kidneys	204
Figure 6.15: High power histology of M283 kidneys	205
Figure 6.16: High power histology of M283 kidneys	206
Figure 6.17: Histology of M2091 kidneys	207
Figure 6.18: Histology of M240 kidneys	208
Figure 6.19: Histology of M236 kidneys	209
Figure 6.20: Histology of M283 knee	210
Figure 6.21: High power histology of M283 knee	212
Figure 6.22: High power histology of M283 knee	213
Figure 6.23: High power histology of M283 knee	214

#### Chapter 7:

Figure 7.1: 3D BSE SEM AKU trabecular bone (field width 2700microns)	226
Figure 7.2: 3D BSE SEM AKU trabecular bone (field width 2700microns)	227
Figure 7.3: 3D BSE SEM AKU trabecular bone (field width 2700microns)	228
Figure 7.4: 3D BSE SEM AKU trabecular bone (field width 2700microns)	229
Figure 7.5: 3D BSE SEM AKU trabecular bone (field width 900microns)	231

Figure 7.6: 3D BSE SEM AKU trabecular bone (field width 900microns)	232
Figure 7.7: 3D BSE SEM AKU trabecular bone (field width 900microns)	233
Figure 7.8: 3D BSE SEM AKU trabecular bone (field width 900microns)	234
Figure 7.9: Histology of AKU trabecular bone (59yr old male)	236
Figure 7.10: Histology of AKU trabecular bone (46yr old female)	237
Figure 7.11: High power histology of Figure 7.10	238
Figure 7.12: Histology of AKU trabecular bone (58yr old female)	239
Figure 7.13: Fluorescence microscopy of AKU trabecular bone (59yr old male)	240
Figure 7.14: qBSE-SEM AKU bone (59yr old male) (field width 2700microns)	242
Figure 7.15: qBSE-SEM AKU bone (59yr old male) (field width 2700microns)	244
Figure 7.16: 3D BSE SEM OA trabecular bone (field width 4050microns)	247
Figure 7.17: 3D BSE SEM OA trabecular bone (field width 1780microns)	248
Figure 7.18: Histology of OA trabecular bone (51yr old female)	249
Figure 7.19: Histology of OA trabecular bone (74yr old female)	250
Figure 7.20: Histology of OA trabecular bone (74yr old female)	251

#### Chapter 8:

Figure 8.1: Macroscopic image of AKU7A1	259
Figure 8.2: Macroscopic image of AKU7B1	259
Figure 8.3: Macroscopic image of AKU7B2	260
Figure 8.4: Macroscopic image of AKU7B3	260
Figure 8.5: Histology of AKU7 submandibular gland	262
Figure 8.6: Histology of AKU7 submandibular gland	263

#### Chapter 9:

Figure 9.1: MRI scans of thorax of AKU17	269
Figure 9.2: Macroscopic image of mediastinal mass	270
Figure 9.3: Histology of fibrous tissue of mediastinal mass	271
Figure 9.4: Histology of fibrous tissue of mediastinal mass	272
Figure 9.5: High power histology of mediastinal mass	273

**Tables**Chapter 1:Chapter 2:

Table 2.1: Patient demographics of AKU samples	52
--	----

Chapter 3:

Table 3.1: Patient demographics with joint location	56
---	----

Table 3.2: Average age of patient joint replacements from AKU patients	57
--	----

Chapter 4:Chapter 5:

Table 5.1: Microscopic features of cellular and matrix presentations of ochronosis	164
--	-----

Chapter 6:

Table 6.1: Details of FAH-/-, HGD +/- mice analysed	191
---	-----

Chapter 7:Chapter 8:Chapter 9:

## 1. Introduction

Alkaptonuria (AKU) is a rare autosomal recessive condition caused by mutation or absence of a single enzyme in the tyrosine metabolic pathway; homogentisate 1,2-dioxygenase (HGD). The lack of the enzyme results in the inability of the sufferer to fully metabolise homogentisic acid (HGA), this results in elevated levels of HGA in the body tissues and massive urinary excretion of the HGA. The disorder is characterised by three clinical features: darkening of urine on standing due to the presence of HGA, ochronosis of collagenous tissues, primarily articular cartilages of the weight bearing joints and subsequent ochronotic arthropathy as a result of the long term deposition of ochronotic pigment.

## **1.1 JOINT TISSUES**

### **1.1.1 Articular Cartilage**

In the human body there are three types of cartilage, these are grouped in relation to their function and properties. They are distinguished by their compositional constituents which are related to their function. The cartilages are elastic, fibrocartilage and hyaline. One of the most distinct properties of cartilage in health is it is avascular, has no nervous innervations and is alymphatic. Elastic cartilage is found in the pinna and parts of the larynx. Fibrocartilage is present in intervertebral discs and the menisci of the knees. Hyaline cartilage is the most predominant cartilage in the body and is seen on the ends of the long bones and is significant in joint function. It is also seen in the nasal septum, tracheal cartilages and the respiratory cartilages. Articular cartilage is a complex highly specialised tissue with numerous functions; shock absorption from locomotion, load distribution of the initial load through to the underlying bone and to provide a smooth and

low friction surface for efficient movement. The complexity of this tissue is further increased as in contrast to parenchymal organs such as liver, brain and kidney the connective tissues of the joints do not function directly via their cells but via their extracellular matrices.

The cartilage matrix consists of collagens, proteoglycans and non-collagen proteins. Within this matrix a single cell type; chondrocytes maintain turnover of certain matrix components within their vicinity. (Goldring, 2009). The cartilage matrix can be subdivided into 4 distinct layers, (uppermost to deepest) superficial, middle, deep and calcified. To date there is no real classification for dividing these compartments up. For many years cartilage had been considered an unresponsive or inert tissue, but it is now clear that the chondrocytes also respond to many of the same types of stimuli which cause responses in bone, such as cytokines, mechanical stimuli and genetic factors (Goldring 2007). The cartilage matrix consists of water, collagen and proteoglycans. Of this between 60-80% is usually water which is held in place by being bound to the proteoglycans in the matrix.

### **1.1.2 Structure, function and composition of cartilage**

The composition of articular cartilage is directly related to its biomechanical function. Within the articular cartilage located on the long bones, there are four distinct layers, each one has its extracellular components organised to meet its biomechanical function. These layers have differing cell densities and matrix organisation related to their structure and function. Throughout these layers, there are also different compartments,



distinguished by their proximity to the cellular components of the cartilage. Immediately around the chondrocytes is the pericellular matrix. The regions furthest from the chondrocytes, is deemed the interterritorial matrix, which constitutes the majority of cartilage given the sparse distribution of cells in this tissue. Between these two compartments is the territorial matrix. Synonymic with this organisational distinction there are also compositional differences of the matrix components. The majority of the articular cartilage is made up of water (60-80%), collagen fibres (10-30%) and proteoglycans (5-10%). Articular cartilage also contains non-collagenous proteins and a single cell type, chondrocytes. Chondrocytes are sparsely located within the matrix and are responsible for maintaining their surrounding matrix. The matrix is predominantly composed of type II collagen, but other types, including; V, VI, IX, X, XI, XII, and XIV are also present in lesser amounts. At the superficial zone collagen fibres are laid down parallel to the surface with the chondrocytes flattened. The preservation of this surface may prove critical for protection of the underlying layers. Collagen IX is found interspersed between the collagen II fibres. The middle layer demonstrates collagen fibres arranged in an oblique manner, this aids in the absorption of compressive and shear forces being placed on the joint. Chondrocytes in this region are spherical. In the deep layer the collagen fibres are arranged perpendicular to the surface along with the chondrocytes, this maximises the absorption of compressive forces through the joint.

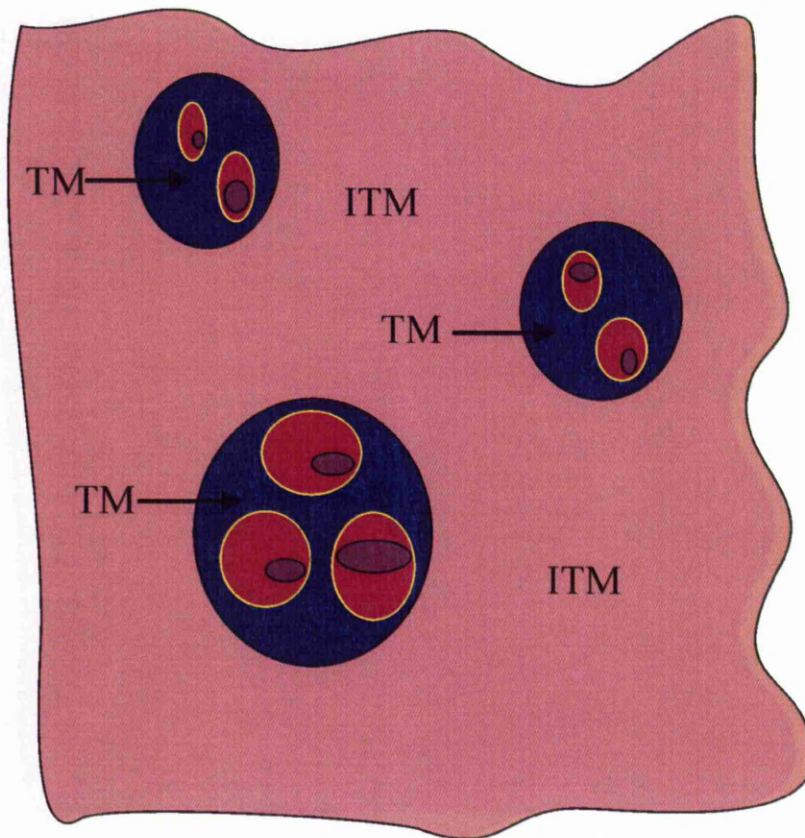


Figure 1.2: A schematic showing the arrangement of cells and their relation to the named regions of matrix. Chondrocytes are usually seen in small groups or clusters known as isogenous groups. The matrix immediately round the cell is the pericellular matrix (yellow). The territorial matrix (TM) is around the chondrocytes, often seen as to be within the isogenous group (purple). The interterritorial matrix (ITM) is located amongst the clusters of chondrocytes (pink).

### **1.1.3 Collagen**

Collagen fibres play a critical role in the structure and function of extra cellular matrix and at the cellular-extra cellular boundary (Kadler, 2008). Collagen exhibits a triple helical structure, with distinct periodicities at 67nm, giving it an unmistakable banding

pattern. The most abundant collagen in cartilage is type II. The collagen fibres are fundamental in maintaining the tensile properties of cartilage. This is facilitated by the crosslinking of collagen fibres, with collagen monomers demonstrating binding sites to mediate fibril formation (Prockop, 1998). Whilst collagen monomers will readily form fibres *in vitro*, this appears not to be synonymic *in vivo*, with other binding factors appearing to play an important role in the process and ensuring that diversity of fibre types, probably related to location and function, is maintained (Di Lullo, 2002 & Kadler, 2008). The collagen molecules themselves are formed from a repeat structure which sees the amino acid glycine located as every 3rd amino acid, to give the motif; Gly – X – Y, whereby X is usually proline and Y is hydroxyproline (Gordon, 2010).

Whilst collagen is the largest solid component of cartilage, other molecules are present and play a significant role in the structure and function of the tissue, these are the proteoglycans. Aggrecan is the largest part of the proteoglycans found in cartilage. Alongside being able to withstand tensile forces, cartilage can absorb compressive forces, enabling deformation under compressive load, whilst being able to return to its original form. This feature is associated with aggrecan and the aggregates it forms with hyaluronic acid and link protein. These aggregates usually consist of <100 aggrecan molecules located off a central hyaluronic acid filament (Martel-Pelletier, 2008). Aggrecan is important in the retention of water within cartilage under mechanical loading.

### **1.1.4 Chondrocytes**

As the sole cell in articular cartilage chondrocytes are responsible for maintaining the extracellular matrix. It has been demonstrated that they turnover matrix components in their vicinity (pericellular matrix) more rapidly than those at a greater distance from them (interterritorial matrix) (Goldring 2008). The longevity of chondrocytes within the matrix must be many years given that the rate of cell division is extremely low.

## **1.2 BONE**

### **1.2.1 Bone structure and function**

Bone is a highly specialised tissue which performs numerous functions. The majority are associated with mechanical function, such as movement, absorbing load, providing soft tissue support and protection. The other function is as a homeostatic store for mineral components utilised by the body during daily function and maintenance. There are two types of bone, cortical and trabecular. Cortical bone is densely packed and provides the external structure of the bone organ. Internally is trabecular bone, which appears as rod and plate like elements, and has a much larger surface area. In amongst the trabecular is the bone marrow, which has haemopoietic potential. Bone is composed of type I collagen fibres which are laid down as osteoid and then mineralised. It is this mineralisation that acts as the homeostatic store of calcium within the body. The structure and function of bone sees it modelled and remodelled during life to ensure the tissue can withstand the necessary load of supporting the body, while minimising the energy costs associated with locomotion of the bone organ. During life the remodelling of bone sees the internal shape

constantly alter in response to the mechanical load that is place on it and also to meet the mineral needs of the body.

The structure of bone is predominantly hydroxyapatite (mineral) with collagenous and non collagenous proteins. The collagen is type I and can become mineralised. The collagen fibres consist of two  $\alpha 1$  chains and one  $\alpha 2$  chain, coded for by separate genes and wound together in a triple helix. The fibres are the finished product of procollagen which is secreted from the cells with an N and C terminal domains which are cleaved extracellularly. Alongside the collagen there are non collagenous proteins found in bone which are instrumental to its maintenance and turnover. These proteins include osteocalcin, matrix Gla protein, osteonectin, proteoglycans, bone sialoprotein and serum proteins (Roach, 1994).

### **1.2.2 Cells within bone**

The turnover and remodelling of the bone organ is a highly ordered process. This process is undertaken by the cells which reside within the bone organ. Collagen is synthesised, secreted and laid down by osteoblasts as osteoid. Once this deposition has occurred the osteoblast either entombs itself into a cavity within the mineralised matrix, becoming an osteocyte, or alters its shape to become flattened and reside on the surface of the bone, becoming a bone lining cell. Removal of mineralised matrix requires a highly specialised cell; osteoclasts. These cells are multinucleated and arise from the fusion of mononuclear haemopoietic precursors. The osteoclasts move to the bone surface and undertake the process of bone resorption.

### **1.2.3 Bone turnover**

Bone is a highly dynamic tissue, altering in response to mechanical, biochemical and genetic stimuli. It repairs constantly at the site of micro-fractures and repeats this feat on a larger scale at sites of fracture associated with trauma. It can also adapt to new or altered loading applied to it over time. Although there are two distinctly different types of bone, the remodelling process is the same. There is a highly ordered process of bone turnover which sees packets of bone only being removed if there is going to be adequate deposition to replace it. This process is mediated by the cells, originally thought only to involve the osteoblasts and osteoclasts, it is now evident that osteocytes are also influential in the remodelling process (Bonewald, 2008). The process is initiated by the bone lining cells moving away from the bone surface to expose the underlying bone matrix. Then osteoclast precursors migrate to the area, fuse to form mature osteoclasts and resorb the bone. The process of resorption ceases prior to the recruitment of osteoblasts to the active surface to fill in the resorption lacunae.

Bone turnover is a general phenomenon which occurs in all regions of all bones. Any deviation from this finely balanced process results in pathological conditions, such as osteoporosis or subchondral bone sclerosis in osteoarthritis (OA).

### **1.2.4 Subchondral bone**

Subchondral bone or the subchondral bone plate lies immediately beneath the layer of calcified articular cartilage at the ends of the long bones. This plate provides a rigid structure to which the cartilage is attached. The two tissues, whilst compositionally and functional distinct share a closely balanced relationship. The subchondral bone and its

continual remodelling shows interdigitations into the calcified cartilage plate. Subchondral bone pathology is extremely important in the initiation and progression of osteoarthritis and has recently been suggested as a possible target for treatment of the disease (Kwan Tat, 2010). Even with this suggestion there is still no clear evidence as to whether the subchondral bone pathology in joint diseases such as OA follows or precedes changes in the overlying articular cartilage.

### **1.3 SYNOVIAL AND SOFT TISSUES**

Whilst cartilage and bone changes are predominantly associated with joint degeneration, the synovial tissues and surrounding musculature cannot be ignored as their functional significance is of great importance. The capsule, ligaments and surrounding musculature contribute to the mechanical stability of the joints and without their normal function cartilage degeneration is often seen, such as in malalignment syndromes resulting from abnormal loading across the cartilage surface. It is also evident that the synoviocytes, or cells that line the synovial surface are of high functional significance. They produce synovial fluid; a filtrate of plasma, but also maintain nutrition flow to the chondrocytes and produce high levels of hyaluronic acids to ensure efficient gliding of the joints. These cells also remove waste products from the joint space and thus balance homeostasis of the joint cavity.

Bone, cartilage and soft tissues are all unique in their matrix and cellular composition in health. These tissues rely on normal and healthy function of all the others to maintain the healthy and function of the joint organ as a whole. In AKU it is originally thought that the

cartilage was the only affected tissue, and that the synovial effects were a secondary result due to the presence of ochronotic shards of cartilage becoming embedded in the synovium. These tissues, whilst each unique all rely on the normal and intact function of the others to maintain joint health and function. In AKU it appears that the changes in the cartilage affect the synovium and to an extent the bone.

#### **1.4 METABOLISM**

Metabolism is a complex mechanism of chemical reactions that are inter-related and an important part of maintaining homeostasis of an organism. The homeostasis is fundamentally important to maintain cellular processes and functionality and converting one substance or compound into another that is readily useable by the organism. Metabolism can often be divided into two functional components; catabolism and anabolism. Catabolism covers processes which see complex molecules broken down to give their principal functional components. For example breakdown of large globular proteins to polypeptides which can be further broken down to amino acids. Anabolism is the opposite and sees these small functional components utilised to build proteins and complex structures useful to the body for processes related to growth, energy or repair from amino acids. There are many underlying reasons for these reactions but some of the most significant are related to the size and cost to the body of moving around large molecules to the site where they are needed in the body. These reactions are usually regulated by highly specific enzymes which facilitate these reactions. Within the body there predicted to be somewhere in the region of 135 metabolic pathways containing over



2700 enzymes. Many of these pathways are found to be conserved amongst species, both complex and simple (Romero, 2005).

#### **1.4.1 Tyrosine Metabolism**

Tyrosine is a non-essential amino acid that is synthesised in the liver from phenylalanine. Tyrosine is a polar, uncharged (hydrophilic) amino acid which is fundamentally important in humans for a number of processes, it is used to synthesis 3 catecholamine hormones; adrenalin, noradrenaline and dopamine. It is also the precursor to thyroxine which is important in the regulation of cellular metabolism, growth and enhancing the effect of other catecholamine effects. It is also used in melanin biosynthesis whereby it forms pigment in the melanocytes of the skin. Tyrosine is also involved in other metabolic pathways where it is enzymatically degraded through a number of steps to fumarate and acetoacetate both products are then used as substrates in the citric acid cycle. It is along this specific pathway that a number of genetic diseases occur.

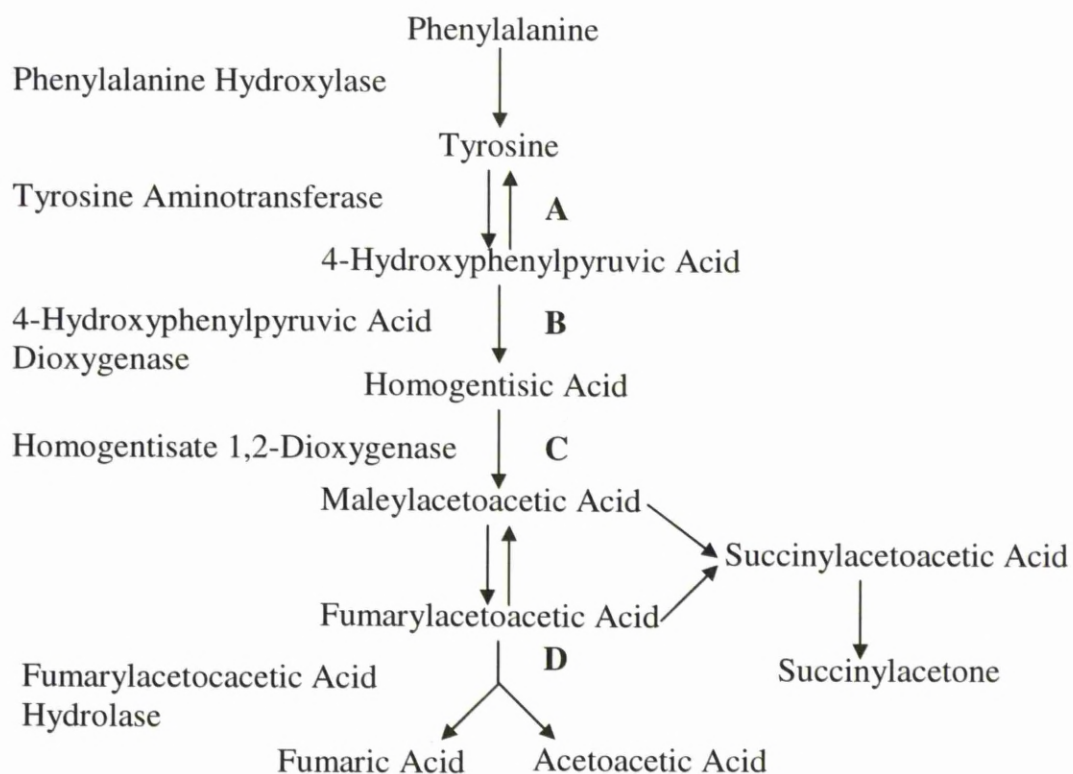


Figure 1.3:- Diagram showing the phenylalanine and tyrosine metabolic pathway with enzymes and defects. **A** = Tyrosinemia type II. **B** = Tyrosinemia type III. **C** = Alkaptonuria. **D** = Tyrosinemia type I.

## **1.5 ALKAPTONURIA**

### **1.5.1 History**

Alkaptonuria (AKU) is a rare autosomal recessive condition resulting from the inability to fully metabolise the amino acids tyrosine and phenylalanine. The disorder is renowned for being one of the first disorders to be described by Sir Archibold Edward Garrod as

“an inborn error of metabolism” and to conform to the laws of Mendelian autosomal recessive inheritance (Garrod, 1902, Garrod 1908). Prior to the deduction by Garrod that AKU is an autosomal recessive condition and is an “inborn error of metabolism” there were numerous published observations that described clear features of AKU.

The earliest documented report of AKU relates to the description of a school boy who passed urine “as dark as ink,” by Scribonius in 1584 (Scribonius, 1584). This was closely followed 25 years later when Schenck described the same phenomena in a Carmelite monk (Schenck 1609). Similar reports were documented by Lusitanus in 1649, Singer in 1775, and Marcet in 1822. In 1859, Boedeker undertook an extensive analysis of urine from a 44yr old man with increasing lumbar spine pain and severely compromised mobility. He identified a reducing substance present in the urine of this individual that reduced alkaline copper solutions consistent with diabetes, however Nylander’s solution remained unchanged (A test for glucose in the urine, which produces a black precipitate). Boedeker deduced that the reducing substance in the urine was not glucose based on these observations and the fact that the individuals urine failed to support yeast fermentation. Further analysis demonstrated silver nitrate, chromic acid, osmic acid and permanganate were all reduced. He also observed, consistent with previous observations, that when left to stand the urine darkened. He further described that this occurred from the surface of the solution downwards. Boedeker demonstrated that this darkening was rapidly accelerated on addition of alkali substances and quickly took up a large volume of oxygen. This finding allowed Boedeker to name the new substance “alkapton” derived from the Arabic “Alkali” (meaning alkali) and the Greek word meaning “to suck up

(oxygen) readily/greedily in alkali. Boedeker was also able to extract his newly named compound by a process involving precipitation with lead and extraction in ether. This process yielded “alkapton” crystals that were not pure; contaminated with nitrogen (Boedeker, 1861). Following Boedeker’s discoveries there was still no knowledge as to the actual compound responsible for the disorder and its features. Prior to its discovery there were numerous attempts to deduce the compound and its’ structure. The compounds suggested in the intermediary included; pyrocatechol, protocatechuic acid, glycosuric acid, urrhodinic acid, uroxanthic acid and uroleucic acid (O’Brien, 1963). Eventually, in 1891 Wolkow and Baumann managed to extract alkapton and its lead salt form (Wolkow, 1891). They also obtained prismatic crystals of the free acid, detailing its melting point and empirical formula;  $C_6H_{12}O_4$ .

In parallel, but unrelated to attempts to distinguish the compound responsible for darkening of the urine, there were interesting observations being made by Virchow in necropsy of a 67yr old man who died from congestive heart failure. He found that the articular cartilages, intervertebral discs, menisci, laryngeal and tracheal cartilages were all black. The ligaments and synovial tissues displayed pigmentation to a lesser extent of the cartilages. Microscopic analysis of these tissues showed that the black pigmentation observed macroscopically actually appeared yellow in colour. As a result of this appearance Virchow termed the phenomena “Ochronosis” derived from the Greek ochros “sallow” and nosos “disease” (Virchow, 1866). It was in 1902 that Albrecht connected the ochronosis of tissues, ochronotic arthritis and alkaptonuria. He concluded that long term suffering from alkaptonuria resulted in ochronosis (Albrecht, 1902). In 1904 Osler was the first person to publish evidence to document the diagnosis of alkaptonuria in

living individuals. The sufferer in question displayed pigmentation of the ears and the sclera. Osler also noted that the sufferer had a brother who displayed similar features, both presented arthritis in the spine (Osler 1904). In 1902 Garrod described the disorder as the result of an alternative course of metabolism, harmless and usually congenital and lifelong (Garrod, 1902). Most famously Garrod presented his work at the Croonian lectures in 1908, whereby he demonstrated that albinism, alkaptonuria, cystinuria and pentosuria were all resultant of Mendelian inheritance, causing variation in metabolism of normal metabolites on normal pathways (Garrod, 1908, Schriver 2008). Garrod demonstrated that there was an association between the intake of the amino acids tyrosine and phenylalanine and this increased the output of HGA in alkaptonuric individuals (Garrod, 1905). Ochronosis has been confirmed in an Egyptian mummy dating back to 1500 B.C. The confirmation of AKU in *Hawra*, was verified by performing radiological and biochemical analysis of the joints most affected by the disease, the knees, hips and intervertebral discs (Stenn, 1977).

### **1.5.2 Epidemiology**

The incidence of alkaptonuria is estimated to be between 1 in 200,000 to 1 in 1,000,000 births in the developed world (Sahin, 2001, Phornphutkul, 2002, Keller, 2004). In regions of Slovakia and the Dominican Republic the prevalence is much higher, around 1 in 19,000. It has been demonstrated that there are numerous mutations within the Slovakian population (Zatkova, 2000), with further independent founder mutations identified in this small country (Gehring, 1997, Müller, 1999, Zatkova, 2000). The prevalence of AKU in Slovakia is further complicated by the discovery that the M368V mutation, the most

prevalent AKU mutation in Europe and a relatively frequent AKU mutation in the neighboring countries, has not been encountered in the Slovak patients (Zatkova, 2000). They also discovered that there are relatively few mutations from the surrounding countries that occur in the Slovakian AKU gene pool, and that there are 3 mutations which show a high prevalence in the this region and are rarely found outside Slovakia. One of the most difficult things in predicting the appearance of AKU in any region is the lack of knowledge of how many carriers (HGD mutational heterozygote's) there are in the general population.

### **1.5.3 Clinical Presentations**

Alkaptonuria has three clinical features which present at different stages through life. The first and earliest presenting symptom is the excretion of HGA in the urine; this darkens on standing or can be darkened rapidly by the addition of alkaline substances. The presence of HGA in urine is used as a diagnostic tool for determining AKU. It has been trialed on over 135,000 children in Wales as part of a screening study looking for inherited metabolic disorders, particularly phenylketonuria (PKU) after the discovery that it causes severe mental retardation if not treated with a low phenylalanine diet from birth. This trial discovered 2 infants with the disorder (Bradley, 1975). It has been reported that darkening of urine in nappies can be seen within 57 hours of birth (Garrod, 1902). This would confirm that the excretion of HGA in the urine is high from birth. The excretion of HGA in the urine and its subsequent darkening and staining of nappies and/or clothing in infants is the only clinical sign of the disorder in the pediatric group (Peker, 2008). Whilst darkening of urine is usually an obvious sign of abnormality, it is not unique to

AKU, it can be caused by accumulation of other tyrosine metabolic compounds such as L-DOPA, melanin or melanogen (Slawson, 1980), or by intake of certain foods in large quantities (Noll, 1980). To ensure AKU is correctly diagnosed further analyses of the urine are usually undertaken in the pediatric age group as the other clinical features, such as the ochronosis of ear cartilages only becomes notable around the 4<sup>th</sup> decade (O'Brien, 1963) and the ochronotic arthropathy, does not present until the 3<sup>rd</sup> or 4<sup>th</sup> decade of life (Phornphutkul, 2002). Further analysis of urine is usually undertaken using either spectrophotometric analysis (Phornphutkul, 2002), HPLC (Bory, 1989 & 1990) or by NMR urinalysis (Yamaguchi, 1986).

Over time levels of HGA accumulate in body tissues and undergo polymerisation by an unknown mechanism to deposit as a dark pigment associated with the extracellular matrix (Helliwell, 2008 & Taylor, 2010). This deposition is termed ochronosis, as coined by Virchow on his microscopic observations (Virchow, 1866). Ochronosis is most noticeable in the sclera of the eyes and pinna where the pigmentation of cartilages can be seen through the skin, this occurs after the 30<sup>th</sup> year of life (Phornphutkul, 2002). The ochronosis occurs in many other tissues of the body, but in the majority it is not as clear as in the pinna or sclera. Other tissues which show ochronosis include the skin (O'Brien, 1963), not only in the dermis but observations have been described in the sweat glands, both intracellularly and in the basement membrane (Friderich, 1951 & Lichenstein, 1954). Occasionally the ochronosis can be the first point of elucidating the diagnosis of AKU in an individual, such as the ochronosis found in the tracheal and bronchial cartilages (Parambil, 2005). The majority of other tissues that demonstrate ochronosis are usually observed post-mortem or are found due to issues related to the deposition of

pigment in those tissues which brings about the need for surgical intervention. Post-mortem macroscopic and microscopic examination of tissues from individuals diagnosed with AKU has demonstrated an extremely wide presentation of ochronosis affected tissues. Tendon pigmentation is widely reported with the Achilles and quadriceps often being ochronotic and this pigmentation is assumed to be the reason for spontaneous failure (Manoj Kumar, 2003 & Chua, 2006). There has also been discussion of pigmentation in other less frequently affected tendons, such as that of the flexor digitorum profundus muscle. Post-mortem pigmentation has been observed in other tendons, including that of the sternocleidomastoid (Helliwell, 2008). It has also been described that there is a distinct lack of involvement of tendons which possess a synovial sheath, except one; the tendon of long head of *m biceps brachii* (Filippou, 2008).

The cardiac system is often seen to be affected by ochronosis. There are numerous reports of valve involvement due to the deposition of ochronotic pigment resulting in the need for replacement in alkaptonuria sufferers (Phornphutkul, 2002, Fisher, 2004,) Cardiac issues due to the presence of ochronotic pigment in the heart valves can sometimes be the initial presentation of alkaptonuria (Ffolkes, 2007). The involvement of the heart valves is well described, but there is also deposition associated with the aorta and main arteries (Helliwell, 2008), the coronary arteries do not appear to be involved before the age of 40, or at least involved to the extent where changes can be detected, although by the age of 59, 50% of patients examined showed coronary artery involvement in the form of calcification detected by CT scan (Phornphutkul, 2002).



There are descriptions of ochronosis in the dura mater (Gladston, 1952, Liu, 2001, Helliwell, 2008). Whilst HGD expression and HGA metabolism occur in the liver, there is no literature to demonstrate that these tissues, along with those of the lymphoreticular, pancreas, gastrointestinal or endocrine structures show macro or microscopic ochronosis (Helliwell, 2008). There is literature detailing the pigmentation in the islets of Langerhans (Helliwell, 2008 & Lichtenstein, 1954), although the significance of this is difficult to interpret as the distribution within the cells and tissue is not described.

There have been reports of numerous presentations of ochronosis in different tissues presenting as the initial symptom of AKU, however it is most common that the first presentation is detected radiographically or clinically as OA-related pain in the joints. Ochronosis in the joints occurs over a prolonged period whereby there is gradual deterioration in joint function. This is termed ochronotic arthropathy. The earliest and most common presentation is often related to the spine, particularly the lower back and is often confused with ankylosing spondylitis. In a study of 163 cases of AKU, the spine was involved in 159, knee in 62, shoulder in 37 and hip in 33 (O'Brien, 1963, Lagier, 1980). The difference between the ochronotic arthropathy in the spine and ankylosing spondylitis is that the sacro-iliac joints usually remain unaffected in ochronotic arthropathy (Perry, 2006), although the presence of ankylosing spondylitis and AKU in the same patient has been described (Balaban, 2006). Spinal changes in AKU also differ from those of the spine in OA; spinal involvement in AKU seems to preferentially affect the thoracolumbar region rather than lumbosacral (Phornphutkul, 2002, Ben Rayana, 2008). Such is the severity of spinal involvement in AKU, a third of 45 patients examined

showed a loss in height (Phornphutkul, 2002). The involvement of the spine sees narrowing and pigmentation of the intervertebral discs along with calcification; osteophytes are usually small or absent. Following spinal involvement in AKU, it is usually proximal joints which are the next to be affected, with hips and shoulders being described as the next joints to present with ochronotic arthropathy (Perry, 2006). Ochronotic arthropathy of the hips presents clinically and radiographically as OA with joint space narrowing and subchondral sclerosis often observed (Araki, 2009). The only current approach for treating the joint arthropathies is pain management and surgical intervention. It is well documented that surgical intervention brings about the diagnosis of AKU (Rose, 1957 & Perry 2006), if all other symptoms and features have been missed or overlooked. Ochronotic femoral heads have been studied extensively following surgical replacement and reveal a wide phenotypic presentation, but what is consistent is the presence of ochronotic pigment associated with the cartilage matrix (Melis, 1994, Di Franco, 2000, Shimizu, 2007, Kefeli, 2008). Even with all the complications and associations of pigment with tissues there is no evidence to correlate a shortened life span of patients with AKU (Srsen, 1985). There are numerous reports of misdiagnosis of rheumatological conditions which are masquerading as AKU following administration of monocycline and tetracycline. This evidence suggests that the most reliable confirmation of AKU is urinary excretion of gram quantities of HGA (Vilboux, 2009).

#### **1.5.4 Therapeutic strategies**

The treatment of AKU, its clinical features and understanding of the pathogenesis are still not completely understood. The majority of therapies have been aimed at preventing

ochronosis of tissues, brought about by the oxidation of HGA to its intermediate and ultimately its pigmented polymer which binds to the connective tissue components.

#### 1.5.4.1 Ascorbic Acid

It has been suggested that treatment of AKU patients with ascorbic acid (ASC) maybe one such approach (Sealock, 1940). It had been previously demonstrated that 10mM ASC inhibited HGA polyphenol oxidase, an enzyme suggested as specific to the polymerisation of HGA (Zannoni 1969). It would be difficult to achieve this concentration *in vivo*. The more significant issue with using ascorbic acid would be the danger that it could contribute to the formation of kidney oxalate stones in AKU sufferers (Phornphutkul, 2003). The usefulness of ascorbic acid has been shown in rats to decrease the binding of homogentisic acid in connective tissues (Lustberg, 1970). It is more notable that ASC may have a far more detrimental effect on HGA than any potential benefit that is yet to be elucidated. Experiments have shown the ascorbic acid is stable at physiological pH and in certain concentrations, however on addition of HGA solution the auto-oxidation rate greatly increases along with the rate of oxygen consumption (Martin, 1987). ASC is a co-factor to 4-hydroxyphenylpyruvate dioxygenase, which may result in the vitamin increasing production of HGA in alkaptonuric patients. Experiments have demonstrated that there is also no beneficial effect of utilising ascorbic acid as it does not lower urinary or plasma HGA levels in adults or 15 month old infants. It also indicated that in the cases of young infants it can have a profound increase on urinary levels of HGA (Wolff 1989). In 1988, Forslind drew the conclusion that ascorbic acid is not an

effective therapy for treating symptomatic ochronosis (Forslind, 1988). It may be that a more beneficial strategy would be to block the formation of HGA itself. It has recently been shown *in vitro* that administration of ASC in combination with N-Acetylcysteine (NAC) to human articular chondrocytes challenged with HGA; decreased apoptosis, increased chondrocyte growth and partially restored proteoglycan release all of which were detrimentally affected by HGA. The results showed a notable increase in efficacy when the antioxidants were used in combination rather than in isolation, the use of NAC in combination with ASC is theorised to counteract the increase in HGA production by use of ASC alone (Tinti, 2010). It is also now being investigated that there are other antioxidants maybe viable therapeutic agents for AKU (Braconi, 2010). Experimental evidence has shown that the minocycline induced pigmentation can be seen in thyroid glands of rats. This pigmentation is absent when rats are fed ascorbic acid in tandem with minocycline (Bowles, 1998).

#### 1.5.4.2 Nitisinone (NTBC)

One of the main issues with treating AKU is that the HGA and its intermediates seem to affect tissues, such as deep in the articular cartilage, where the presence of any gene therapy would be unable to have any action. One of the most promising recent developments has come in the form of an early triketone which was originally developed as a herbicide (Schulz, 1993). This substance is NTBC, or 2-(2-nitro-4-trifluoromethylbenzoyl)-1,3-cyclohexanedione, which is already administered orally to sufferers of tyrosinaemia type I (Lindstedt, 1992). NTBC is one of a family of triketone herbicides, all of which function to inhibit 4-hydroxyphenylpyruvate dioxygenase

(HPPD). This enzyme is responsible for the conversion of hydroxyphenylpyruvate to HGA. In hereditary tyrosinaemia type I (HTT1), NTBC acts by inhibiting the production of HGA, resulting in a partial block to the formation of fumarylacetoacetate. Prevention of this product reduces the concentration of any oxidizing metabolites which result in often fatal features of the disorder in children; these include severe liver disease, hepatocellular carcinoma and kidney tubule dysfunction (Anikster, 1998). The safety and functional significance of NTBC in treating HTT1 was demonstrated in a murine model of the disease. FAH mutation is normally fatal in neonates with the phenotype. FAH is normally produced in the foetal mouse on day 16 of gestation. It was demonstrated that subcutaneous injection of NTBC into the mother on day 15 would correct this disorder in the pups, they would then be administered a daily oral dose of NTBC following birth (Grompe, 1995). Following the verification of safety and use of NTBC for HTT1 in mice and humans it was shown that NTBC could be used to treat a murine model of alkaptonuria, whereby mice that exhibited urine which darkened on contact with NaOH soaked filter paper were maintained on NTBC and their urinary HGA levels analysed alongside plasma NTBC levels. These results showed that NTBC caused a dose dependant reduction in the urine levels of HGA in these mice, providing initial proof for the treatment of AKU by NTBC (Suzuki, 1999). Initial trials of NTBC in humans demonstrated that there was at least a 69% reduction in urinary HGA in 2 patients with AKU when the drug was administered in low doses. In this study there was significant elevation of tyrosine plasma levels which produces the risk of corneal crystal formation, corneal epithelial damage, and photophobia (Phornphutkul, 2005). The deposition of corneal opacities has been described in individuals taking NTBC for HTT1, believed to

be due to elevated plasma and serum tyrosine and possibly exacerbated by poor dietary compliance (Ahmad 2002). A larger scale study looking at 9 patients with AKU was undertaken to investigate the effect of NTBC and its effects on HGA excretions and plasma levels (Suwannarat, 2005). Both NTBC and ASC have been used in combination with low protein diets to reduce dietary intake of tyrosine and phenylalanine.

#### 1.5.4.3 Low protein diet

There are a small number of reports documenting the use of restricted protein intake as a way to reduce the level of HGA in the body of alkaptonuric individuals and investigate the effect on pigmentation. The studies show mixed results; one such study shows that there is little effect of ASC on urinary excretion of HGA; furthermore there is a suggestion that it increases the amount of the speculated causative intermediate, BQA (Mayatepek, 1998).

Another study describes protein restriction as lowering urinary HGA excretion levels in patients under the age of 12; however this effect is lost beyond this age group. Furthermore there are often issues with compliance to a restricted protein diet, particularly as age progresses (de Haas, 1999). Questions must also be raised about the effect of physical and mental progression in children who have their diet restricted of protein during their key developmental stage. Another issue with restricting dietary protein is that the majority of HGA is generated from protein breakdown within the body.

#### 1.5.4.4 Enzyme replacement therapy

Since it is a single enzyme that is deficient in AKU, the ideal treatment would be the immediate replacement of HGD in the metabolic pathway to give normal tyrosine catabolism. In theory this technique should be feasible, but due to the intracellular function of the tyrosine metabolic enzymes there are more lethal complications that could arise. Whilst the lack of the HGD gene results in deposition of ochronotic pigment, this phenomenon is not fatal. Following the degradation of HGA in the liver and kidneys, the production of MAA and subsequent reversible conversion to FAA results in the spontaneous formation of succinylacetone; this is toxic and highly mutagenic. For this reason any enzyme replacement would have to ensure that the functional HGD is delivered to the cellular location of tyrosine metabolism to prevent the buildup of succinylacetone occurring around the body and in the bloodstream.

### **1.6 HMOGENTISATE 1,2-DIOXYGENASE PRODUCTION, FUNCTION AND MUTATIONS**

AKU results from the mutation in the gene encoding for the enzyme HGD. The normal human HGD gene is 54,363bp long and codes a 1715 nucleotide sequence that is divided into 14 exons, which vary in lengths of between 35 and 360 bp (Granadino 1997). The 445 amino acid protein forms a dimer of two trimers which constitutes a functional hexamer (Vilboux, 2009). The crystalline protein structure has been resolved. It consists of a 280 residue N-terminal domain with a central  $\beta$ -sandwich structure flanked by a  $\beta$ -sheet that interacts with the 140 residue C-terminal domain of neighboring subunits. The active site binds iron in a domain defined by 3 side chains; His335, Glu341, and His371.

(Vilboux, 2009 & Titus, 2000). The HGD protein is responsible for catalysing the breakdown of HGA to MAA. HGA is the last metabolite in Tyrosine metabolism to retain the benzene ring, HGD metabolises HGA to form MAA by cleavage of the benzene ring between C1 and C2 giving the linear compound (Knox, 1955). The presence of HGA in normal individuals is limited to the kidney and liver due to the production of the tyrosine metabolic enzymes in these tissues. It is believed that the majority of the HGD production and function occurs in the liver and kidneys. Work in rats has shown that the highest functional activity of HGD is in the liver, followed by the kidneys and then essentially inactive amounts of enzyme activity are seen in spleen, heart, skeletal muscle or small intestine (Crandall, 1954). This is consistent with work of others to show that this liver and kidneys demonstrate the majority of HGD functional activity. The demonstration of essentially inactive amounts of HGD in other tissues is both in confirmation with and contrary to the findings of others who had shown that HGD was functionally expressed in non-renal and hepatic tissues (Crandall 1954 & Bernheim 1944). This work also demonstrated that the tyrosine metabolic pathway proceeds intracellularly (Crandall 1954). More recently, HGD expression has been detected in small intestine, colon and prostate of humans, alongside the liver and kidneys (Fernandez-Canon, 1996). To date at least 91 mutations have been identified covering a number of mutation types: 62 missense, 13 splice site, 10 frameshift, 5 nonsense, and 1 no-stop mutation. It is also suggested that the majority of HGD variants occur in exons 3, 6, 8 & 13 (Vilboux, 2009). Interestingly attempts have been made to correlate genotype and phenotype in AKU, however given that the human liver can produce enough HGD to metabolise 1.5kg of HGA/day any mutation must result in at least 99% reduction in



functional enzyme production in order to present the AKU phenotype (Scriver, 2001 Vilboux, 2009). To date there is no correlation with type of HGD mutation, the amount of HGA in the urine, HGA plasma level or severity of the disease. (Introne, 2003). The build up of HGA does not normally happen in normal individuals as once formed it is cleaved to MAA and further metabolised to FAA and then fumarate and acetoacetate. In alkaptonuric individuals it has been demonstrated that the HGD is the only missing enzyme in the metabolic tissues, all subsequent enzymes are present and functional (La Du, 1958).

### **1.7 HOMOGENTISIC ACID**

HGA is a small highly water soluble molecule of molecular weight 168.15 and a linear formula of  $(\text{HO})_2\text{C}_6\text{H}_3\text{CH}_2\text{CO}_2\text{H}$ . The crystals are off-white to tan in colour. It is also known as 2,5 dihydroxyphenylacetic acid.

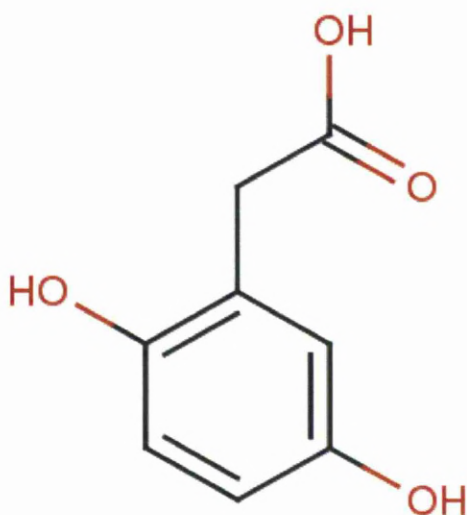


Figure 1.4:- Chemical structure of homogentisic acid.

It undergoes chemical changes on addition of NaOH or when left to stand in the presence of molecular oxygen to form its quinone intermediate; benzoquinone. This intermediate is highly unstable and believed to undergo polymerisation to form the pigmented polymer observed in patient tissues. It is theorised that this process has many similarities to the formation of melanin from tyrosine.

### Metabolic Pathway of Ochronotic Pigment Production

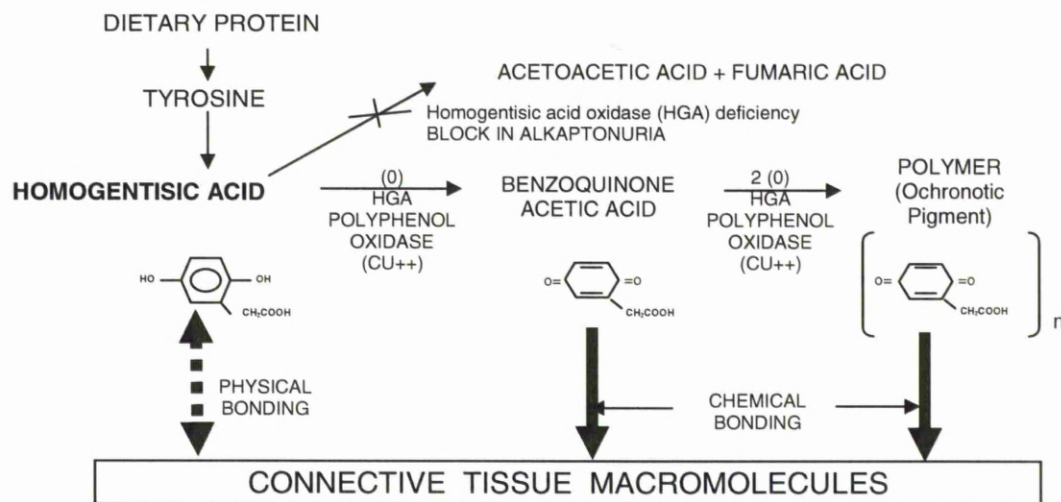


Figure 1.5:- Diagram showing the theorised metabolic pathway of ochronotic pigment production. (Adapted from Stanbury, 1978).

### 1.8 AKU IN OTHER ORGANISMS

AKU has been described in other organisms. It has been shown in other primates such as the crab-eating macaque which displayed the typical darkened urine associated with the disorder but failed to show any signs of ochronosis or joint involvement in this 8yr old animal (Johnson, 1993). Prior to the discovery of this macaque there have been two descriptions of AKU occurring in other primates, much closer to the *homo sapien*

lineage. These occurred in the chimpanzee (Watkins, 1970) and the orangutan (Keeling, 1973). Diagnosis was based in the discolouration of urine but no ochronosis or joint involvement was detailed. HGA in urine has also been observed in Dalmatians (Lonsdale, 1994). There are also early reports of the appearance of ochronosis in cattle, horses and dogs and a rabbit which displayed darkened urine (Lewis, 1926, O'Brien, 1963).

### **1.9 AKU ANIMAL MODELS**

Many human disorders benefit from animal models to help progress their understandings and to trial therapeutic strategies. It was noted that there was limited research into the attempts to induce ochronosis and ochronotic arthropathy as way to study AKU in animals (O'Brien, 1963). The earliest attempts at an animal model of AKU were undertaken by intraperitoneal or intravenous injection of HGA into rabbits. The investigators also injected HGA into the joints of rabbits (1g, 0.25g, 0.125g, 0.06g/1ml of saline). Animals which received multiple injections exhibited darkening of urine along with ochronosis of joint tissues and surrounding fat, tendon and muscles in a non-specific nature. Intraperitoneal and intravenous injections of HGA did not produce ochronosis. This study demonstrated the damaging effects of HGA; consistent results were obtained when buffered or unbuffered HGA solution was injected into tissues (Moran, 1962). One interesting note of the study is the observation of tubular casts in the kidney resulting from the excretion of HGA initially injected into the joints or peritoneum suggesting that there may be localised damage due to the HGA. The investigators also looked at the reaction of injecting ochronotic pigment from a necroscopied case of AKU into the knee joints of rabbits. Thickening and swelling of the synovium was noted with the presence

of macrophages and giant cells around pigment. The significance of this is diluted by the fact that a standard immunological response would be expected from the injection of human material into a rabbit. The authors also suggested an adaptation of their method whereby overloading of the animal with HGA by exposing to a high tyrosine and low ascorbic acid diet (Moran, 1962). The first model study was made in rats whereby feeding them for a minimum period of 9 months from the age of 1 month on a diet of 8% L-tyrosine appeared to induce ochronosis and arthropathy. The induction of AKU was confirmed by presence of HGA in the urine (Blivaiss, 1966). A murine model of AKU was produced in 1993 by mutagenesis. These mice arose by intraperitoneal injection of ethylnitrosourea (250mg/kg) of eight week old mice from an inbred stock carrying seven recessive mutations. Following recovery, these animals were then mated to 129/Sv-T/+ mice. Independent micro-pedigrees were achieved by systematic sibling mating for more than 10 generations. The AKU mutation was then backcrossed onto both the BALB/cByJ (albino) and the C57/BL/6J (pigmented) backgrounds. These animals were previously thought not to exhibit ochronosis, despite the mutant phenotype exhibiting darkened urine and high levels of urinary and plasma HGA, both of which were absent from wild type and heterozygotes. (Montagutelli, 1994). The mice have a truncated protein form of the HGD enzyme resulting from a splice mutation (Manning, 1999). Macroscopic and microscopic analysis of these animals revealed an absence of ochronosis of tissues (Montagutelli, 1994). It is well known that mice endogenously produce the anti-oxidant ascorbic acid and this maybe a protective mechanism in the mouse (Levine, 1986). As part of the investigation into the murine model, the detection of the mutation in the mouse genome was found to be in an area that was highly

homologous with the human 3q (Montagutelli, 1994). The mode of transmission of the murine disorder was demonstrated to be autosomal recessive consistent with the human transmission of the disorder. This demonstrated that heterozygote's, even with 50% of wild type production of HGD can sufficiently clear HGA from their systems (La Du 1989, Montagutelli, 1994). The mapping of the human alkaptonuria gene was based on the inter species conservation of genetic linkage groups (Janocha, 1994).

### **1.10 FUNGAL MODEL**

AKU is a metabolic disorder in the same metabolic pathway as the more serious a HTT1. In murine HTT1 there is neonatal lethality which makes it a difficult model for studying the disorder. *Aspergillus nidulans* shows an interesting versatility in its metabolic ability, it proceeds through two different phenyl compounds for carbon sources that are both metabolised to 2,5-dihydroxyphenylacetic acid, or HGA, and then metabolised further to maleylacetoacetate and fumarylacetoacetate. The species demonstrates a highly conserved amino acid sequence when compared to the human sequence. Loss of the FahA results in phenylalanine toxicity and secretion of succinylacetone consistent with human HTT1. Furthermore loss of the HGD prevents phenylalanine toxicity and results in an alkaptonuric type phenotype; in this culture system induction of the phenylalanine/phenylacetate catabolism results in production of HGA which accumulates in the media and undergoes oxidation and polymerisation to become dark brown (Fernandez-Canon, 1995).

### **1.11 SUMMARY**

Alkaptonuria is identified by clinicians as the first disorder to be demonstrated as an inborn error of metabolism. HGA is the molecule responsible for deposition as a pigmented polymer in joint tissues of sufferers of AKU. The accumulation of this molecule is the result of a single enzyme deficiency; HGD, the gene for this enzyme and its chromosomal location are known. Whilst these represent large advances in knowledge of the disease; the understanding of the pathogenic mechanisms that see HGA converted to its pigmented polymer, or other intrinsic and extrinsic factors that may be influential in determining the tissues and regions that are affected by the pigment are not fully understood. These unknowns represent a large gap in the knowledge of the disease and gaining insights into these areas would open up more therapeutic opportunities for treatment of this rare and debilitating condition. There are also numerous individual case reports in the literature many are descriptive of end-stage ochronosis and arthropathy, whilst informative, these describe a stage that is possibly beyond the opportunity for treatment. There is evidence to suggest that in these patients that HGA alone is not the sole or limiting factor determining pigmentation. Alongside this, due to the rarity of the disorder there is little in the way of models and longitudinal data to enable study of the disease, which may have limited the advancement into understanding of the disorder. The formation of the findAKUre project has allowed access to the numerous AKU specimens which will enable the comparison of patient tissues and investigation of unknown factors that may elucidate currently unknown mechanisms in the disorder, which will be a large advancement in understanding of the pathogenesis of the disease.

### **1.12 AIMS OF THE STUDY**

Alkaptonuria is a rare autosomal recessive disease with no known cure or treatment. The causative molecule, HGA, and missing enzyme has been identified and cloned (HGD). Despite this little is known about how or why specific tissues and components of tissues are preferred for the deposition of the pigmented polymer. Furthermore there is little evidence describing the variation of pigment presentation from one patient to another, and within a patient. Therefore the aims of this study were to compare and contrast presentations of pigmentation in AKU patient tissue samples and to increase the understanding of the biochemical and molecular pathogenesis of the disease in order to open up more therapeutic strategies for the treatment of the disease.

## **2. Materials and Methods**



## **2.1 ETHICAL APPROVAL**

All human tissue samples used in this project were obtained under ethical approval from Liverpool REC (07/Q1505/29). Patients involved signed a fully informed consent form and the data was anonymised to protect the patients confidentiality. All joint tissues were obtained at time of surgery and dissected as required before either being passed into PBS or DMEM for transport back to the laboratory, or fixed in PBFS. Once back in the laboratory, unfixed tissues were further dissected and plated out as described in this chapter.

## **2.2 CELL CULTURE**

### **2.2.1 Reagents**

Dulbeco's modified eagles medium (DMEM) and DMEM with Ham's F12 1:1 was purchased from Gibco and supplemented with 10% foetal calf serum (FCS), purchased from Biosera, 1% penicillin/streptomycin (P/S), 1 % L-glutamine purchased from Sigma. Trypsin/EDTA (ready to use), hyaluronidase, collagenase, homogentisic acid, L-ascorbic acid 2-phosphate and dexamethasone were purchased from Sigma. PBS was made up in laboratory (PBS: 0.286 M sodium chloride, 5.55 mM potassium chloride, 16.4 mM disodium hydrogen phosphate, 2.94 mM potassium dihydrogen orthophosphate distilled water, pH 7.4 and then autoclaved).

### **2.2.2 Plasticware**

No. 10 Swann Morten disposable scalpels were purchased from Sarstedt. Plasticware was purchased from Sarstedt and BD Falcon.

### **2.2.3 Culture of human osteosarcoma and chondrosarcoma cells**

Human osteosarcoma cells SaOS-2, MG63 & Te-85 were taken from laboratory stocks. C20-A4 chondrosarcoma cells were a kind gift from Dr Mary Goldring (Hospital for Special Surgery, NY, USA). Cells were maintained in 9 cm petri dishes and passaged every 3 days. Cells were cultured to confluence, media removed, washed twice with sterile PBS. 3-5ml of trypsin EDTA was then added to cells and incubated for 5-7mins at 37°C. Trypsin action was halted by addition of 12mls of fresh DMEM containing 10% FCS. This solution was distributed across 3 9cm petri dishes and then had 5mls of fresh DMEM added to each dish prior to being replaced in the incubator. Cells were cultured in a humidified incubator at 37°C in an atmosphere of 95% air and 5% CO<sub>2</sub>.

### **2.2.4 Preparation of HGA stock solution**

HGA stock solution was prepared by dissolving 0.102 g of HGA crystals into 6.07 ml of PBS to give a  $1 \times 10^{-1}$  M stock solution. Solution was then aliquoted out and stored at -80°C for future use.

### **2.2.5 Preparation of HGA supplemented cultures**

Cells were passaged as described previously and then plated out into 6, 12 or 24 well plates depending on the experiment being undertaken. Following passaging one of the dishes of cell suspension was pipetted into a 25ml universal and had 20mls of fresh DMEM added to it. The cell suspension was then vortexed and distributed evenly across the well plates. Following one day to allow cells to become attached to the plasticware HGA medium was

added at one of the following concentrations;  $3.3 \times 10^{-4}$  M,  $3.3 \times 10^{-5}$  M or  $3.3 \times 10^{-6}$  M. The  $3.3 \times 10^{-4}$  M solution was made by taking 9ml of fresh DMEM and placing into a labelled universal, 29.7 $\mu$ l of HGA stock solution was then added to this universal. A serial dilution was then made into another universal containing 9ml of fresh DMEM which then had 1ml added to it from the universal containing the  $3.3 \times 10^{-4}$  M solution. This gave a concentration of  $3.3 \times 10^{-5}$  M. The final concentration was then made by adding 1ml of the  $3.3 \times 10^{-5}$  M solution to another universal containing 9ml of fresh DMEM. Volumes and dilutions were adjusted accordingly depending on which size petri dishes or well plates were being used. Medium on these cultures was changed every 3 days and the supernatants were stored in labelled eppendorfs at  $-80^{\circ}\text{C}$ .

#### **2.2.6 Preparation of ASC stock solution**

L-Ascorbic acid 2-phosphate was prepared by adding 289mg to 10ml of PBS. The solution was aliquoted out and stored at  $-80^{\circ}\text{C}$ .

#### **2.2.7 Addition of ASC to culture plates**

ASC was added to designated cultures at a concentration of 1  $\mu\text{l/ml}$  of DMEM.

### **2.2.8 Preparation of Dexamethosone stock solution**

Dexamethosone was prepared by adding 39.3mg to 1ml of 100% ethanol to give a  $1 \times 10^{-1}$ M solution. This was then made upto 100ml in 100% ethanol and serially diluted to give a final concentration of  $1 \times 10^{-5}$  M solution which was stored at  $-80^{\circ}\text{C}$ .

### **2.2.9 Addition of Dexamethasone to culture**

Dexamethasone stock was added to designated cultures at a concentration of  $10 \mu\text{l/ml}$  of DMEM.

## **2.3 HISTOLOGY**

### **2.3.1 Reagents**

Haematoxylin, eosin, potassium ferricyanide, ferric chloride, nuclear fast red and DPX microscopy mountant were all purchased from VWR. EDTA, chrome potassium sulphate and bovine gelatine were purchased from Sigma. Glass slides and coverslips were purchased from BDH.

### **2.3.2 Fixation**

All tissues were fixed in 10% PBFS containing phenol red indicator solution. Following fixation tissues were placed into 70% ethanol in preparation for histological processing.

### **2.3.3 Decalcification of mineralised tissues**

Following fixation mineralised tissues were dissected to the required size and thickness (<1cm) and deposited into 10% formalin/12% EDTA solution for decalcifying and left until the mineralised tissue was soft enough to bend. Tissues were then passed through three changes of distilled water for a minimum time of 12 hours.

### **2.3.4 Processing of samples for embedding**

Pieces of tissue were removed from fixative, placed through changes of increasing grades of alcohols up to 100% ethanol before being subject to 2 changes of xylene followed by 2 changes of wax. Tissues were removed from molten wax and placed into warmed metallic boats before being submerged in molten wax and then had a microtome chuck placed on top of them. Blocks of tissue were then left to solidify before being removed from their metallic mould and trimmed to give a rhomboidal cutting surface for sectioning on the microtome.

### **2.3.5 Subbing of glass slides**

#### **2.3.5.1 Subbing solution**

- 1) 0.2% bovine gelatine (1mg in 500ml)
- 2) 0.2% chromium potassium sulphate

#### **2.3.5.2 Subbing procedure**

- 1) Dissolve gelatine in warm distilled water (do not heat over 50°C)

- 2) Add chrome sulphate, use the same day
- 3) Treat clean slides with 100% ethanol for at least 2mins.
- 4) Drain for 5mins.
- 5) Stand in subbing solution for at least 1min.
- 6) Drain excess. Cover slides to keep out of dust and dry overnight at room temp.

### **2.3.6 Sectioning of tissues**

5µm sections were cut using a microtome. Ribbons of sections were floated out onto 45°C water in a water bath before being mounted on subbed glass slides and left in the incubator at 50°C overnight.

### **2.3.7 Histological staining of slides**

In preparation for staining slides, were deparaffinised placing the slides in the following solutions for the following length of time:

- 1) Xylene for 5mins
- 2) Xylene for 5mins
- 3) 100% ethanol for 5mins
- 4) 100% ethanol for 5mins
- 5) 90% ethanol for 5mins

6) 70% ethanol for 5mins

7) dH<sub>2</sub>O for 5mins

Stains were prepared as described by Bancroft, specifically as follows:-

#### 2.3.7.1 H&E

1) Sections to water

2) Stain in haematoxylin for 3-5 mins

3) Rinse in 1% HCl solution for <5 seconds

4) Differentiate in running warm water for 3-5mins, or until slides are “blue”

5) Stain in eosin for 3-5 mins

6) Rinse in tap water for <30 seconds

7) Dehydrate through graded alcohols to xylene

8) Mount with DPX

#### 2.3.7.2 Schmorl's

1) 1% aqueous ferric chloride (or sulphate)

2) 1% aqueous potassium ferricyanide

3) Distilled H<sub>2</sub>O

Add the following together:-

1) 37.5 ml of ferric chloride solution

2) 5 ml of potassium ferricyanide solution

3) 7.5 ml of dH<sub>2</sub>O

#### 2.3.7.3 Method

- 1) Sections to water
- 2) Immerse for 5-10mins in Schmorl's reagent
- 3) Wash well in running H<sub>2</sub>O to remove any residual ferricyanide
- 4) Counter stain for 5mins using NFR
- 5) Dehydrate through graded alcohols and xylene
- 6) Mount with DPX

### 2.4 TRANSMISSION ELECTRON MICROSCOPY

#### 2.4.1 Reagents

Gluteraldehyde was purchased from Sigma. Osmium tetroxide solution and Agar 100 resin were purchased from Agar Scientific. Reynold's lead citrate was produced by combining lead nitrate (Agar Scientific) and sodium citrate (Sigma) (see below).

##### 2.4.1.1 Preparation of lead citrate solution

- 1) Boil fresh 18.2 mega Ohm dH<sub>2</sub>O for 10 minutes to remove any CO<sub>2</sub>. Cover with Petri dish and cool for 30 minutes before use.
- 2) Make 10 ml of 1M NaOH using the freshly prepared water.
- 3) Add 30 ml of freshly prepared water to the 1.33g lead nitrate and 1.76g sodium citrate; shake/sonicate for 60 minutes to allow conversion of lead nitrate to citrate.



- 4) Add 8 ml of 1M NaOH; solution should clear, make up to 50 ml with freshly prepared water.
- 5) Store in foil-lined plastic container at 4°C. The stain is stable for up to 6 months; discard if it becomes cloudy.
- 6) Before use, microfuge aliquot at 5,000 rpm for 5 minutes. (1677g)

#### **2.4.2 Preparation of specimens for transmission electron microscopy**

Tissues were obtained from surgery and washed in PBS. Tissues were micro-dissected to give pieces less than 1mm<sup>3</sup>. Tissues were then fixed by immersion in 4% paraformaldehyde with 2.5% gluteraldehyde in 0.1M sodium cacodylate (pH 7.4) overnight. Samples were then washed in 0.1M sodium cacodylate buffer wash pH 7.4 for 5mins. Samples were immersed in 1% osmium tetroxide in distilled water for 1.5hr in a rotator. Samples were then stained with 5% alcoholic uranyl acetate for 3 cycles of 30minutes. Samples were then dehydrated through graded alcohols and infiltrated with Agar 100 resin as listed below:

##### **2.4.2.1 Dehydration at room temperature**

- 1) 50% ethanol for 5mins
- 2) 50% ethanol for 5mins
- 3) 70% ethanol for 5mins
- 4) 70% ethanol for 5mins
- 5) 90% ethanol for 5mins

- 6) 90% ethanol for 5mins
- 7) 100% ethanol (High purity) for 10mins
- 8) 100% ethanol (High purity) for 10mins
- 9) 100% ethanol (High purity) for 10mins
- 10) 100% acetone (high purity) for 5mins
- 11) 100% acetone (high purity) for 5mins
- 12) 100% acetone (high purity) for 5mins

#### **2.4.2.2 Resin infiltration**

- 1) 30% resin / 100% acetone for 1 hour
- 2) 70% resin / 100% acetone for 1 hour
- 3) 100% resin for 1 hour
- 4) 100% resin for 1 hour

Tissues were then placed into a resin mould, labelled and submerged in fresh resin. Resin moulds with tissues were then polymerised overnight in an oven at 60°C overnight.

#### **2.4.3 Sectioning and post staining of tissues in resin blocks**

70 nm sections were cut using a Reichert Ultracut E microtome and post stained using uranyl acetate in 50% ethanol and lead citrate. TEM was performed using an FEI 120kV Tecnai G2 Spirit BioTWIN, images were obtained using digital image capture using SIS Megaview III camera.

## **2.5 SCANNING ELECTRON MICROSCOPY**

### **2.5.1 Reagents**

Tergazyme was purchased from Alconox, Alconox inc, NY, USA. PMMA was purchased from Sigma. Hydrogen peroxide was purchased as stock concentrate from Aristar.

### **2.5.2 Sample processing**

Samples were removed from 70% ethanol and cut into 4mm thick slices using an ethanol cooled diamond saw. Slices were then embedded in PMMA, the block surfaces trimmed and polished, and coated with carbon by evaporation. They were imaged using backscattered electrons (BSE) in a Zeiss DSM962 SEM with external computer control. Images were recorded at 20kV, 0.5nA probe current and 17mm working distance using halogenated dimethacrylate standards to calibrate the electron backscattering (Boyde, 1999). Bone slices were macerated for 18 days in 4% Tergazyme, bacterial pronase enzyme detergent, followed by 29 days in 5% hydrogen peroxide solution (i.e., 6 fold dilution of the Aristar stock concentrate) to remove all cells and normal hyaline cartilage matrix and leave all calcified matrices. After washing and drying, these slices were carbon coated from both sides and imaged using 3D BSE SEM.

### **2.5.3 Fluorescence Light Microscopy**

Direct view stereoscopic fluorescence microscopy was conducted on unstained histology sections and SEM blocks using an Edge 3D microscope fitted with twin Canon digital cameras (Greenberg, 1997).

## **2.6 MURINE EXPERIMENTS**

### **2.6.1 Reagents**

NTBC powder was a kind gift from Swedish Orphan. Sodium bicarbonate ( $\text{NaHCO}_3$ ) was purchased from Sigma. Ultrapure  $\text{H}_2\text{O}$  (18 M $\Omega$  filtered).

### **2.6.2 NTBC Stock solution preparation:** (makes 250 mL sterile 2 mg/mL NTBC stock)

- 1) Dissolve 3g  $\text{NaHCO}_3$  in 30 mL  $\text{H}_2\text{O}$  and place at  $5^\circ\text{C}$  for ~2 hours, vortex until dissolved.
- 2) Add 500mg NTBC to  $\text{NaHCO}_3$  solution and dissolve at  $10^\circ\text{C}$  for ~3 hrs whilst stirring.
- 3) As NTBC dissolves the solution will turn yellow.
- 4) When fully dissolved, add remaining 220 mL  $\text{H}_2\text{O}$  to reach final volume.
- 5) Sterile filter in a laminar flow hood.
- 6) Wrap in foil and store in refrigerator.

### **2.6.3 NTBC working solution preparation**

- 1) Autoclave 1 L  $\text{H}_2\text{O}$  and refrigerate overnight.
- 2) Place autoclaved  $\text{H}_2\text{O}$  and NTBC stock solution into a sterile laminar flow hood.
- 3) Add 8 mL of 2 mg/mL NTBC stock to 1L  $\text{H}_2\text{O}$  and cap tightly before removing from hood.

#### **2.6.4 Mouse care**

C57/Bl6 FAH  $-/-$ , HGD  $+/-$ , mice were housed in the Grompe laboratory at Oregon Health & Science University (in accordance with the Institutional Animal Care & Use Committee) and maintained on NTBC (Nitisinone™) for periods of time up to two months following birth, NTBC was then withdrawn.

The time periods of withdrawal were as follows:-

- 11 months off NTBC
- 2 weeks off NTBC
- 2 days off NTBC
- 1 day off NTBC

Mice were sacrificed by exposure to CO<sub>2</sub>. Sacrificed animals were dissected as described below to ensure standard harvest procedures

#### **2.6.5 C57/Bl6 FAH $-/-$ , HGD $+/-$ dissection**

##### **2.6.5.1. Skin**

- 1) Remove ears by snipping skin starting at the top of the head in between each ear, and tracing around each ear and fix.
- 2) Cut the skin around the neck and peel off over the eyes and nose, cutting at nose if necessary.
- 3) Cut the skin down the back of the mouse to the base of the tail.

- 4) Stretch the skin out to the sides of the mouse, and peel off the skin over each limb.
- 5) Detach skin entirely and fix.

#### 2.6.5.2. Abdomen

- 1) Lift belly skin and cut up to sternum and down each side following the ribcage.
- 2) Remove the viscera (guts), cutting just above stomach to leave oesophagus intact, and fix.

#### 2.6.5.3. Thorax

- 1) Cut ribs on each side up to forelimb armpits (clamshell) and across neck above sternum and fix.
- 2) Remove/tease apart white tissue on top of heart. Lift up heart and tease free from surrounding tissue by cutting from below. Cut heart completely free above aortic arch (leaving arch intact) and wash in PBS to remove excess blood before fixing.

#### 2.6.5.4. Limbs

- 1) Pinch top of lower limb close to spine and cut leg free by cutting into pelvic bone, to protect the head of the femur. Fix leaving muscle attached.
- 2) Repeat with 2<sup>nd</sup> lower limb, but remove muscle from detached leg. Sever bones above and below knee joint to allow fixative penetration and formalise.

#### 2.6.5.5. Head and Trachea

- 1) Open jaw with scissors and cut through cheek muscle and bone to free lower jaw and tongue. Cut toward abdomen, pulling lower jaw down till tracheal passage visible. Cut upper

head away and fix. Carefully lift and cut away neck muscle till trachea exposed for fixative penetration.

2) Sever spine just below remaining ribcage and fix thorax including attached upper limbs, trachea and lower jawbone/tongue.

3) Cut away muscle close to spine on lower body including attached tail, and fix.

Each body part was formalin fixed for 1 day before removing from solution and wrapping in formalin soaked gauze, and placing in ziplock bag. Each bag should contain all the body parts from one mouse and labelled with treatment, date of dissection and initialled. Samples were then shipped to Liverpool for analysis.

## **2.7 ssNMR**

### **2.7.1 Reagents**

4mm zirconia rotors and Bruker AVANCE-400 9.4 Tesla wide bore spectrometer were purchased from (Bruker, Karlsruhe, Germany).

### **2.7.2 Method**

Ochronotic and nonochronotic cartilage samples were prepared for NMR by grinding under liquid nitrogen in a pestle and mortar to a consistency resembling that of a fine powder. The highly pigmented ochronotic cartilage was noticeably harder to grind. After brief drying under vacuum to remove surface moisture, samples were packed into 4 mm outer diameter zirconia rotors (Bruker, Karlsruhe, Germany) and  $^{13}\text{C}$  NMR spectra obtained using a Bruker AVANCE-400 9.4 Tesla wide bore spectrometer equipped with a standard dual channel broad band probe, at a magic angle spinning

rate of 12.5 kHz and radio frequencies of 400.1 MHz ( $^1\text{H}$ ) and 100.5 MHz ( $^{13}\text{C}$ ).  $^{13}\text{C}$  signal intensity was enhanced using standard cross polarization (CP) MAS techniques ( $^1\text{H}$   $\pi/2$  pulse length 2.5  $\mu\text{s}$ ,  $^1\text{H}$  cross polarization field 70 kHz,  $^1\text{H}$ - $^{13}\text{C}$  cross-polarization contact time 2.5 ms, broadband TPPM15 decoupling during signal acquisition at a  $^1\text{H}$  field strength of 100 kHz, recycle time 2 s, typical number of scans accumulated per spectrum ca. 20,000). Chemical shifts were referenced to the methylene signal from solid glycine at 43.1 p.p.m. relative to tetramethylsilane at 0 p.p.m.

## **2.8 MECHANICAL TESTING**

### **2.8.1 Mechanical testing protocol**

Unfixed tissues were washed in sterile PBS immediately following surgery. Cubes of articular cartilage were dissected from the articular surface. Cartilage cubes were removed from the sample as close to the subchondral bone as possible and were then measured. Samples were stored overnight at 4°C in pH 7.4 PBS. Wet samples were placed on a 9cm petri dish. Excess saline was removed from the surface and around the periphery of the tissue. Samples were mechanically tested by compression on a Nene M5 tensile tester using Nene software with a 500N load cell. Samples were loaded at a rate of 0.5mm/minute. Data was recorded as load-displacement. The stress strain curves were plotted for each sample and Young's modulus calculated.

### **2.8.2 Statistical analysis**

Statistical differences were determined by applying Kruskal Wallis with Dunn's Multiple Comparison test using Graphpad Prism 5 software.



## **2.9 PATIENT DEMOGRAPHICS AND SYMPTOMS**

<u>Sample</u>	<u>Age</u>	<u>Sex</u>	<u>Joint</u>	<u>Symptoms prior to removal</u>	<u>Sample characteristics</u>
AKU1	59	M	Hip	Chronic kidney disease, previous Achilles rupture and muscle rupture. Previous joints replaced, 1 <sup>st</sup> age 55.	Full depth blanket pigmentation of articular cartilage.
AKU2	53	M	Knee	Previous surgeries, Diagnosed aged 16.	Patchy surface pigmentation and extensive in deep zone.
AKU3*	59	M	Hip	Both knees previously replaced. Eye pigmentation. Prostate stones.	Patchy absence of cartilage from the articular surface and extensive full depth pigmentation of remaining articular cartilage.
AKU4	46	M	Knee	Previous hamstring tear. No previous joint replacements. Ear pigmentation.	Faint pigmentation close to the subchondral junction, absence of pigmentation from the middle, superficial and articular layers.
AKU5	58	F	Knee	Previous spinal surgery related to AKU. Diagnosed age 54	Extensive pigmentation of femoral condyles, particularly in the central regions of both condyles, with full depth pigmentation in these areas. Peripheral to these regions; pigmentation at subchondral boundary and into middle zone, but absent from superficial and articular surface.
AKU6	69	F	Knee	3 previous joint replacements, L Knee, L shoulder & L hip.	Dense pigmentation of condyles, particularly medial condyle, which had dark fissures in the surface. Cartilage had full depth pigmentation. Lateral condyle showed patchy pigmentation, located at the subchondral boundary and into middle zone.
AKU7	60	F	Hip	Previous fracture, 2 arthroscopies, previous hamstring and tendon tears. Cervical, lumbar & sacroiliac joint disease. Joint pain in both knees, shoulders, hands and feet, L hip & R ankle. Eye & ear pigmentation. No previous joints replaced.	Loss of articular cartilage with a thin rim remaining around the equator, this showed full depth ochronotic pigmentation.
AKU8	53	M	Knee	Previous arthroscopy, renal stones, previous fracture, pain in both knees. Lumbar and sacroiliac joint disease. Ear pigmentation. No previous joints replaced.	Dense central pigmentation of condyles, which was less at the peripheral surfaces. Pigment was present in full cartilage depth at contact surfaces. At the peripheral surfaces pigment was seen at the subchondral boundary and deep zone.
AKU9*	61	M	Hip	Both knees and hip previously replaced. Eye pigmentation. Prostate stones.	Extensive loss of articular cartilage, a small thin amount was left on the periphery of the head, all that remained was heavily pigmented.

OA1	51	F	Knee	Previous partial medial menisectomy. X-Ray showed mild osteoarthritis in the medial tibio-femoral compartment and in the superior aspect of the patello-femoral compartment. Joint effusion noted. No intra-articular bodies. Normal patello-femoral alignment. MRI demonstrated degenerate meniscal remnant. Subchondral oedema and marginal osteophyte formation.	
OA2	74	M	Knee	End stage medial tibio femoral arthrosis noted on the left with varus deformity and severe lateral PTFJ OA with lateral patella migration noted. Old healed proximal fibular diaphyseal fracture noted on this side.	
OA3	62	M	Knee	Bilateral end stage medial tibiofemoral OA was noted with severe lateral tibiofemoral and patellofemoral arthrosis. There was a large amount of marginal eccentric bone formation on the trochlear and patellae bilaterally with a 28mm calcified chondral body noted within a right popliteal cyst. Bilateral genu varus was present.	

Table 2.1: *A table demonstrating the demographics and symptoms of patients involved in this study.*

*\*Denotes same patient*

### **3. Macroscopic presentation of AKU joint samples.**

### **3.1 INTRODUCTION**

The first objective of this Thesis is to document the presentation of ochronosis in joint replacement samples from AKU patients. Joint replacement for ochronotic osteoarthropathy in alkaptonuria is common and is the most effective treatment at alleviating joint pain in patients with this condition. There are numerous case reports detailing the end stages of the disease, all with varying severity and presentation. The clinical presentations are often similar across patients; with darkening of the urine easily identifiable if AKU has already been made. The presentation of joint pain in many cases is generally earlier than would be expected of someone who had joint degeneration associated with osteoarthritis, although the radiographic and clinical symptoms are similar (Bálint 2000 & Lagier 2006). The presentation of individual cases is often accompanied by a review of literature on the disorder. Most reports are generally descriptive of the patients' presentation and condition of the surgical specimen and any interesting abnormalities that arise that may in part be attributed to the underlying ochronosis. In surgical specimens it is common for large areas of cartilage to be pigmented, and in places missing from the surface of the bone. There is usually little description of involvement of bone pigmentation, although pigmentation of cells has been seen. Even in cases where multiple joints have been replaced, there is little comparison between these joints to distinguish common regions of pigmentation in these patients. (Demir 2003 & Carrier 1990). Determining regions of pigmentation that are common across surgical samples may be indicative of regions predisposed to early onset, or the most rapidly progressive pigmentation.

This study was aimed at detailing and describing the macroscopic presentation of ochronosis in specimens obtained from patients with AKU undergoing joint replacement surgery due to ochronotic osteoarthropathy. Where feasible, samples, were photographed during surgery, then on return to the laboratory environment in order to obtain an overview of distribution of

pigmentation, across a sample, across the AKU population in this study and from within the same patient where possible.

### **3.2 RESULTS**

<b>Sample</b>	<b>Age</b>	<b>Sex</b>	<b>Tissue</b>
AKU3	59	M	Hip
AKU5	57	F	Spine
AKU6	59	M	Hip
AKU8	42	M	Arthroscopy
AKU9	46	M	Knee
AKU10	58	F	Knee
AKU11	69	F	Arthroscopy
AKU12	69	F	Knee
AKU13	59	F	Hip
AKU14	65	M	Hip revision
AKU15	53	M	Knee
AKU16	61	M	Hip
AKU18	70	F	Knee
AKU19	59	F	Knee
AKU21	51	F	Knee

Table 3.1:- *Demographics of patient with AKU from whom samples collected as part of this project*

<b>Average. age of hip replacement (yrs)</b>	<b>61.6</b>
<b>Average. age of knee replacement (yrs)</b>	<b>56</b>
<b>Average. age of male hip replacement (yrs)</b>	<b>59.6</b>
<b>Average. age of female hip replacement (yrs)</b>	<b>64.5</b>
<b>Average. age of male knee replacement (yrs)</b>	<b>49.5</b>
<b>Average. age of female knee replacement (yrs)</b>	<b>59.25</b>

Table 3.2:- *Average age of patient joint replacements from the patient samples obtained in this project.*

### **3.2.1 Ochronosis in hips**

In order to understand the presentation of ochronosis in the hip joint, 5 surgically resected femoral heads and their accompanying tissues were examined. Samples were photographed and documented from a pathological point of view.

#### **AKU3**

A 59 year old male with known alkaptonuria attended surgery for a left THR. The femoral head displayed normal spherical shape over the majority of the head, but displayed abnormal thickening and shape at the neck of femur, where this region was as wide as the equatorial regions of the head of femur. The whole articular cartilage surface was ochronotic. There was a large osteophyte located on the neck of the femur and this in parts displayed ochronotic darkening consistent with that seen in the articular cartilage. Areas overlying the greater trochanter and parts of the joint capsule displayed dense ochronosis (Fig.3.1).

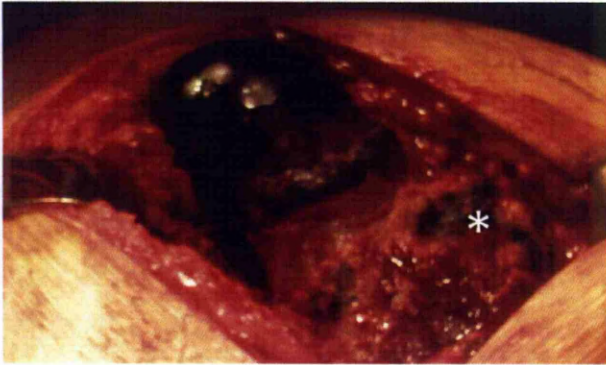


Figure 3.1:- *Photograph showing the macroscopic appearance of AKU3 femoral head at the time of surgery. The black colouration is ochronotic pigment which is located uniformly across the cartilage on the femoral head and sporadically on the soft tissues (\*).*

Following surgical removal the femoral head was sawn into an anterior and posterior half through the fovea. Consistent with the macroscopic observation of the whole hip, the cut surface showed full depth pigmentation of the articular cartilage, from the subchondral bone through to the articular surface. There was thinning of the cartilage superior and inferior to the fovea and also on the lateral aspect of the femoral head towards the neck of the femur. The neck of the femur showed a diameter similar to that of the widest point of the head of the femur. This was particularly easily identified on the lateral aspect. The cut surface also showed that there was no comparable ochronotic pigmentation in the bone matrix as to that seen in the cartilage matrix. However there were darker aspects of the bone matrix compared to other regions. These darker regions appeared in the areas that would be consistent with transmitting the highest loading from the pelvis down into the neck of the femur and onto the diaphysis.

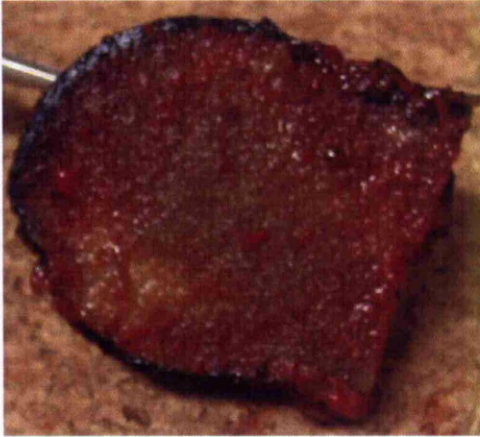


Figure 3.2:- *Photograph showing the macroscopic appearance of the internal cut surface of AKU3 femoral head at time of surgery.*

#### AKU6

A 59 yr old male with known AKU presented for a right hip replacement due to ochronotic arthropathy.

#### AKU13

A 59 yr old female attended hospital for a left total hip replacement. The femoral head showed a large area of denuded bone around the superior surface. There were numerous osteophytes seen in this region which displayed no evidence of ochronosis. The equator of the femoral head showed dense ochronosis of the articular cartilage, although it was clearly evident that the cartilage layer in this region was extremely thin. The descent from the equator of the femoral head down to the neck of the femur showed a gradual loss of ochronosis in the cartilage resulting in regions which then demonstrated no macroscopic pigmentation. There was little pigmentation of the surrounding capsular tissues. Observations of the acetabulum demonstrate that the acetabular labrum was densely pigmented. There were peripheral regions, away from the socket that showed less pigmentation, but were still



noticeably darker in colour. Macroscopic observations of the neck of femur demonstrated the presence of pigment beneath the periosteal surface. The internal cut surface of the femoral head showed darkening of the bone matrix, suggestive of ochronotic pigment located in the bone domain. This darkened matrix ran from the fovea obliquely across to the neck of the femur.

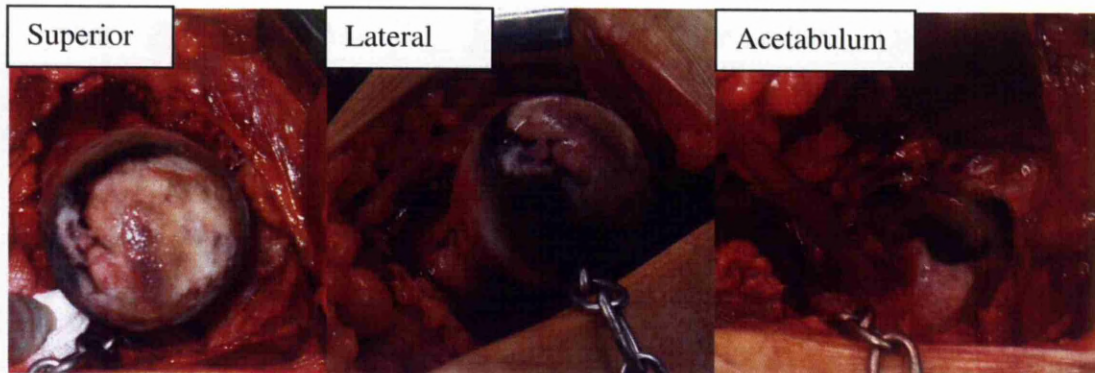


Figure 3.3:- Photographs showing the superior view (left), lateral view (middle) of AKU13 femoral head at time of surgery. Photograph showing the macroscopic appearance of the acetabulum at time of surgery (right). All tissues demonstrate ochronosis in some region.

#### AKU16

A 61 year old male with known AKU attended surgery for a left THR. The presentation of the patient was due to a rapid onset of progression, from normal to pain, discomfort and limited range of motion in the hip in the period of 18 months since attending hospital previously for his right THR. Once removed the femoral head was sawn into two halves. Articular cartilage was present in places (predominantly below the equator) and was completely full of ochronotic pigment. There was no unpigmented articular cartilage. The cartilage, although pigmented demonstrated a smooth articular surface and was only thinned towards the periphery. The halves both displayed numerous pathological features. The most striking of which were the deformed shape of the femoral head, the posterior aspect of which

appeared to have collapsed and flattened as part of the arthropathic remodelling process. On the superior and posterior aspect of the head the articular was large regions of denuded bone. On parts of this region were numerous osteophytes, some of which had grown over the ochronotic articular cartilage although the osteophytes showed no sign of ochronotic pigment (Figure 3.5). In amongst the osteophytes and on the denuded area were numerous minute pieces of ochronotic cartilage, these appears to be impacted into the bone surface. The femoral neck appeared normal, with no suggestion of widening. The synovial and capsular tissues were densely ochronotic and fibrosed. In places these tissues had spread over the surface of the ochronotic articular cartilage, progressing up from the region of the neck of femur. The acetabulum displayed dense ochronosis. The cut surface of the femoral head demonstrated a lack of pigmentation comparable to that seen in the articular cartilage. There were however darker regions of bone matrix and periosteum.

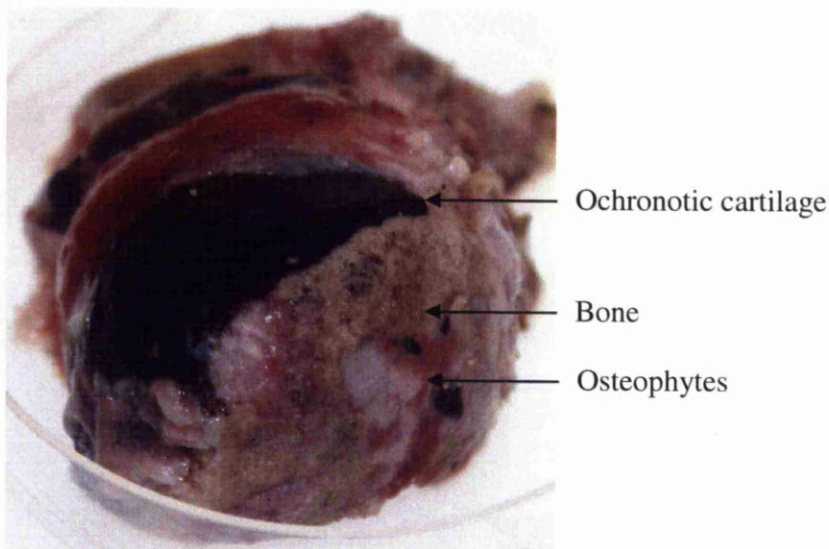


Figure 3.4:- *Photograph showing the macroscopic appearance of the superior aspect of half of the AKU16 femoral head following surgical excision.*

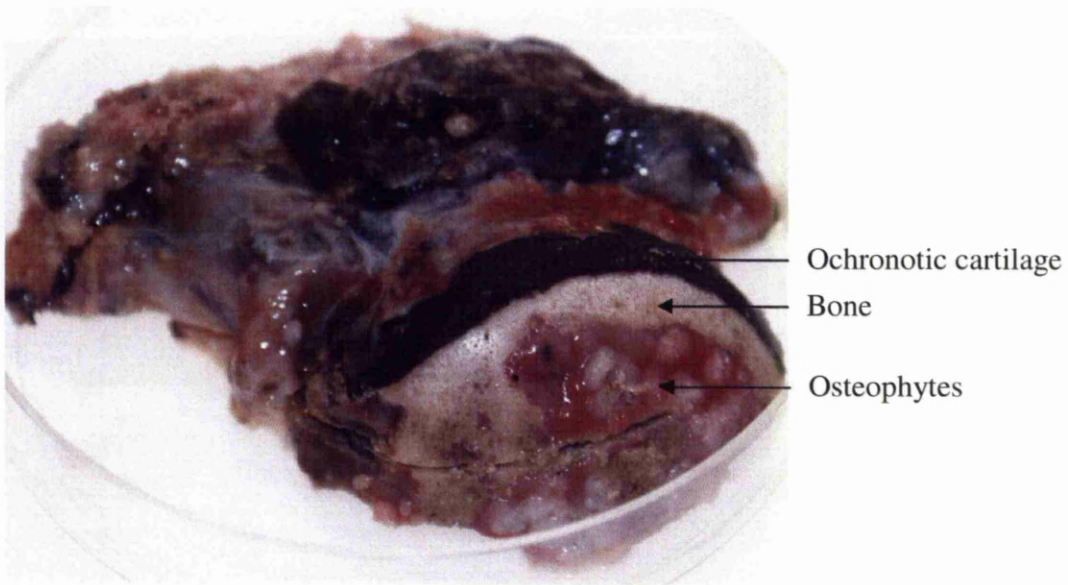


Figure 3.5:- *Photograph showing the macroscopic appearance of superior aspect of the AKU16 femoral head following surgical excision. Note numerous small osteophytes located on the bone on the superior aspect.*



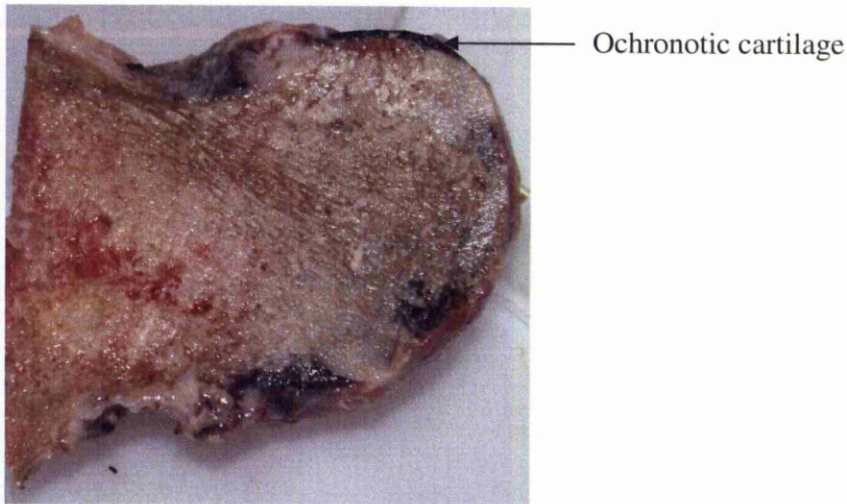


Figure 3.6:- Photograph showing the macroscopic appearance of internal cut surface of the midline of the AKU16 femoral head. Pigmented articular cartilage can clearly be seen located on parts of the femoral head and pigmentation can be seen located in the bone domain in parts. Note the abnormal shape of the cross section as a result of aggressive remodelling. Pigmentation also appears to be in the periosteum in the surface towards the top of the image.

### AKU18

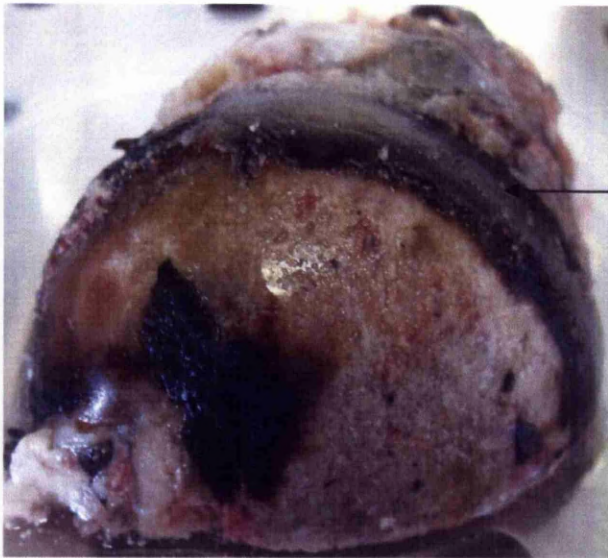
A 70 year old female with known AKU attended surgery for a right THR. The femoral head demonstrated a normal spherical shape. There was cartilage present around the equator and down to the neck of the femur. All cartilage was ochronotic, with regions appearing extremely thin. Superior to the equator there were large regions of denuded bone, on this region were numerous small osteophytes and numerous minute pieces of ochronotic cartilage that appeared to have been impacted into the exposed bone surface. In the fovea of the hip the insertion of the *ligamentum teres* showed dense ochronotic colouration. The neck of femur showed no change in shape. It was also covered in capsule, some of which was heavily ochronotic, some areas darker in appearance and some showing normal colouration. The

periosteum of the neck of femur showed colouration, appearing more ochronotic than the trabecular matrix underlying it.



*Ligamentum Teres*

Figure 3.7:- A photograph showing the macroscopic appearance of superior view of AKU18 femoral head following surgical excision. Note the pigmentation of the ligamentum teres in the fovea.



*Ochronotic cartilage*

Figure 3.8:- A photograph showing the macroscopic appearance of the superior articular surface of AKU18 femoral head.

### **3.2.2 Ochronosis in knees**

#### **AKU9**

A 46 yr old male with known AKU attended hospital for a left TKR. Observations of the tibial plateau demonstrated darkened appearance of central regions of the medial plateau; similar presentation was seen on the lateral plateau. Away from the central load bearing areas pigmentation was difficult to identify with the articular cartilage looking normal. On the medial plateau there were small abrasions on the articular cartilage surface around the contact points, correlating with the densest ochronotic pigmentation. There were no similar abrasions seen on the lateral plateau. There was distinct pigmentation present within both the lateral and medial menisci. The pigmentation in the menisci appeared beneath the surface with the articular edges appearing free from pigment. A cross sectional observation of the menisci revealed that the pigmentation in the meniscus was in the centre with the periphery of the cross section appearing free from pigment. The densest pigmentation was seen in the medial meniscus on the anterior surface. Macroscopic observations of the cut underside surface of the tibial plateau showed a slight darkened appearance in the medial side within the bone matrix. There was no pigmentation consistent with that seen in the cartilages.

The cruciate ligaments demonstrated ochronosis, appearing slightly darker in colouration, suggesting deep pigmentation with absence of pigment at the external surfaces. There was also a large ochronotic body present in the soft tissues of the infrapatella bursa. This was solid in consistency with fibres of ochronotic tissues interspersed with non-ochronotic regions. The femoral condyles displayed a spectacular distribution of pigment, with regions free from ochronosis, to areas which were dense with pigmentation. The ochronotic regions correlated with the main articular contact points of both the medial and lateral condyles. Towards the periphery of these regions the pigmentation was not as evident and disappeared

into areas which showed no pigmentation at all. The surfaces of the condyles, even in regions which were showing underlying pigmentation showed no notable degenerative changes. The only exception to this was the posterior surface of the patella. This displayed a band of ochronotic pigmentation running horizontally in the articular cartilage. In the middle of the patella there was a large lesion, which showed dark ochronotic pigmentation and a large unpigmented osteophyte. The cut surface of the underside of the patella demonstrated dark ochronosis, suggesting the presence of pigmentation in the bone matrix.

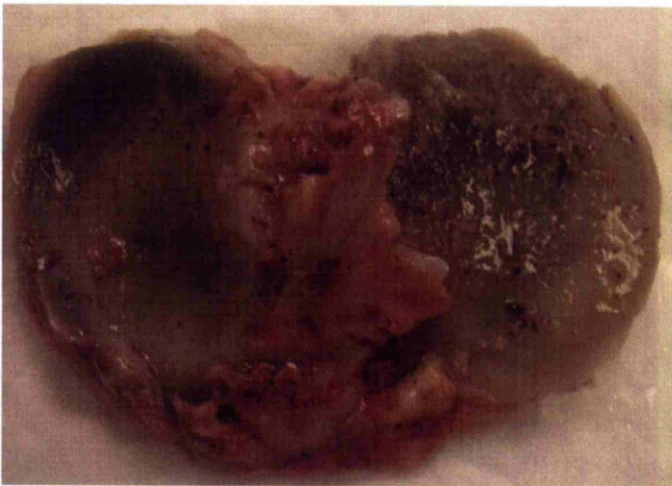


Figure 3.9:- A photograph showing the macroscopic appearance of the articular surface of the AKU9 tibial plateau. Pigmentation is dark in appearance and not present in all cartilage.





Figure 3.10:- A photograph showing the macroscopic appearance of the posterior articular surface of AKU9 patella. A large lesion is seen with dense ochronosis around its periphery.



Figure 3.11:- A photograph showing the macroscopic appearance of ochronotic loose body removed from AKU9. This body shows large regions of dense ochronotic fibres within it.

#### AKU10

A 58 year old female with known AKU attended hospital for a right TKR. Examination of the distal femur demonstrated dusky articular cartilage across all regions of the articular surface. Periphery of the distal femur showed numerous periarticular osteophytes which did not demonstrate any noticeable ochronotic pigmentation. On the medial femoral condyle was a large lesion which measured 4cm in length and 1.5cm in width. In comparison the lateral femoral condyle demonstrated less pigmentation with only focal regions of dense pigmentation. The posterior surface of the patella showed large regions of denuded bone, with only a small rim of pigmented articular cartilage present around the periphery.



Numerous osteophytes were seen on the posterior surface. Beyond this rim of cartilage numerous periarticular osteophytes were present, these displayed no ochronotic pigmentation. Examination of the menisci demonstrated a dusky ochronotic appearance to these structures. The anterior surface displayed dense pigmentation whilst there was no pigmentation at the surface of the other sides. However, the rest of the menisci had a dusky colouration to it, appearing to be manifest from deposition deeper in the tissues.

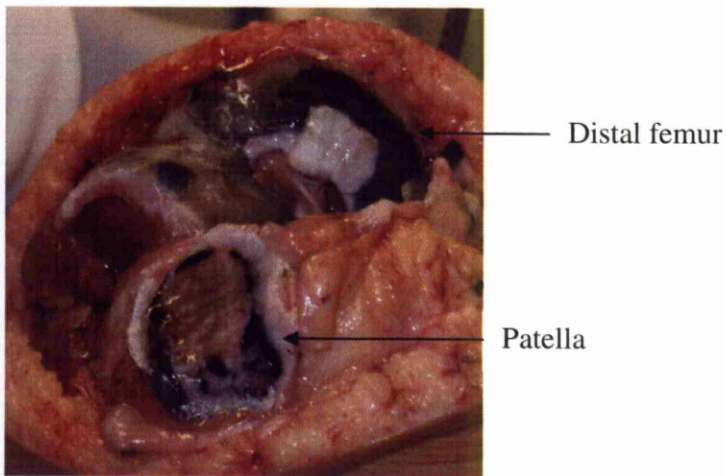


Figure 3.12:- A photograph showing the macroscopic appearance of right distal femur of AKU10 during TKR surgery. Note the large lesion in the medial femoral condyle. The posterior surface of the patella shows a rim of normal and then ochronotic cartilages surrounding an area of denuded bone.

### AKU12

A 69 yr old female attended hospital for a right total knee replacement. The cartilage covering the medial aspect of the tibial plateau showed a dusky appearance across the majority of the surface. The medial weight bearing aspect showed the darkest pigmentation with lighter pigmentation towards the periphery. This presentation was also evident on the lateral plateau. The meniscus of the medial side was snapped off during surgery, but

displayed dense ochronotic pigmentation within the whole structure. There were only the peripheral surfaces that failed to display pigmentation. The lateral meniscus displayed dense pigmentation throughout with only the external edges failing to show pigmentation. The lateral meniscus was also damaged during the surgery, with it fracturing in half, dividing it into an anterior and posterior half. The soft and connective tissues, including the cruciate ligaments also displayed ochronotic pigmentation in a patchy presentation.

Dissection of the tibial plateau into an anterior and posterior half revealed the macroscopic distribution of pigment through the articular cartilages. There were large differences between the presence and distribution between the lateral and medial sides. The medial side demonstrated pigmentation of the articular cartilage from the subchondral bone almost to the full depth of the articular cartilage. The pigmentation was absent from the most medial aspect. There was dense pigmentation in the cartilage overlying the intercondylar eminence. On the lateral aspect there was almost full depth ochronosis of the cartilage, except in the most lateral aspect. There was also some apparent damage to the cartilage in the medial aspect of the tibial plateau, this appeared lesion-like in presentation, similar to the lesions that are observed in osteoarthritis, although it did not extend through to the subchondral bone, with the damage appearing in the superficial and medial zone.

The posterior aspect of the patella showed dense ochronotic pigmentation in places. These were intermittently dispersed between areas of exposed bone. The pigmented cartilage remained predominantly on the superficial and medial surfaces. There was numerous osteophytes present, the largest of which was on the inferior medial aspect and was unpigmented. In the centre of the lateral half of the patella there was also a smaller unpigmented osteophyte. On the underside of the patella there appeared to be dense ochronosis within the bone matrix on the lateral aspect.

The femoral condyles also displayed a large variation in the presence of ochronotic pigment, some regions were completely pigmented and others appeared macroscopically unaffected by pigment. In particular the medial condyle showed dense black pigmentation on the medial aspect with regions where articular cartilage was missing from the surface. The pieces of synovium which were obtained showed variation in pigmentation, with some areas showing dense ochronosis and other regions appearing macroscopically unaffected.



Figure 3.13:- A photograph showing the macroscopic appearance of the tibial plateau of AKU12 following its surgical excision and removal of a 5mm slice through the midline. Note the dense ochronosis of the meniscus that is still attached.

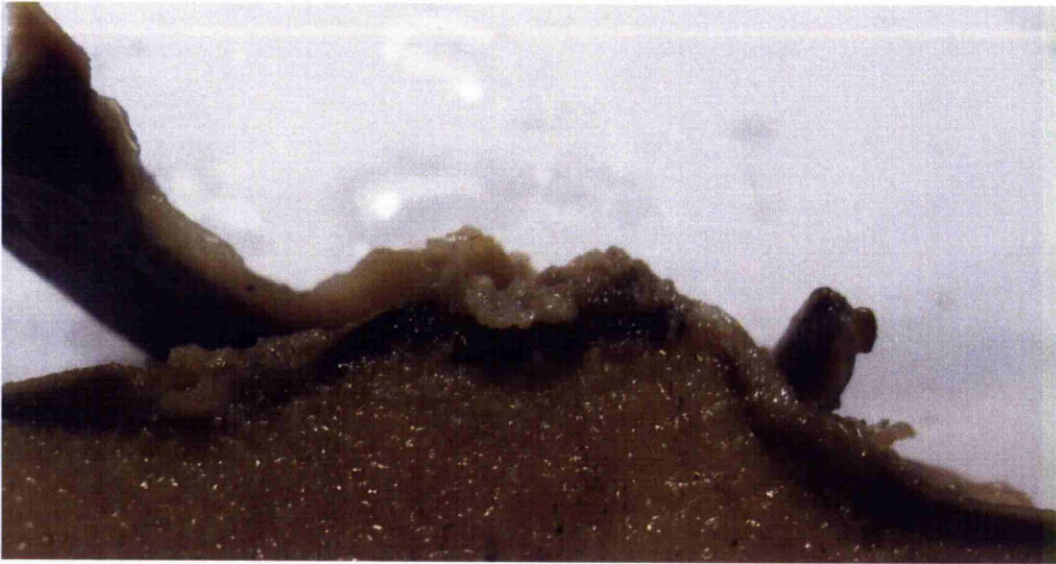


Figure 3.14:- A photograph showing the macroscopic appearance of internal cut surface at the midline of AKU12 showing distribution of pigment through the cartilage. Pigmentation appears to be more prevalent in the deep cartilages.



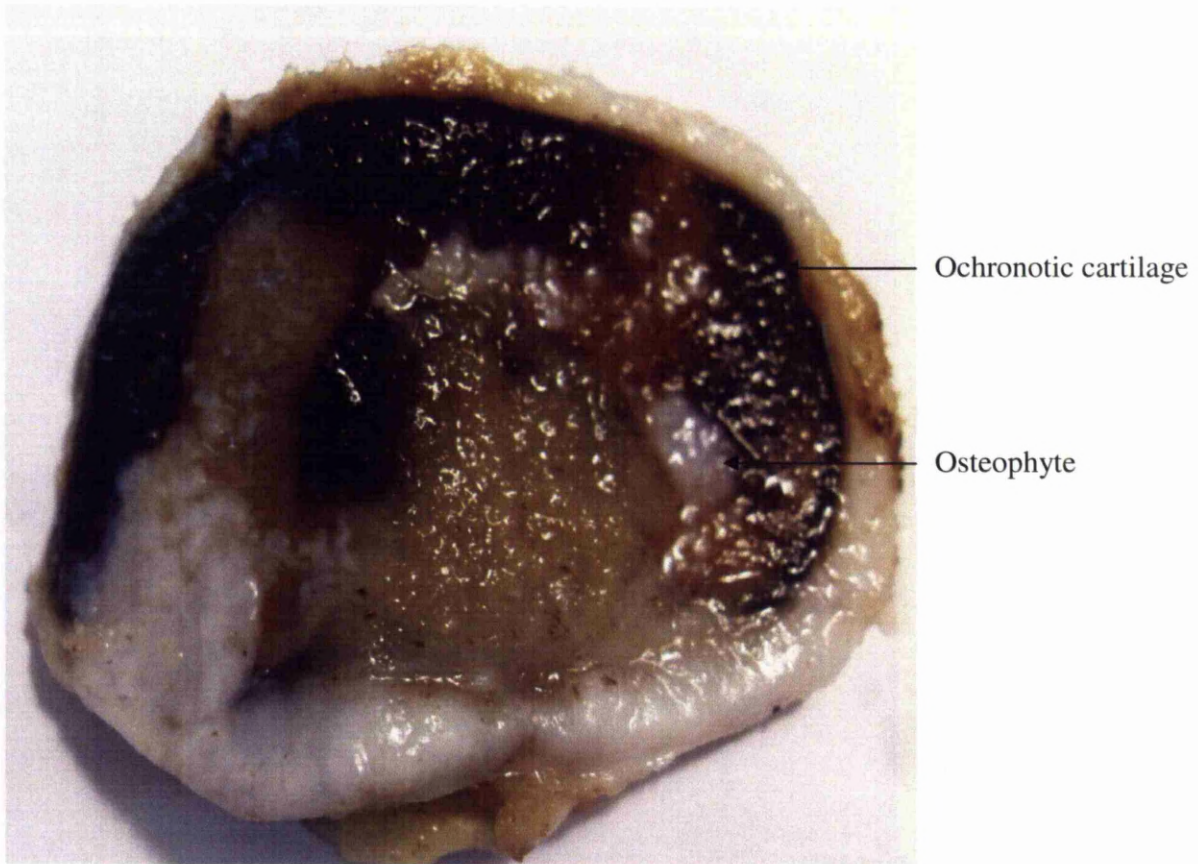


Figure 3.15:- A photograph showing the macroscopic appearance of the posterior articular surface of the patella from AKU12 sample. Note the ochronotic, non-ochronotic and absent cartilage.

### AKU15

A 53 year old male with known AKU attended surgery for a left total knee replacement. The tibial plateau demonstrated dense regions of ochronosis on both the medial and lateral sides. The heaviest ochronosis was seen in the centre of the medial tibial plateau and on the lateral plateau, which showed a densely uniform dark colouration. Pieces of capsular and soft tissue that were still attached to the plateau displayed little evidence of ochronosis when compared to the articular cartilage. The posterior femoral condyles both showed a degree of pigmentation. The lateral condyle was much more severely pigmented, with a dark uniform

pigmentation across the whole of the surface; the peripheral regions appeared normal and white. The articular surface of this region appeared topographically normal, with no evidence of damage to the surface. The medial condyle was less pigmented, with approximately half the surface showing ochronotic pigment. The peripheral surfaces showed large osteophytes, which were not pigmented. The remaining chamfers from the lateral and medial sides displayed a similar distribution of pigment seen on the tibial plateau and the posterior condyles, with the lateral side being more widely affected and demonstrating the most ochronosis. Both lateral and medial sides displayed little in the way of damage to the articular surfaces, other than the presence of the ochronotic pigment in the tissue. The macroscopic distribution of pigment in the articular cartilage was seen as full depth in the lateral side. Medially the regions where macroscopic pigmentation was seen showed almost full depth pigmentation. As progression to non-pigmented regions was made the distribution of pigment was associated with the deeper cartilages. There was no evidence of pigmentation at the articular surfaces without it also being present in the deeper zones. The menisci showed regions of dense ochronotic pigmentation. The lateral meniscus showed a more uniform ochre colouration than that of the medial. The medial meniscus was also much smaller than the lateral, both in size and diameter. The pigmentation in the menisci was present through the middle of the structure, with little in the way of pigmentation present towards the insertions, these appeared macroscopically normal. The ACL showed no macroscopic ochronosis. There was a loose body removed from the joint which showed dense regions of ochronosis within the tissue. The mass was extremely hard, both in regions with and without ochronotic material present.



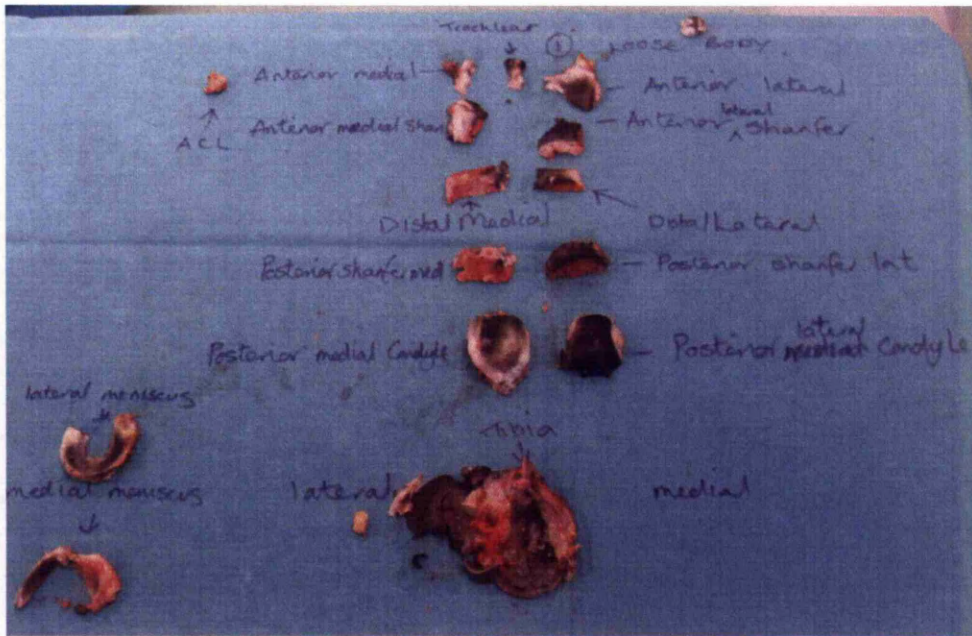


Figure 3.16:- A photograph showing the macroscopic appearance and anatomical distribution of the pieces of AKU15 surgically resected specimen

#### AKU19

A 59 year old female with known AKU attended surgery for a left TKR. The tibial plateau showed regions of dense ochronosis. The medial plateau was dark in colouration with only the very periphery showing any obvious white cartilage colouration to it. The lateral plateau was more severely affected by ochronosis than the medial aspect. The central part of the lateral side showed denuded bone, surrounded by a dark rim of ochronotic cartilage. Radiating out from this rim was less pigmented cartilage, but this was not possible to identify any unpigmented cartilage on the lateral articular surface. Both menisci showed dense ochronosis with only the outer most regions showing the absence of pigmentation. The insertions of the menisci also showed very little in the way of pigmentation. The femoral condyles display regions of dense pigmentation, particularly the lateral condyles. There was a large lesion on the lateral condyle where denuded bone and a large non-pigmented osteophyte

could be seen growing over the pigmented articular cartilage. There was only non pigmented cartilage present on the most lateral aspect of the lateral condyle. On the lateral aspect, the lateral epicondyle displayed dense ochronosis of the overlying fascia. The patellar surface of the distal femur showed large regions of denuded bone, particularly on the lateral side. The medial condyle was pigmented across all pigmented surfaces, the only region that showed no pigmentation was the most medial aspect of the cartilage. On the medial condyle there was a large fissure, approximately 2cm in length, running through the midline. The synovial and capsular tissues displayed patchy ochronosis. There was no obvious ochronosis of the adipose tissues surrounding the joint. The posterior surface of the patella showed large areas of denuded bone in the centre, with a rim of dark ochronotic cartilage surrounding the denuded area. There were large osteophytes at the periarticular regions of the patella. The denuded bone also showed numerous osteophytes overlying parts of the rim of ochronotic cartilage.

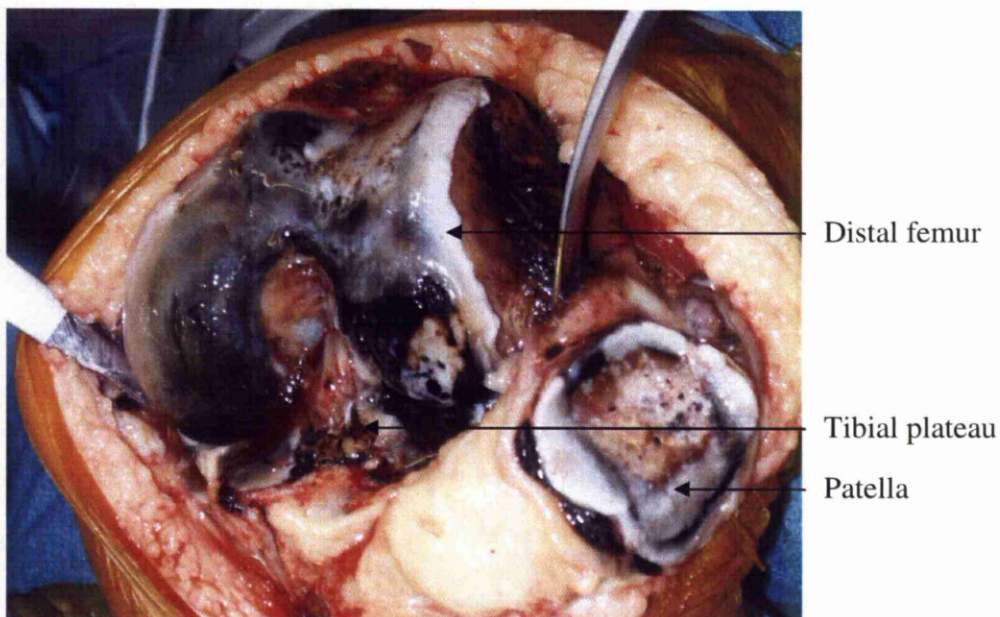


Figure 3.17:- A photograph at time of surgery showing the anatomical distribution of pigment across the knee joint of the AKU19 specimen. Note the pigmentation of the fascia overlying the periosteal surface on the lateral aspect.



AKU21

A 51 year old female with known AKU attended surgery for a right TKR. The tibial plateau displayed regions of dense ochronosis. The medial plateau had large regions of denuded bone demonstrating no signs of ochronosis. There was a densely ochronotic region at the anterior medial aspect of the intercondylar eminence. On the lateral aspect there was a dusky appearance across the entire articular surface, with densely ochronotic regions at the anterior region. The femoral condyles showed regions of dense ochronosis at the midline and the peripheral regions demonstrated less pigmentation. The posterior surface of the patella showed dense degeneration. The periarticular surface showed large osteophytes; internal to this was a dense rim of ochronotic cartilage. The central part of the patella consisted of denuded bone with numerous osteophytes, which in parts were overlying ochronotic cartilage.

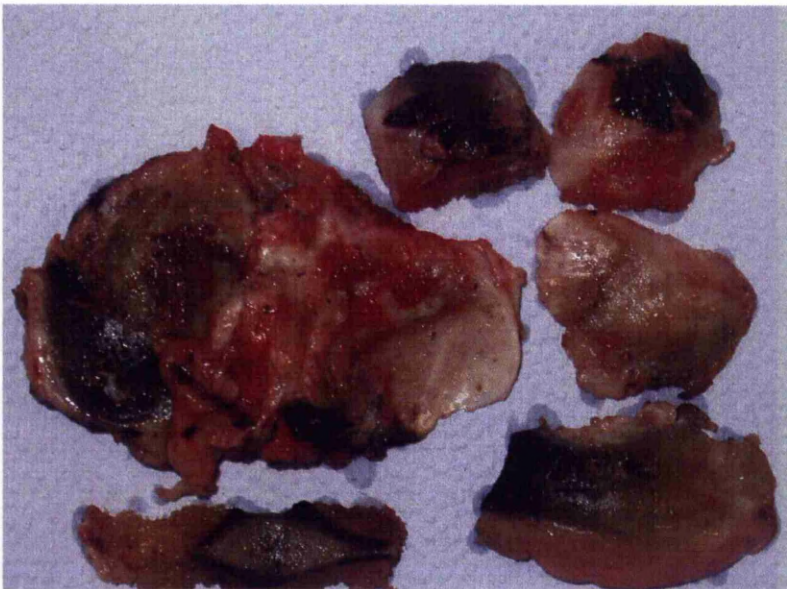


Figure 3.18:- A photograph showing the macroscopic distribution of ochronotic pigment across the tibial plateau and femoral condyles.

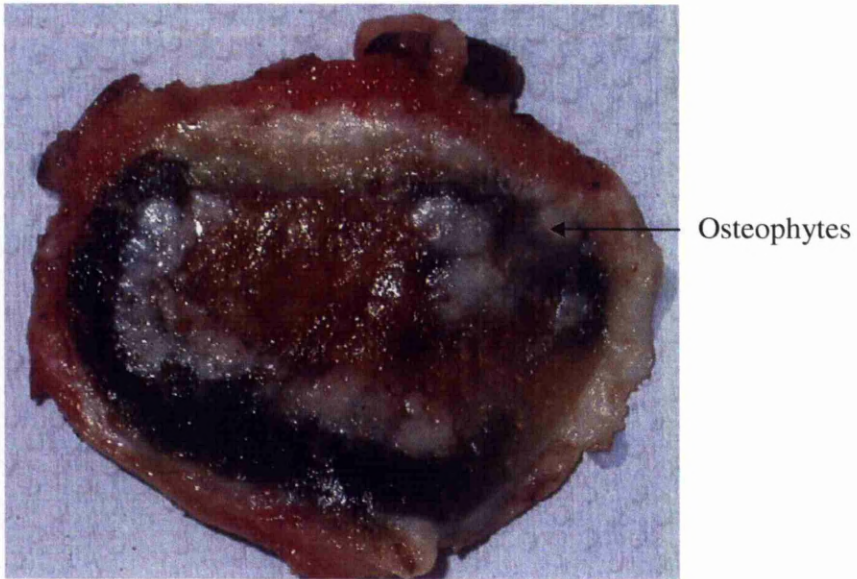


Figure 3.19:- A photograph showing the macroscopic appearance of posterior articular surface of the patella from AKU21. Note the osteophytes growing within the rim of ochronotic cartilage.

### **3.2.3. Arthroscopies**

#### **AKU8**

A 42 yr old male with known AKU attended hospital for bilateral arthroscopy due to bilateral knee pain. He attended clinic previously in 2006 to assess ochronosis of both knees following complaints of pain. On attending clinic the anaesthetic strategy was aimed to be a spinal block, however due to the patients highly calcified and degenerated discs it was not possible to administer this so a general anaesthetic was administered. This visit to clinic was to observe the left and right knees. The patient complained of right knee pain and no pain was associated with his left knee. Arthroscopic observations revealed no pigmentation in the right knee. Observations in the left knee revealed ochronosis of the menisci and darkened appearance of the articular cartilage. There were also large pieces of ochronotic cartilage loose in the synovial fluid, although it was not possible to observe exactly where these had become detached from.

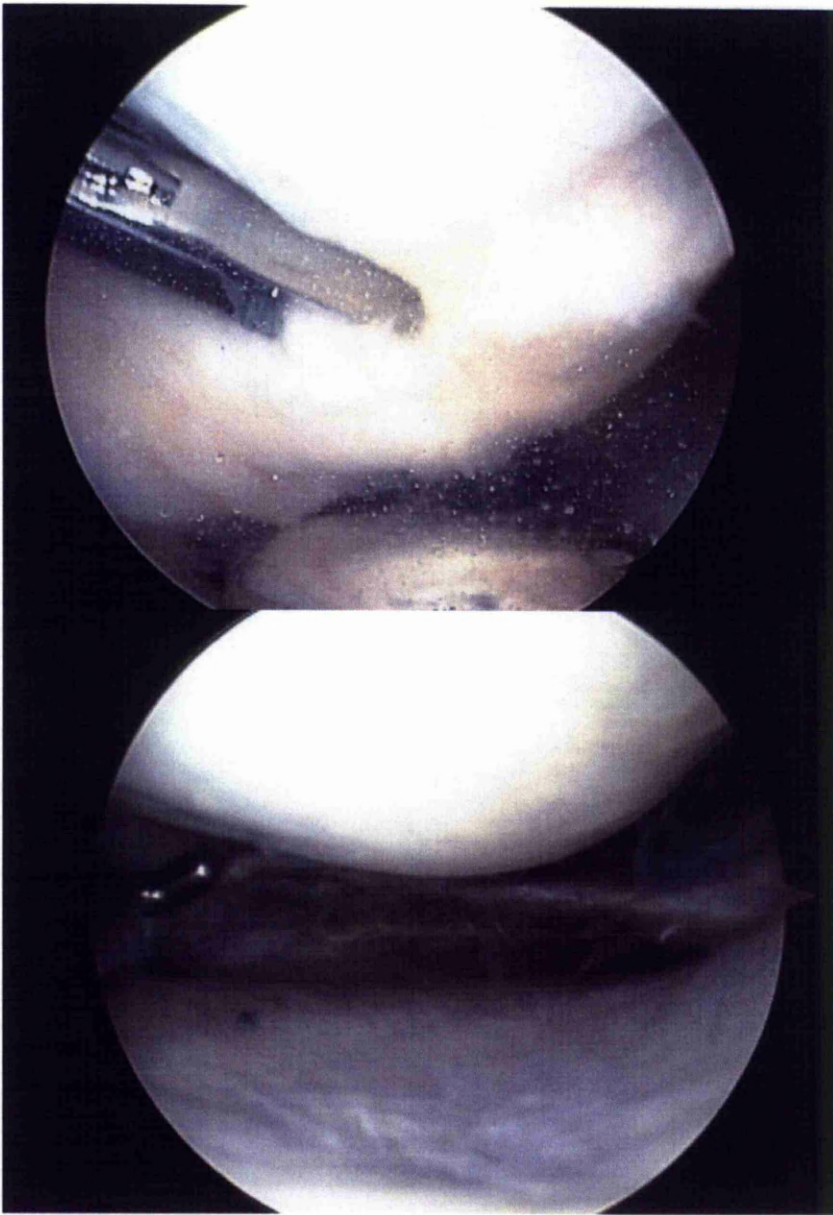


Figure 3.20:- Images taken at the time of bilateral arthroscopy showing the appearances of the articular cartilages. Note the top image shows no sign of ochronosis of the cartilages whereas the bottom images shows ochronosis of the tibial cartilage and the meniscus as indicated by the location of the probe. (Images kindly provided by Mr Clarke, Rugby St Cross Hospital)



AKU11

A 69 year old female with known AKU attended hospital for a right knee arthroscopy.

Samples removed demonstrated a mix of ochronotic and non-ochronotic matrix.

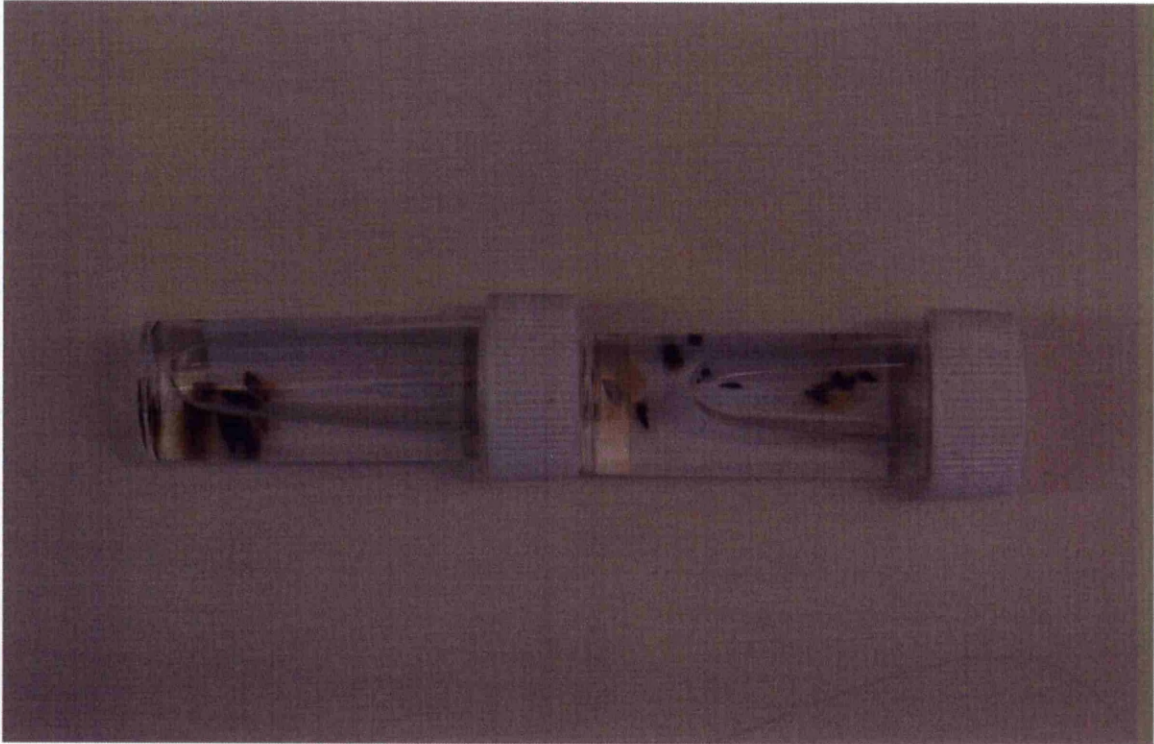


Figure 3.21:- A photograph showing the appearance of cartilage samples taken from arthroscopy which demonstrate areas of ochronotic and non-ochronotic cartilage. These samples came from the knee that would later be replaced (sample AKU12).

### **3.2.4 Spine and revision surgeries**

#### **AKU5**

A 57 yr old female with known AKU, presented for elective surgery due to chronic pain and stiffening of the lower thoracic and proximal lumbar spine. The T12 and L1 vertebrae were fused in order to alleviate pain related to calcification of the intervertebral disc between these two vertebrae. Tissues obtained were articular facet L1, vertebral body of T12, fat, muscle and over lying skin. The skin showed no obvious signs of ochronosis. The facet showed a dark colouration, typical of ochronosis, but not to the extent of articular cartilage. Both the joint facet and lamina showed ochronotic pigmentation. The ligament overlying these tissues was the most ochronotic piece of this sample.

#### **AKU14**

A 65 yr old male with known AKU attended hospital for a left revision total hip replacement. Due to the complexity of the operation, numerous pieces of bone were removed from around the existing prosthesis to enable its removal and prepare the bone surface for insertion of the new prosthesis. Macroscopic examination of the removed tissues revealed no presence of ochronotic pigment of the tissues. Interestingly no pigmentation or discolouration was seen on the surfaces of the removed prosthesis.

.

### **3.2.5. Discussion**

These observations demonstrate the largest single study of alkaptonuric joint specimens undertaken. The combined specimens of 6 knees, 5 hips, 2 biopsies from arthroscopies and a spinal surgical specimen provide a unique gross anatomical insight into the distribution of pigment across joint tissues, both within a patient and across a small percentage of the AKU sufferers in the UK (believed to be in the region of 300, although to date 78 have been identified) (Ranganath, 2010). The most striking feature was the non-uniform distribution of ochronotic pigment across the joint tissues. Within the hips and knees there was no uniform observation of the deposition of pigment in a specific area compared to another. Samples from within a patient (AKU10 & AKU19; Figs. 3.12 & 3.17 respectively) show no similarities in the distribution of pigment at the macroscopic level. The lateral aspect of AKU19 showed a much more degenerative change than the lateral aspect of AKU10; which had a far more medial degeneration. Similarly the right sided samples from with a patient AKU12 (knee – Fig. 3.13) & AKU18 (hip – Fig. 3.8) show differential distribution of pigmentation, although the time between the degeneration of the knee and hip (approx 5 months) is of interest the significance cannot be determined.

Examination of the hip specimens reveals interesting pathology; only one specimen demonstrated the presence of macroscopically observable non-ochronotic cartilage. The femoral head (Fig. 3.3) from this sample showed non-ochronotic cartilage near the neck of femur. All other femoral heads demonstrated the presence of ochronosis in the regions of cartilage still present. There was a common absence of cartilage from the superior aspect of 3 of the femoral heads, suggesting that the wear and tear of routine use results in loss of

cartilage. This may in part be attributed to the hard ochronotic cartilage of the femoral head being articulated against the hard pigmented articular cartilage of the acetabulum, consistent with those seen in Fig. 3.3. The presentation of these regions is interesting, as this would usually be seen in osteoarthritic samples, where focal lesions had initiated the breakdown of cartilage, causing the underlying bone to become exposed. The large areas of exposed and denuded bone on the hips demonstrate presence of ochronotic cartilage, present in the joint space for a period of time, before becoming embedded in the denuded bone surface. This is in part similar to the process of osteoarthritic degeneration, which sees cartilage fragments released into the joint space as fibrillation occurs, degeneration of the menisci which become prone to tearing and proliferation of synovium can all increase the presence of detritus in the usually fluid filled joint space (Felson, 2010).

The knee samples show non-uniform distribution of pigment. There was no medial or lateral trend, which is not surprising given the differences in gait throughout the human population. Across the knee samples the most consistently degenerated area was the posterior surface of the patella. This region consistently showed large denudation of bone, with an ochronotic rim of cartilage and osteophytes. Amongst the knees there were also large loose bodies removed. These were hard in composition with a mixture of ochronotic and non-ochronotic regions.

All osteophytes seen on both hip and knee samples demonstrated an interesting lack of ochronotic pigment, the absence of pigmentation of these structures raises an interesting question about the timing of pigmentation, with the chondrocytes in these structures displaying all major components and the distribution of articular cartilage when fully formed (Gelse, 2010). This would suggest that the cartilage structures in the body do not pigment during or immediately following formation.



Whilst the pigmentation of cartilage was widespread in the tissues of the patient samples, there were few other signs of degeneration of the cartilage, the articular surface was predominantly normal in most regions of all samples. There were a few lesions present across the patient samples; however there is little evidence to suggest that these are due to matrix degradation associated with arthritis, particularly given the presence of large pieces of pigmented cartilage throughout the joint synovium, embedded in the denuded bone surface and free in the joint spaces.

The description of ochronotic osteoarthropathy being of early and rapid onset (Maxwell, 2005) is supported by the mean age of primary surgery of our patient cohort compared with a sample representing national mean ages of hip and knee replacements (hips; M =67.5, F=70.4, knees; M=69.4, F=70.9) (Culliford, 2010). The AKU patients in this study demonstrated a younger mean age (hips; M = 59.6, F = 64.5, knees; M = 49.5, F= 59.25) for their primary surgery.

#### **4. Ultrastructural analysis of ochronotic tissues**

## **4.1 INTRODUCTION**

This chapter describes the ultrastructural presentation of ochronosis throughout bone cartilage and joint tissues. The literature describes in depth the ultrastructural presentation of ochronotic synovium and the cartilage that is embedded within it. Chapter 3 of this Thesis describes the macroscopic presentation of ochronosis as seen in tissues from patients with alkaptonuria. As seen with the macroscopic presentation there are large differences in the presence of pigment across tissues, both across bone, cartilage and soft tissues. This chapter provides a comprehensive analysis of alkaptonuric joint tissues at the ultrastructural level, providing an in depth look at the most affected component of alkaptonuric tissues, the collagen fibres. This chapter also describes for the first time a distinct pattern of binding and the earliest noted sign of pigment nucleation.

## **4.2 RESULTS**

### **4.2.1 TEM of AKU Cartilage**

At low magnification collagen fibres were difficult to distinguish in the matrix and were surrounded by numerous dark deposits when observed in longitudinal section. Amongst the collagen fibres, the extracellular spaces were filled with dark globular and granular deposits that appeared extremely electron dense. Inside of some these deposits there was crystalline material (Fig. 4.1).

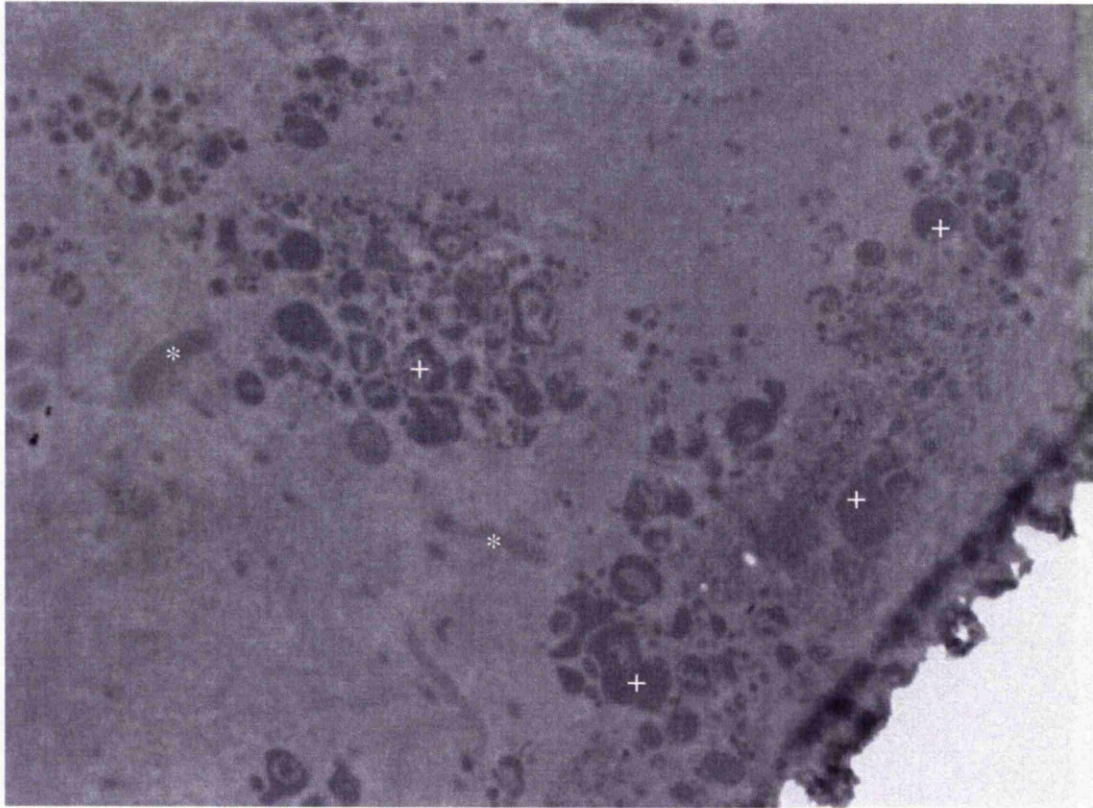


Figure 4.1:- *Low power photomicrograph showing numerous ochronotic granules and globules present in the cartilage matrix (+). A few short collagen fibres (\*) can be seen in the field of view. (x9,900).*

With increasing magnification collagen fibres became more clearly identifiable in the matrix, particularly in longitudinal section. The 67nm banding pattern typically associated with the fibrillar collagens could clearly be seen. An observation of collagen fibres in transverse section was more difficult, except in regions where the fibres had been completely encrusted by ochronotic pigment, this gave a negative outline of the body of the collagen fibre in the matrix.

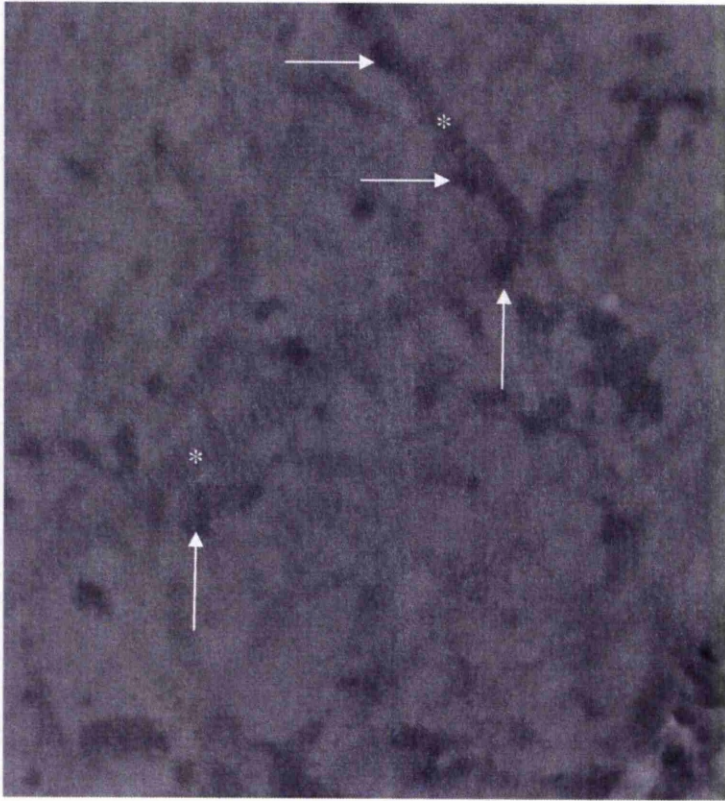


Figure 4.2:- An electron photomicrograph showing numerous collagen fibres (\*) in longitudinal section with sporadic ochronotic deposits located along their length (arrows). It is more difficult to distinguish collagen fibres in transverse section but some can be seen amongst ochronotic deposits. (x20,500).

Across the matrix collagen fibres demonstrated large variations in their diameter along short distances of the fibre, although these did not always appear to be in relationship to the presence of detectable ochronotic pigment on their external surfaces. There were also small granules of ochronotic pigment present on the surface of some fibres, much smaller than along the fibres.



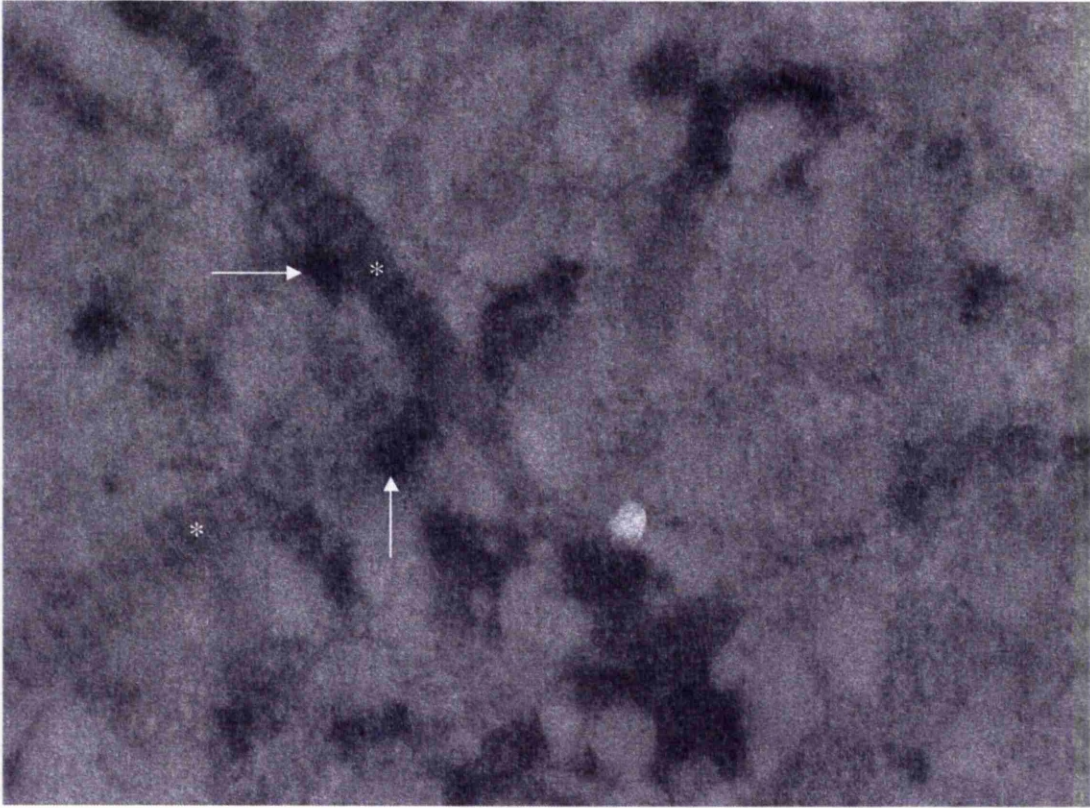


Figure 4.3:- A high power electron micrograph showing numerous collagen fibres (\*) with large electron dense ochronotic granules located along their length (arrows). (x43,000).

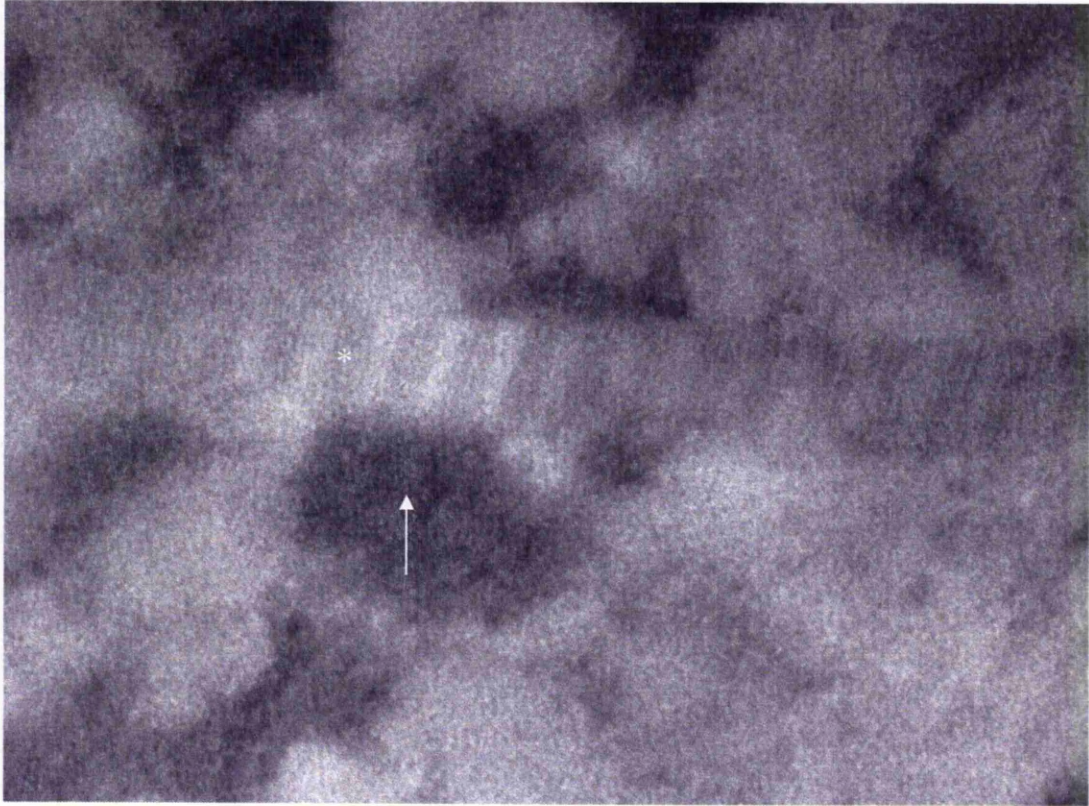


Figure 4.4:- A high power photomicrograph showing the close relationship between ochronotic pigment (arrow) and collagen fibres (\*) in the matrix. (x87,000).



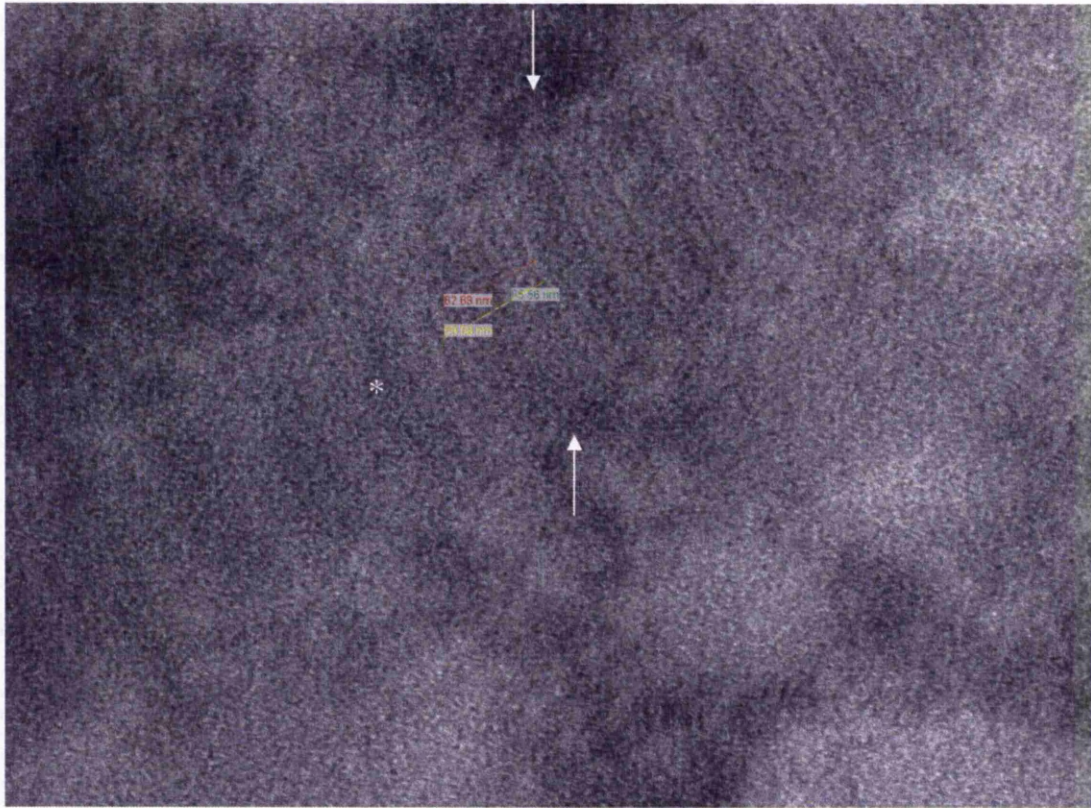


Figure 4.5:- A high power photomicrograph showing the presence of ochronotic pigment (arrows) on the superior and inferior surfaces of a collagen fibre (\*). Lines of measurement have been placed onto the image to attempt to demonstrate the periodicity of the collagen fibres. Yellow = 69.58nm, Red = 62.68nm, Green = 65.56nm. (x160,000).

Throughout the examination of the cartilage sections it was difficult observe any chondrocytes within the tissue sections examined.



#### **4.2.2. TEM of OA cartilage**

Examination of OA cartilage demonstrated numerous collagen fibres present in the matrix. It was clear that there was no ochronotic pigment present in the spaces of the extracellular matrix.

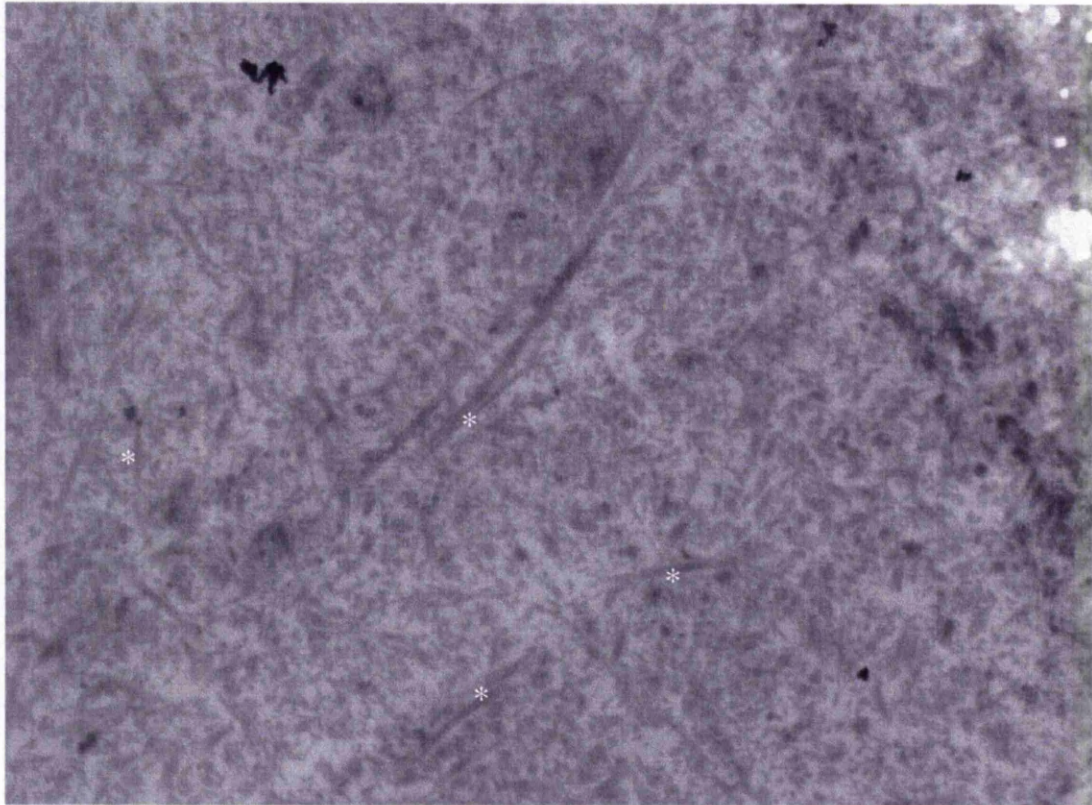


Figure 4.6:- A low power electron photomicrograph showing numerous collagen fibres (\*) in both transverse and longitudinal section. There is no evidence of any ochronotic pigment associated with the fibres and spaces can clearly be observed between matrix components. (x8,200)

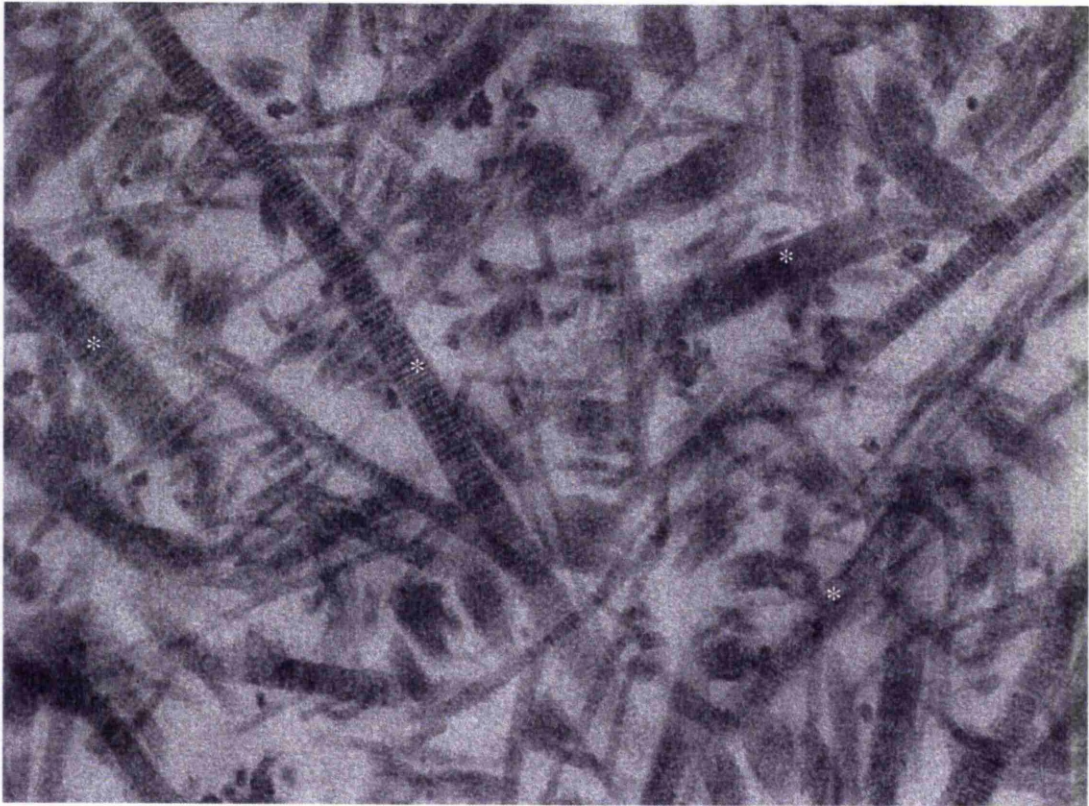


Figure 4.7:- An electron micrograph of osteoarthritic cartilage matrix showing numerous randomly oriented collagen fibres (\*).67nm banding can clearly be seen on the fibres. (x43,000).



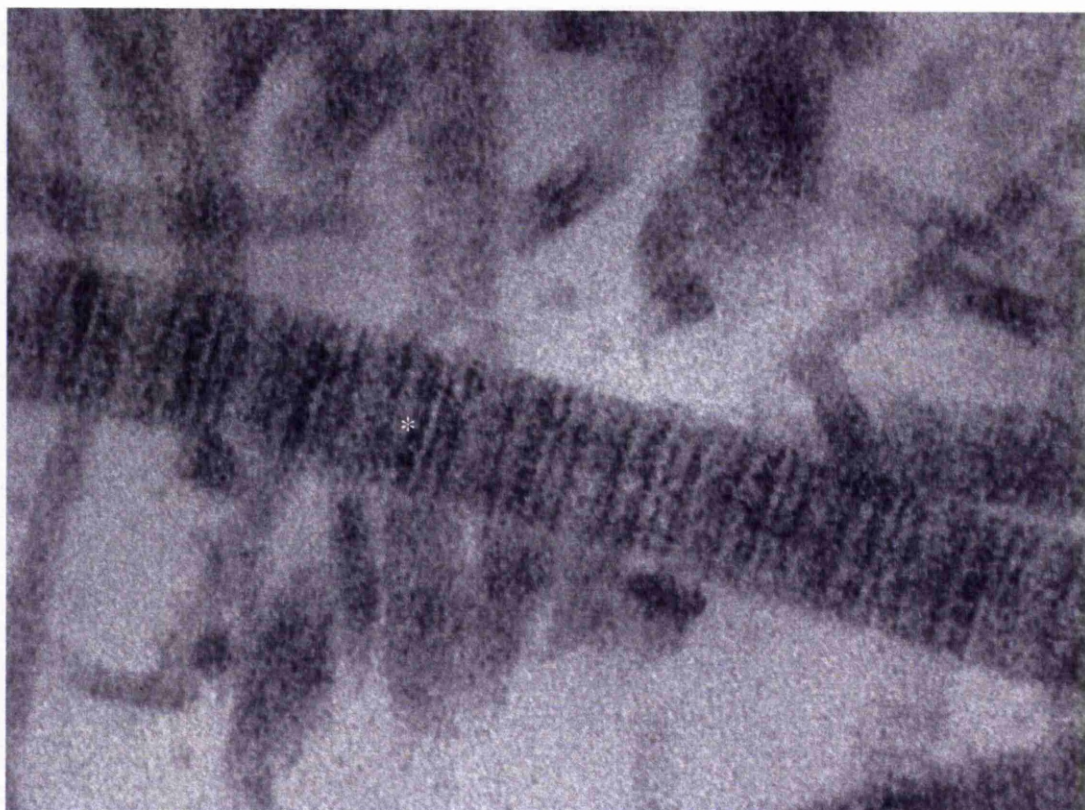


Figure 4.8:- A high power electron micrograph of an individual collagen fibre (\*) demonstrating no electron dense ochronotic deposits along the fibre body from OA cartilage. 67nm banding is clearly seen. (x160,000).

Fibres were clearly seen both longitudinally and transversely. Those fibres seen in transverse section demonstrated normal cross sectional appearances and had no evidence of dark ochronotic deposits passing through their fibre body, or around their peripheries.

#### **4.2.3 TEM of AKU bone**

Examination of mineralised bone from the vertebrae of an individual with alkaptonuric ochronosis revealed no pigmentation in the bone matrix. Collagen fibres could clearly be observed in the matrix. Mineralised collagen could be seen at the edge, along which an osteoclast appeared to be located.

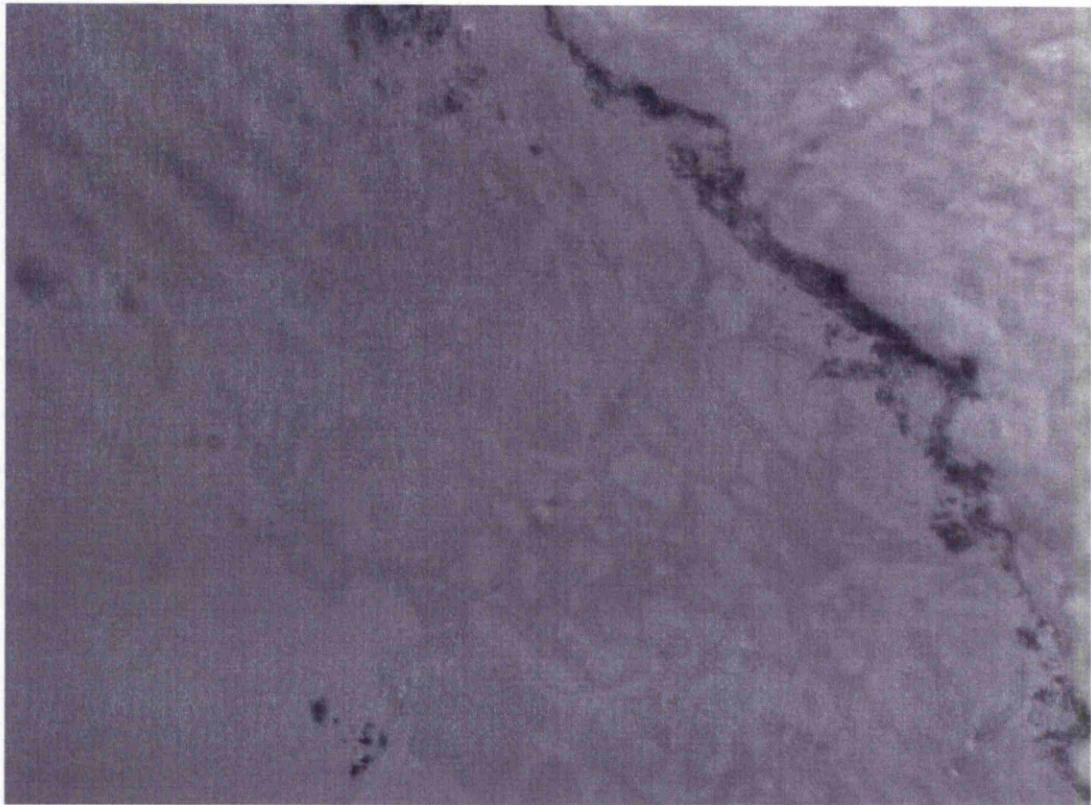


Figure 4.9:- *Low power electron micrograph showing the presence of mineralised collagen matrix (top right) and a large region of cellular organelles (bottom/middle left).*



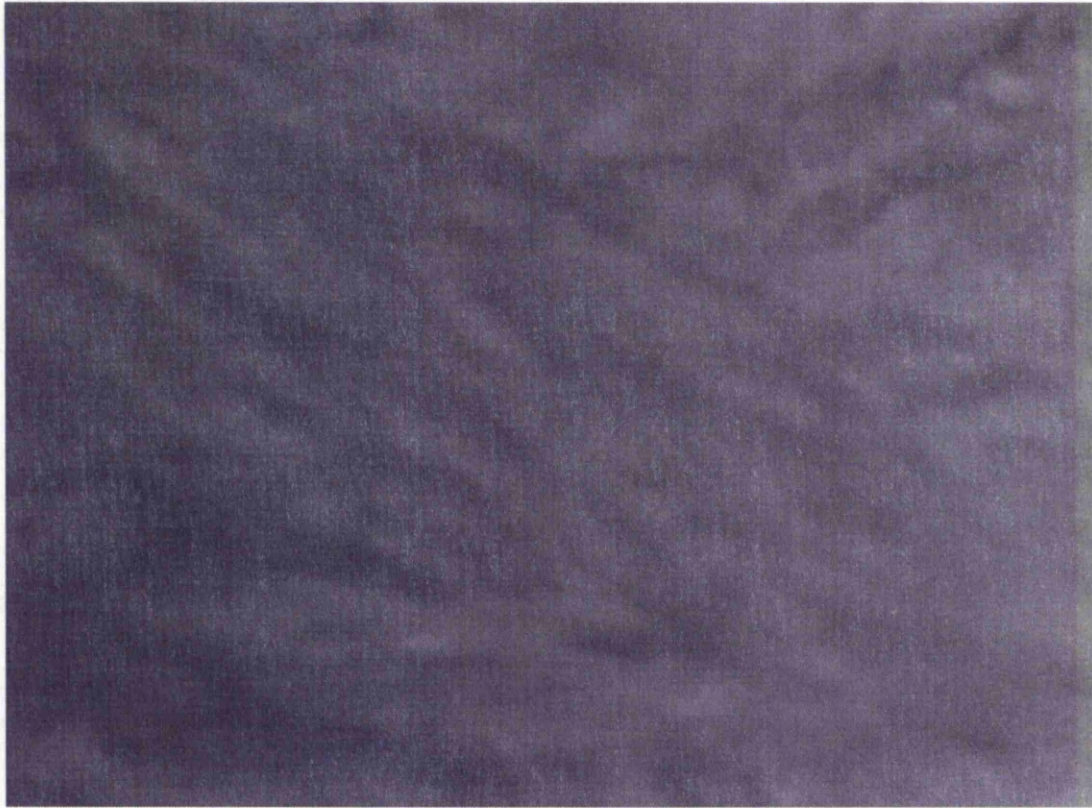
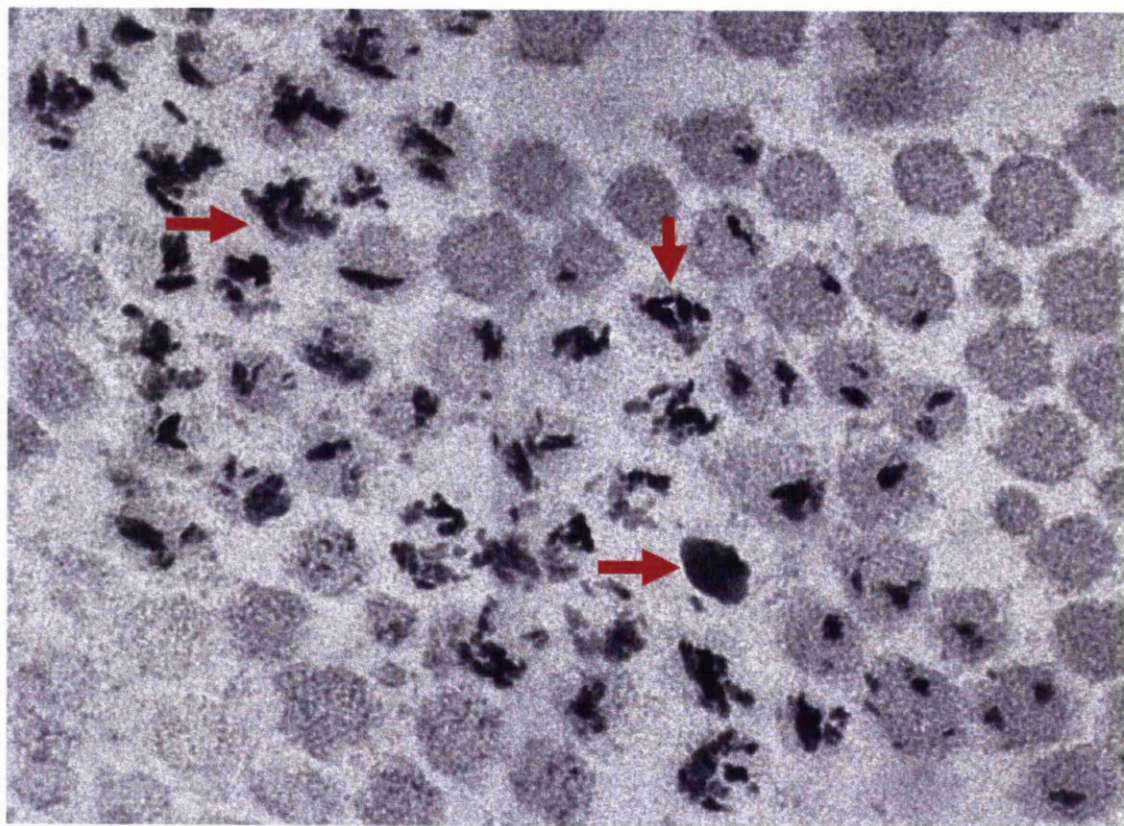


Figure 4.10:- A low power electron photomicrograph shows mineralised collagen can be seen with the typical 67nm banding. No electron dense deposits can be identified. (x26,500).

High power examination of the bone matrix did not reveal any obvious sign of large ochronotic deposits or early signs of ochronosis like those seen associated with the collagen fibres in the cartilage and capsule matrices.

#### **4.2.4 TEM of AKU Capsule**

At low magnification collagen fibres are easily identifiable in transverse and longitudinal section. Present amongst the fibres were numerous electron dense granules of ochronotic pigment. These granules varied in position amongst the fibres. Some fibres had single granules of pigment located within the visible cross section of the fibre, or sometimes connected to the periphery of the fibre. Other fibres possessed more than one pigment granule inside the fibre body. In some instances multiple pigment granules had no identifiable connection with the perimeter of the fibre. In proximity to these granulated fibers there were also fibres which appeared to have been completely replaced or encrusted in pigment (Fig. 4.11).



*Figure 4.11:- A high power TEM photomicrograph showing collagen fibres in transverse section. Numerous fibres appear with small electron dense granules located within the fibre body. Other fibres appear to have been completely replaced by pigment (arrows). Some fibres show no obvious association with pigment. (x87,000).*

Analysis of other regions showed a more severe or possibly advanced form of pigment associated with the fibres when viewed in transverse section. This pigmentation appeared again as electron dense shards but much more crystalline in structure and often protruded from the body of the fibre. The shards also appeared to bridge between fibres often connecting one fibre to another neighbouring fibre, or in some instances more than one neighbouring fibre. These large shards were sometimes seen attached to a large granules

located in the centre of an individual fibre. There were often fibres in the region of interest that had no notable shards associated with them. Fibres with pigment sticking out from them often appeared swollen when compared to their non pigmented neighbours. Pigment protruding from fibres was in some instances observed binding to “extra-fibrillar” pigment (Fig. 4.12). Fibres which appeared free from pigmentation appeared structurally abnormal. They did not show the circular cross section associated with collagen fibres but presented as more of a pentagonal or hexagonal cross section (Fig.4.12).



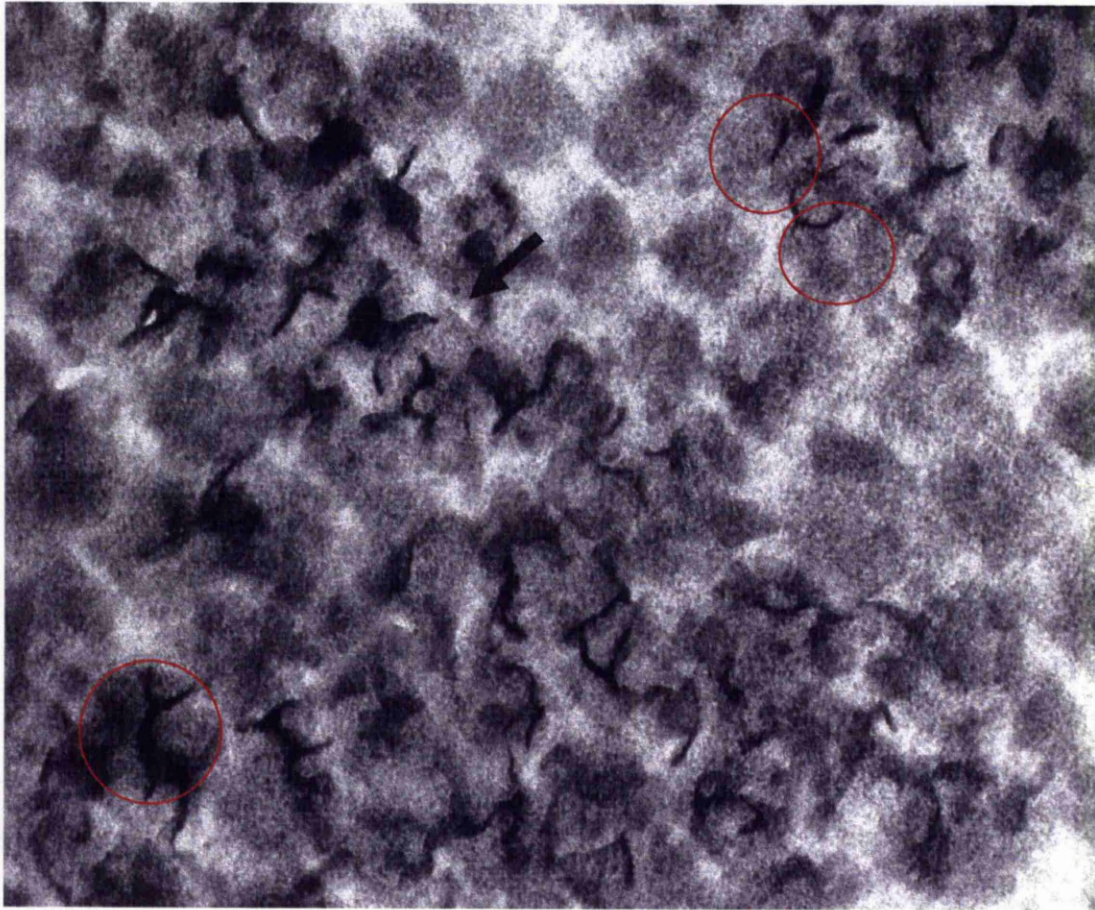


Figure 4.12:- TEM photograph showing large electron dense ochronotic shards located within the fibre body and often protruding out into the interfibrillar space and connecting to other fibres (top right). (Circles represent overlay of fibre perimeter to show protrusion of shard from fibre). Shards can also be seen originating from large granules located within fibre bodies.(arrow). Numerous fibres show no notable dense pigmentation but appear structurally abnormal displaying many variations on shape and diameter. (x160,000).

Numerous novel observations were noted when viewing the collagen fibres in longitudinal section. It was easy to identify the typical 67nm cross banding that is

normally associated with the fibrillar collagens. The most distinct feature is the presence of many electron dense ochronotic shards on the surface of the collagen fibres giving a speckled appearance. It is also of interest that there is often more than one pigment granule/shard associated with a single collagen fibre. The pigment is present on fibres of all diameters, in all different shapes and sizes across the tissue. It is clear that there are also regions of fibres and whole fibres that are free from any form of pigmentation. It was seen in some regions that there was a gradient of pigmentation running from collagen fibres that were totally free from pigment across to regions of heavy pigmentation. It was also observed that there were regions of pigmentation there were so heavy and dense that the collagen fibre had been completely replaced, or encrusted into pigment. This phenomenon was observed across a distance of less than a few hundred nanometres (Fig. 4.13). Most noticeable is the presence of a periodic banding pattern of ochronotic shards on an individual collagen fibre. The pigmentation overlaps with the periodic banding associated with the fibrillar collagens. (Fig. 4.13 inset).



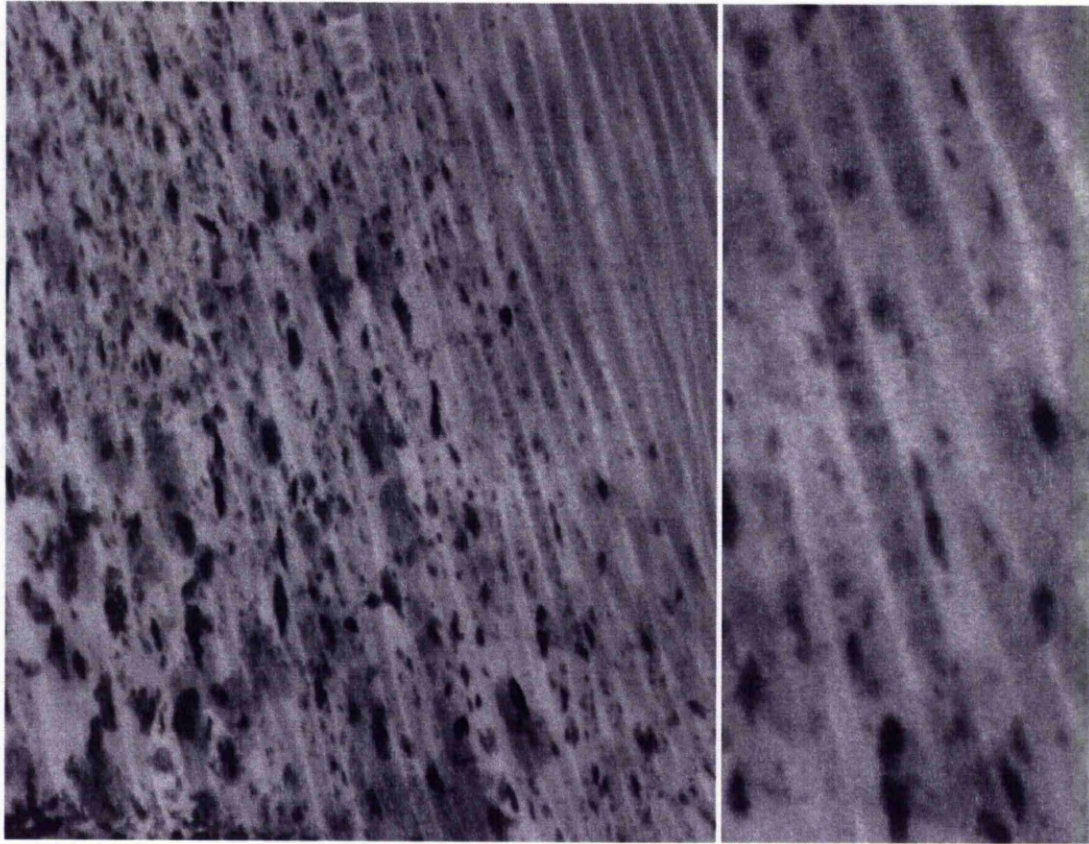


Figure 4.13:- *Ultrastructural appearance of ochronotic ligamentous capsule. Collagen fibres viewed in longitudinal section show a distinct electron dense pigment on their surface. Not all fibres present with pigment deposition. Numerous pigment shards can be seen on a single fibre. Gradient of pigmentation can be seen running right (no pigment on fibres) to left (large electron dense shards replacing fibres) (x20,500). Inset shows a distinct periodic binding pattern associated with pigment granules on a single fibre.*

This regular periodicity of ochronotic pigment binding was seen on more than one fibre within the tissue (Fig. 4.14). Alongside the regular pattern observed on some fibres we were able to note very early signs of pigment deposition. These small granules were seen to appear in a regular pattern on the longitudinal surface of the collagen fibres. These

deposits appear to be the earliest noted and detectable signs of pigment deposition (Fig. 4.14). High power magnification of larger pigment shards on the longitudinal surface of the fibres shows shards to be bridging some of the cross bands on the fibrillar surfaces (Fig. 4.14).

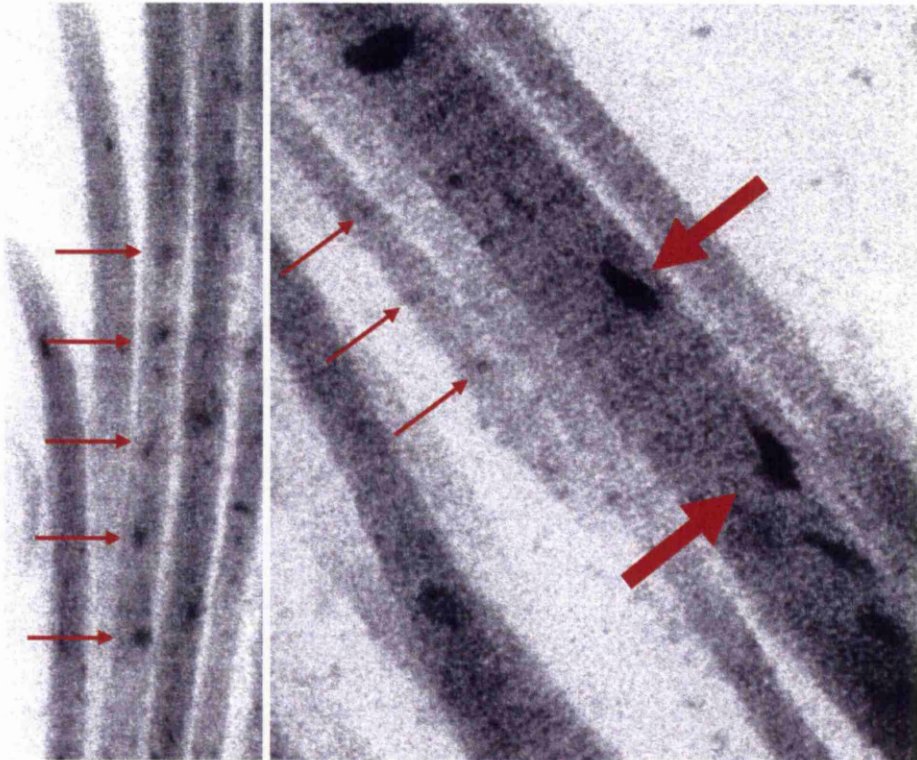


Figure 4.14:- Ultrastructural appearance of collagen fibres from ochronotic ligamentous capsule. (Left) Individual collagen fibre showing a regular binding pattern along the surface (thin arrows) (left x20,500). (Right) Collagen fibre showing nucleation of ochronotic pigment in a distinct pattern (thin arrows). Pigment can also be seen bridging across the cross bands of the collagen fibres (thick arrows) (right x87,000).

TEM examination of the cells within the ligamentous capsule displayed numerous features of interest. Many cells displayed small dark shards of ochronotic pigment (Fig



4.15). These were comparable in shape and size to those observed on the collagen fibres within the matrix. Some of the fibroblasts observed showed comparable small electron dense granules located within the cell nucleus (Fig.4.16). In some areas fibroblasts displaying cytoplasmic pigmentation showed no sign of necrosis. Cells displaying larger amounts of pigmentation and they also displayed more signs of necrosis, such as organelle disruption and discontinuities in the plasma membrane (Fig. 4.16 bottom inset).

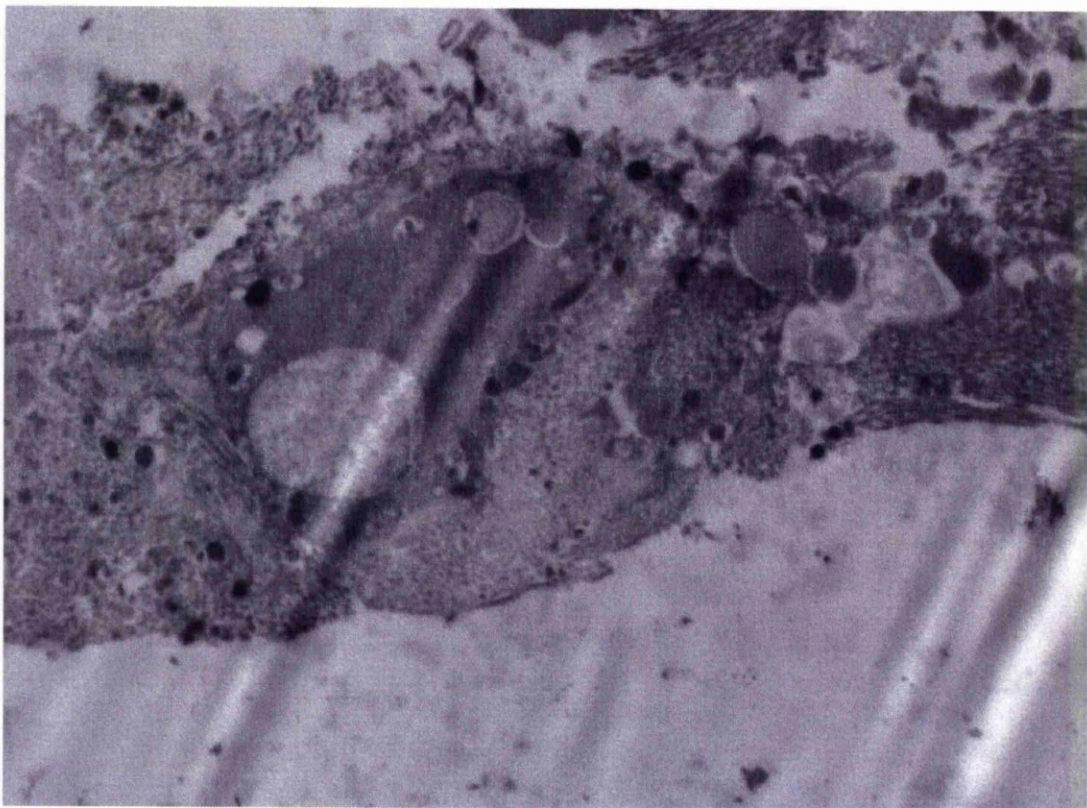


Figure 4.15:- A low power electron photomicrograph showing a fibroblast amongst the collagen matrix with numerous electron dense deposits located within its cytoplasm. (x6,000).

Cells were also seen with numerous small fibrillar structures located within their cytoplasm. On and around these fibrillar structures were numerous small electron dense granules suggesting association between the two (Fig. 4.16 top inset). Fibroblasts were also seen in some regions without notable electron dense granules within their cytoplasm.

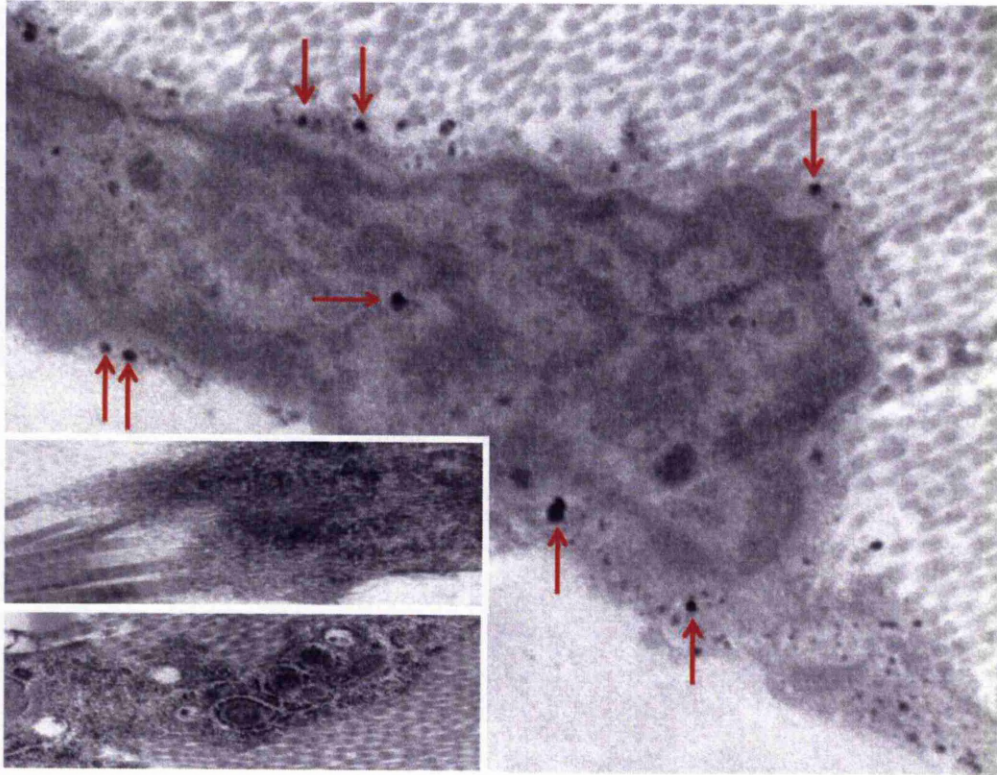


Figure 4.16:- TEM photograph of a fibroblast on the periphery of collagen fibres in the ligamentous capsule. Numerous small electron dense granules can be seen in the cytoplasm (large arrows). There are also electron dense granules located within the nucleus of the cell (small horizontal arrow). (x26,500). Insert :- (bottom) TEM photograph showing fibroblast with numerous electron dense ochronotic granules within the cell. Cell organelles are difficult to distinguish due to the cell being in necrosis (x20,000). (top) TEM photograph showing abundant electron dense granules in the cell cytoplasm associated with fibrillar structures (x60,000).

#### **4.2.5 TEM of spinal ligament**

Regions of spinal ligament examined by TEM revealed large regions of collagen fibres interspersed with large elastic fibres and large electron dense ochronotic deposits. Fibroblastic cells were seen frequently throughout the matrix. Elastic fibres were easily identifiable due to the vastly increased size compared to individual collagen fibres, these were normally at least 3 times larger in diameter, but occasionally seen in excess of 10 times the diameter. (Fig. 4.17)





Figure 4.17:- A low power electron micrograph showing the location of numerous bundles of collagen fibres (c) interspersed by elastic (e) fibres and large ochronotic deposits. The green line shows the cross-sectional diameter of an ochronotic deposit which is 1371.18nm. The red line demonstrates the thickness of a bundle of elastic fibres passing through the field of view, this bundle is 715.66nm in diameter. The yellow line demonstrates a large ochronotic deposit present amongst the collagen fibres and in close proximity to an elastic fibre. Three other ochronotic deposits can be seen in this column of collagen fibres, there is another ochronotic deposit amongst the collagen fibres in the bottom left of the image. A fibroblast (f) can be seen amongst the collagen fibres on the right hand of the image. (x9,900).

The fibroblasts within the matrix showed no sign of necrosis, they were seen both in regions of ochronotic and non-ochronotic matrix. Fibroblasts were observed in non-ochronotic matrix with ochronotic deposits located intracellularly (Fig. 4.18 & Fig. 4.19).

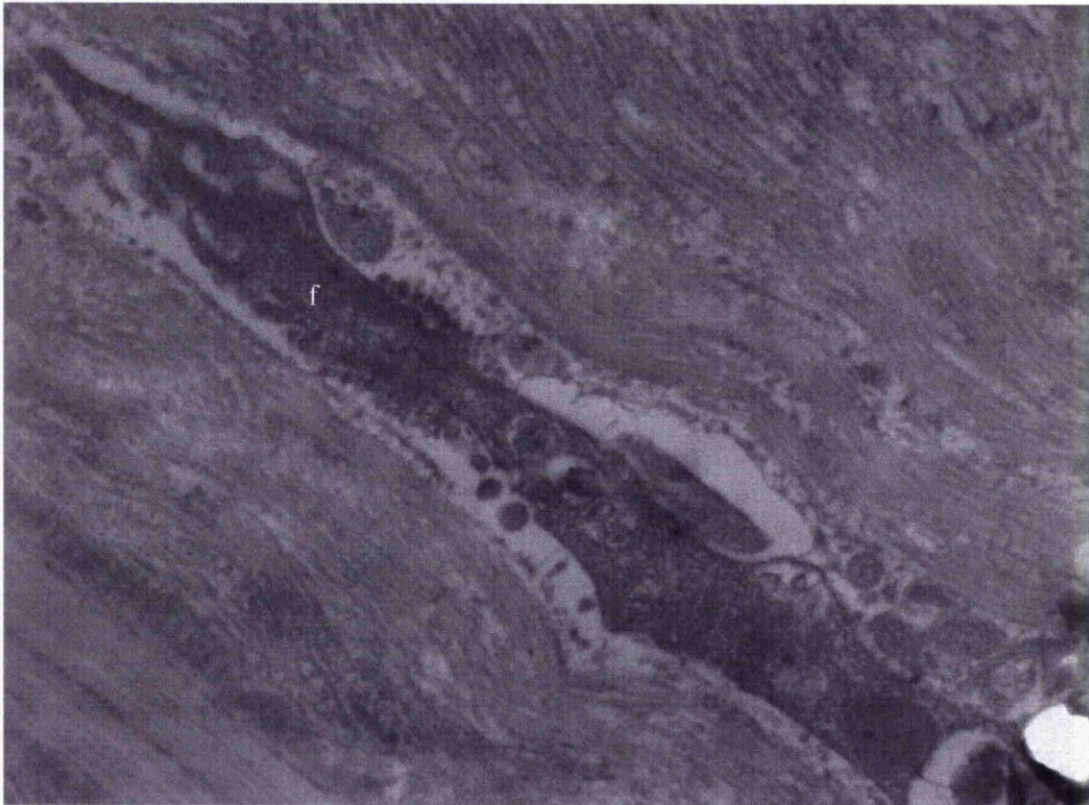


Figure 4.18:- A low power electron micrograph showing a fibroblast (f) in the ligamentous matrix with ochronotic pigment in a cytoplasmic vacuole. Collagen and elastic fibre bundles can be clearly seen. (x20,500).



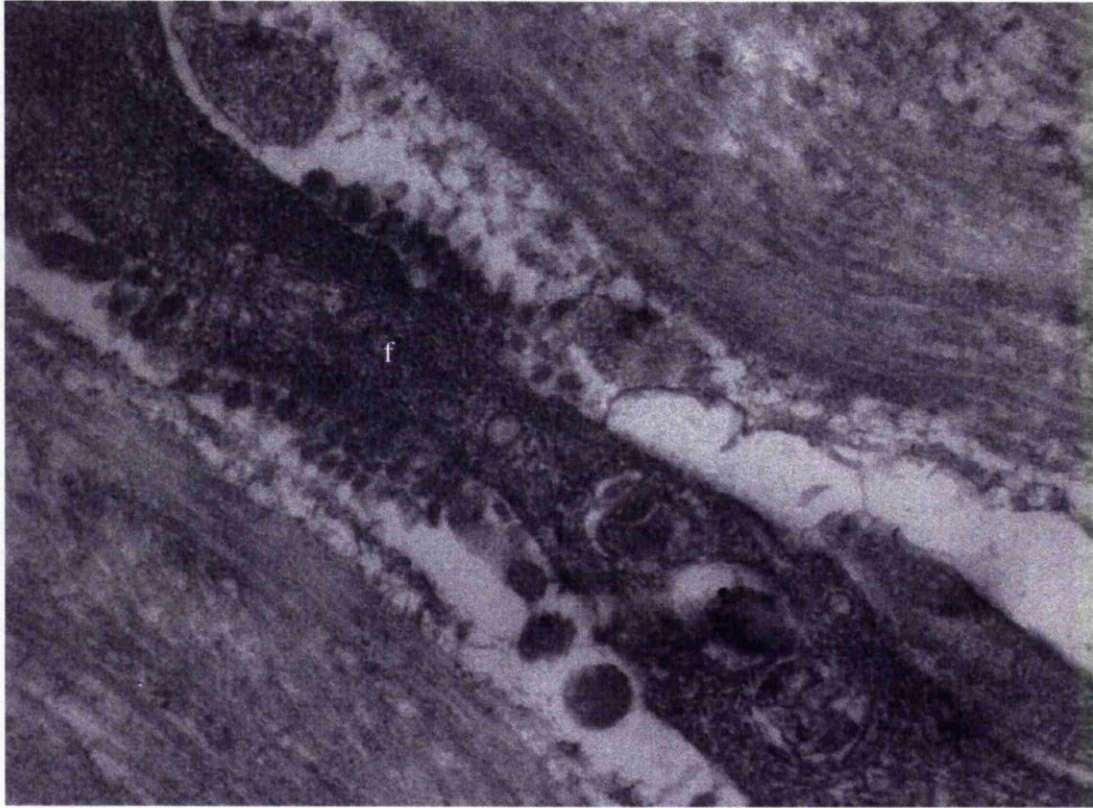


Figure 4.19:- A high power electron micrograph showing a fibroblast located amongst the collagen fibres with ochronotic like deposits located in vacuoles within its cytoplasm. (x43,000).

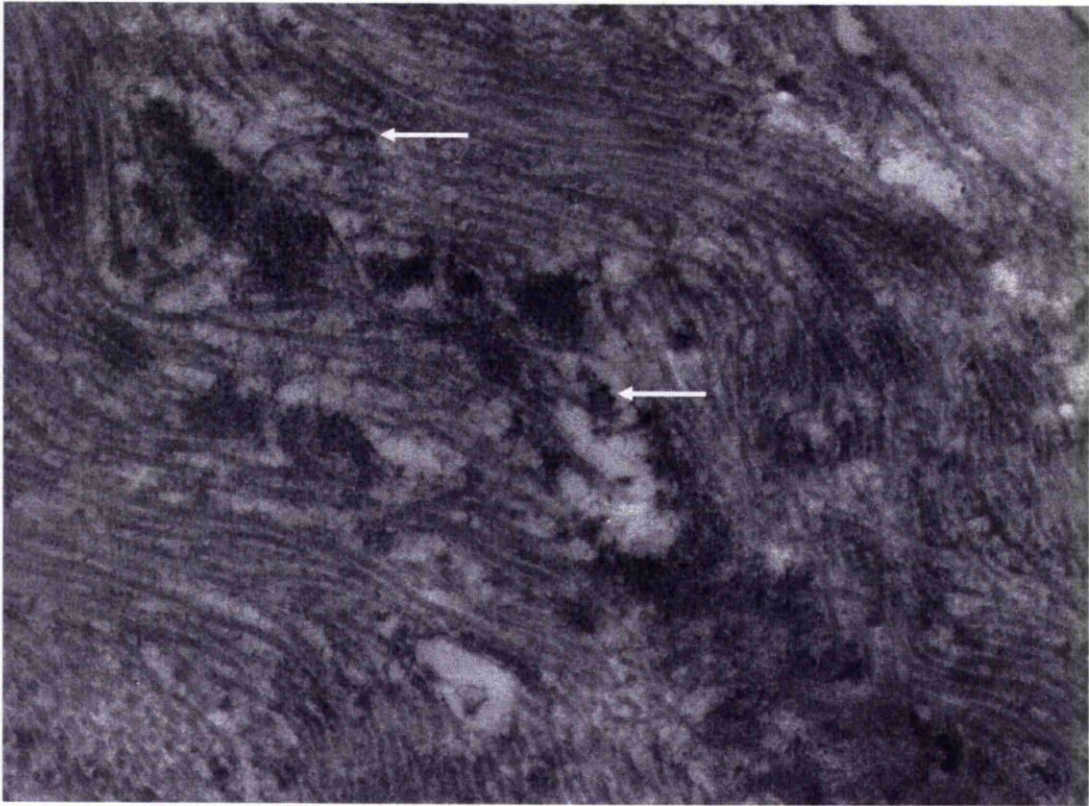


Figure 4.20:- *A low power electron micrograph showing the appearance of ochronotic like deposits associated with the collagen fibres in the matrix (arrows). (x26,500).*

When the matrix was examined at high power there were large regions of collagen fibres in proximity to large ochronotic deposits. When observed in transverse section the collagen fibres displayed highly irregular shapes. Although it was often difficult to distinguish detectable ochronotic pigment associated with these fibres.



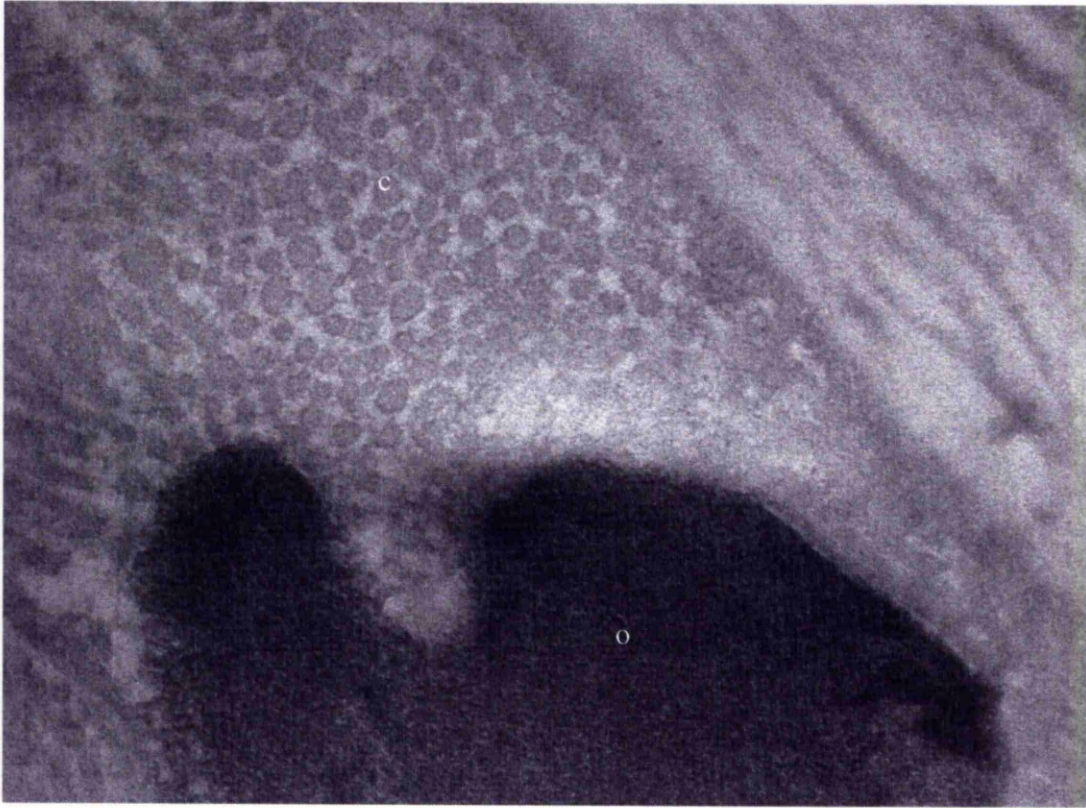


Figure 4.21:- A high power electron photomicrograph demonstrating the presence of abnormally shaped collagen fibres in the matrix. No dense ochronotic deposits are seen associated with the fibres in the field of view. There is a large ochronotic deposit (o) present in the bottom of the image, which appears in part to be associated with a large elastic fibre. (x60,000).

#### **4.2.6 TEM of *in vitro* cultures**

As described in literature; deposition of ochronotic pigment occurs in cultures of osteosarcoma cells (SaOS-2 and MG63) with HGA added to their culture medium (Tinti, 2010). As part of this chapter and the paper described in the previous reference, an electron microscopic study of these cultures along with my own novel cultures of C20 human chondrocytes was undertaken. Alongside this a study of the formation of HGA polymerised product from pure HGA crystals in water was also performed. This chapter and part of the referenced paper represents the first time anyone has studied *in vitro* models of ochronosis and pure polymerised HGA using ultrastructural techniques.

Examination of all cultures revealed numerous cells and sporadic regions of cell matrix (Fig. 4.22 & 4.23). Regions of matrix looked extremely primitive compared to the highly ordered matrix seen in human joint tissues such as cartilage and fibrous capsule. The matrix was most evident in regions immediately surrounding cells and within fibroblastic like structures of the cells themselves (Fig. 4.22 & 4.23). The fibres that were observed looked pro-collagen like in structure with thin wispy fibres that displayed no evidence of the 67nm periodic banding pattern synonymous with fibrillar collagens. Similar fibres were observed in both the osteosarcoma and chondrosarcoma cultures. When these fibres were viewed in longitudinal section there were numerous dark electron dense deposits observed in association with the fibres. These were also seen intracellularly.

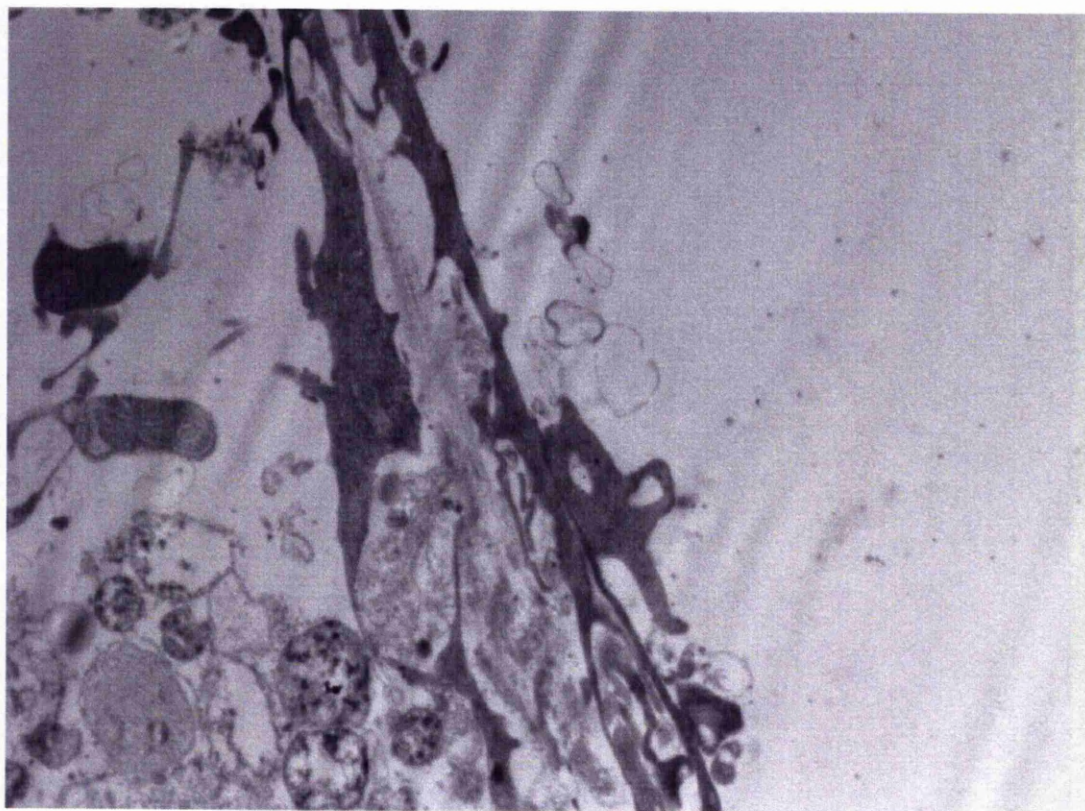


Figure 4.22:- A low power electron photomicrograph showing the relationship between cellular and extracellular culture components in MG63 cells cultured in  $3.3 \times 10^{-4} M$  HGA. Electron dense ochronotic deposits can be seen associated with structures in the bottom right hand corner of the image. (x6,000).



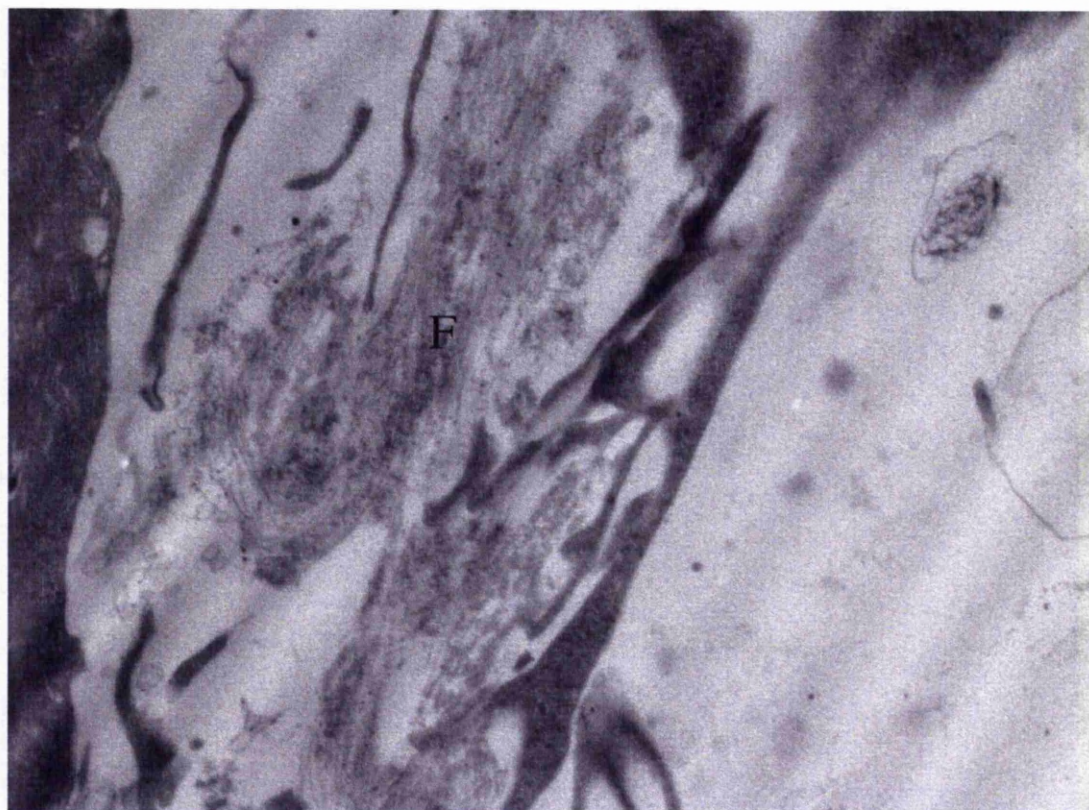


Figure 4.23:- A low power photomicrograph of MG63 cells cultured in  $3.3 \times 10^{-4} M$  HGA. Numerous thin fibres (F) can be seen in the middle of the image amongst cellular structures. Small dark granules can be seen associated with these fibres. (x9,900).

As seen in Figure 4.22 & 4.23 there are clear fibres located between regions of individual cells, possibly fibropositor structures. These were also seen in SaOS-2 cultures (Fig. 4.24) and chondrosarcoma cultures (Fig. 4.25).



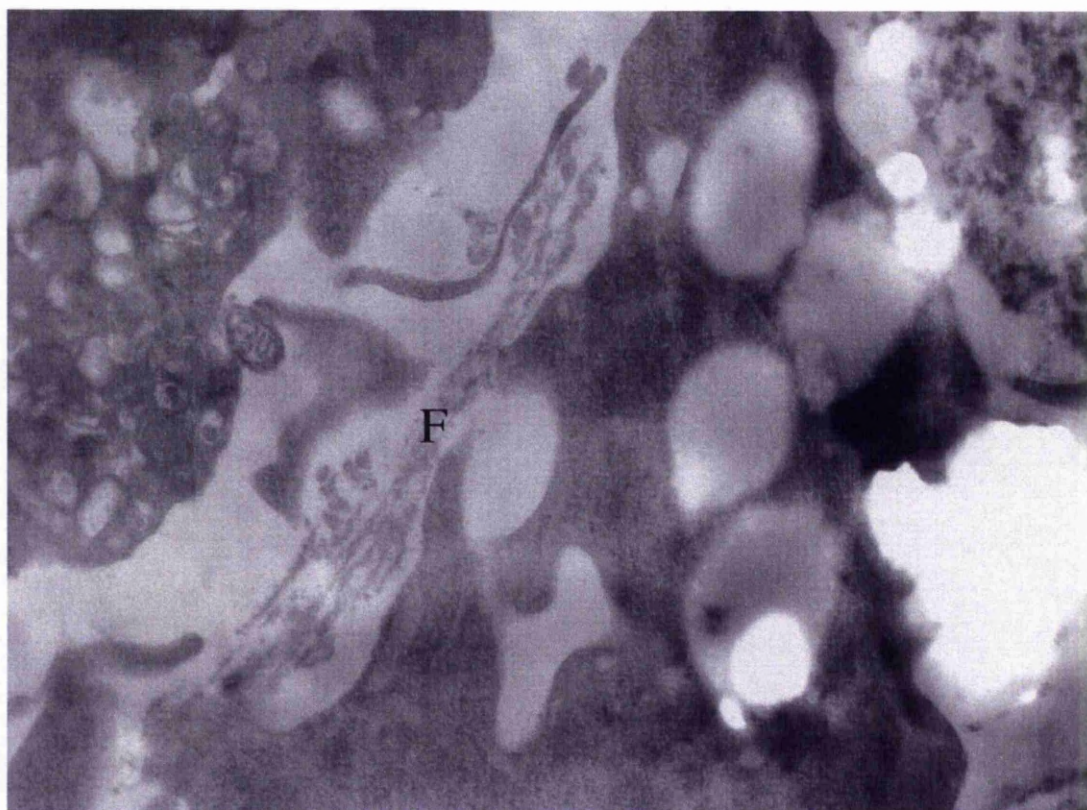


Figure 4.24:- A low power electron micrograph showing the presence of fibres and cellular components in SaOS-2 cells cultured in  $3.3 \times 10^{-4} M$  HGA. (x16,500)

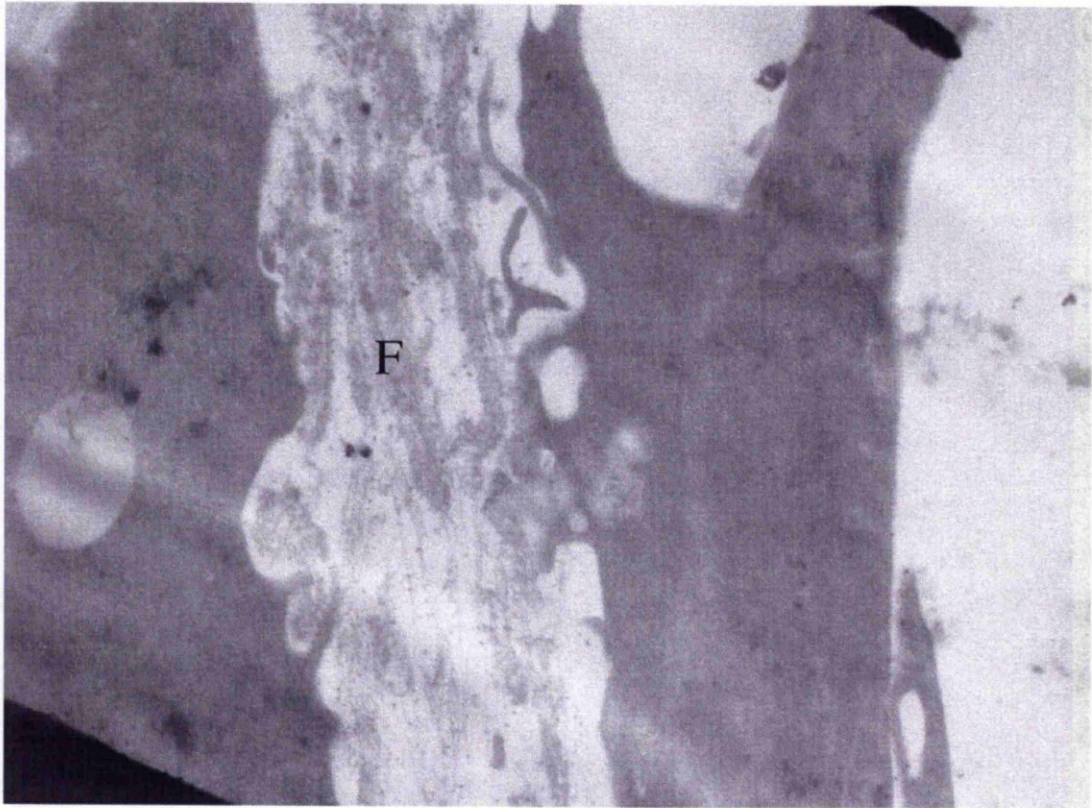


Figure 4.25:- A low power electron micrograph showing the relationship between cellular and extracellular components in C20 human chondrosarcoma cells cultured in  $3.3 \times 10^{-4} M$  HGA. (x8,200).



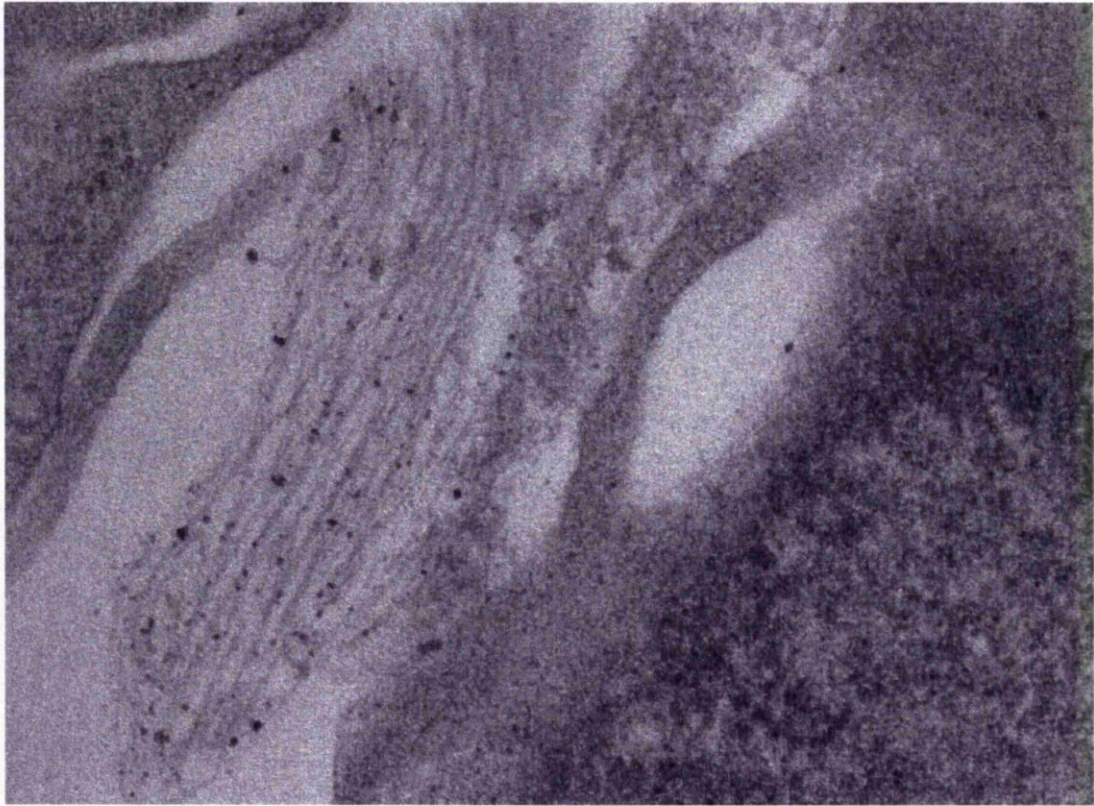


Figure 4.26:- A high power electron photomicrograph of C20 human chondrocytes cultured in  $3.3 \times 10^{-4} M$  showing the presence of numerous extracellular fibrils with dark ochronotic granules present amongst them. (x43,000).

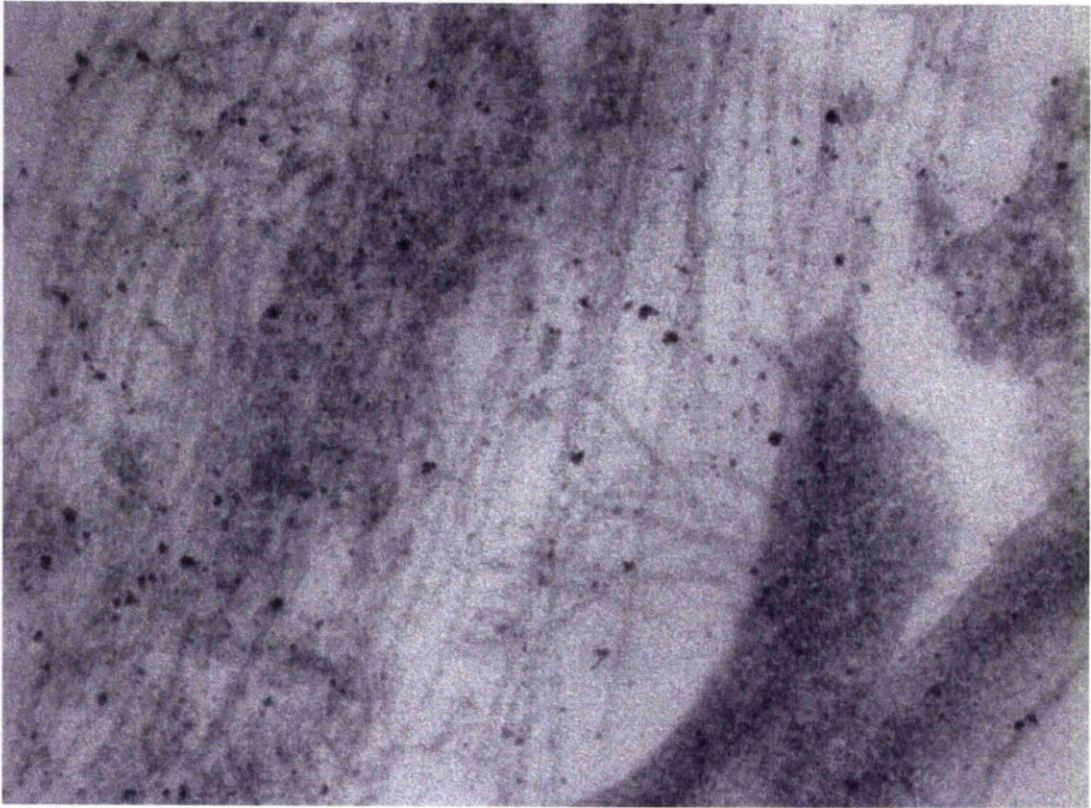


Figure 4.27:- A high power electron photomicrograph showing the presence of ochronotic granules with extracellular matrix fibres in cultures of MG63 cells cultured in  $3.3 \times 10^{-4} M$  HGA (identical to those seen in figure 4.26, chondrocyte cultures). (x60,000).



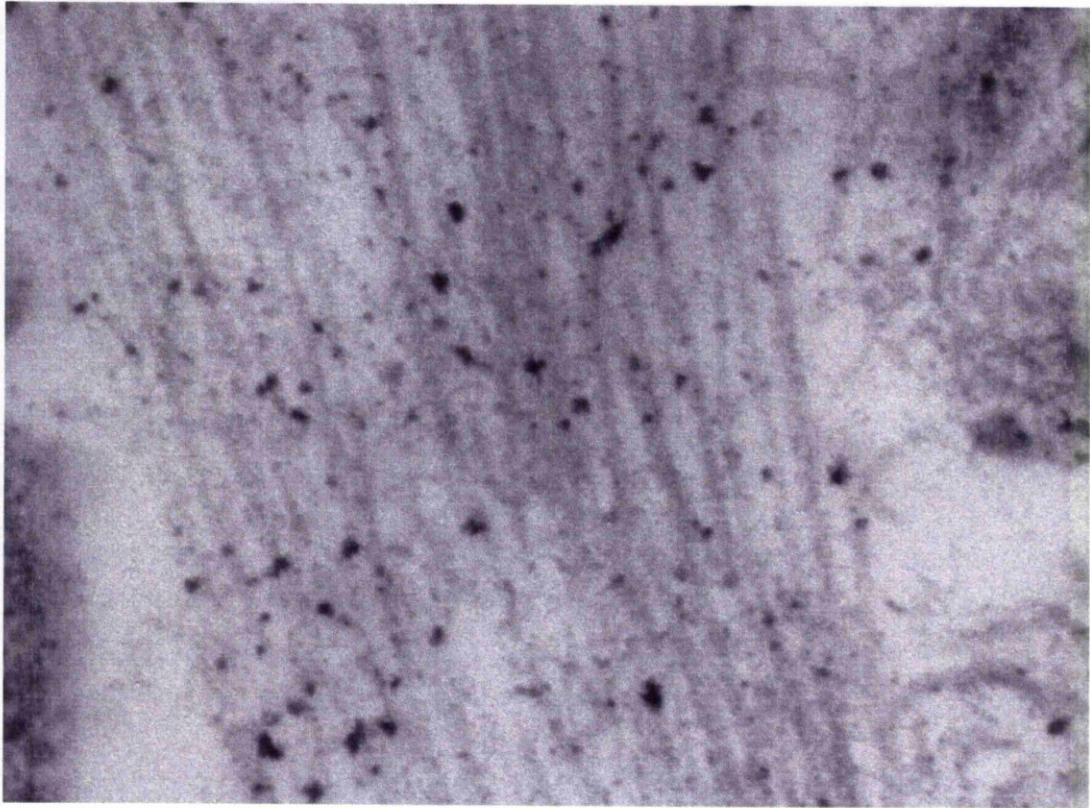


Figure 4.28:- A high power electron photomicrograph showing the presence of electron dense ochronotic deposits associated with the extracellular fibres of MG63 cells cultured in  $3.3 \times 10^{-4} M$  HGA. ( $\times 105,000$ ).

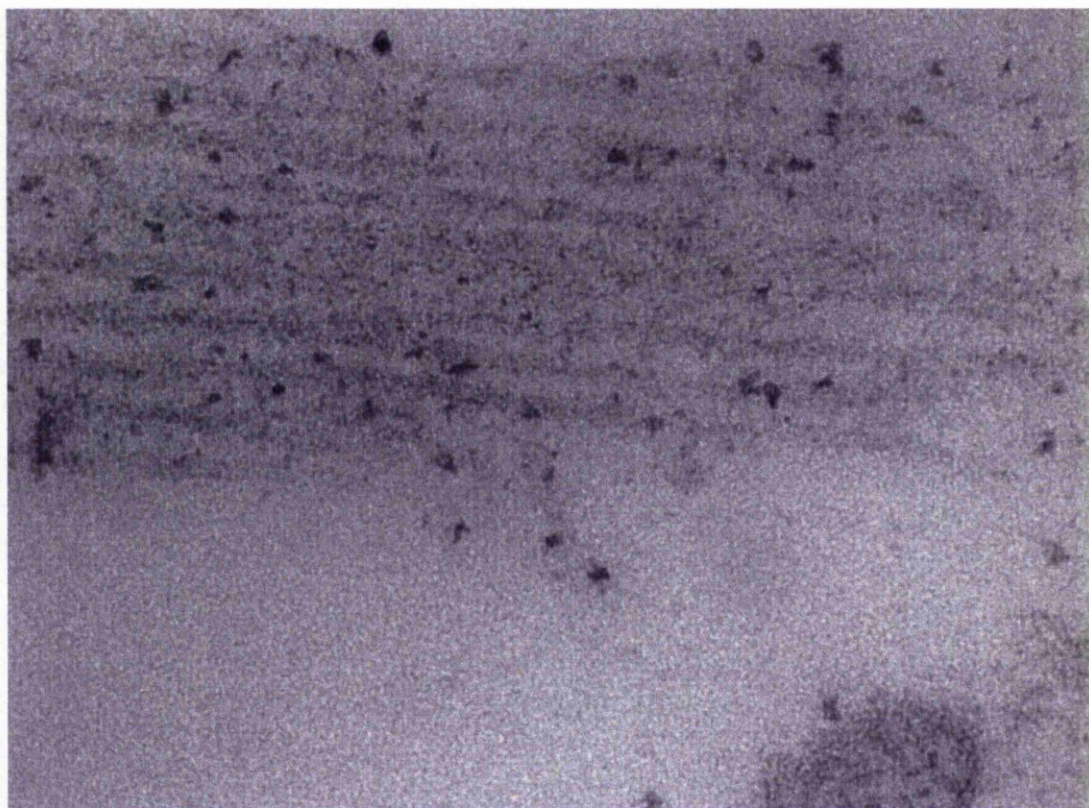


Figure 4.29:- A high power electron photomicrograph showing the close association of ochronotic pigment with extracellular fibres in the matrix of C20 cells cultures in  $3.3 \times 10^{-4} M$  HGA. (x135,000).

Examination of regions of matrix reveals transversely sectioned fibres that demonstrated a variety of cross sectional shapes including oval, hexagonal and pentagonal. Fibres showed varying sizes of electron dense ochronotic deposits. These deposits were seen around the periphery of some fibres and in the internal part of other fibre bodies. These fibres and the associated deposits were observed in both the osteo and chondro cell cultures in HGA.



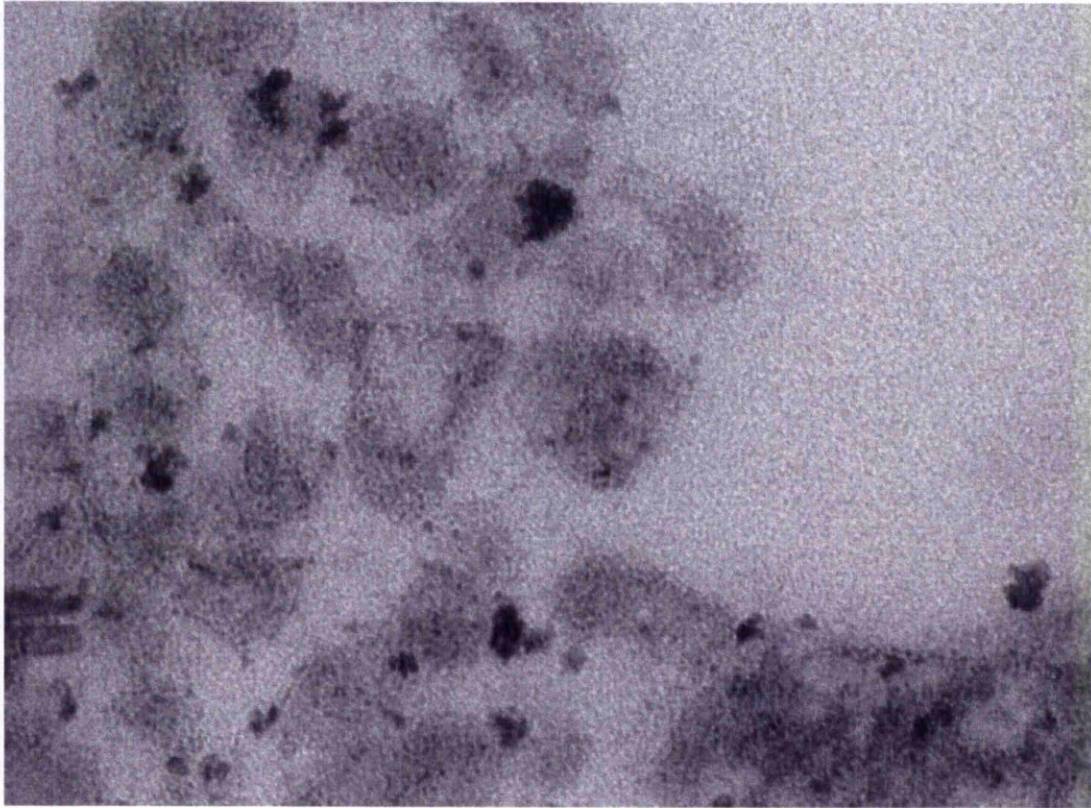


Figure 4.30:- A high power electron photomicrograph demonstrating fibres in transverse section in cultures of C20 chondrocytes cultured in  $3.3 \times 10^{-4} M$  HGA. Fibres demonstrate notable ochronotic deposits associated with there periphery and within their body. (x160,000).

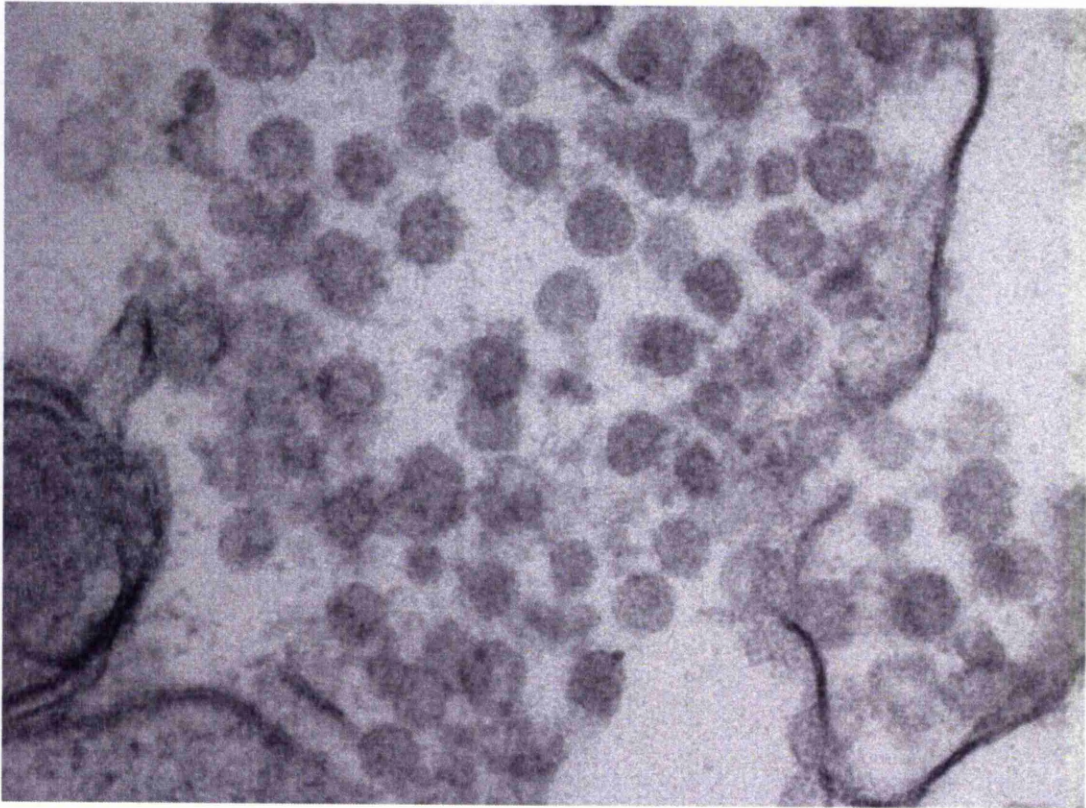


Figure 4.31:- *A high power electron photomicrograph showing fibres in cross section in cultures of SaOS-2 osteosarcoma cells cultured without HGA. (x105,000).*

One of the most striking features of these cultures under the TEM was the necrotic appearance of many cells in both the osteosarcoma (SaOS-2 and MG63) (fig. 4.32) and chondro (C20) (Fig. 4.33) cultures. These were characterised by disruption of the plasma membrane and rearrangement of the cellular organelles. These characteristics were evident of cells in all cultures regardless of the presence of ochronotic pigment within the cytoplasm or in the immediate extracellular domain.



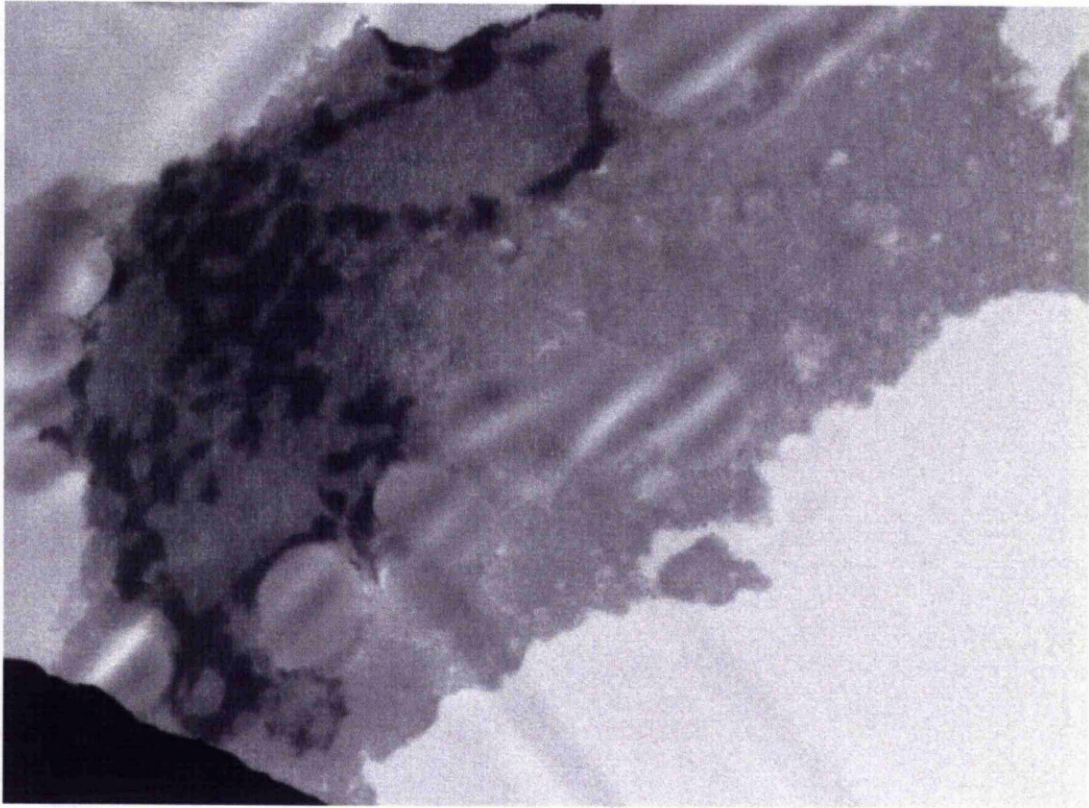


Figure 4.32:- A low power electron photomicrograph showing the rearrangement of cellular organelles and disruption of the plasma membrane representing cell necrosis in an MG63 cells cultured in  $3.3 \times 10^{-4} M$  HGA. (x8,200).

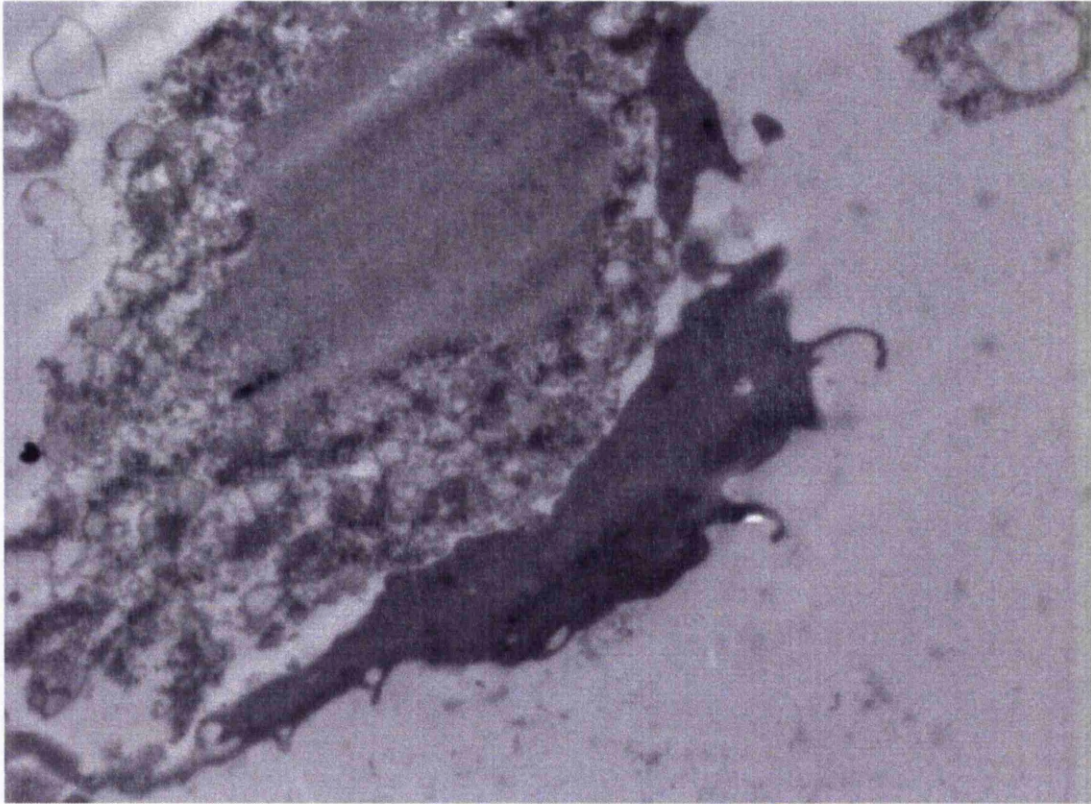


Figure 4.33:- A low power electron photomicrograph showing necrosis of a C20 cell cultured in  $3.3 \times 10^{-4} M$  HGA, with organelle rearrangement and disruption of the plasma membrane. (x6,000).



#### **4.2.7. TEM analysis of pure HGA polymer**

Pure HGA polymer, which appeared as a dark black tar like material that was insoluble in water, 70-100% ETOH and acetone was observed under the TEM. Large dark crystal like granules were observed at low magnification (Fig. 4.34). Within these deposits large even more electron dense shards were observed.

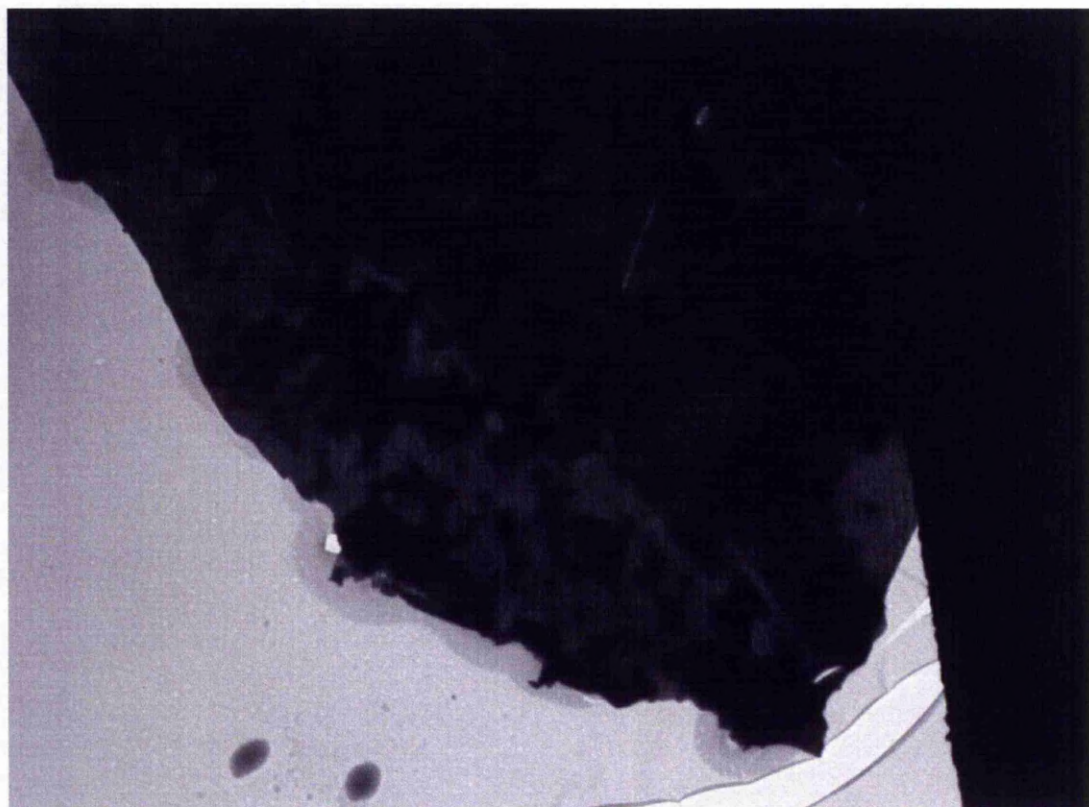


Figure 4.34:- A low power electron micrograph showing the presence of a pure HGA polymeric derivative located on the TEM grid. The large granule shows a darkened appearance with numerous large electron dense ochronotic granules located within its structure. (x1,250).

Examination of these granules at a high power revealed that dense ochronotic shards were over  $10\mu\text{m}$  in diameter. Numerous granules were located within the large less dense deposit (Fig. 4.35)

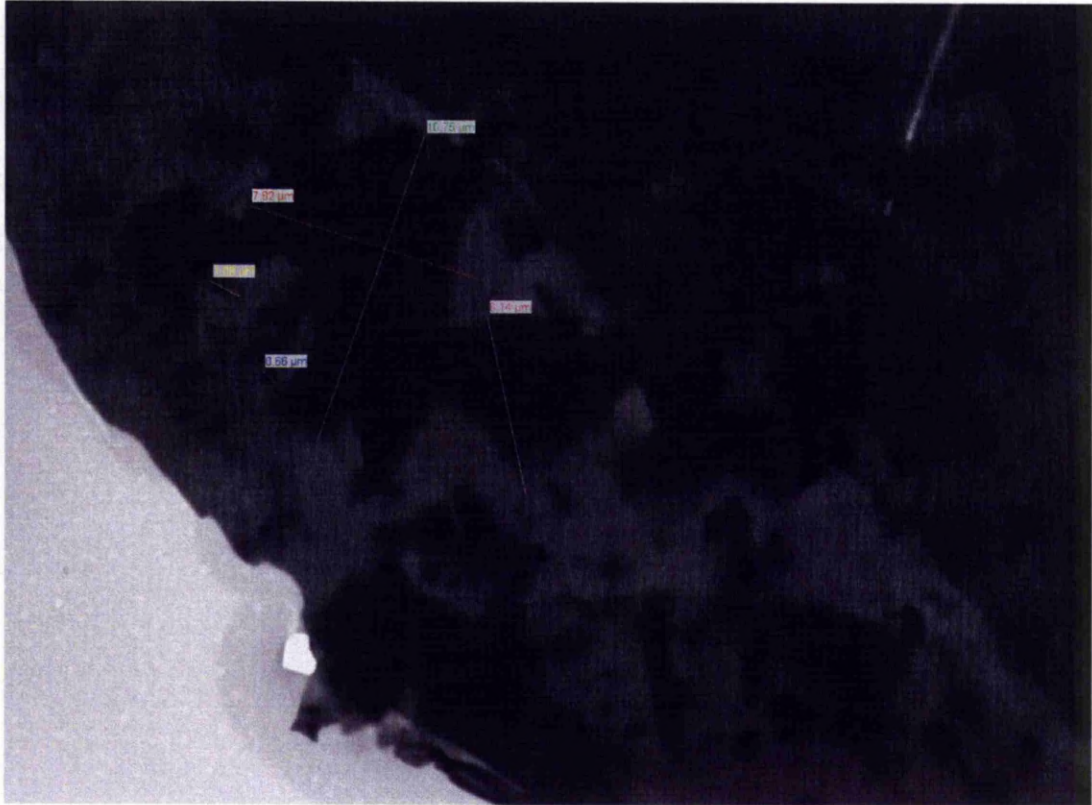


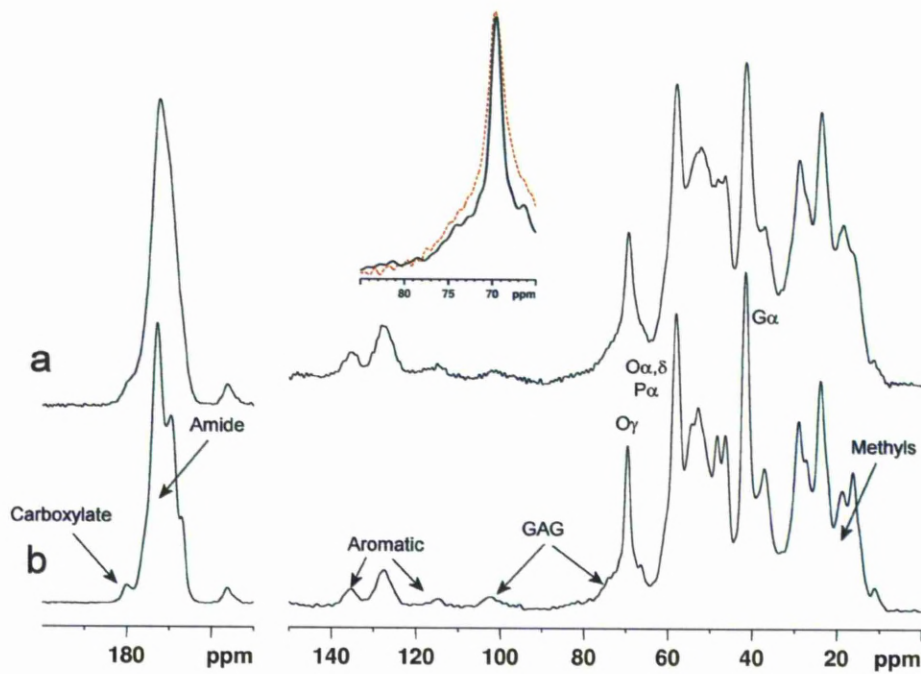
Figure 4.35:- A low power electron photomicrograph of pigment granules measuring the diameters of the more dense ochronotic deposits. Green =  $10.75\mu\text{m}$ , Red =  $7.82\mu\text{m}$ , Purple =  $6.14\mu\text{m}$ , Yellow =  $1.08\mu\text{m}$  & Blue =  $0.66\mu\text{m}$ . (x2,550).

#### **4.2.8 ssNMR of ochronotic cartilage**

$^{13}\text{C}$  solid state NMR spectra of ochronotic cartilage and non-ochronotic cartilage from an alkaptonuric patient (AKU12), are shown in Figure 4.36. Both datasets were acquired using the solid state NMR technique known as cross polarization, involving transfer of NMR intensity from highly sensitive and abundant  $^1\text{H}$  atoms to inherently less sensitive, low abundance (ca. 1.1% of all carbon)  $^{13}\text{C}$  atoms. The method greatly enhances the intrinsically weak signal from  $^{13}\text{C}$  in the sample, and in fact in many cases, such as the present one, is essential for achieving adequate signal in reasonable time. The method however is selective for molecules which are fairly rigid and therefore does not permit observation of, for instance, the abundant highly mobile glycosaminoglycan (GAG) species which are major constituents of cartilage. Indeed the spectrum of the control material is dominated by signals from rigid collagen molecules, although some GAG signals, presumably from immobilized GAG chains, are also visible. A few assignments of signals to GAG, and to specific protein functionalities (methyl groups, aromatics, amides, carboxylates) or amino acid carbons (glycine, proline, hydroxyproline) are indicated.

The most striking difference between the spectra of the control and the ochronotic cartilage is a marked broadening of most, if not all, signals in the ochronotic material. This is emphasized by the inset in Figure 4.36 which shows the signal from the  $\gamma$ -carbon atoms of hydroxyprolines (a convenient well resolved spectroscopic marker of this amino acid and therefore of collagen itself) in the control cartilage overlaid with that from the ochronotic cartilage. The most likely explanation of this generalized signal broadening is

a decrease in collagen molecular order. The precise atomic level nature of this disordering cannot yet be defined; it could be attributable to disruption of the regular tropocollagen triple helical structure by the presence of HGA and its polymeric derivative



in the matrix.

Figure 4.36: Solid state  $^{13}\text{C}$  NMR spectra acquired under cross polarization conditions from heavily pigmented ochronotic articular cartilage from an alkaptonuric patient (a), and "control" non-pigmented articular cartilage from the same patient (b). A selection of signal assignments, to collagen functional groups, amino acids and GAGs, are shown. The inset is an overlay of the hydroxyproline  $\gamma$ -carbon signal from control (black) and ochronotic (red) material; it demonstrates the increased signal linewidth in the spectrum of the ochronotic cartilage relative to control.



### **4.3 DISCUSSION**

Macroscopic examinations of the tissues from patients revealed widespread variations in the pigmentation observed in all regions. Areas show dense ochronosis whereas millimeters away demonstrate regions of no macroscopic ochronosis. This is further confirmed by the histological examination of tissues.

Ultrastructural examination of cartilage reveals that there is widespread pigmentation in the matrix, associated with collagen fibres and possibly other matrix components such as proteoglycans, which has been described previously (Mohr, 1980). However it appears that not all the matrix components when examined ultrastructurally show the features of ochronosis in tissues that appear macroscopically completely pigmented. It also appears that there are large deposits present in the matrix that do not have any distinguishable matrix components associated with them, although it may be that any nearby components have in fact been completely engulfed by polymerised pigment and thus are not distinguishable. Interestingly in the large ochronotic deposits observed in the cartilage matrix there appeared to be other crystalline material that may be other material(s) or proteins that have been incorporated into the polymerisation process and are not HGA or any of its intermediary or end stage derivatives. The process of polymerisation is clearly related to the presence of HGA, as similar electron dense deposits were not observed in the OA cartilage that was analysed as control tissue, but it is unclear *in vivo* whether other circulating or location specific molecules or proteins are incorporated into the pigment as part of the polymerisation process.

There is an interesting association between deposition of HGA pigment and calcium as observed in calculi of certain tissues and organs; such as that described in the submandibular calculi of a patient with AKU in chapter 8. More in depth analysis of kidney and prostate stones from patients with AKU has revealed that there is the usual calcium compounds present in these calculi along side an amorphous material (probably ochronotic pigment). Although it is difficult to deduce whether calculi induce pigmentation or if the alkaline conditions that the stones are constantly subjected to due to their anatomical location results in a separate polymerisation that results in deposition in these stones (Sutor, 1970). Whilst the presence of ochronotic pigment in the matrix of cartilage at the ultrastructural level is not blanket, its overall presence in the tissues is sufficient to bring about numerous pathologies; alteration of local biochemical, biomechanical factors and cellular homeostasis that result in the end stage arthropathy observed.

The association with calcium is an interesting point given that the time taken for bone to mineralise to 2/3<sup>rd</sup>s its final mineral content is only 3 weeks (Fuchs, 2008), which *in vitro* is sufficient time for osteoblast like cells to synthesise matrix which undergoes microscopical and ultrastructurally detectable deposition of pigment, although the final mineral content *in vivo* takes approximately a year to achieve. This would suggest that there maybe other protective mechanisms involved in bone, such as that the nucleation site required for initiation of deposition of ochronotic pigment is one of the first occupied by the apatite in the mineralisation of bone collagen. The examination of ligamentous capsule was consistent with previous examinations of soft joint tissues, that pigmentation

was patchy with both pigmented and non-pigmented regions (Helliwell, 2008 & Lagier, 1980). Whilst macro and microscopic observations of collagen in capsule reveal distinct differences in the presence of ochronotic pigment across the tissue, ultrastructural examination shows that there are often unaffected fibres within the heavily pigmented regions, similar to my observations in densely ochronotic cartilage. Analysis shows a previously unobserved ultrastructural feature in the capsular tissue, a gradient of pigmentation across numerous collagen fibres where pigmentation is absent on a number of fibres and across a short distance of only a few hundred nanometres pigmentation appears to initiate and then become blanket on the collagen fibers. The identification of a pattern on the fibres may suggest that there is a promoter or favourable point of nucleation which once commenced may recruit other matrix proteins into the polymeric pigment. The initiation or nucleation may occur in a manner analogous to the mineralisation which occurs on the collagen fibres of calcifying bone. The small nucleating pigment appears as a regular pattern and as such may provide clues to the exact point to which the HGA is attracted in these tissues and could be used in the future to elucidate the binding mechanism as a therapeutic target. The identification of this earliest point of binding is an important discovery as this confirms that collagen is indeed the preferential binding site, but as yet the exact site on the fibre is unknown. What is positive about this discovery is that the large amount of HGA that is present in these tissues doesn't appear to be the limiting factor in what is driving or initiating pigment binding or deposition. If this were not the case pigmentation would be much more severe and widespread over every fibre. We know that HGA is a very small and highly water soluble molecule due to its excretion in massive quantities in urine of affected individuals

(Suwannarat, 2005) as well as its presence in joint fluids, prostatic secretions (Krizek, 1971), and possibly in the cerebrospinal fluid (Liu, 2001).

Examination of spinal ligament by TEM revealed ochronosis associated with some matrix collagen fibres and intracellularly. There were appearances of elastic fibres that had electron dense deposits on parts of their periphery. This observation is in contradiction to another case where examination of arterial tissue showed no pigment associated with the elastic fibres (Gaines, 1989); although the comparison between the two tissues is not exactly the same, the elastic fibres are unlikely to be different in structure, even given that they are from different sites.

It looks as though there maybe a further process by which pigmentation and polymerisation may occur intracellularly, whether this is related to deposition on collagen fibres is difficult to determine due to the observations that are seen in surgical samples often represent the end stage of a deposition process that is not well understood. I can confirm in my observation that there are numerous deposits present within the cells that are consistent with the extracellular deposits seen on the collagen fibres.

It is clear that there are still many questions over the pigmentation that occurs in alkaptonuria. Pigmentation may occur during collagen synthesis; this would be likely to affect the final triple helix of the collagen causing changes in functionality, of both the cartilaginous and capsular tissues. This maybe supported in part by the detection of numerous pigment shards running through the body of the collagen fibres examined. It appears most likely that the collagen in tissues acts a nucleation site for pigment

deposition and polymerisation occurring on a currently unknown site or part of the fibre, consistent with my observations. This nucleation may occur at neighbouring sites and then join together to form larger deposits as seen by the bridging of shards across numerous collagen fibre cross bands.

Intracellular deposition may occur due to the presence of HGA within the cytoplasm. The prolonged presence of HGA may result in a concentration threshold being achieved within the cell causing the auto oxidation and polymerisation of HGA to its pigmented polymer. This would be consistent with the auto oxidation of other dihydroxy aromatic compounds such as tyrosine and L-DOPA (Foster, 1950). Questions must be asked as to why not all collagen fibres in cartilage and capsule are affected. The presence of HGA cannot be the limiting factor, there must be other local factors which are limiting to the deposition of pigment. One such limit may be the availability of nucleation sites. It is clear from my evidence that there is more than one site of initiation and deposition per collagen fibre in tissues as demonstrated by the numerous deposits on a single fibre. This would suggest that there are preferential sites of nucleation and possibly local factors within tissues such as pH, or presence of other currently unidentified factors that may play a role in promoting deposition. Numerous decades of exposure of collagen fibres should present sufficient time for deposition to occur on all fibres to some extent. This may not be the case if pigment is broken down within the tissues by a currently unidentified mechanism, or there are local protective mechanisms. Similar to those which protect mineralised collagen fibres as a whole. However other evidence in this thesis

suggests that the breakdown of pigment, particularly when in its bound form to matrix proteins is not possible.

Pigmentation in cells of different tissues, not just those of joint tissues, for example the urinary system supports the suggestion that pigmentation may occur when local concentrations of HGA pass a specific threshold. Alternatively the local factors such as the pH in some tissues, such as the urinary system, or prostate may be alkaline enough to promote pigmentation in a manner parallel to the oxidation that occurs in urine (Krizek, 1971).

Examination of the ultrastructural appearance of *in vitro* cultures reveals widespread pigmentation of matrix fibres in both osteosarcoma and chondrosarcoma cultures, although my previous data shows that in *in vitro* cultures the chondrosarcoma cells show more rapid and severe deposition, this cannot be distinguished in TEM examination. It is suggested that pigmentation in tissues takes many years and that there may be protective mechanisms, which with the ageing process become less efficient or cease to function. In the osteosarcoma cultures the pigmentation of the synthesised collagen fibres, presumed to be type I, but may also be type V or XI (Fernandes, 2007), shows that the protective mechanisms *in vivo* are not present in these cultures – one of which may be mineralisation – as the matrix of these cells does not mineralise in our routine culture media, but may also be other currently unidentified factors. The confirmation of pigmentation of the collagen fibres in these cells is a promising tool for further investigations into the pathogenesis of ochronosis, as the earliest points of detectable



ochronosis are the time when treatment would need to be administered to prevent further pigmentation. Consistent with the observations *in vivo* the specific nucleation sites for the pigment appear to occur multiple times along individual fibres *in vitro*.

This chapter describes for the first time the earliest signs of pigment deposition in tissues from patients with AKU, as seen in the cartilage and ligamentous capsule. This is also the first description and analysis of ultrastructural deposition in an *in vitro* model of ochronosis. Here I demonstrate a clear pattern of binding of ochronotic pigment to collagen fibres. Furthermore we show the earliest nucleation point of pigment deposition on these fibres. I also confirm the presence of pigment in fibroblasts at the electron microscopic level. It is clear that whilst there is a vast knowledge of the end point of the disorder there is little to suggest a clearer understanding of the early stages and mechanisms of the disorder. These results represent a vast advancement in this area. Further investigations using this model may provide some information about whether collagen is pigmented pre or post assembly and whether fibres are pigmented prior to their excretion from the cell. There is evidence in both these cultures that the fibres are pigmented in fibro-positor like structures in these cultures which would indicate that pigmentation may occur as cells are excreting fibres from their cell. Whilst pigment is seen in the cells in both cultures it is difficult to ascertain whether these intracellular deposits are associated with fibres.

It should be noted that the ability to obtain high quality sections for TEM imaging of bone (undecalcified) and ochronotic cartilage are extremely difficult due to the brittleness

of bone tissues due to the presence of mineralised matrix in bone and the ochronotic pigment in cartilage which causes fracturing and shattering of sections, even when cut on a diamond knife. Furthermore, the ochronotic cartilage appears highly hydrophobic when floated out on to water making it difficult to float onto copper grids for imaging, should sectioning be successful. OA cartilage sections did not exhibit similar hydrophobia when being floated out for sectioning.

**5. The role of calcified cartilage and subchondral bone in the initiation and progression of ochronotic arthropathy in alkaptonuria**

## **5.1 INTRODUCTION**

As described in chapters 3 & 4 of this thesis the striking results of numerous years of exposure to HGA in the joint tissues can be seen. Over many years, HGA polymerises and becomes deposited by a currently unknown mechanism in these collagenous tissues, a process termed ochronosis (O'Brien, 1963, Helliwell, 2008, Zannoni, 1969). Recent work has shown, as described in chapter 4, that there is pigmentation associated with the periodicity of fibrillar collagen, possibly suggesting that there is a preferential binding site for the ochronotic pigment on the collagen fibres (Taylor, 2010). Although cartilage is a preferential site for ochronosis, pigmentation is observed in other tissues, such as the submandibular gland, even in the absence of cartilaginous matrices (Helliwell, 2008, Taylor, 2010, Krizek, 1971). With increased exposure to HGA and continued polymerisation in joint tissues, the end stage of the disorder is a severe osteoarthropathy. Although there is no proven link between the presence of HGA and shortened lifespan, the quality of life is severely affected and the only current treatments to have any proven clinical benefit are either liver or renal transplantation or more commonly joint replacement surgery (Introne, 2002, Kobak, 2005, Araki, 2009, Spencer 2004, Phornphutkul, 2002). This chapter, describe the progression of articular cartilage degeneration in ochronotic arthropathy from initiation of pigmentation to complete joint failure. It has been previously suggested that the presence of HGA alone is not the determining factor in pigment deposition; Chapter 8 of this Thesis (Taylor, 2010). Although AKU is rare there are numerous publications detailing the end stage of the disease resultant from pigment deposition and recently the earliest observed signs of ochronosis associated with collagen fibres have been seen (Taylor, 2010). However little is known about the mechanism(s) involved in progression from this initiation to the clinical end point. This Chapter provides evidence that intact tissues are initially resistant to

pigmentation and that focal cellular and extracellular matrix abnormalities cause joint tissues to be susceptible to pigmentation. Pigmentation initially manifests at the boundary of the subchondral bone and calcified cartilage before proceeding towards the articular surface.

## **5.2 RESULTS**

### **5.2.1. Macroscopic**

Examination of samples revealed a spectrum of pigmentation from focal ochronosis to complete pigmentation across all zones of cartilage (Table. 1). In the samples that were not completely pigmented, the focal deposits were in regions known to be subjected to the greatest load bearing during locomotion, e.g. knee medial tibial plateau compared to lateral. (Andriacchi, 2009) It was also observed that pigmentation of the articular surface was central rather than peripheral in advanced ochronosis (Chapter 3, Fig 3.12 in particular). These are the region(s) associated with initiation and severe pathology in primary knee osteoarthritis (Pelletier, 2007). The medial tibial plateau of heavily pigmented samples showed high mottling and fissuring of the articular surface (Fig. 3.12 in chapter 3).

### **5.2.2. Material Properties of cartilage samples**

Surgical dissection of cartilage from the joint specimens revealed an interesting phenomenon. Dissection revealed that the pigmented cartilage was difficult to remove from the bone and was much stiffer than non-pigmented cartilage (findings that were subsequently confirmed by mechanical testing – Fig. 5.2). This was even evident when compared to aged osteoarthritic cartilage as well as healthy cartilage. Alongside this numerous orthopaedic surgeons commented on the “brittle and stubborn” properties of the ochronotic cartilage. In some instances it was noted that the ochronotic cartilage presented more resistance than the bone which it was overlying (n=5).



### **5.2.3. Mechanical loading of cartilage**

Routine processing of samples for SEM revealed that the enzymatic action of Tergazyme (alkaline bacterial pronase), which effectively digests non-calcified ECM, was unable to break down the pigmented hyaline articular cartilage (Fig. 5.5).

#### **5.2.3.1. Mechanical loading**

Loading of articular cartilage cubes from freshly surgically resected medial femoral condyles revealed large differences in Young's modulus of heavily pigmented vs nonpigmented and osteoarthritic cartilage (Fig. 5.2). The mean Young's modulus of pigmented cartilage showed a more than 5x greater modulus than cartilage which was non-pigmented (136MPa vs 22MPa). Similar differences in the Young's modulus between the ochronotic and osteoarthritic cartilage were also observed. This demonstrates the vast increase in stiffness attributed to the presence of ochronotic pigment in the cartilage of patients with ochronotic osteoarthropathy. The difference in stiffness of these tissues was significant,  $p < 0.01$  (Fig.5.2). Interestingly there was no significant difference between the non-pigmented alkaptonuric cartilage and the osteoarthritic cartilage.

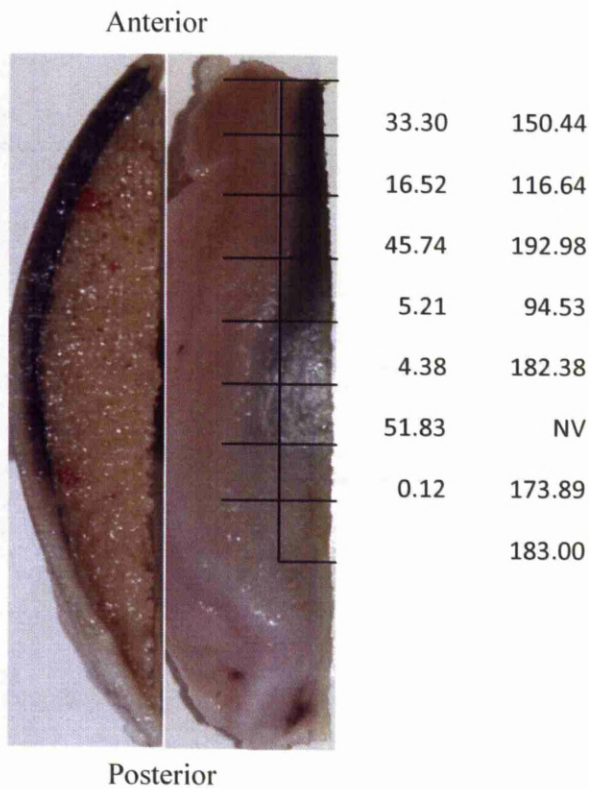


Figure 5.1:- Macroscopic images and raw values demonstrating the location from which the cartilage samples were removed from a medial femoral condyle and mechanically tested in order to determine Young's modulus. NV = no value. Left: cut surface of medial aspect of medial femoral condyle demonstrating the distribution of pigment within the cartilage matrix. Right: view of articular surface of medial femoral condyle demonstrating the distribution of ochronotic pigment.

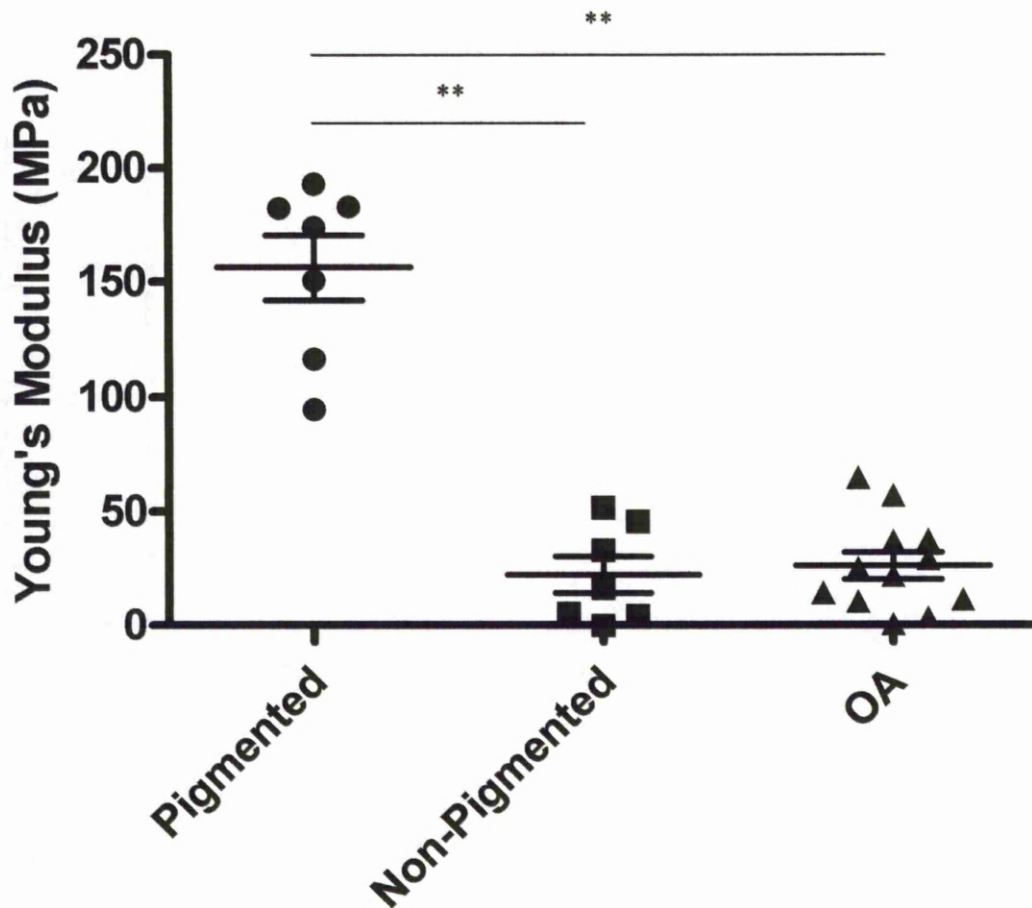


Figure. 5.2: Graph showing Young's modulus of pigmented, non-pigmented and osteoarthritic cartilage. Graph demonstrating the differences in Young's modulus of pigmented, non-pigmented cartilage and osteoarthritic cartilage. Differences between the pigmented vs. non-pigmented, and pigmented vs. osteoarthritic were highly significant.  $p < 0.01$ .

#### **5.2.4. Enzymatic digestion of cartilage**

Attempts were made to culture chondrocytes from samples obtained at surgery. These were digested out from the matrix as described in Chapter 2. Samples were treated with hyaluronidase, trypsin and collagenase. AKU cartilage was predominantly ochronotic, with a few regions that were relatively normal in colour. The OA cartilage showed no ochronosis (Fig.5.3). Following

incubation in the enzyme solutions the ochronotic cartilage showed no change in its appearance or presence on the culture dishes. Whereas the OA cartilage matrix had been completely digested and chondrocytes liberated from their matrix (Fig. 5.4).

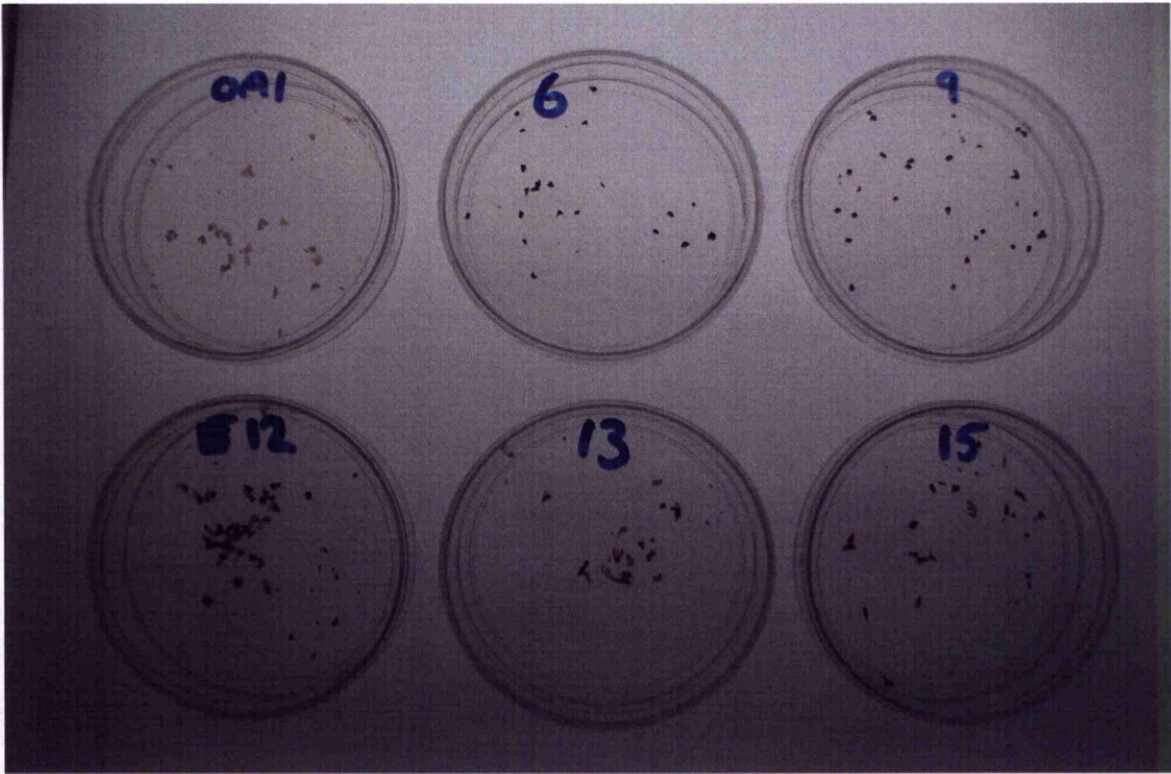


Figure 5.3:- *Photograph showing the appearance of cartilage shards prior to addition of proteolytic enzymes required to release cells from the cartilage matrix in order to culture in monolayer. Samples are as follows (top left to bottom right): OA1, AKU6, AKU9, AKU12, AKU13, AKU15.*



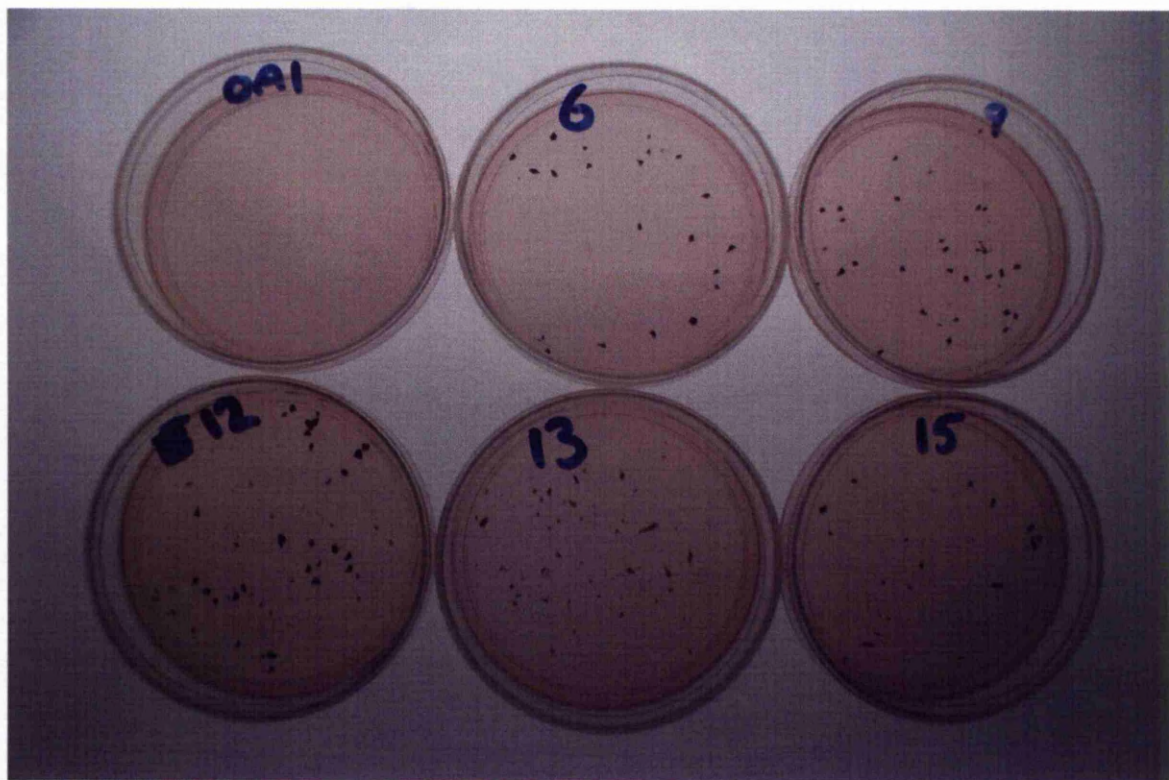


Figure 5.4:- Photograph showing the appearance of cartilage shards following the addition of proteolytic enzymes required to release cells from the cartilage matrix in order to culture in monolayer. Samples are as follows (top left to bottom right): OA1, AKU6, AKU9, AKU12, AKU13, AKU15. Note the absence of cartilage shards from the OA1 dish, demonstrating the function of enzymes on non-ochronotic cartilage.

As part of routine preparation for SEM analysis (see chapter 2) samples were treated with Tergazyme, an alkaline bacterial pronase which routinely removes all non-mineralised matrices and cells from tissues. It was surprising to observe that the ochronotic cartilage was impervious to the action of this solution, whereas non-ochronotic alkaptonuric cartilage and that from OA samples is routinely digested away (Boyde, 2003).

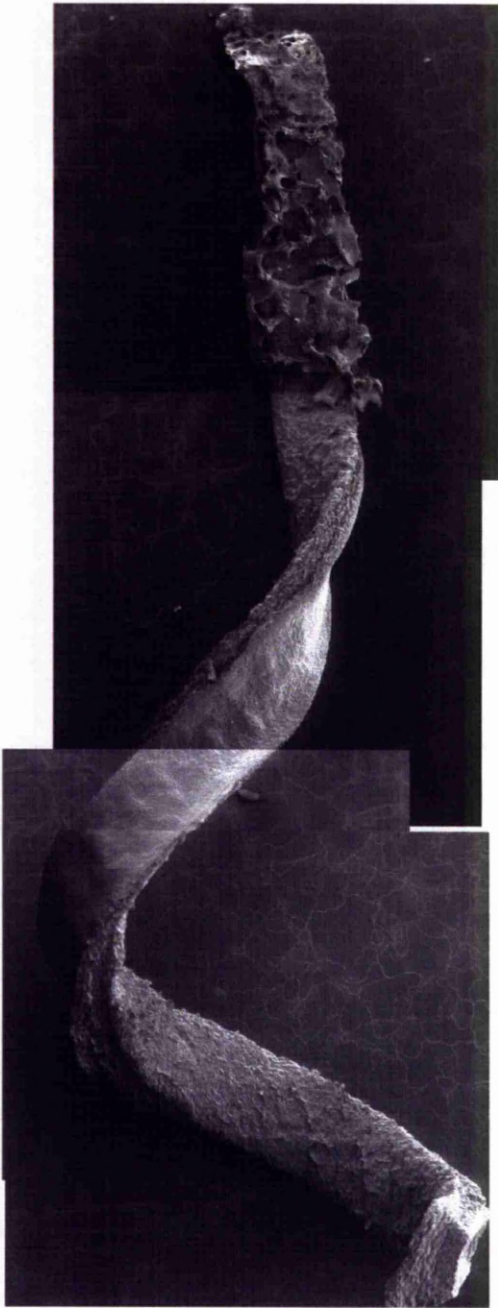


Figure 5.5:- An SEM photomicrograph (10x) showing the sliver of ochronotic hyaline articular cartilage that was removed from an ochronotic femoral head (AKU1). This strip was impervious



*to Tergazyme action. The smooth surface seen is that of the articular surface. The rough side is the subchondral side.*



Figure 5.6 : *A high magnification (20x) SEM photomicrograph showing the subchondral side of the strip of ochronotic hyaline articular cartilage which fractured off from the underlying calcified matrix of an ochronotic femoral head (AKU1). Note that the chondrocyte morphology can clearly be seen (within square). This would not normally be evident in non-ochronotic*

*cartilage because the pigment would not be there to give an outline of the lacunae, but also the matrix would have been digested away.*

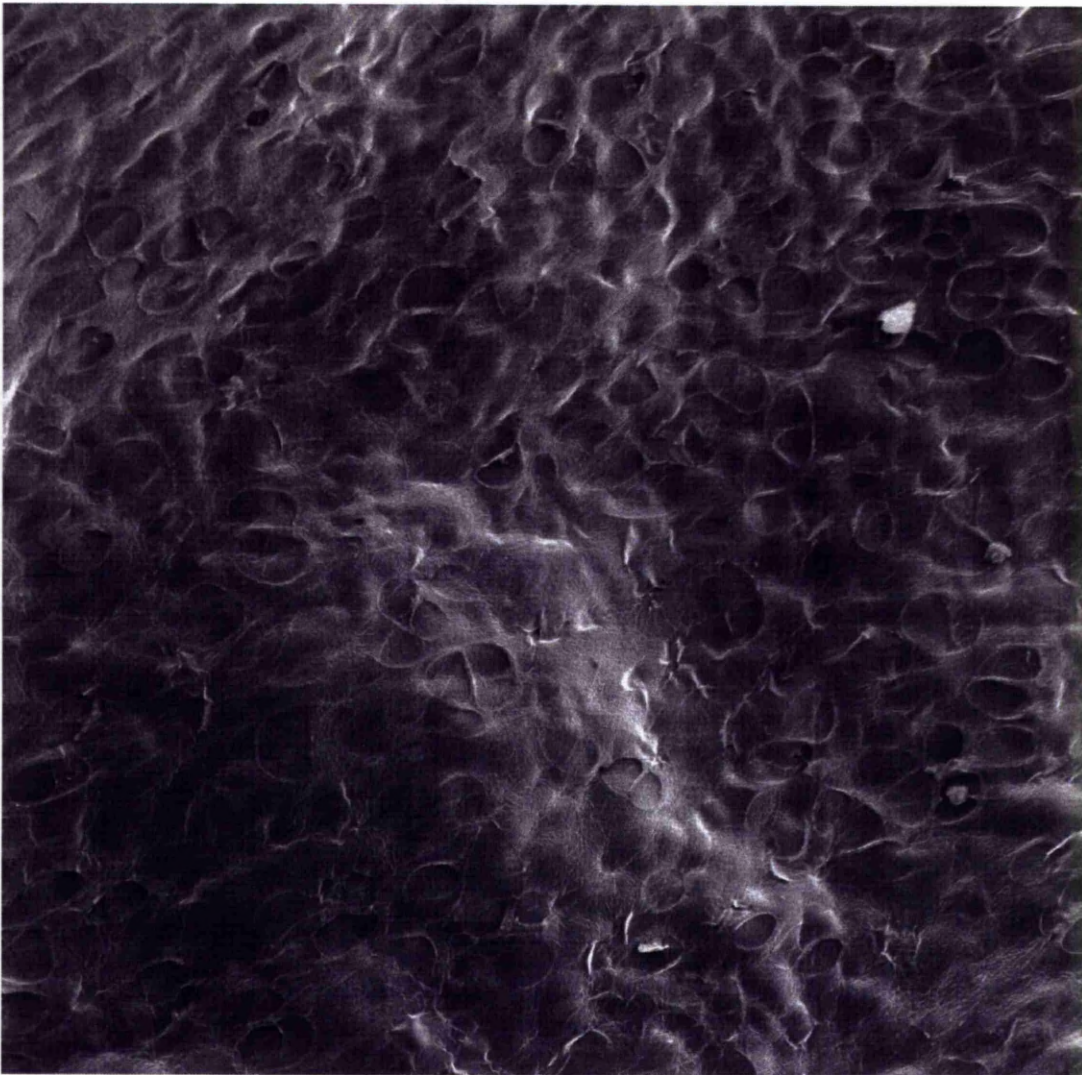


*Figure 5.7:- A higher power (100x) SEM photomicrograph showing the location and morphology of chondrocytes located in the ochronotic cartilage matrix.*

### **5.2.5 Histological observations**

Histological analysis of H&E stained sections confirmed macroscopic observations regarding the presentation of pigmentation. There was a large variation in pigmentation across samples and within samples. Mildly pigmented samples showed that pigmentation was associated with individual chondrocytes in the calcified cartilage and included both intracellular and pericellular pigmentation of the chondrocyte lacunae and territorial matrix (Fig. 5.8a & c). At this stage, there was no pigmentation in other (more superficial) cartilage zones and little evidence of advanced arthritic changes at the articular surface (Fig. 5.8a & b).



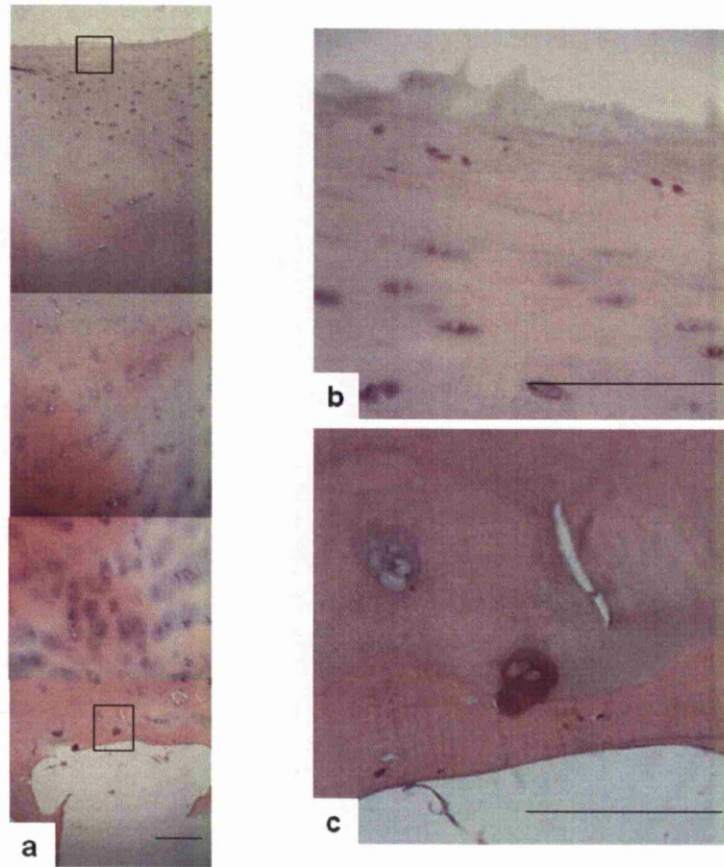


**Figure 5.8:-** Photomicrographs of articular cartilage in AKU sample showing the earliest detectable pigmentation in the calcified cartilage. (a) A merged stack of 4 photomicrographs showing the full thickness of articular cartilage. Note the pair of chondrocytes and their territorial matrix on the bone/calcified cartilage boundary with ochronotic pigmentation of the matrix. The rest of the articular cartilage shows no ochronotic pigmentation and no microscopical evidence of degeneration. H&E. Bar = 50 $\mu$ m. (b) Higher power view of articular surface of cartilage demonstrating healthy chondrocytes. Bar = 20 $\mu$ m. (c) Higher power view of pigmented chondrocytes in calcified cartilage showing the initiation of ochronosis in their territorial matrix. Bar = 20 $\mu$ m.

Samples with more widespread ochronosis had a greater frequency of chondrocyte intracellular pigmentation in the calcified cartilage and territorial matrix. With the widespread ochronosis, pigment was absent from the interterritorial matrix. As pigmentation of chondrocytes and territorial matrix became more widespread, there was still no evidence of pigmentation in the hyaline cartilage and at the articular surface. When, the pigmentation front extended into the non-calcified hyaline cartilage matrix, the deep and middle zones had blanket pigmentation and the territorial matrix in these zones was even more intensely pigmented. However, alongside this widespread pigmentation the interterritorial matrix of the calcified cartilage matrix was unpigmented. Pigmentation was also absent from the superficial zone and articular surface. Hyaline cartilage began to show fissuring at the deep surfaces close to the subchondral interface. Pigmentation of the interterritorial matrix and the articular cartilage was only observed in samples with the most advanced and widespread pigmentation. In addition, the most pigmented samples had dense pigmentation of the extracellular matrix in all deep and middle zones of the hyaline cartilage. There was no calcified cartilage present and the subchondral bone was absent in almost all of the section in these most pigmented samples. In regions where there was subchondral bone still present, osteoclasts could clearly be seen resorbing the thin bone matrix to the point of contact with the pigmented hyaline articular cartilage (Fig. 5.9). Pigmented cartilage was adjacent to, and impacted onto, the trabecular structures which were thin and showed evidence of osteoclastic resorption. The pigmentation in the calcified cartilage was consistently associated with the territorial matrix and at no stage showed the pattern of blanket pigment deposition observed in the non-calcified hyaline cartilage matrix.

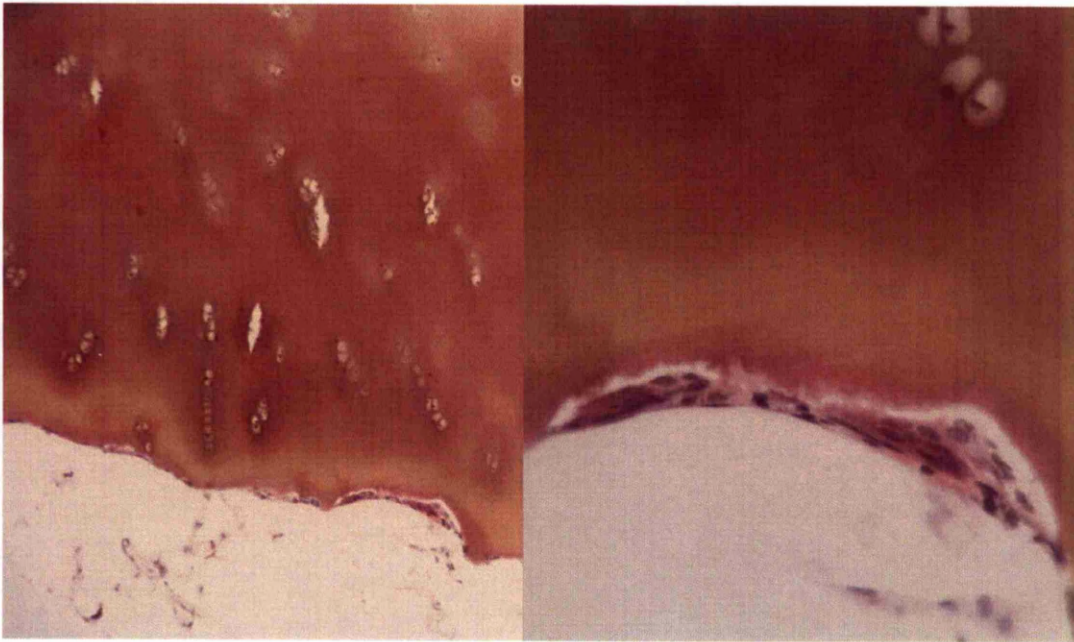


Figure 5.9:- *Pigmentation in the full depth of the articular cartilage. (left) Calcified cartilage and subchondral bone plates have been almost completely resorbed. Osteoclasts can be seen resorbing the last remnants of the subchondral bone plate. (right) Higher power view of osteoclastic resorption of subchondral bone and calcified cartilage up to the pigmented hyaline cartilage. Bar = 50 $\mu$ m.*

There was a general lack of pigment in bone matrix in all samples but intracellular ochre-coloured deposits were observed in osteocytes and their lacunae (Fig. 5.10 & 5.11). Pigmentation observed in osteocytes was present in two types; granular and blanket pigmentation. Pigmentation could also be seen in the canalicular network. In some sections, osteoclasts were seen engulfing pigmented osteocytes as they were released from the surrounding matrix, (Fig. 5.11). Pigmentation was seen in the osteocytes from all samples showing cartilage matrix pigmentation.



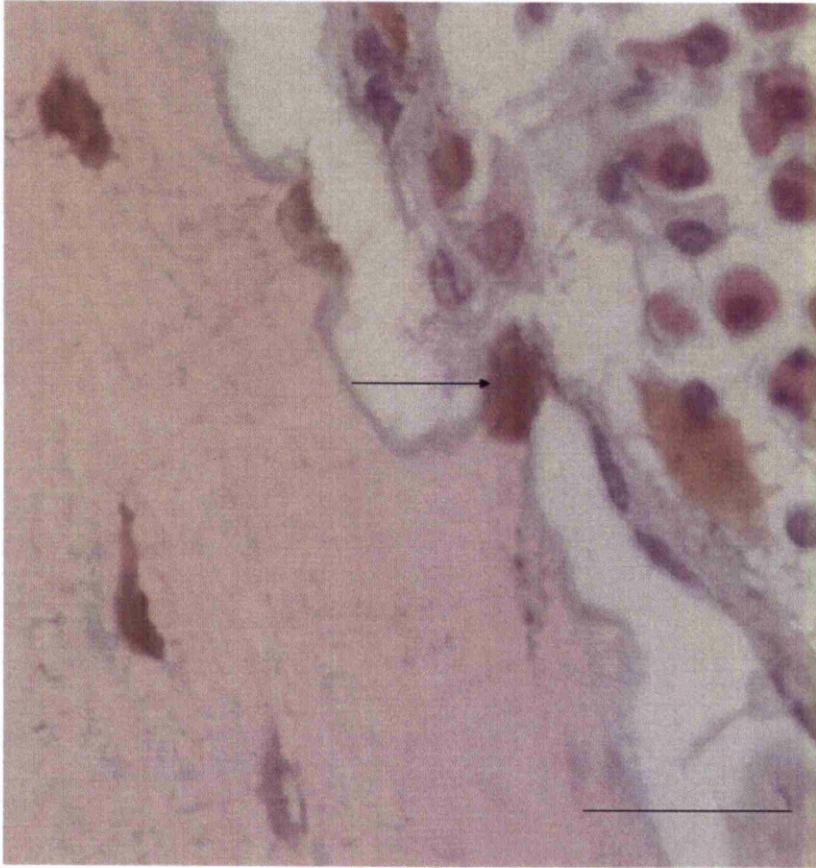


Figure 5.10:- *Osteocyte liberated from the mineralised matrix following osteoclastic action on the surrounding matrix (arrow). Bar = 20µm (AKU1).*



Figure 5.11:- *Photomicrograph showing the overview of bone matrix with numerous dead and necrotic osteocytes in the bone matrix, demonstrating granular intracellular pigmentation. In the marrow space numerous multinuclear cells, presumed to be osteoclasts can be seen, some of which display large intracellular ochronotic deposits. Numerous liberated pigmented osteocytes can be seen in the marrow space.*



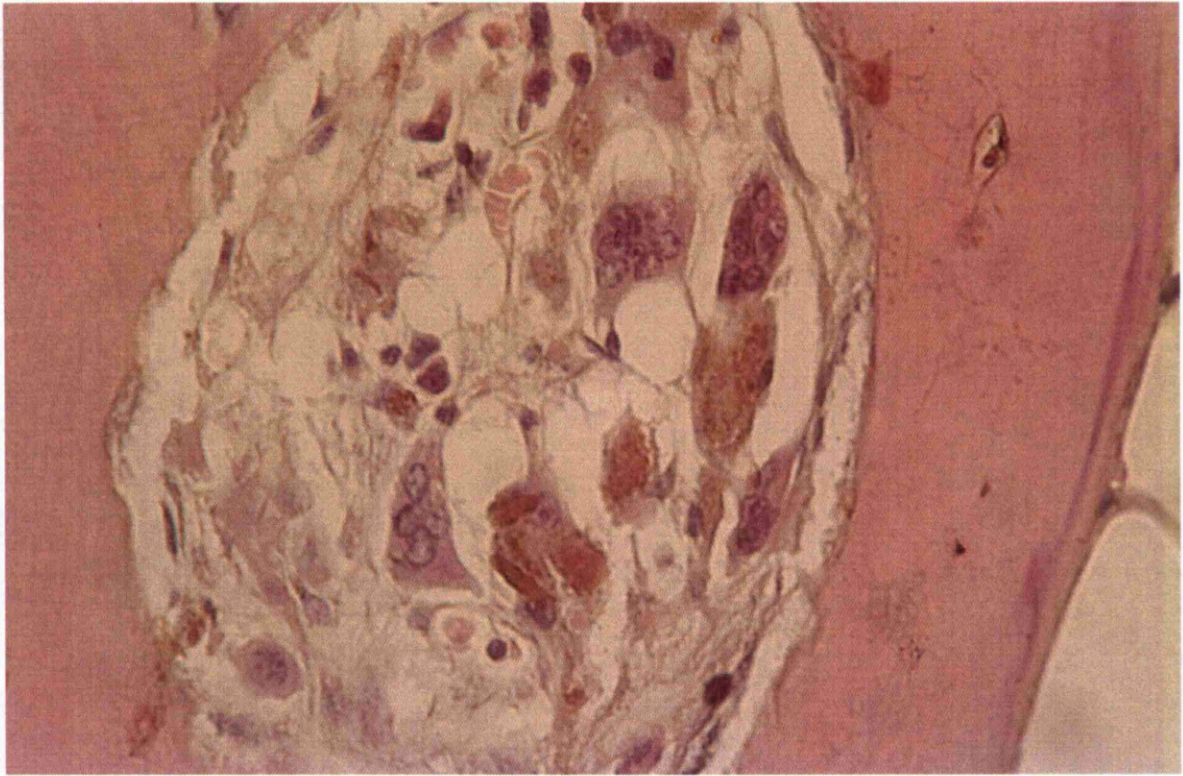


Figure 5.12:- *Photomicrograph showing numerous multinuclear cells in the marrow space. One of which shows multiple ochronotic deposits within its cytoplasm, some of these appear to be pigmented osteocytes.*



Figure 5.13:- *Multinuclear cells engulfing pigmented osteocytes following liberation from the resorbed matrix (arrows). Bar = 20µm.*

In samples with advanced ochronosis, shards of pigmented cartilage were embedded in the marrow space cavity between trabeculae. The ochronotic fragments were surrounded by fibrous tissue, mononuclear and multinuclear cells all showing intracellular ochronotic pigmentation. Shards of pigmented cartilage, lost from the articular surface, could be observed embedded in synovium; this was present in 8 out of the 8 samples. (Fig. 5.14 & 5.15).



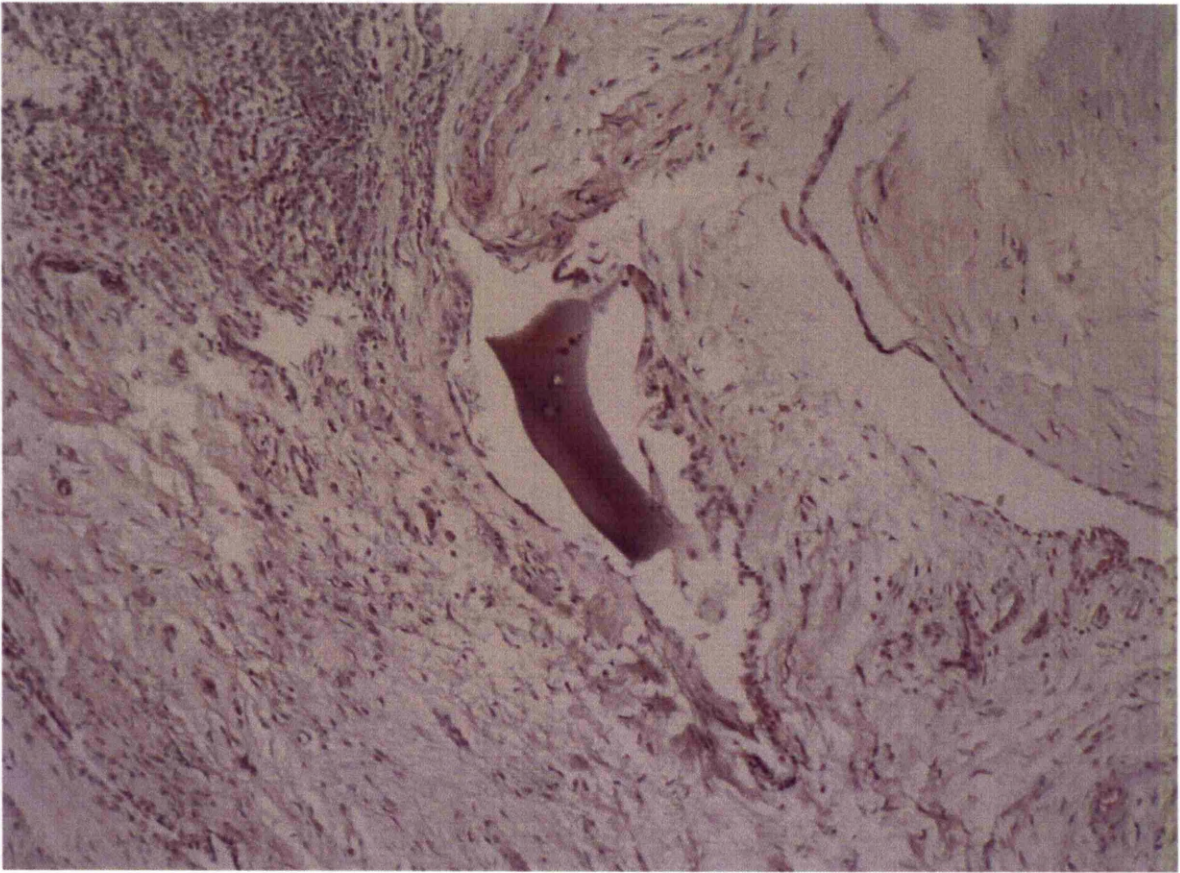


Figure 5.14:- *A large piece of ochronotic cartilage is seen embedded in inflamed synovial tissue. Note the chondrocyte lacunae present in the ochronotic matrix.*



Figure 5.15:- *A high power photomicrograph showing the presence of another ochronotic shard of cartilage located in the synovial tissue. Pigmented chondrocytes can be seen located within their lacunae in the ochronotic matrix.*

Examination of the most severely pigmented samples revealed that there were two types of pigmentation in the matrix (Fig. 5.16). There was blanket pigmentation in the deep zone, which was more intense around the territorial matrix (Fig. 5.16d). In some samples in the superficial and middle zones, there was a granular rather than blanket pigmentation with a ground pepper-like appearance (Fig. 5.16c). This was also observed in the chondrocyte lacunae and the chondrocyte cytoplasm (Fig. 5.16).



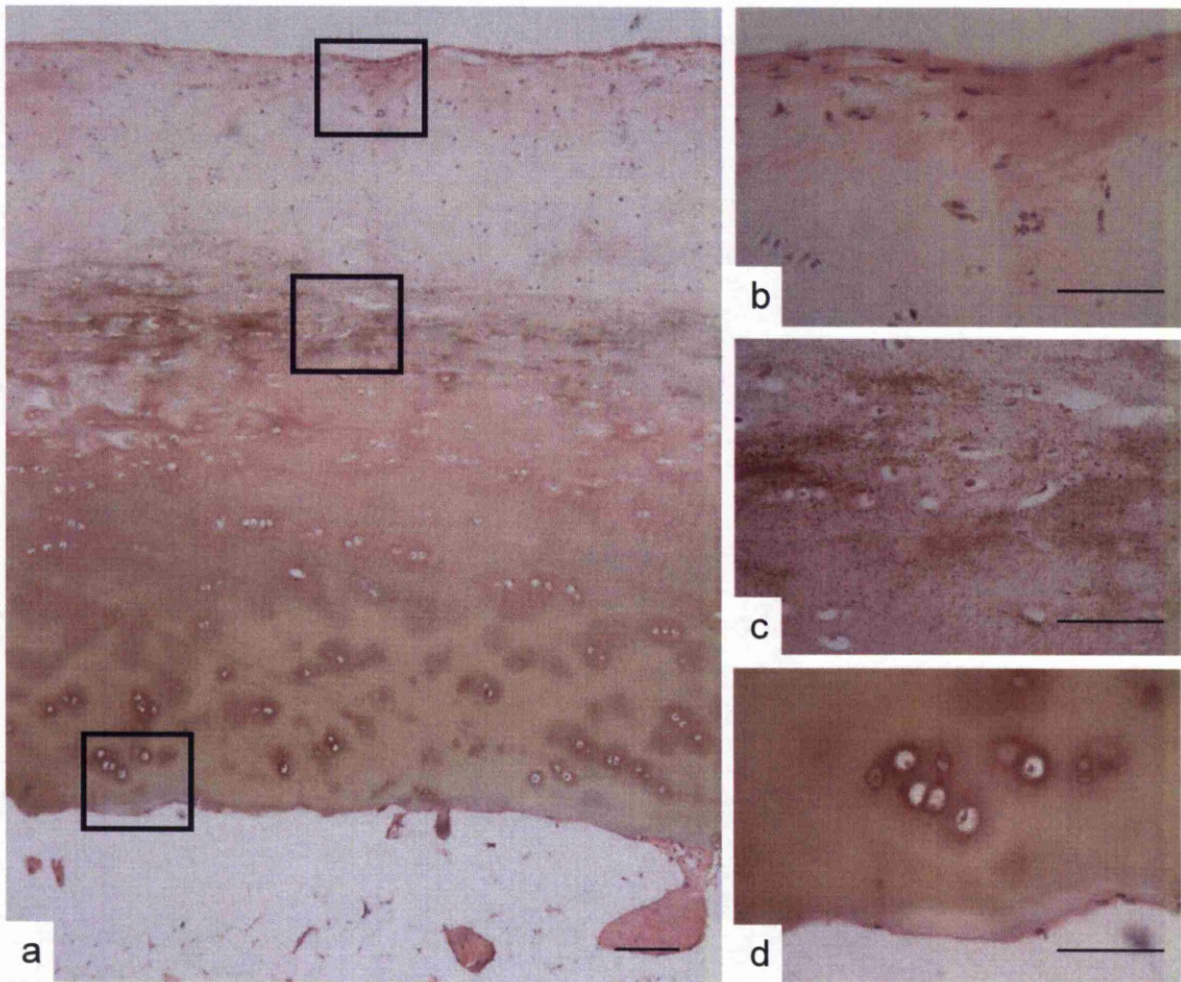


Figure 5.16:- (a) Overview of full thickness depth of AKU femoral condyle showing ochronotic pigmentation at the deep and middle cartilage layers. Bar = 50 $\mu$ m (b) High power photomicrograph of the articular surface showing the absence of pigmentation from the matrix. Chondrocytes show dense intracellular ochronotic granules. Bar = 20 $\mu$ m. (c) High power photomicrograph of the middle zone showing dense ochronotic granular pigment in the extracellular matrix. Chondrocytes show intracellular deposits. Bar = 20 $\mu$ m. (d) Blanket deposition in the extracellular matrix of the deep zone, chondrocytes show intracellular pigmentation, some are also necrotic. Bar = 20 $\mu$ m. H&E. Necrotic cells were identified by their shriveled and homogeneous glassy appearance. Their nuclear and cytoplasmic components are difficult to distinguish.

Pigmentation of the chondrocytes, osteocytes and osteoclasts was widespread in heavily pigmented samples. Interestingly there was also pigmentation observed in mononuclear cells within the marrow space and in the synovial tissues (Fig. 5.17). These pigmented mononuclear cells were seen alongside pigmented fibroblastic cells in the fibrous tissues. Also within the marrow space ochronotic deposits were observed associated with the adipocytes and their collagenous matrices (Fig. 5.17 & 5.18).



Figure 5.17: *High power photomicrograph of the marrow space and bone domain showing numerous pigmented mononuclear cells located within the fibrous tissue of the marrow space. Superior to this multinuclear cells can be seen engulfing pigmented ochronotic cartilage, some of which show pigmented osteocytes and other ochronotic deposits in their marrow space.*



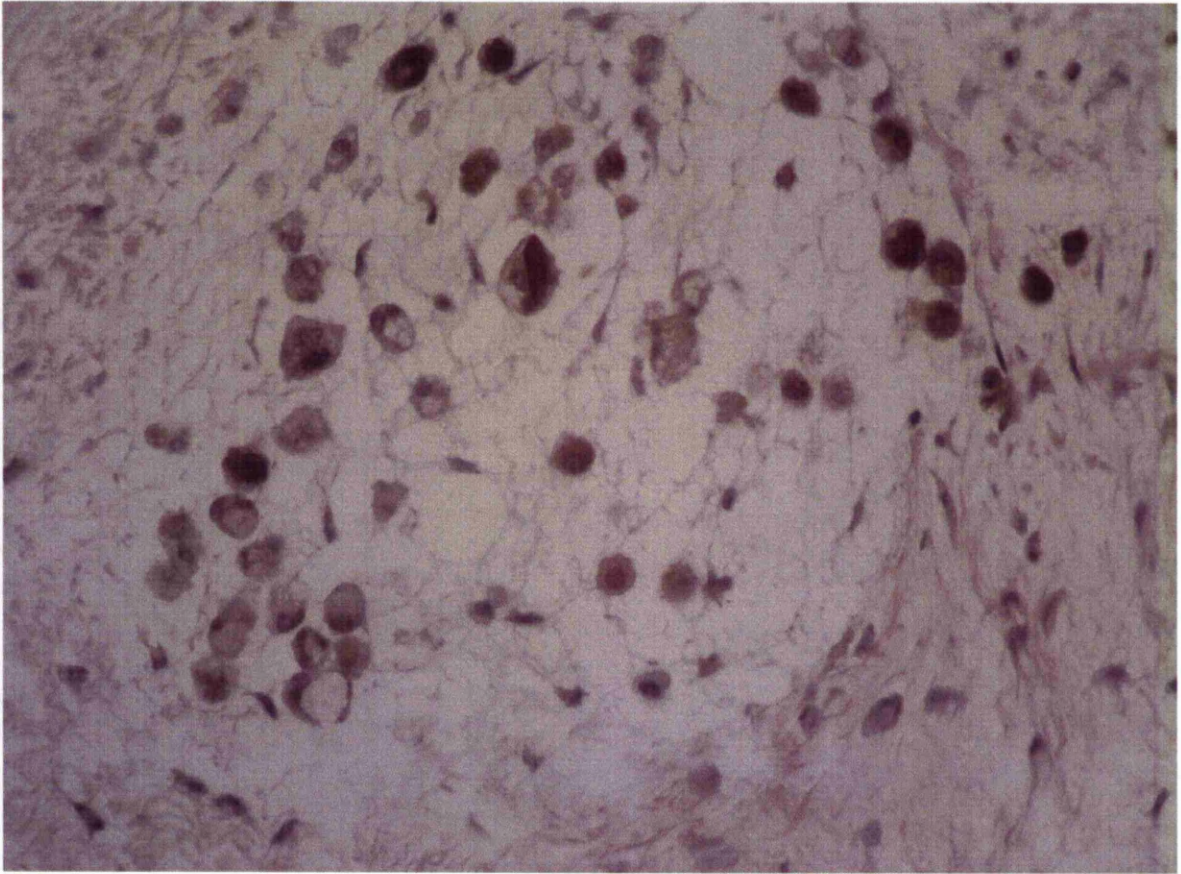


Figure 5.18: *Photomicrograph showing numerous pigmented and partially pigmented mononuclear cells in the synovial tissue. The cells appear pigmented in the absence of detectable pigment associated with the surrounding collagenous matrix.*



Figure 5.19:- *Photomicrograph showing the adipocytes and their collagenous matrices in the marrow space. Numerous ochronotic deposits can be seen amongst the collagen network.*



This variation of pigmentation allows observations of macroscopic pigmentation to be correlated with microscopic presentation, as seen in table 5.1.

<u>Severity of Pigmentation</u>	<u>Cartilage</u>					<u>Bone</u>		
	<u>Calcified</u>	<u>Deep</u>	<u>Middle</u>	<u>Superficial</u>	<u>Articular</u>	<u>O/cyte</u>	<u>O/clast</u>	<u>Lacunar /Canalicular</u>
<u>Initiation/Mild</u>	F,P,TM	No	No	No	No	IC	No	No
<u>Moderate</u>	Y,P,TM	F,IC	No	No	No	IC	No	No
<u>Advanced</u>	Y,P,TM	Y,IC,BM	Y,IC	No	No	IC,P	Y	Y
<u>Severe</u>	Y,P,TM	Y,IC,BM	Y,IC,BM	Y,IC,BM	Y,IC,BM	IC,P	Y	Y
<u>End Stage</u>	No	Y,IC,BM	Y,IC,BM	Y,IC,BM	Y,IC,BM	IC,P	Y	Y

Table 5.1:- A table showing the microscopic features of cellular and matrix presentations of ochronosis when correlated with the severity of pigmentation. Key: BM=Both Matrices, i.e. territorial and interterritorial, F=Few, IC=Intracellular, P=Pericellular, TM= Territorial matrix, Y=Yes. At end stage hyaline cartilage is often missing from the joint surface, so has been scored from cases where it was present, calcified cartilage is no longer present and thus shows no pigmentation at this stage.



#### **5.2.6. Fluorescence microscopy**

Consistent with histological examination, fluorescent microscopy confirmed the presence of ochronotic pigment in the articular cartilage, commencing in the calcified zone and being absent at the articular surface with no notable arthritic changes. There was also confirmation of the lack of calcified cartilage and loss of subchondral bone in the most pigmented sample(s).

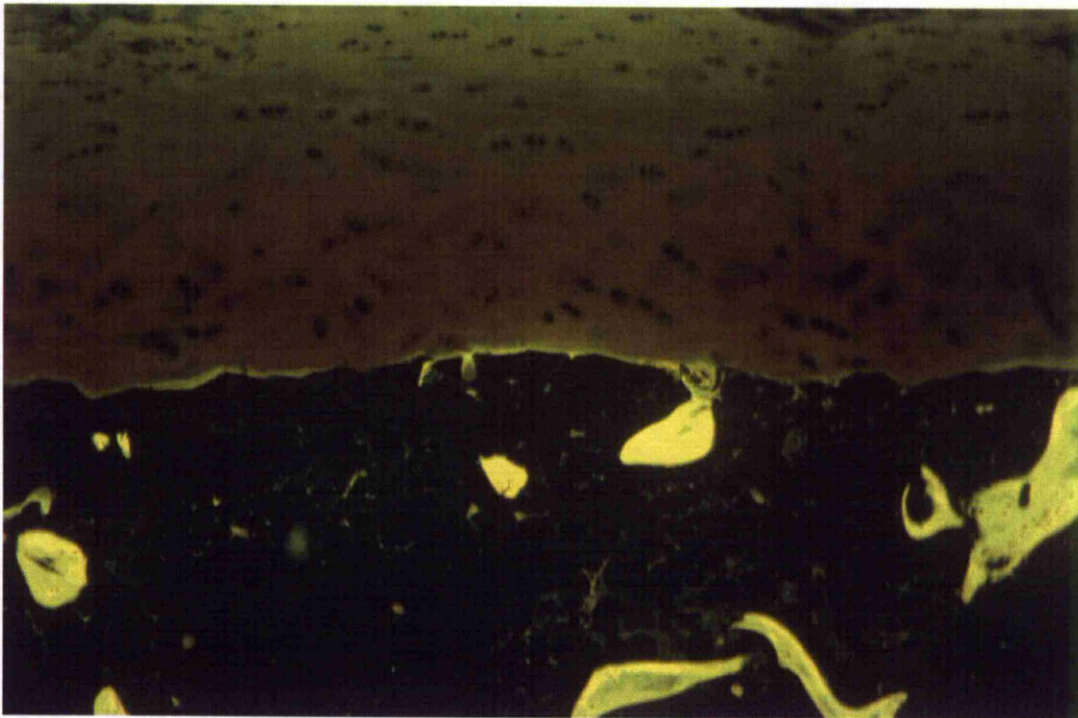


Figure 5.20: *A fluorescent photomicrograph of the deep articular cartilage and subchondral region. Ochronosis can be seen in the deep cartilages which show little fluorescence. In the more superficial regions there is more fluorescence from the matrix consistent with less pigmentation of the matrix.*

In some regions pigmented ochronotic cartilage projected deep into the bone domain. The cartilage at the articular surface exhibited high fluorescence as pigmentation progressed, whilst

the deeper zones, where pigment had been deposited, hardly fluoresced and appeared dull ochre in colour (Fig. 5.20 & 5.21).



Figure 5.21:- A fluorescent photomicrograph showing the fluorescence of the articular surface and the pigmentation front beneath it, which shows no fluorescence due to the presence of ochronotic pigment. No arthritic changes are seen at the articular surface.

Bone exhibited a high autofluorescence, except in the osteocytes which exhibited the same colouration as the pigmented chondrocytes and their pericellular matrix (Fig. 5.22). Other osteocytes exhibited no fluorescence.

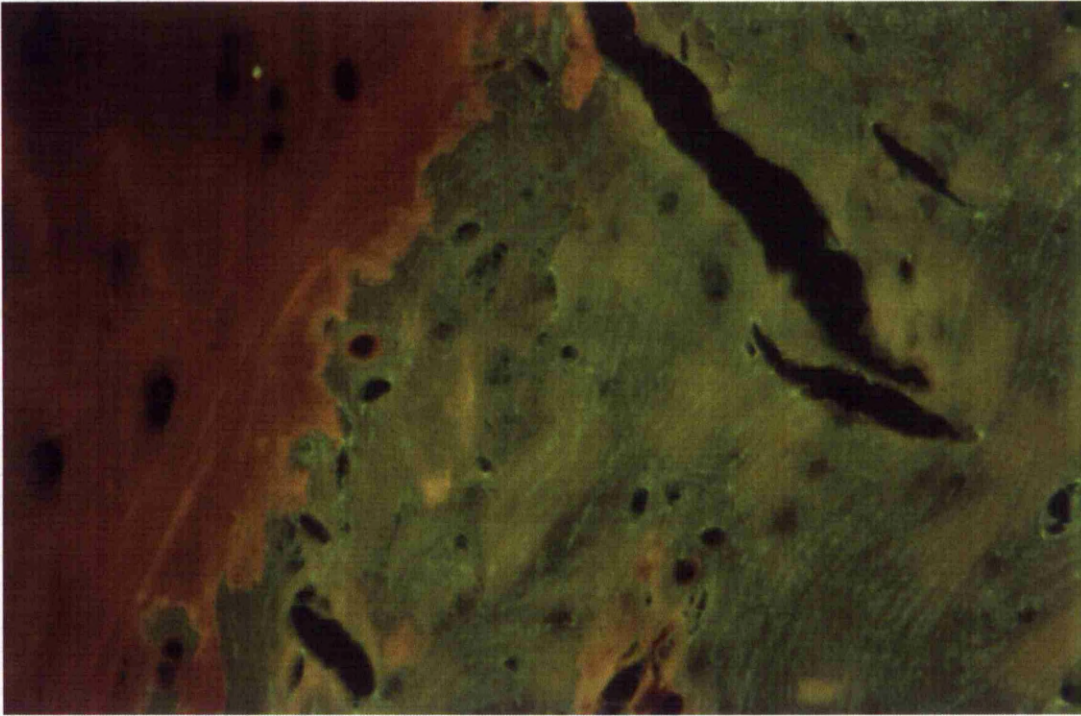


Figure 5.22: A *fluorescent photomicrograph showing the ochre appearance of regions of bone matrix in ochronotic samples. These regions appear non-ochronotic under transmitted light microscopy.*

Interestingly, in the transmitted light examination of the unstained histological sections, there appeared to be no pigment associated with the bone matrix, but regions of the bone matrix exhibited colouration similar to the ochre coloured matrix under fluorescence light, indicating the presence of pigment. These areas of pigmentation appeared to be located in between the lamellae (Figure 5.23a&b).



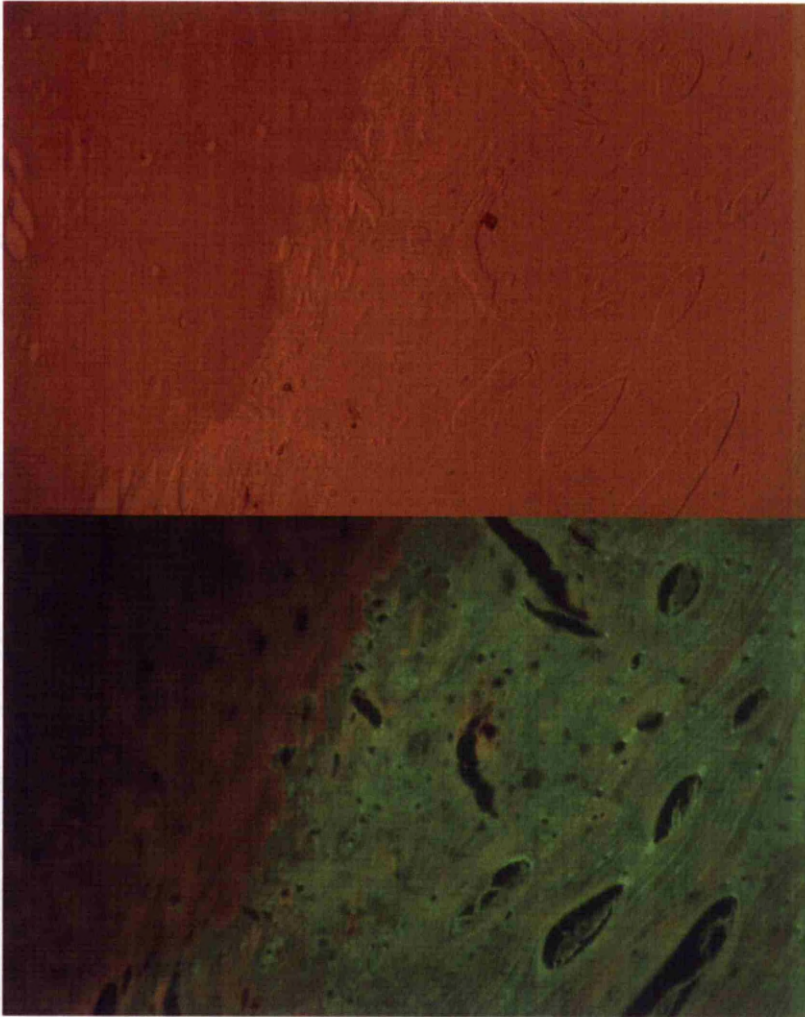


Figure 5.23a&b:- a) Top – An unstained section from an ochronotic femoral head showing the ochre appearance of unstained cartilage. There are ochronotic chondrocytes located in regions, with pigmentation surrounding their pericellular matrix. b) Bottom – Fluorescent image of the same unstained section. Ochronotic cells and their matrix appear dull in colour, consistent with the appearance of the densely pigmented hyaline articular cartilage. Regions of the bone matrix exhibit dull colouration similar to the appearance of ochronotic cartilage, suggestive of pigment present in the bone matrix, appearing to be between the lamellae.

Fluorescence microscopy also confirmed the presence of ochronotic shards of cartilage in the

marrow cavity, surrounded by fibrous tissue which appeared to engulf the fragmented shards (Fig. 5.24). The fragments of cartilage were often seen enclosed within thick fibrous bands of tissues bridging from one trabecular structure across to another (Fig. 5.25).

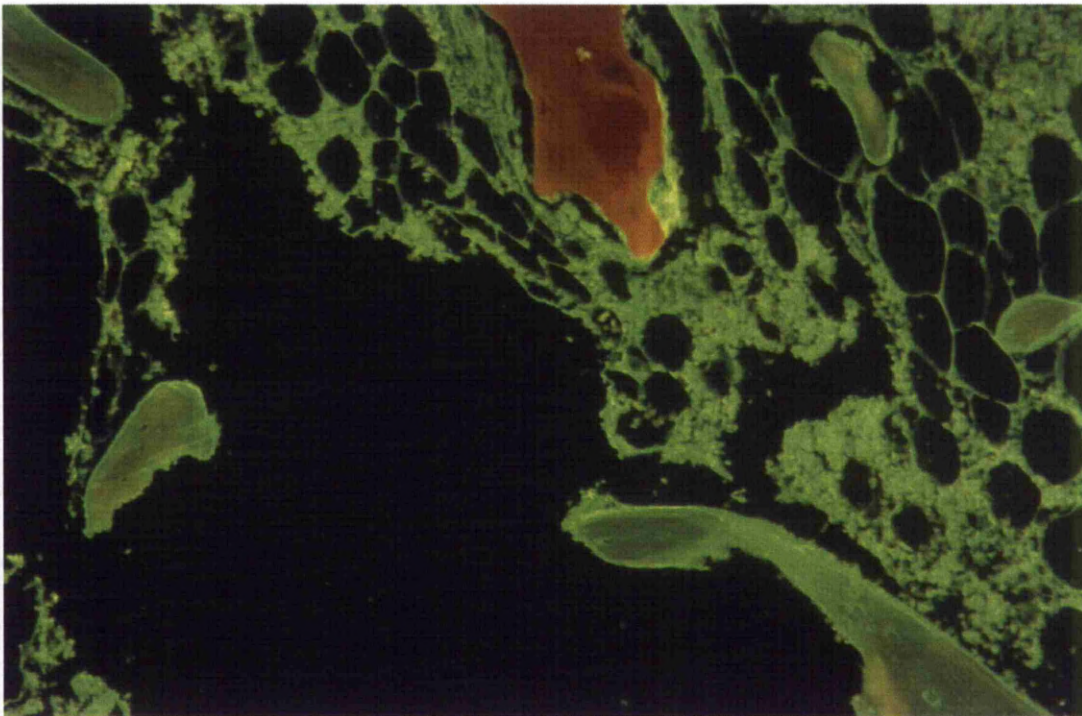


Figure 5.24:- *A fluorescent photomicrograph showing the presence of large ochronotic shards of cartilage present in the marrow space and surrounded by mononuclear cells and collagen fibres.*



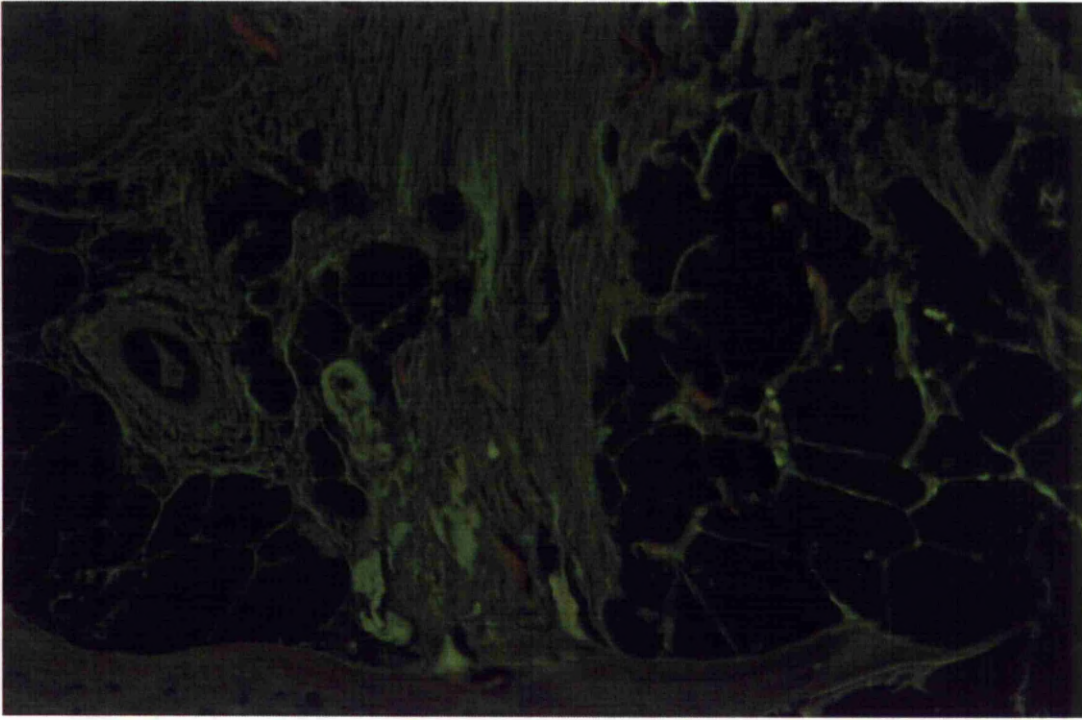


Figure 5.25:- *A photomicrograph showing the presence of pieces of ochronotic cartilage located in the marrow space and engulfed in fibrous tissue which is seen bridging between existing trabeculae. Regions of the fibrous tissue exhibit brighter fluorescence than the pre-existing matrix to which it is attached.*

### **5.2.7. SEM**

3D BSE SEM analysis in the most pigmented, macerated sample showed the complete absence of the subchondral bone plate. There was no calcified cartilage present in the sample (as seen in Fig. 5.9). Pigmented hyaline articular cartilage appeared as the dark (because it is not mineralised) substance attached to the trabecular bone structure that had survived intact through the routine processing of the sample (Fig. 5.5).

2D compositional qBSE SEM imaging of the most pigmented sample revealed mineralised matrix with numerous dead osteocytes, identified due to their dense lacunar mineralisation. The bone outline could clearly be observed, but there was no mineralised cartilage or subchondral bone plate present. Overlaying topographical and compositional images showed the presence of non-mineralised bone where the subchondral junction should be (Fig.5.27). The bone cartilage interface appeared as non-calcified cartilage in contact with unmineralised bone.

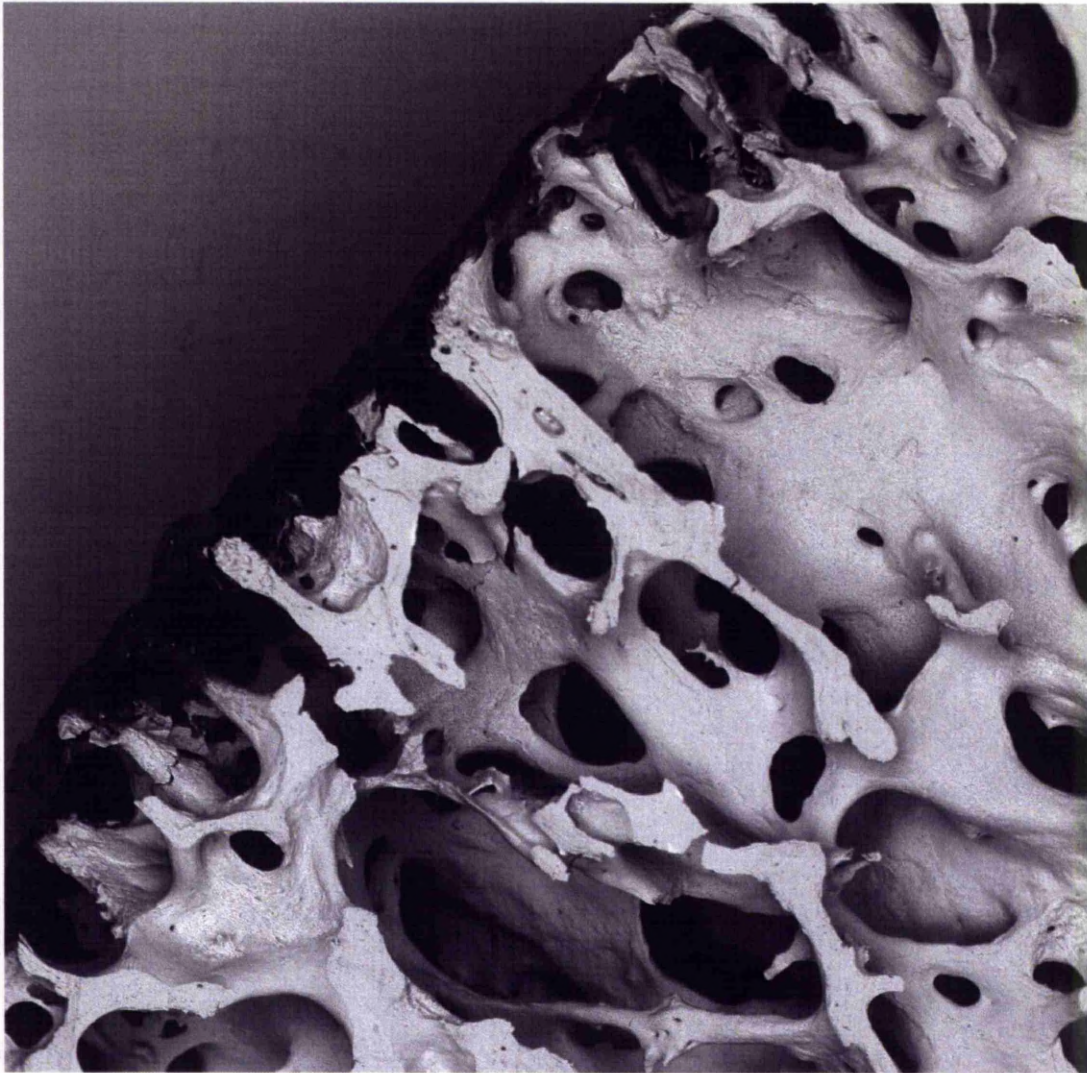


Figure 5.26:- 3D BSE SEM image showing the bone architecture from a Tergazyme macerated ochronotic femoral head (as seen in Fig. 3.1 & 3.2, chapter 3). Note that there is no subchondral plate. Remnants of pigmented hyaline articular cartilage are visible as dark stained material on the proximal surfaces of the trabeculae.



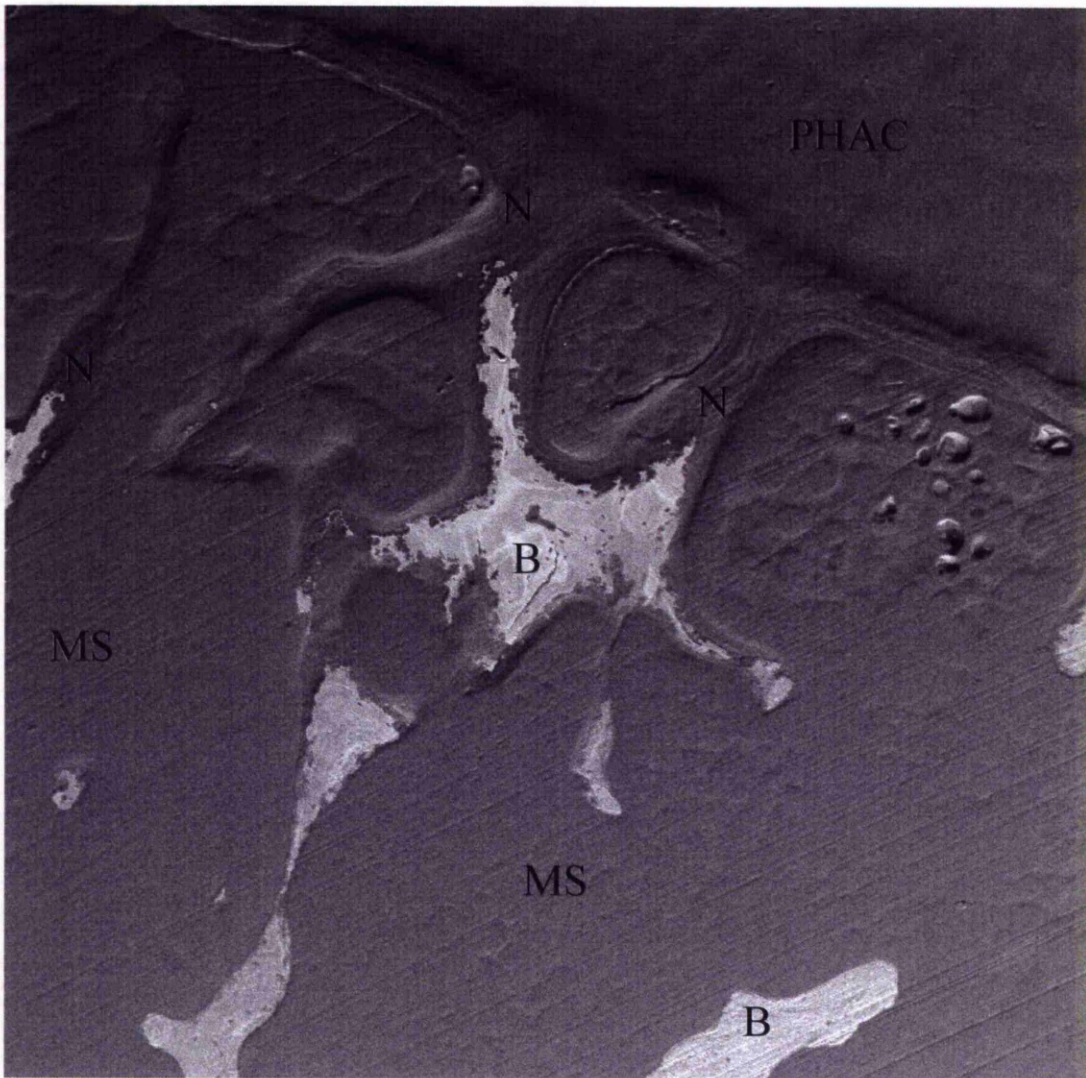


Figure 5.27: *Topographical BSE SEM image with grayscale compositional BSE image of mineral density overlaid. Pigmented hyaline articular cartilage (PHAC) is present in the upper right hand. Some of the bone matrix is not mineralised (N). Normal mineralised trabecular bone can be seen (B) located within the marrow space (MS).*

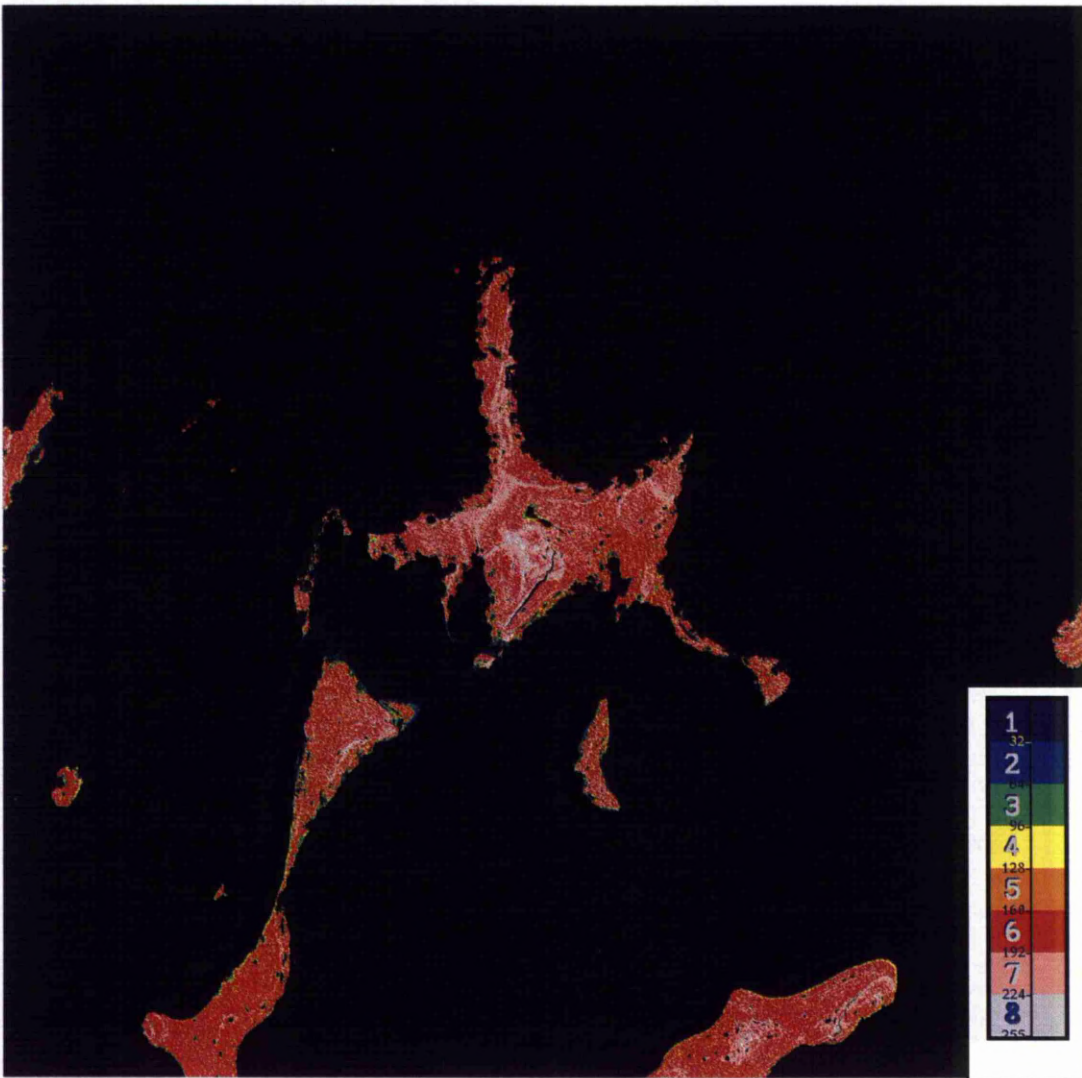


Figure 5.28:- Colour coded qBSE-SEM of same region in Figure 5.27 with halogenated standards applied showing the mineral density of the matrix. Regions of normal mineral can be seen, alongside regions of lower mineralisation towards the articular surface and around resorption lacunae. The key demonstrates mineral density with red being normal mineral density, pink and grey are hypermineralised regions and blue, yellow and green hypomineralised regions.



qBSE-SEM analysis revealed a range within normal limits of mineralisation densities in regions of trabecular bone (red colouration in Fig. 5.28), whilst additionally showing completely unmineralised bone matrix patches. In the most severely pigmented sample, there was no mineral content in any region of the cartilage, confirming absence of cartilage mineralisation and loss of any pre-existing calcified cartilage. The mineralised bone trabeculae showed regions of lower or zero mineralisation density that were in contact with the non mineralised tissues (blue, green and yellow colouration in Fig. 5.28) and showed evidence of osteoclastic action in the form of resorption lacunae (Fig. 5.28). This demonstrates that pigmented, unmineralised hyaline articular cartilage was confluent with non-mineralised bone. 3D BSE SEM of femoral condyles from AKU and OA patients revealed an interesting comparison. OA femoral condyle showed little evidence of damage to the articular cartilage with no sign of fissures or abrasions on the surface (Figure 5.29).



Figure 5.29: *Macroscopic image of surgical samples from a 51 yr old female who underwent surgery for pre diagnosed unicompartmental OA. Samples show little in the way of surface damage indicative of moderate or late stage OA.*

The subchondral architecture of the OA samples revealed widespread sclerosis with subchondral trabeculae showing distinctive thickening, particularly in the midline. There was no evidence of bone marrow lesions in this sample (Fig. 5.30).

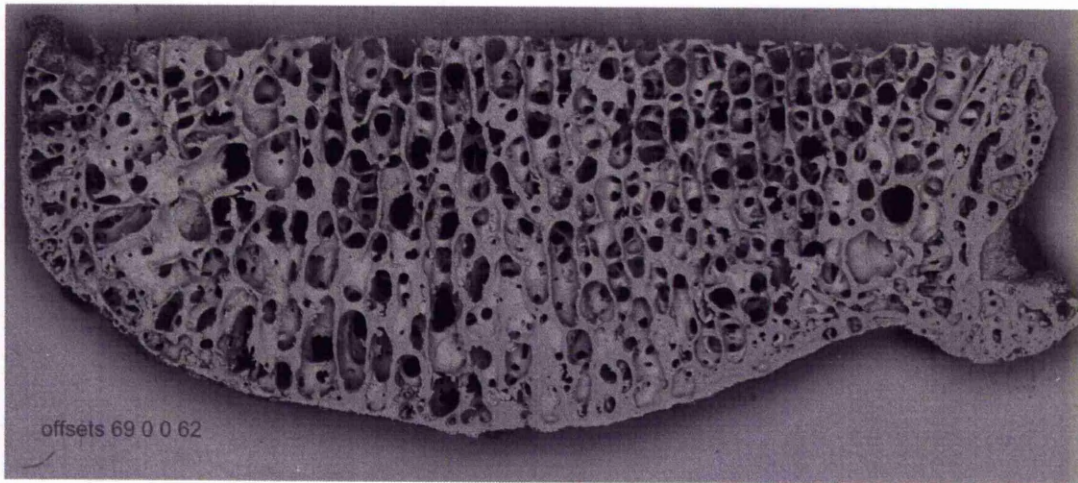


Figure 5.30:- 3D SEM image of OA femoral condyle demonstrating subchondral sclerosis. A small osteophyte can be seen. The subchondral plate can clearly be seen.

The AKU femoral condyle showed incomplete cartilage pigmentation, with the pigment present extensively in the cartilage matrix but not completely up to the articular surface (Fig. 3.16, chapter 3). The subchondral architecture showed evidence of thinning with presence of a bone marrow lesion located in the periphery of the condyle. The trabeculae showed no sign of sclerosis comparable to that seen in the OA sample (Fig. 5.30).



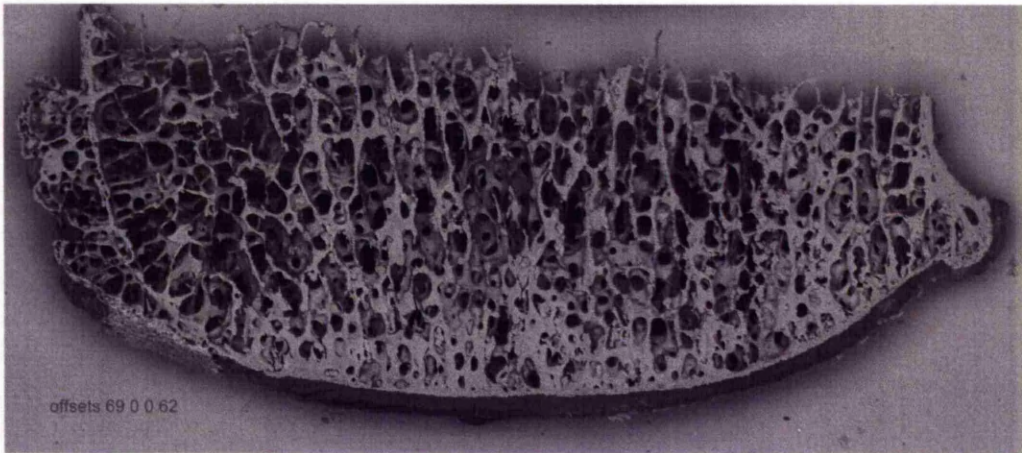


Figure 5.31:- 3D SEM image showing AKU femoral condyle with focal subchondral thinning, early stage and BML presence.

The most severely pigmented AKU sample was a femoral head that showed a focal bone marrow lesion towards the periphery of the sample. There was sporadic evidence of sclerosis. However most interesting was the complete absence of the subchondral plate (Fig. 5.32).

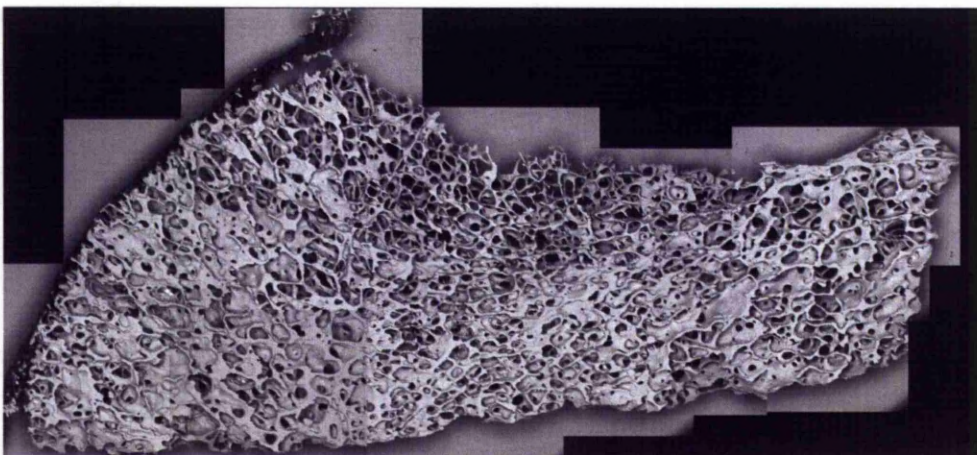


Figure 5.32:- 3D SEM image showing end stage arthropathy following subchondral remodelling of AKU femoral head showing complete loss of the subchondral plate across the sample, with impacted pigmented hyaline articular cartilage on bone trabeculae. Evidence of focal sclerosis and regions of porosis were clearly seen.

Another 3D SEM imaged femoral head showed similar regions of focal sclerosis and porosis. This femoral head is seen macroscopically with cartilage missing from the articular surface (Fig. 5.33).

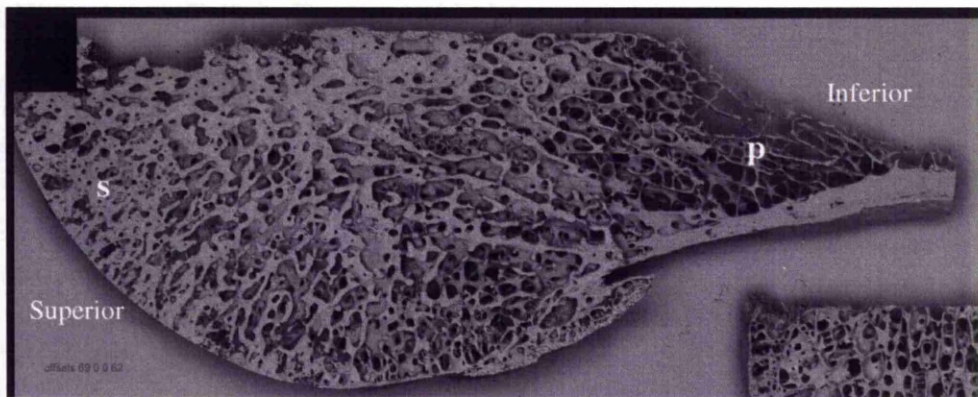


Figure 5.33:- 3D SEM showing end stage arthropathy following subchondral remodelling of AKU femoral head. Note subchondral plate absence, sclerosis (s) and porosis (p).



### **5.3. Discussion**

This chapter describes the deposition of ochronotic pigment in articular cartilage from the initial focal deposition associated with individual chondrocytes in calcified cartilage, through proliferation of pigment throughout the hyaline cartilage and associated resorption of the subchondral plate ending in complete joint destruction. These findings add weight to the theory that extracellular matrix is normally resistant to ochronosis, but becomes susceptible to pigmentation in response to tissue injury. The injury to tissues to induce pigmentation may begin with microtrauma (Meyer, 2008). Once pigmentation is initiated, it appears to spread, preventing matrix degradation by proteolytic enzymes and cells, having a protective effect on the collagen fibres. However with the increase in stiffness due to the presence of the pigment, it appears whilst pigmentation is protective against degradation it may induce mechanical damage through normal loading of ochronotic cartilage, causing shards to become broken off and embedded in the synovium (Figs. 5.24 & 5.25). Although it has previously been suggested that the calcified matrices do not undergo ochronosis (Di Franco, 2000), our results suggest that the initial pigmentation starts deep in the cartilage, at or close to the mineralising front, associated with individual chondrocytes and their territorial matrices. The conditions that allow pigmentation have not been identified but could be related to mechanical or oxidative damage, or alteration in chondrocyte gene expression. Given the observed *in vitro* toxicity of HGA (Tinti, 2011), this may be considered an etiological factor of the disease. There is a wide range of concentrations used *in vitro*; 0.1  $\mu\text{M}$  to 1 mM which covers the physiological range of HGA *in vivo* (Taylor, 2007 & Tinti, 2011). The relationship between intracellular and extracellular pigmentation is not understood. Focal pigmentation is always associated with pigmented cells, indicating that the cellular action is required for the initiation of pigmentation. However, even though pigmentation

might commence intracellularly there is no doubt that it can proceed extracellularly and the vast majority of ochronosis arises from the spread of pigmentation to established matrix - not by secretion of newly pigmented matrix. Once pigmented, ochronotic matrix appears to be resistant to turnover by matrix-degrading enzymes as demonstrated by its resistance to Tergazyme and the presence of ochronotic cartilage shards embedded in the synovial tissues, with presence of multinuclear cells in the vicinity, but no evidence to suggest they are degrading the ochronotic tissue.

The route whereby HGA reaches the site of initial pigmentation is not clear. It could diffuse from the synovial fluid, where the concentration is thought to be similar to plasma, through the hyaline cartilage, or it could permeate through the calcified cartilage from the underlying subchondral bone consistent with the transit of other low molecular weight compounds (Arkill, 2008).

Observations of samples with more advanced ochronosis indicate that once the initial pigment has been deposited, there is proliferation to other chondrocytes and then to inter-territorial matrix. This proliferation of pigmentation suggests that focal ochronosis alters the biomechanical and/or structural properties of adjacent tissue making it susceptible to pigmentation. This additional pigmentation leads to further damage and a downward spiral of tissue destruction. Dissection revealed that pigmentation alters the mechanical properties of cartilage, making it brittle and hard to cut indicating an increase in the Young's modulus which has been confirmed by mechanical testing (Figs. 5.1 & 5.2). Focal changes in mechanical properties lead to stress concentrations or risers, which could consequently induce, further mechanical damage in adjacent tissue (Hoch, 1983 & Alexopoulos, 2005). Mechanical damage and or inflammation are

known to up regulate stress genes in early OA (Goldring, 2008). Pigmentation is shown to begin in the pericellular and territorial matrices of individual chondrocytes, and thus matrix turnover events in these regions could be an important factor for initiation of pigmentation (Catterall, 2009), and may provide evidence for why pigmentation commences around the cells prior to moving into the inter-territorial matrices. This is one possible mechanism for the proliferation of pigmentation, but other mechanism(s) cannot be ruled out including chemical damage to the matrix by, for example, oxidative stress resulting from the initial deposition of pigment (Braconi, 2010).

In association with extensive hyaline cartilage pigmentation, there is remodelling of the calcified cartilage and underlying bone leading to a presentation reminiscent of bone marrow lesions. Eventually the aggressive resorption leads to complete loss of the subchondral plate. This extraordinary phenotype has not previously been reported in pathological conditions. It is likely to be a consequence of stress shielding of the underlying calcified cartilage beneath the stiff shell of pigmented cartilage, with enhanced osteoclastic activity resorbing the shielded subchondral bone and calcified cartilage. There is thinning and hypomineralisation of some underlying trabeculae and sclerotic changes in others similar to that previously reported in bone marrow lesions in OA (Hunter, 2009, Intema, 2010 & Intema, 2010). Although the aggressive resorption appears to be focal, it is noteworthy that enhanced urinary excretion of crosslinked N-telopeptides of type I collagen has been reported in alkaptonuric patients (Aliberti, 2003). Although remodelling of subchondral bone and articular cartilage has been reported in rheumatoid arthritis (Goldring, 2003), the complete loss of the subchondral bone seen in AKU is exceptional. Although a previous report concluded that bisphosphonates were not beneficial in

patients with advanced ochronosis (Aliberti, 2007), our findings suggest that bisphosphonate therapy maybe worthy of reconsideration with administration, either before significant subchondral bone and calcified cartilage loss (i.e. primary prevention) or during early phase of subchondral bone and calcified cartilage loss (secondary prevention/treatment).

As a consequence of the subchondral bone loss, the brittle pigmented cartilage becomes impacted onto the poorly mineralised trabecular bone. Fracturing of the cartilage causes fragments to be displaced into the marrow space and engulfed by the marrow cells and become embedded in the synovium and capsular tissues (Araki, 2009 & Gaines, 1987). The end stage of the disorder shows complete loss of pigmented cartilage from the articular surface (Fig. 3.3).

Pigmentation was not detected in mineralised bone matrix, but osteocytes, osteoclasts and osteoblasts all displayed intracellular pigmentation, as well as the canalicular network and osteocyte lacunae. Osteoclasts were also seen phagocytosing pigmented osteocytes. Although generalised rates of bone formation have been observed to be almost normal in ochronotic individuals (Aliberti, 2003), these observations demonstrate focal hypomineralisation. There was no evidence of generalised osteomalacia and previous studies show no evidence of vitamin D deficiency in AKU patients (Fisher, 2004).

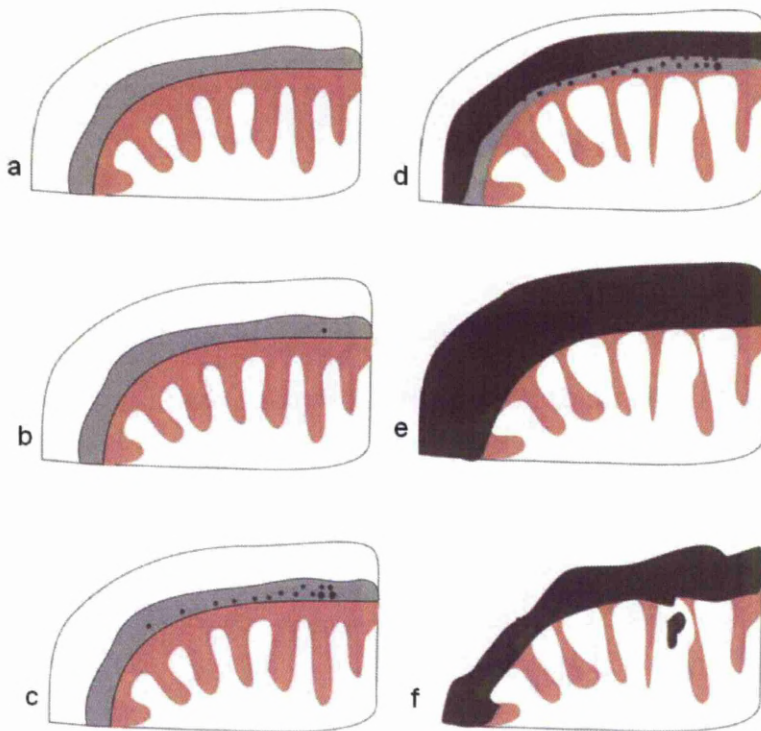


Figure 5.34:- Schematic diagram showing the progression of joint destruction in ochronotic osteoarthropathy from initial pigmentation to eventual loss of cartilage based on the findings in this chapter. (a) Normal articular cartilage and subchondral bone plate. (b) Initiation of pigmentation around a single chondrocyte. (c) Pigmentation spreads to neighbouring chondrocytes. (d) Pigmentation progresses into the matrix of the non calcified hyaline cartilage. (e) Extensive hyaline cartilage pigmentation and complete loss of calcified cartilage and subchondral plate. Pigmented articular hyaline cartilage now sits directly on bone trabeculae. Trabecular structures are thinned by osteoclastic resorption. (f) Pigmented hyaline cartilage is brittle and prone to fracture(s). Shards of pigmented cartilage from the articular surface become embedded in synovium, whereas on the subchondral aspect, fragments become embedded into the marrow spaces.



This research clearly highlights the central role that the bone cartilage interface plays in the initiation of ochronosis in AKU, and the importance of the calcified cartilage and subchondral bone in the subsequent arthropathy. The absence of the calcified cartilage itself is of major pathological significance. Calcified cartilage has often been neglected in the study of joint degeneration in OA, but it is clearly the tissue through which loads are distributed from the hyaline articular cartilage to the underlying subchondral bone (Ferguson, 2003). There are, however, many reports highlighting a role for subchondral bone in the pathogenesis of OA (Karsdal, 2008). It has been suggested that the structural integrity of articular cartilage is reliant on normal subchondral bone turnover, intact chondrocyte function and normal biomechanical stresses (Karsdal, 2008, Felson, 2004 & Hayami 2004).

AKU has already been documented as mimicking or causing premature OA (Bálint, 2000 & Lagier, 2006). The examination of our results show there may be a large overlap of OA with the pathogenesis of AKU, and there is also growing evidence that in OA, alterations in the composition and biomechanical properties of cartilage are facilitated by increased bone turnover (Karsdal, 2008, Hayami, 2004 & Hayami, 2006).

It is tempting to speculate that the initial pigmentation is associated with pre-existing, possibly OA-related changes which make the cartilage matrix susceptible to pigmentation and that HGA is acting as an endogenous marker of degenerative changes. Joint arthropathy in AKU has some parallels with other joint diseases including OA but also has some unique characteristics. Further study of this rare disorder may contribute to the understanding and treatment of joint

degeneration in AKU but also of OA.

## **6. Ochronosis in a murine model of alkaptonuria**

## **6.1. INTRODUCTION**

Other studies in this Thesis have demonstrated that ochronosis of cartilage is initiated in individual chondrocytes and their territorial matrix, before progressing to a more widespread pigmentation of the cartilage matrix (Taylor, 2011). Elucidation of the mechanism of initiation and progression of ochronosis will indicate new opportunities for intervention. Whilst therapies for AKU have been suggested and in some instances trialed, there is still not a clear direction about treatment(s) for AKU.

It has been suggested that NTBC, the therapeutic agent used in treating tyrosinaemia type I, may prove beneficial in treating AKU by blocking the production of HGA in the breakdown of tyrosine (Suwannarat, 2005). The efficacy and safety associated with the use of this drug for treating AKU has not yet been determined. Recent research has shown that there is an increase in oxidative stress to cells associated with high HGA (Braconi, 2010). Furthermore, preliminary *in vitro* work has demonstrated that anti-oxidants may prove useful in treating the disorder (Braconi, 2010 & Tinti, 2010). These results support numerous published reports suggesting that ascorbic acid may be of benefit in treating AKU (Morava, 2003, Wolff, 1989 & Forslind, 1988). Mixed results have been observed when using ascorbic acid *in vivo*, however, ascorbic acid itself is a co-factor of p-hydroxyphenyl pyruvate dioxygenase, the enzyme immediately upstream of HGD, in the breakdown of tyrosine to HGA and thus pigment formation (Lorenzini, 2003). The benefit of low protein diets to slow ochronosis in AKU is questionable given that people who have observed the low protein diet still go on to develop ochronosis in their tissues (de Haas, 1998). This is probably due to the fact that HGA production arises from tissue turnover in the body as well as from the breakdown of ingested protein. The understanding of the progression of ochronosis in AKU has not advanced significantly towards defining a therapeutic strategy since Garrod described the disorder as

“an inborn error of metabolism” over 100 years ago (Garrod, 1902 & Garrod 1908). Even with the groundbreaking identification of the enzyme responsible (HGD) and the cloning of the HGD gene (Fernandez-Canon 1996 & Granadino, 1997), sufferers of the disorder are still subject to the debilitating effects of the polymeric derivative of HGA in their tissues.

There is a clear need for a mouse model for this disorder to provide longitudinal data into the disease progression, because of the nature of the human specimens being a single time point in the progression of an individual sufferer's disease, these time points are usually late or end stage, which is beyond when any possible therapy may have beneficial action. Humans are also subject to intrinsic and extrinsic factors which are person specific, it is difficult to understand the complete time course, and an understanding of when pigmentation commences, and what lifestyle factors may influence this at a given point. Whilst the discovery of the mechanism has demonstrated the possibility of novel therapeutic interventions, a novel model is needed for studying the points and efficacy of each intervention. A mouse model would also provide valuable data on any new therapy, but more importantly may also have given valuable data on the effects of existing therapies. Whilst AKU mice do exist, even with elevated plasma HGA and urinary excretion of HGA, they do not appear to exhibit the human arthropathic features. The murine model of AKU was produced in 1993 by mutagenesis. These mice arose by intraperitoneal injection of ethylnitrosourea (250mg/kg) of eight week old mice from an inbred stock carrying seven recessive mutations. Following recovery, these animals were then mated to 129/Sv-T/+ mice. Independent micro-pedigrees were achieved by systematic sibling mating for more than 10 generations. The AKU mutation was then backcrossed onto both the BALB/cByJ (albino) and the C57/BL/6J (pigmented) backgrounds. These animals were previously thought not to exhibit ochronosis, despite excreting sufficient HGA to cause darkening of urine



(Montagutelli, 1994). The mice have a truncated protein form of the HGD enzyme resulting from a splice mutation (Manning, 1999).

FAH (fumarylacetoacetate hydrolase)  $-/-$  HGD $+/-$  animals were originally produced by crossing AKU mice (obtained from Montagutelli at the Pasteur Institute in Paris) with FAH $\Delta_{\text{exon5}}$ . These mice were then crossed to obtain the desired phenotype (without controlling for strain background) (Manning, 1999). A proportion of these animals appeared to show a reversion to the less severe AKU phenotype following withdrawal of NTBC. The FAH/HTT1 strain would normally succumb to the tyrosinaemia type 1 that follows withdrawal of NTBC. The reversion of nodules within the liver to the homozygous negative form for HGD is thought to arise from the production of mutagenic compounds in the liver due to the FAH deficiency, namely the presence of fumarylacetoacetic acid (FAA) and maleyl acetoacetic acid, (MAA) and subsequent spontaneously formed derivatives. These mutagenic compounds appear to cause a deletion or conversion from the wild type HGD allele, resulting in double mutant HGD and FAH hepatocytes, and these have a selective advantage within the population of liver cells because they do not produce the toxic FAA and MAA derivatives (Manning, 1999). Other experimental models have been reported, but are generally not useful or viable for experimental studies (Keeling, 1973 & Bonduranat, 1965). Following anecdotal descriptions of ochronosis in these mice, this chapter describes a recently undertaken a macro and microscopic study of the tissues of FAH $-/-$ ,HGD  $+/-$  mice which have been withdrawn from NTBC. This chapter details the detection of ochronosis in a murine model of AKU for the first time and similarities between the initial stages of the pigmentation in the murine model and those of the human condition. This murine model may also prove beneficial for screening therapeutic agents for treating the condition.

## **6.2. RESULTS**

<b>Mouse ID</b>	<b>Sex</b>	<b>Time off NTBC</b>
<b>271</b>	<b>M</b>	<b>11 Months</b>
<b>272</b>	<b>M</b>	<b>11 Months</b>
<b>280</b>	<b>F</b>	<b>11 Months</b>
<b>282</b>	<b>M</b>	<b>11 Months</b>
<b>283</b>	<b>M</b>	<b>11 Months</b>
<b>285</b>	<b>F</b>	<b>11 Months</b>
<b>2089</b>	<b>F</b>	<b>2 Weeks</b>
<b>2091</b>	<b>F</b>	<b>2 Weeks</b>
<b>240</b>	<b>F</b>	<b>2 Days</b>
<b>241</b>	<b>F</b>	<b>2 Days</b>
<b>236</b>	<b>M</b>	<b>1 Day</b>
<b>237</b>	<b>M</b>	<b>1 Day</b>

**Table 6.1:-** *details of FAH-/-, HGD +/- mice analysed as part of this chapter and amount of time off NTBC prior to analysis*

Mice were dissected as described in Chapter 2.

### **6.2.1 Macroscopic observations of murine tissues**

The skin and ears, abdominal viscera, femoral heads or knee joints displayed no similar pigmentation to that seen in aged human organs and structures in mice of any age. The livers of mice that had been withdrawn from NTBC for 11 months showed pale discolouration in regions. This was only seen in the mice which had been removed from NTBC for 11 months, all other livers appeared normal. The kidneys of some the mice which had been removed from NTBC for 11 months displayed regions of ochronosis; these were interspersed across

the kidneys, with non-ochronotic regions showing pale discolouration. These regions of ochronosis appeared as large dark nodules, bulging from the external surface of the kidneys. These were only seen in 4 of the 6 mice which had been off NTBC for this amount of time; these three mice were all male. The female kidneys, showed similar regions of pale discolouration but lacked the ochronosis seen in their male counterparts. The ochronotic nodules were located beneath the fibrous capsule; they protruded deep down into the cortex. It was difficult to ascertain whether they were located in the renal columns or the medulla.



Figure 6.1:- Macroscopic image showing kidneys of mouse M283 (male) in situ; which had been off NTBC for 11 months. Large dark ochronotic nodules are seen in the kidney tissues.



Figure 6.2:- Macroscopic image of kidneys from mouse M271 (male) sectioned through the midline to show the internal surface and large ochronotic deposits can be seen with the medulla. Mouse had been off NTBC for 11 months.



Figure 6.3:- Macroscopic images of kidneys from mouse M272 (male) sectioned through the midline to show the internal surface with ochronotic deposits. Mouse had been off NTBC for 11 months.



Figure 6.4:- Macroscopic images of kidneys from mouse M282 (male) sectioned through the midline to show the internal surface with ochronotic deposits. Mouse had been off NTBC for 11 months.



Figure 6.5:- Macroscopic images of kidneys from mouse M283 (male), as seen in situ in figure 6.1, sectioned through the midline showing ochronotic deposits. Mouse had been off NTBC for 11 months.

The kidneys from mice which had been off NTBC for 2 weeks displayed a speckled appearance but showed no external or internal signs of ochronosis. The kidneys from the

mice which were off NTBC for 1 and 2 days respectively displayed a light colouration but no sign of ochronosis.



### **6.2.2. Histology**

Mouse M283 off NTBC for 11 months

#### **6.2.2.1. Heart**

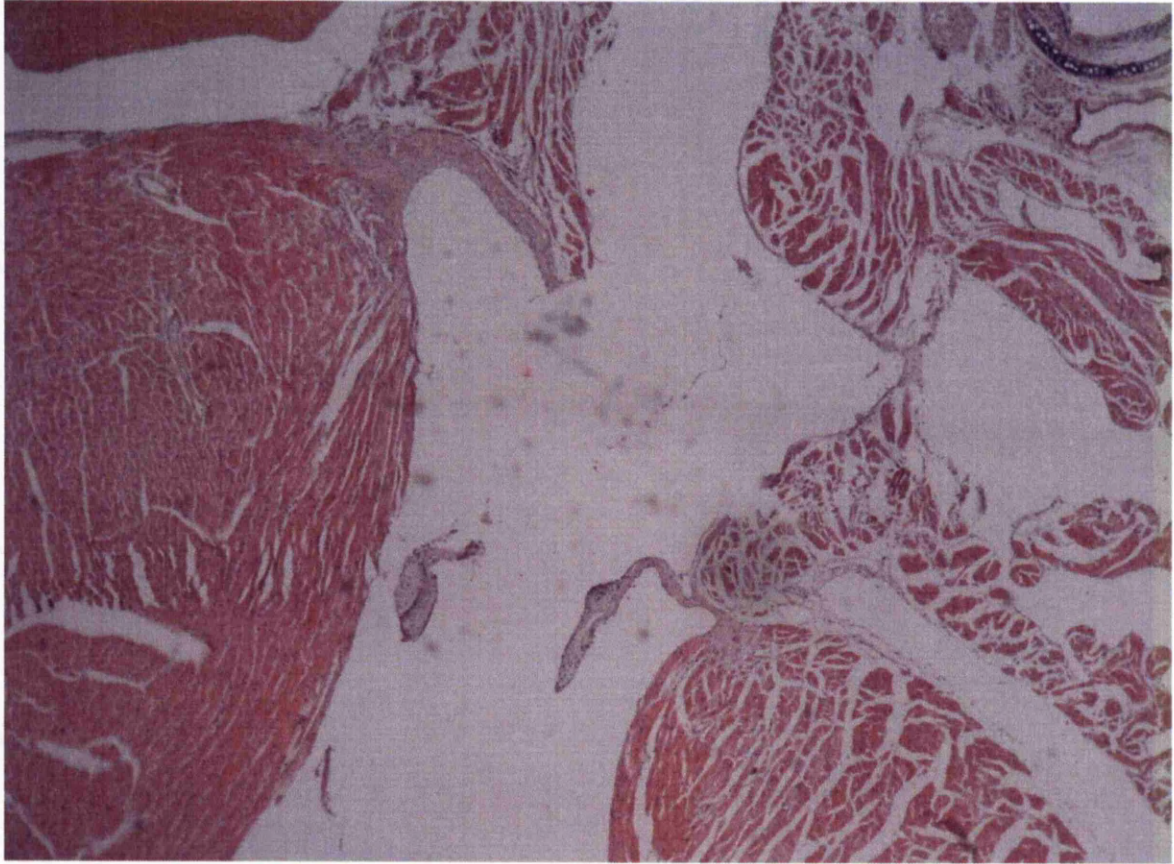


Figure 6.6:- *Low power photo micrograph showing the aortic valves and heart musculature from the heart of M283. No obvious ochronosis can be seen.*

Microscopic observations of the heart tissues revealed absence of ochronotic pigmentation from all tissues. High magnification observation of the heart valve revealed that no ochronosis associated with extracellular matrix or intracellularly, either chondrocytes or fibroblasts. There was also no pigment present in the muscular tissues. The cells all appeared healthy.

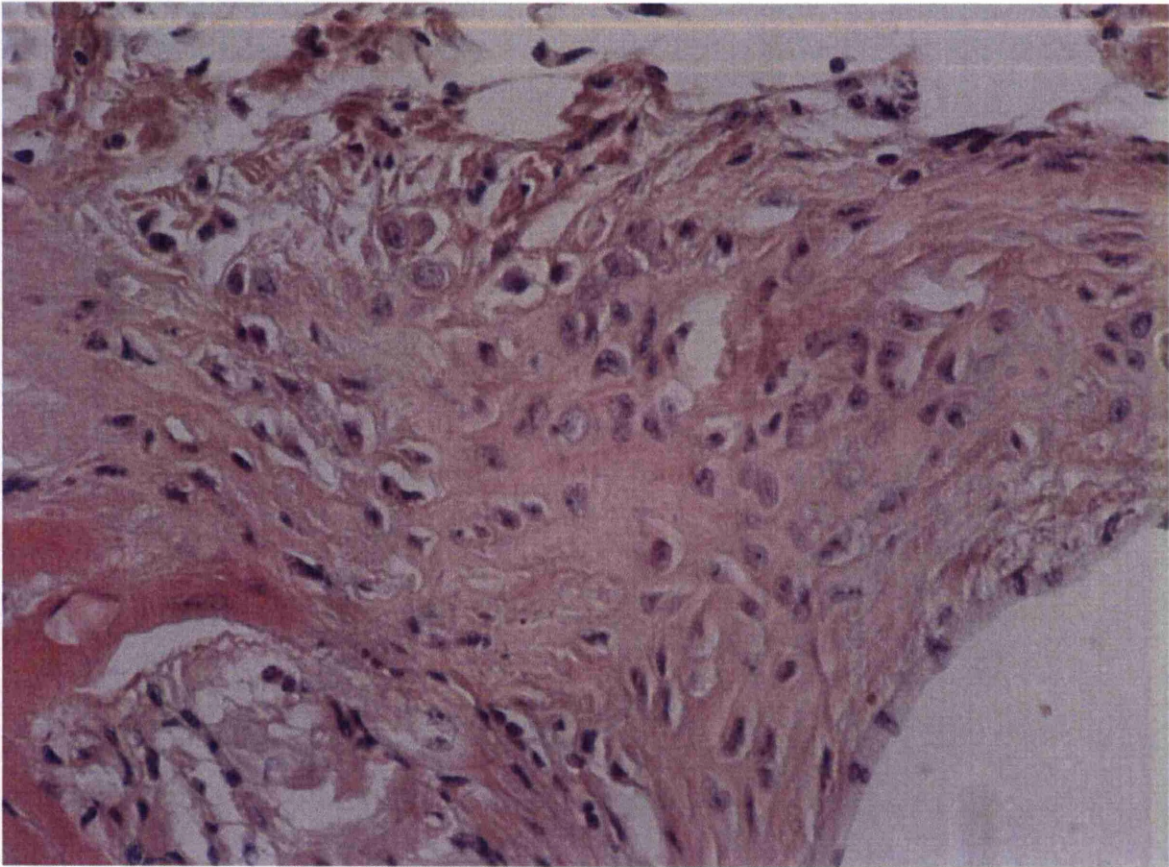


Figure 6.7:- A high power photomicrograph showing fibroblast-like cells and their matrix of the aortic valve. No extra or intracellular ochronosis is seen.

#### 6.2.2.2. Tracheal cartilages

Observation of the tracheal cartilages showed no evidence of ochronosis. The extracellular cartilage matrix and the surrounding fibrous tissue matrix appeared normal. The cartilage matrix stained heavily for proteoglycans. The chondrocyte lacunae were empty, with no evidence of the presence of chondrocytes in the majority of the lacunae; those that were present showed signs of necrosis. It is possible that within this tissue, absence of chondrocytes could be the earliest detectable pathological change. The epithelial lining cells of the trachea showed no sign of intracellular ochronosis.



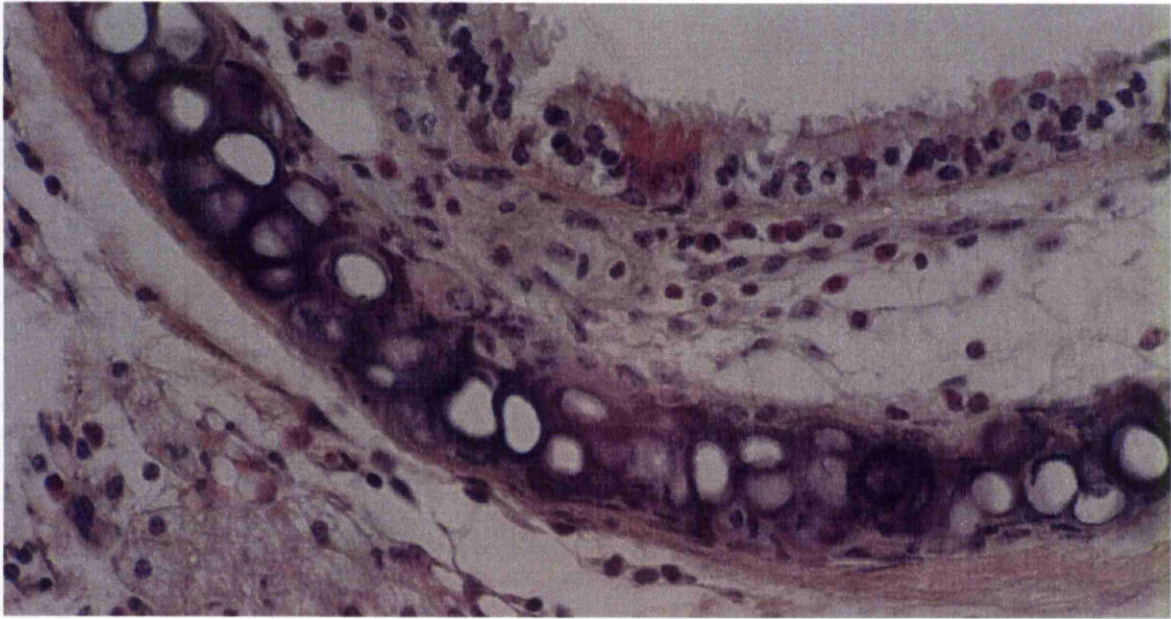


Figure 6.8:- A high power photomicrograph showing the cartilaginous rings of the trachea with no evidence of ochronosis intra or extracellularly. Numerous lacunae are empty and those chondrocytes that are present appear necrotic.

The thyroid cartilage displayed no evidence of ochronosis. There was dense matrix proteoglycan staining. Examination of the chondrocytes displayed some necrotic looking chondrocytes located in their lacunae.

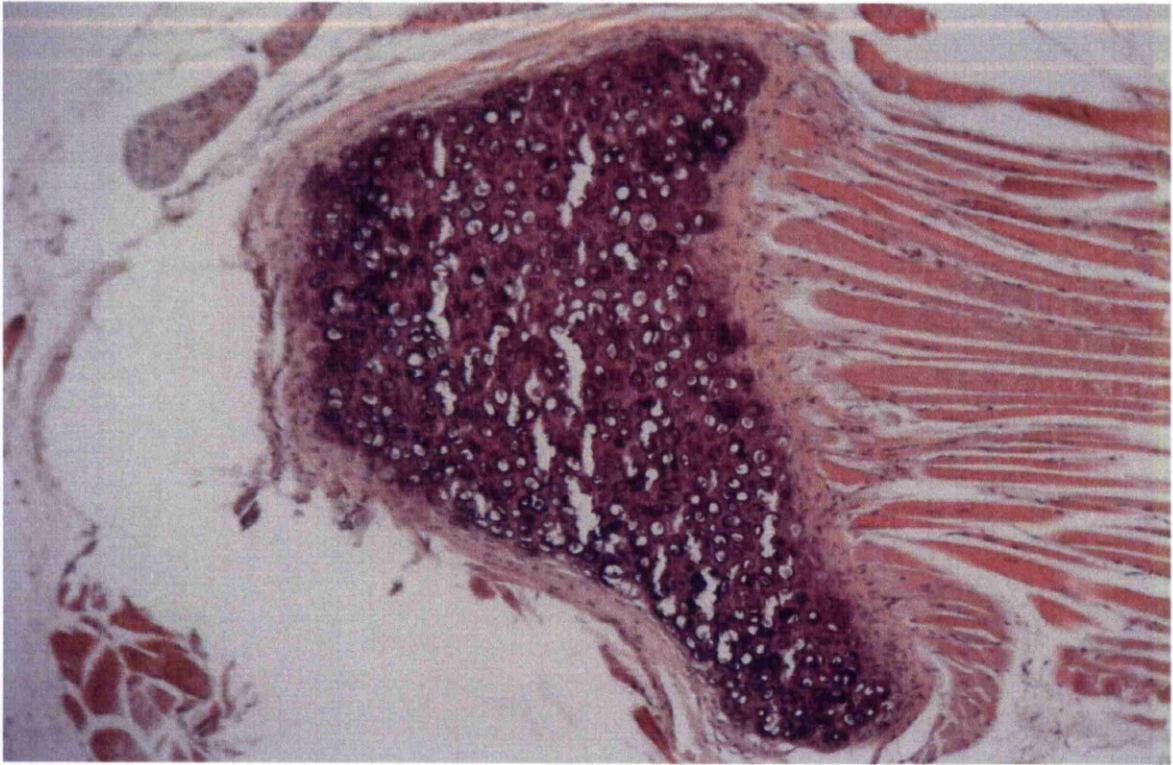


Figure 6.9:- A lower power photomicrograph showing an over view of the thyroid cartilage from M283. No obvious sign of ochronosis is seen in the cartilage matrix or with the entheses of the thyro-arytenoid muscles.



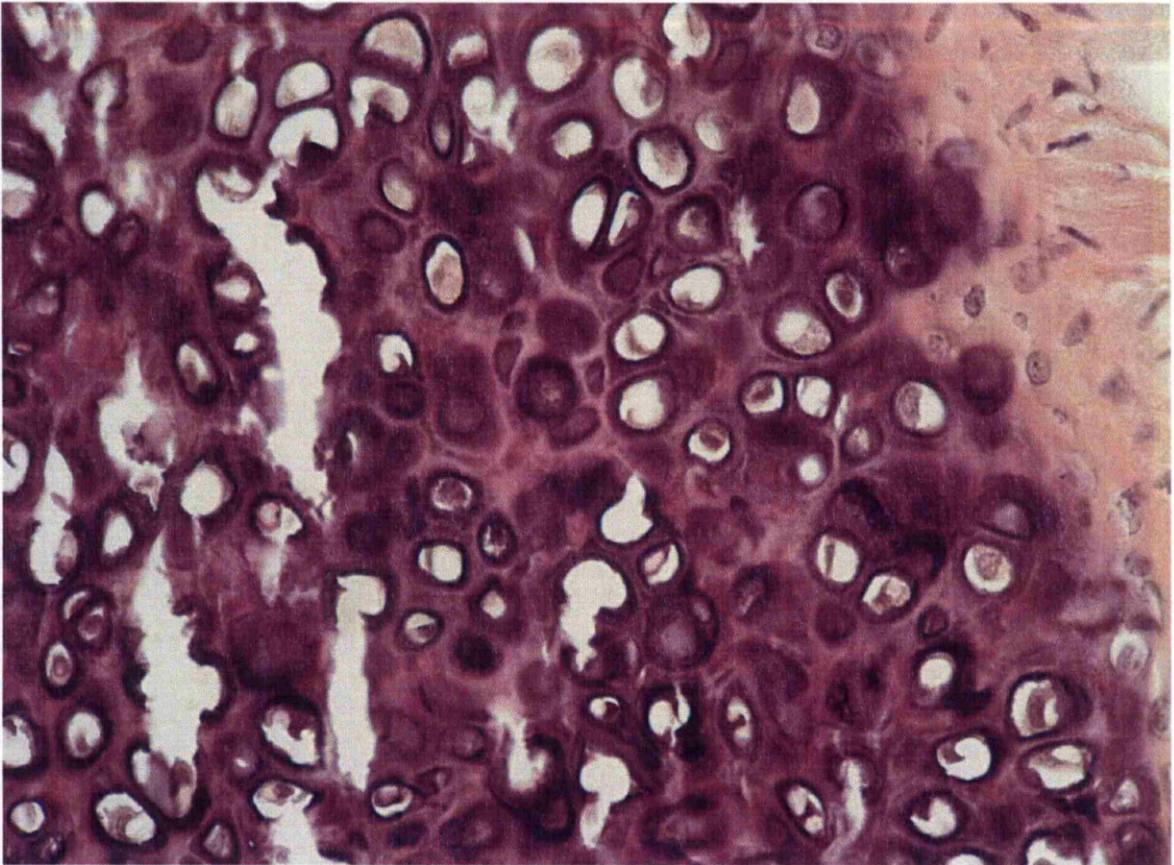


Figure 6.10:- A high power photomicrograph showing the chondrocytes in their matrix within the thyroid cartilage. Many chondrocytes look necrotic and some display an ochre colour suggestive of intracellular ochronosis.

High magnification examination of the chondrocytes showed that some displayed ochre colouration of the cytoplasm. The enthesis of the thyro-arytenoid muscles displayed no pigmentation.



### 6.2.2.3. Kidneys

Microscopic examination of the kidneys revealed widespread pigmented nodules throughout. H&E staining demonstrated the pigment was present in numerous large cast-like structures. The peripheral fibrous capsule around these casts showed granules of ochronotic pigment associated with the fibrous matrix components, these granular deposits were also seen in the cytoplasm of fibroblasts in these regions. Within these pigmented casts were numerous mononuclear cells. These cells showed numerous dense granular deposits of ochronotic pigment within their cytoplasm. There were often numerous mononuclear cells at the periphery of these cast-like structures and they displayed large cytoplasmic deposits of ochronotic pigment.

In the tubules of the kidney numerous ochronotic deposits were seen, presumed to be urine which had undergone polymerisation. Surrounding some of these tubular deposits were had columnar cells in the vicinity that had numerous granules of pigment located in their cytoplasm and also associated with the nearby matrix.

There were numerous tubules in the kidneys of these animals which demonstrated sloughing of cells, indicative of acute tubular necrosis. The inflammation and deposition of pigment in these kidneys made determination of some regions of microscopical anatomy difficult to interpret. It was difficult to distinguish proximal from distal tubules and both of these from collecting ducts. Kidneys from younger mice which had been off NTBC for a shorter period of time displayed no similar pigmentation (Figs. 6.17-6.19).

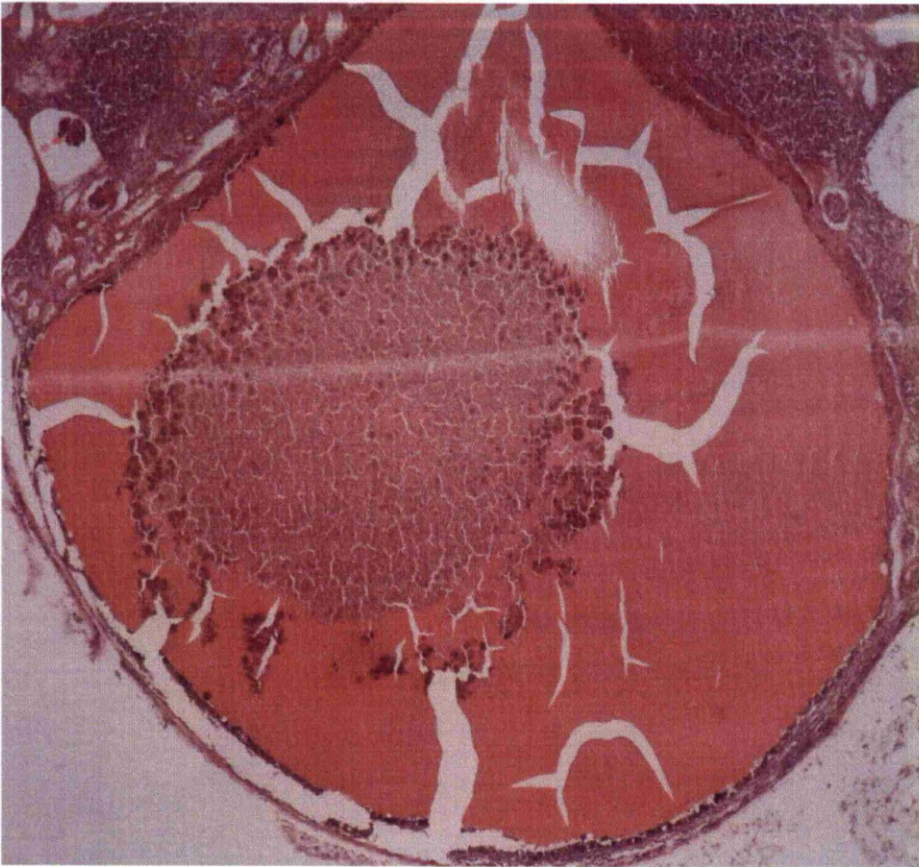


Figure 6.11:- A low power photomicrograph showing a large cyst-like structure from the kidney of M283 (as seen in Figure 6.1) Ochronotic pigment is clear around the periphery of the structure and large amounts of intra and extracellular pigment are seen in the centre of the structure. The intracellular pigmentation is clearly located within mononuclear cells.

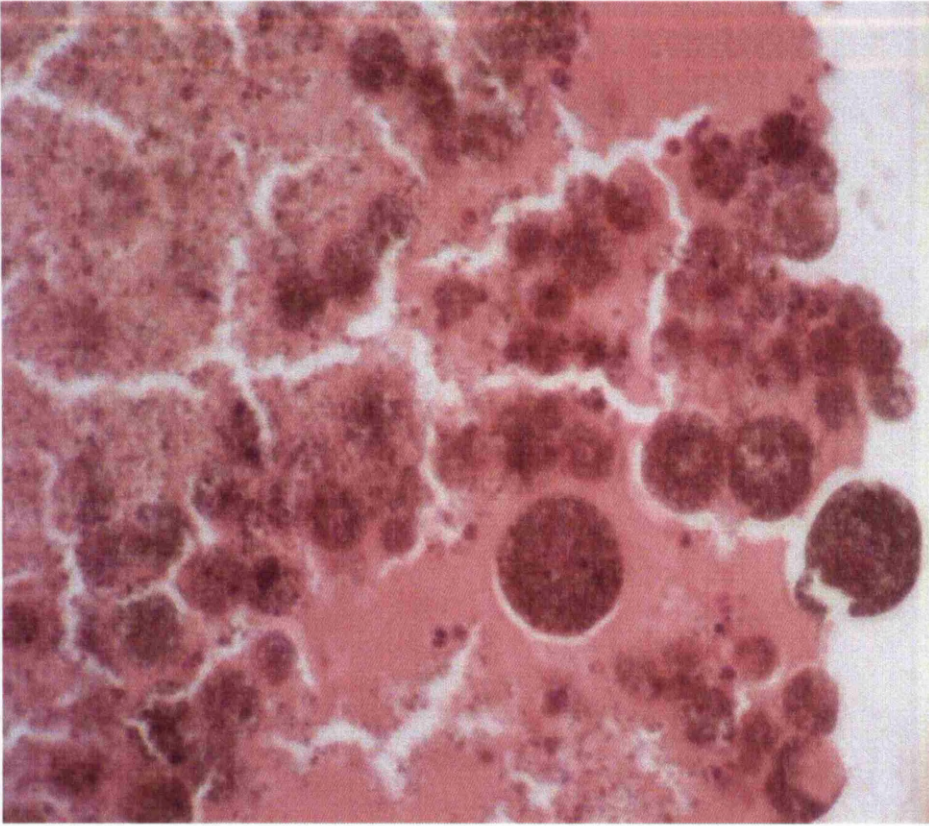


Figure 6.12:- A high power photomicrograph showing the presence of intracellular granular deposits in mononuclear cells within the cyst. There is also extracellular pigment seen amongst these cells.





Figure 6.13:- *High power photomicrograph of the periphery of the cyst like structure. This demonstrates intracellular pigmentation in fibroblast like cells and extracellular pigmentation associated with the fibrous tissues.*

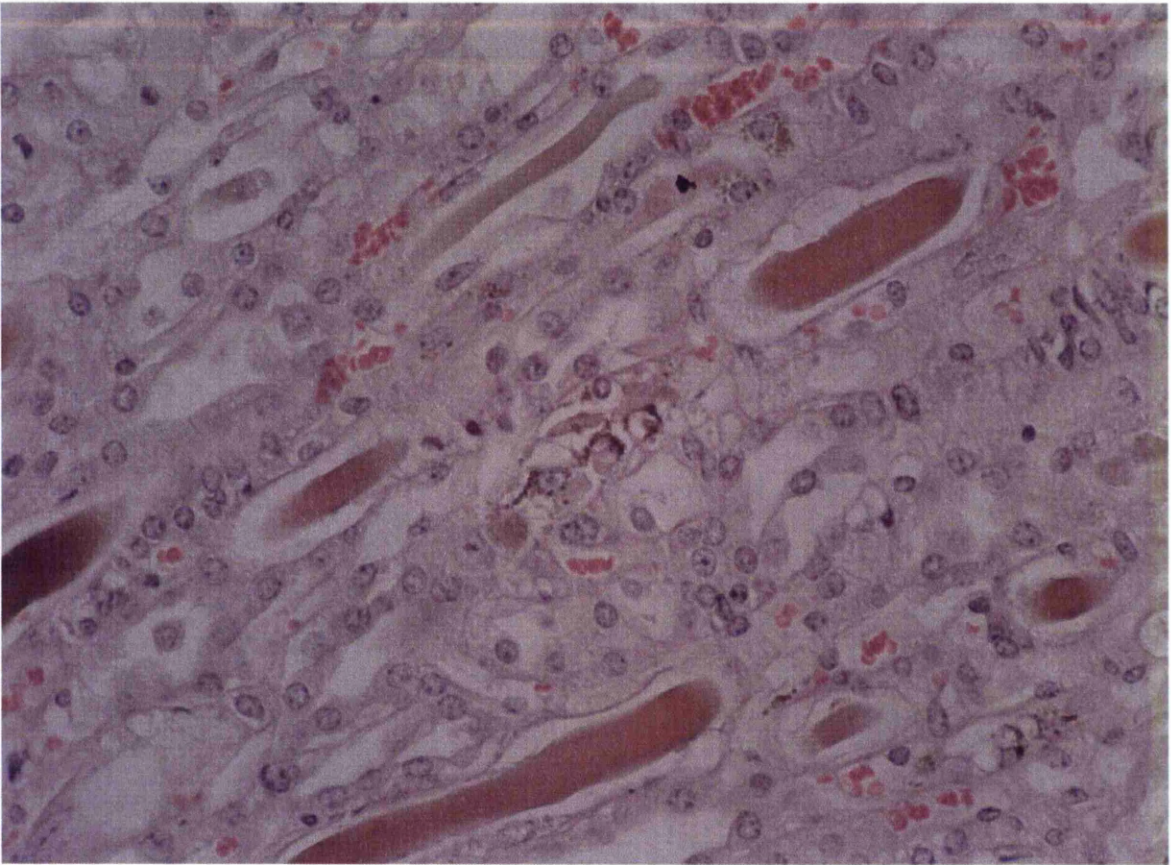


Figure 6.14:- A high power photomicrograph showing the ochronotic appearance of urine in the tubules of the kidney from M272. Granular pigment is also seen within fibroblasts in the collagenous matrix.

#### 6.2.2.4. Schmorls staining of kidneys

Staining of near serial sections of kidneys from mice off NTBC for 11 months confirmed the observations seen in the H&E sections. It also highlighted pigmentation around the casts that were undetected by H&E staining.



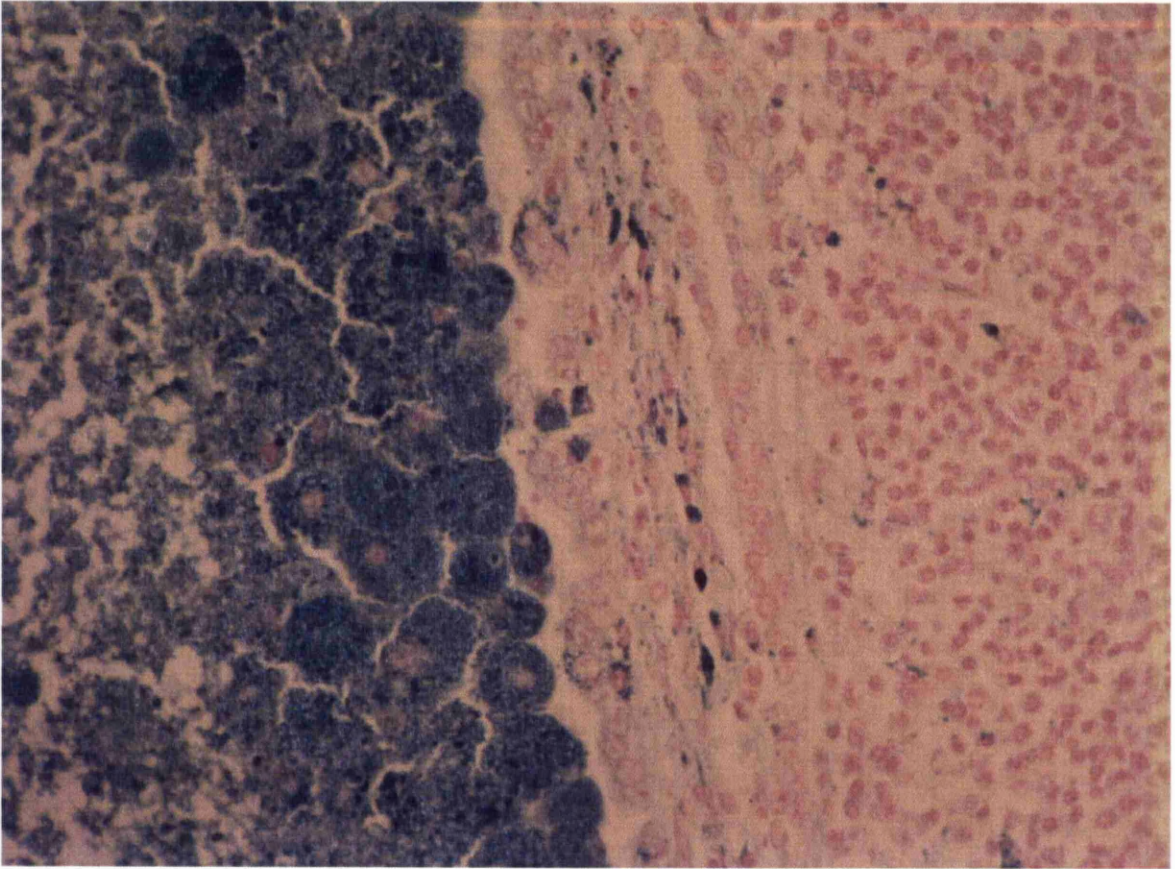


Figure 6.15:- *High power photomicrograph showing the presence of intracellular ochronotic deposits within the mononuclear and fibroblast like cells.*

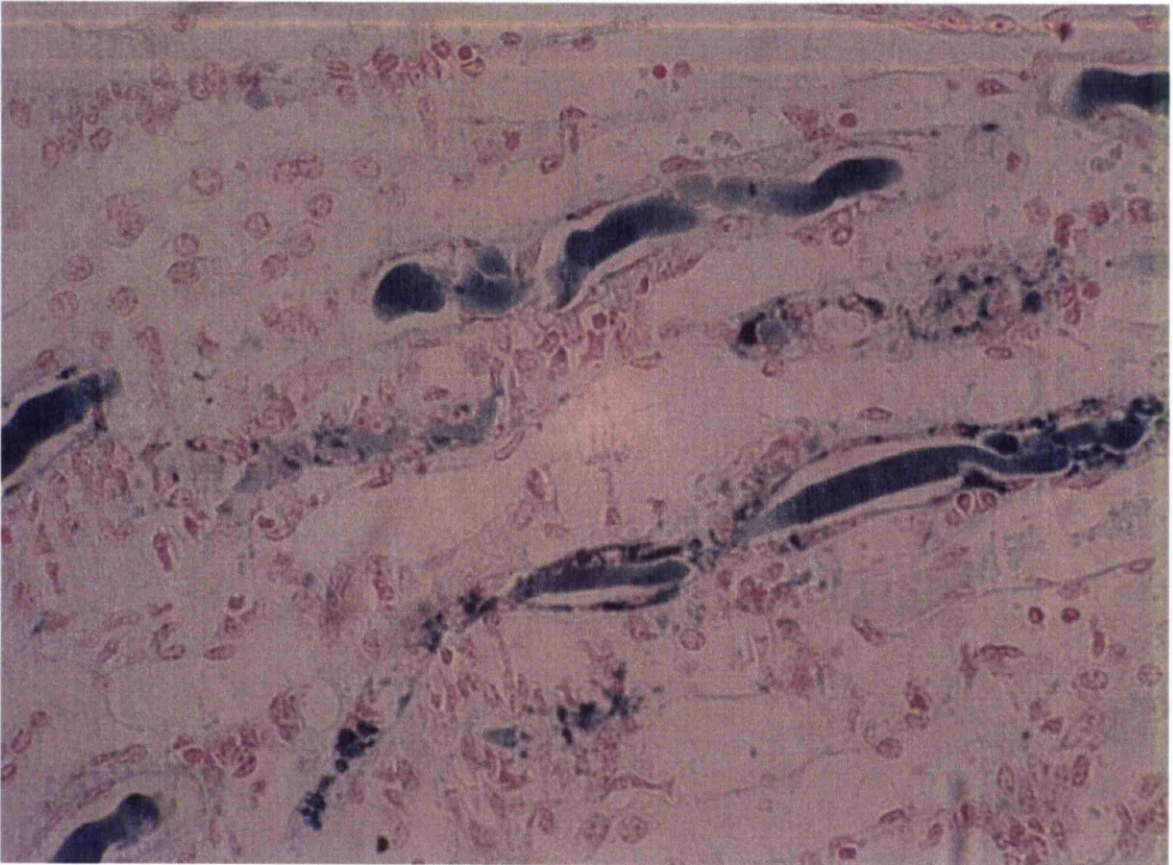


Figure 6.16:- A high power photomicrograph showing the ochronotic urine in the tubules of the kidney from M283. This staining also detects ochronosis associated with the lining cells of the tubules, fibroblastic cells and their associated matrices.



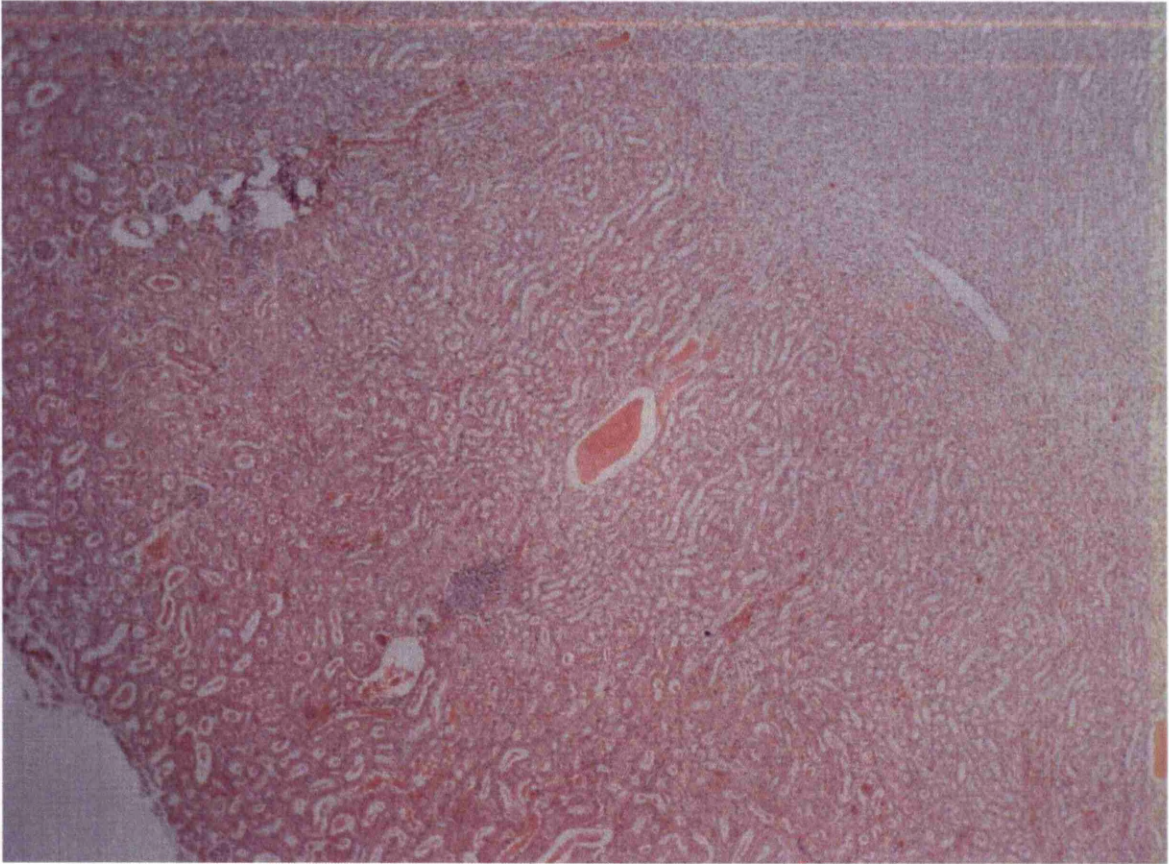


Figure 6.17:- A low power photomicrograph from the kidney of mouse off NTBC for 2 weeks (M2091). No detectable intra or extracellular ochronosis.

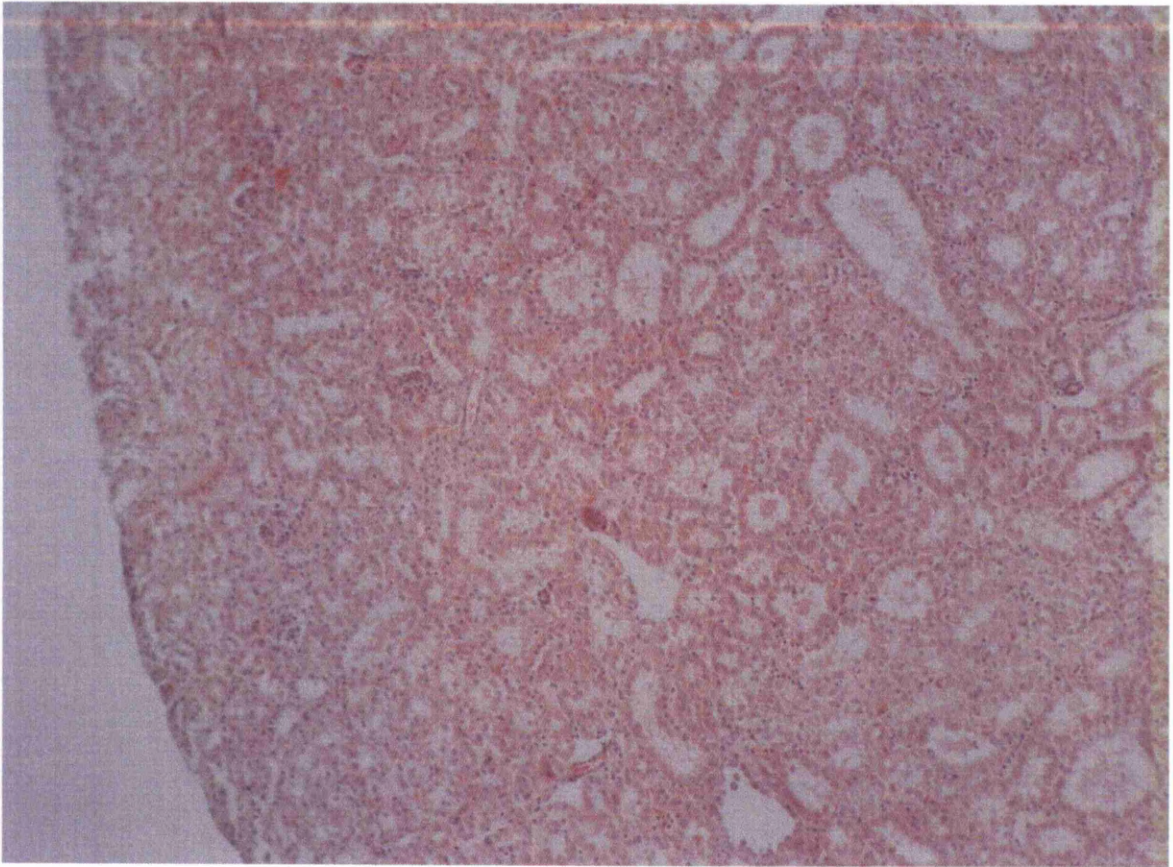


Figure 6.18:- A low power photomicrograph showing the kidney of mouse off NTBC for 2 days (M240). There is no detectable sign of ochronosis either intra or extracellularly.



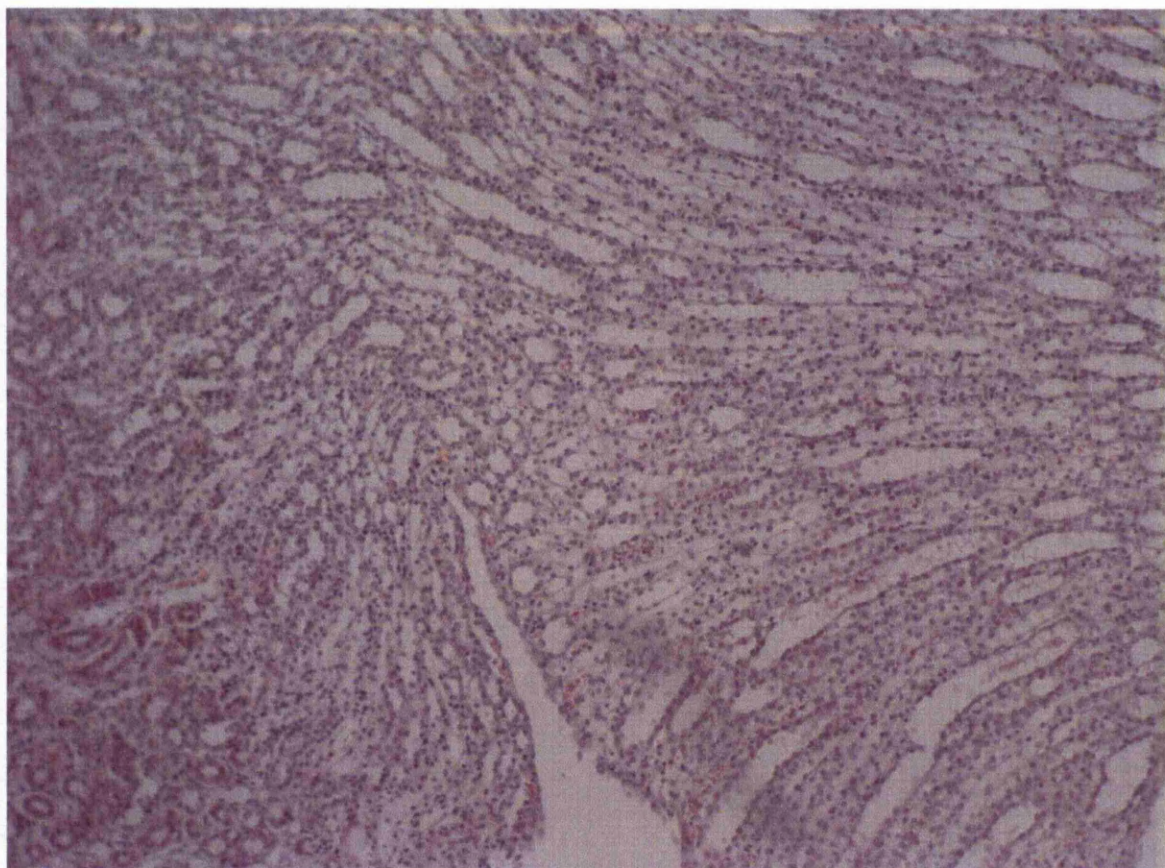


Figure 6.19:- A low power photomicrograph showing the kidney of mouse off NTBC for 1 day (M236). There is no detectable intra or extracellular ochronosis.

#### 6.2.2.5 Knee Joints

Overview of the knee joints revealed normal cartilage matrix located on the underlying bone architecture. There was no ochronosis of the cartilage matrix on the distal femur or proximal tibia; as seen widespread in the human joint articular cartilage matrix. The surface of the articular cartilage appeared normal with no pigmentation or degeneration.



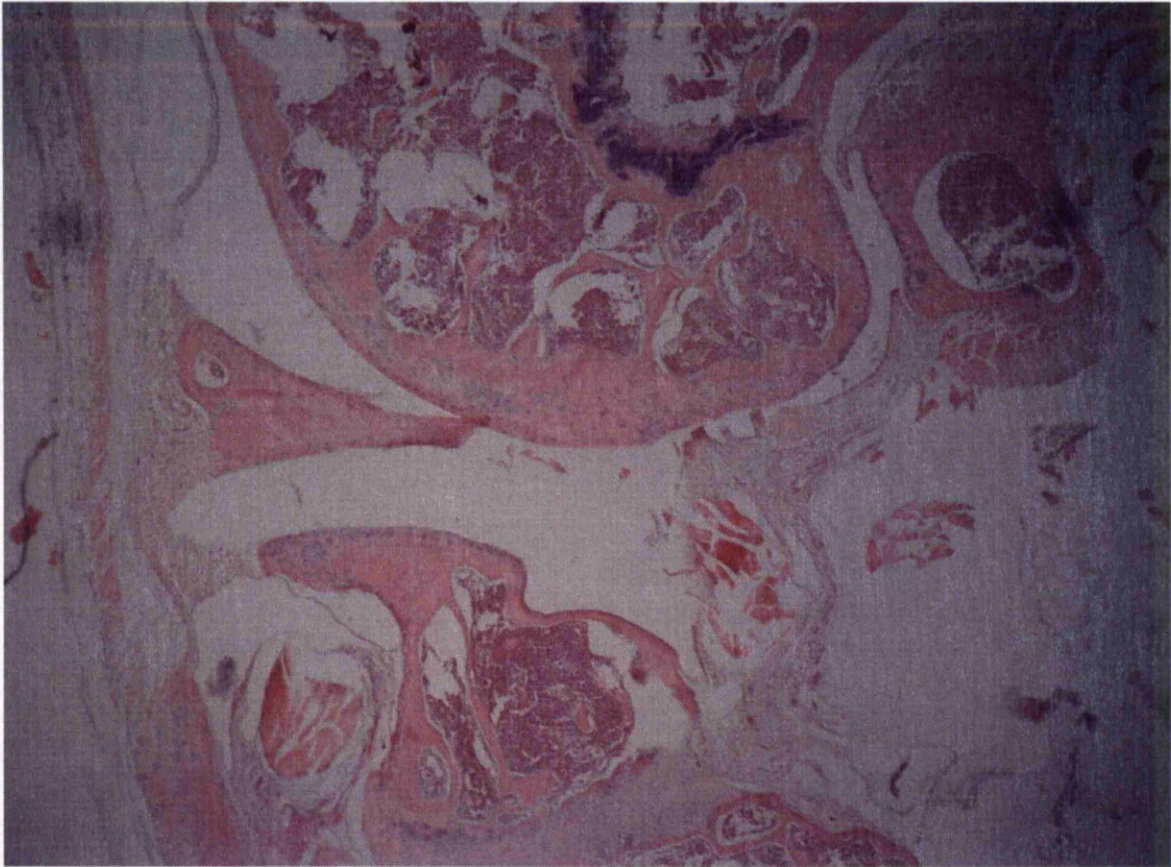


Figure 6.20:- A high power photomicrograph showing the overview of the knee joint from M283. all major anatomical features of the knee joint are seen: distal femur, tibia, fibula, patella and meniscus.

High power observations of the distal femur revealed numerous chondrocytes deep in the cartilage matrix, in close proximity to the subchondral bone, with a dusky appearance to their pericellular matrix. The chondrocytes were a mixture of isolated cells and pairs of chondrocytes. These chondrocytes and their lacunae showed a spherical shape. There were regions on the distal femur that displayed an absence of subchondral plate beneath the articular cartilage.

The proximal tibia showed numerous hypertrophic chondrocytes, some of which showed intracellular pigmentation. In other regions of the proximal tibia the articular surface showed discontinuity at the surface and underlying chondrocytes showed dense pigmentation. The

head of the fibula also showed chondrocytes in singular and groups that had dense pigmentation of their territorial and pericellular matrix. These again were closest to the subchondral bone, no similar pigmentation was seen in the chondrocytes close to or at the articular surface. The meniscus displayed a small number of chondrocytes on the superior surface which had a dusky appearance around their periphery. There were no chondrocytes in the centre of the structure which displayed this pigmentation.

There was also pigmentation in the enthesis of the muscle inserting into the fibula showed pigmentation in the fibrocartilagenous insertion. The chondrocytes showed intra and pericellular pigmentation.



Figure 6.21:- A high power photomicrograph showing the distal femur (top), meniscus (central) and proximal tibia (bottom). Deep chondrocytes of the distal femur show ochronosis in their pericellular matrix.





Figure 6.22:- A high power photomicrograph of the proximal fibula show clear intracellular ochronosis of the deep chondrocytes along with their pericellular and territorial matrices, some cells appear dead or necrotic. No comparable ochronosis is seen at the articular surface of in the osteocytes.

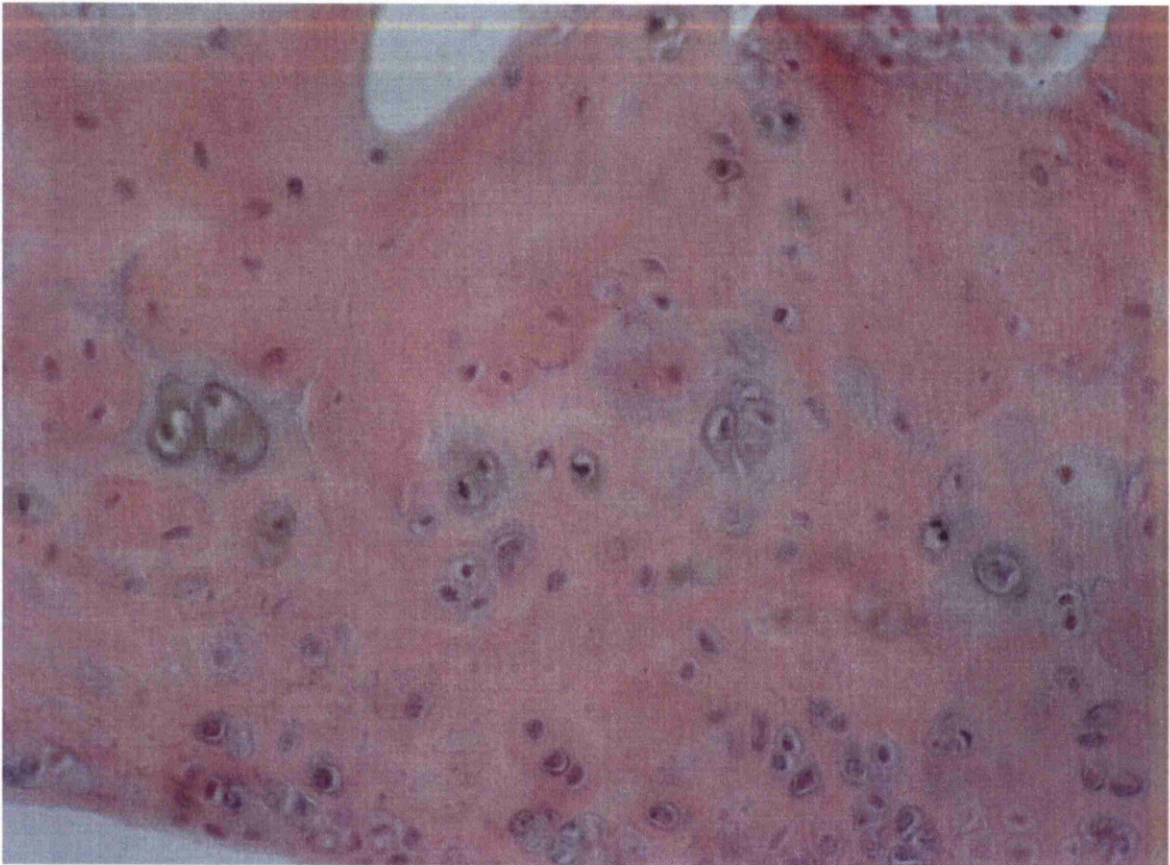


Figure 6.23:- A high power photomicrograph showing the distal femur. Numerous chondrocytes and their periceelular and territorial matrices show ochronosis. There is no comparable pigmentation in the interterritorial matrices and at the articular surface.

### **6.3 DISCUSSION**

This Chapter presents the first data showing ochronosis of tissues in a murine model of alkaptonuria. It has previously been published that mice with the AKU genotype do exist (Montagutelli, 1994). However, these animals do not go on to display the usual phenotypic ochronosis seen in the adult human, even though they have elevated levels of urinary HGA (Montagutelli, 1994, Suzuki, 1999). It has been suggested that the endogenous production of ascorbic acid is a protective mechanism against the gradual ochronosis of tissues in these animals (Kamoun, 1992), or that they do not live long enough to allow deposition to occur in their tissues, or that urinary excretion is so complete that tissues do not experience high



concentrations of HGA. Here we show that tissues, including those of the joints, show ochronosis in mice carrying the mutation for the disease and displaying the high urinary excretion of HGA, when combined with the effects of a second mutation in the FAH gene.

It has been proposed that ascorbic acid, which is produced endogenously in these animals may act as a protective factor. These results suggest that the presence of ascorbic acid is not sufficient to completely prevent pigmentation in all mice. While mice that have been AKU from birth have not yet been shown to display any pigmentation, longitudinal studies of their lifespan do not exist, so it is difficult to completely rule out pigmentation in aged specimens. It has previously been suggested that HGA is not the sole determining factor in pigmentation (Taylor, 2010). The sporadic distribution of pigmentation in the HGD/HTT1 animals would lend further weight to that theory that not all animals or regions of these animals show pigmentation following the initial conversion to the AKU phenotype many months before sampling. 10 months off NTBC with buildup HGA should be sufficient for pigmentation to occur across numerous cartilaginous structures.

Detection of pigmentation within the kidneys in these animals is not surprising from a functional point of view given this is the site of filtration of the blood and the high metabolic activity that occurs here. It is well documented that the darkening of urine is a sign of ochronosis and kidney manifestations in humans are not uncommon: for example, the passing of pigmented kidney stones. There are also descriptions of pigmentation within the kidneys in humans and histologically associated manifestations of the deposition in these tissues (Helliwell, 2008 & Gaines, 1989).

The kidneys in these animals are of interest as it maybe that the effects of the withdrawal of NTBC on these animals and the effects of FAA on the non AKU regions of the kidneys, causing damage, would seriously affect the ability of the kidneys to perform their function, the loss of normal functionality may also be similar to the renal slow down experienced by human AKU sufferers with ageing, limiting the ability of the kidneys to excrete HGA (Lindeman, 1985). However, there is currently no longitudinal data detailing the urinary (and plasma) levels of HGA in AKU patients prior to known ochronosis, or the change over time. Such data would indeed be useful, perhaps observations at a young adolescent age and then compared following a removal of a known ochronotic joint or detection of ochronosis in the sclera or pinna.

It has been shown and widely accepted that there is HGA present in the urine of the HGD<sup>-/-</sup> and FAH<sup>-/-</sup>HGD<sup>+/-</sup> knockouts. There is currently no evidence describing the concentration of the HGA in the urine, or more importantly the plasma of these animals. However, we show that regardless of the concentration, it is sufficient to undergo polymerisation and deposit as ochronotic pigment in multiple tissues. Absence of deposition in the cardiac connective tissues are not of major note, given that not all AKU patients present with cardiac involvement, this suggests that lifestyle factors may play a role in the deposition process. Whatever these factors may be, they are yet to be elucidated.

Deposition in the cartilage of these mice shows that there is sufficient HGA present to allow for polymerisation and deposition. It has been shown in chapter 5 that deposition in the human condition starts focally, associated with single chondrocytes in the calcified cartilage,

progressing towards the articular surface with intracellular deposition appearing to precede the extracellular deposition (Taylor, 2011). It appears that the initiation in these animals is the same, demonstrating that these animals may be valuable for screening therapeutic strategies for inhibiting or reversing pigment deposition in AKU. Whilst bone changes are seen in the human disorder (Taylor, 2011), they were not observed in these mice, bone matrix was devoid of pigmentation, and also bone cells. This also adds weight to the hypothesis that mineralisation is protective in the disorder. It must be appreciated that bone changes appear secondary to the cartilage changes in the progression of AKU, so while bone changes were not observed in these animals, they may occur at a later stage, once the cartilaginous changes become more widespread.

The observations within the murine chondrocytes of two distinctly different types of pigmentation (granular and blanket) is interesting, as this suggests that similar to the human condition, pigmentation may actually arise under two different mechanisms within these tissues (Taylor, 2010). This adds further weight to our claim of synonymy with the human condition. Murine models have proved useful for investigation into disorders on the tyrosine metabolic pathway, particularly with the AKU mouse model which was influential in decoding the location of the then unknown human mutation (Montagutelli, 1994, Pollak, 1993 & Janocha, 1994). The proposed treatment of alkaptonuria using NTBC came about from investigations into mice deficient in the FAH gene. These animals are exposed to the buildup of toxic tyrosine metabolites neonatally, once FAH production begins around day 16. The homozygous animals do not survive beyond 24 hours of birth; however administration of NTBC to mothers whilst pregnant, on day 15 of gestation results in the neonatal effect of FAH deficiency being abolished (Grompe, 1995). The use of NTBC for treatment of HTT1 is now a widely used treatment, although it is not without risks - patients are vulnerable to

hepatocarcinomas (from the underlying hereditary tyrosineamia) and there are further complications associated with the elevated tyrosine plasma levels (Manning, 1999).

The animals which were FAH knockout or FAH knockout and HGD heterozygote showed deterioration with their health following withdrawal from NTBC. In contrast to this the animals which were double knockouts at the FAH and HGD gene were healthy at 4, 7, 9 & 11 weeks off NTBC (Manning, 1999). A similar phenotype and spontaneous mutation has also been described in *Aspergillus* (Fernandez-Canon, 1995). The reversion to the AKU phenotype of both these systems showed the distinct darkening of urine and media (Manning, 1999 & Fernandez-Canon, 1995). Furthermore it has been shown that kidneys from FAH<sup>-/-</sup> animals are pale and increased in size, confirming that they are abnormal (Grompe, 1995). This in itself may result in an increase in the stresses in the kidneys which in turn promotes ochronosis in the surrounding AKU genotype/phenotype regions of these kidneys.

It is encouraging that the earliest signs of pigmentation in these animals have been observed and are synonymous with that of the human condition. It is this critical time point that the ochronosis would need to be treated in human AKU, to prevent full ochronotic osteoarthropathy developing. From our published evidence and that described in the literature it is unlikely that once the pigment is deposited it can be turned over, as seen by the inability of Tergazyme to degrade ochronotic cartilage in Chapter 5 (Taylor, 2011). This time point in the murine model will provide a useful tool for screening potential therapeutic agents. Detection of ochronosis in murine tissues represents a distinct advance in the knowledge and understanding of alkaptonuric osteoarthropathy and will allow us to gain a better understanding into the molecular pathogenesis of the disorder.





**7. Identification of trabecular excrescences, novel microanatomical structures, present in bone in osteoarthropathies**

## **7.1 INTRODUCTION**

Turnover of skeletal tissues occurs as part of development and continues throughout life, in both health and disease. It is usually held and widely stated that skeletal architecture is finely regulated in accordance with homeostatic requirements by bone modelling (net deposition or resorption) and remodelling (resorption and subsequent deposition) and that one of the major influences on remodelling is mechanical loading. The tissue level responses at the micro and ultrastructural levels are complex chains of events involving a number of specialised layers within the joint, namely; hyaline articular cartilage (HAC), articular calcified cartilage (ACC), subchondral bone (SCB), trabecular and cortical bone. The relationships between bone and cartilage are highly dependent on reciprocal normal functions of the tissues. Under normal loading, HAC transmits forces down through the ACC to SCB, resulting in high shear stresses at the osteochondral junction region brought about by differences in the material properties of the calcified and non-calcified tissues. Remodelling of bone is usually highly regulated with a balance of bone removal and formation (Frost, 1964) in what is generally considered to be a coupled mechanism (Parfitt, 1982). However, alterations in trabecular architecture with the normal ageing process suggest that the coupling mechanism is not as tightly regulated as it appears to be in earlier life (Jayasinghe, 1993 & Jayasinghe, 1994).

Remodelling is regulated by a complex interaction of systemic and local factors including paracrine and autocrine signals. The topography of the surface that is produced by the osteoclasts is also important in regulating new bone formation (Gray, 1996). While coupling and (re)modelling is focal at multiple locations at any given time (Frost, 1991), the systemic hormones and the cells exhibit a multitude of wider reaching effects which

result in the replication of undifferentiated cells, recruitment of cells and the differentiated function of cells (Hill, 1998).

Deviation from the finely balanced and highly regulated (re)modelling process results in numerous recognised pathological conditions in the mineralised tissues. These include osteoporosis, in which resorption exceeds formation (Russell, 2003). Aberrant remodelling of bone underlying cartilage is frequently observed in arthropathies, the most common of which is osteoarthritis (OA). There is still much debate about what instigates pathological change(s) in tissues in OA and whether the defect occurs in the HAC or the SCB first, or whether they occur simultaneously. However, the changes in both tissues bring about altered loading across the joint tissues.

The recognition of AKU as a rare form of OA is also supported by common end point treatment of both disorders - joint replacement (Kraus, 2011). In AKU, it is commonly held that cartilage is the predominantly affected tissue, although it has been shown that capsular tissues are also involved. Ochronotic pigment derived from polymerisation of homogentisic acid (HGA) is initially associated at the ultrastructural level with the periodicity of the collagen fibrils, as seen in chapter 4 (Taylor, 2010). The evidence for the association of HGA pigment with collagen is clear, but until recently it was accepted that bone is relatively unaffected, particularly compared to cartilage (Di Franco, 2000). It has been shown that part of the progression of the destructive mechanism in AKU involves an up-regulation of the osteoclastic activity in the mineralised joint tissues of these patients resulting in the unprecedented complete resorption of the SCB plate and ACC, as seen in chapter 5 (Taylor, 2011). This resorption may be induced by altered loading, possibly as a result of stress shielding due to the altered mechanical properties of

the overlying HAC. Ochronotic pigment deposition increases the stiffness of the HAC matrix, resulting in abnormal distribution of load through the tissues and Chapter 5 of this Thesis (Taylor, 2011). Alternatively, HGA polymer deposition may inhibit the mineralisation of HAC to become ACC and the reserve of ACC may eventually be used up.

In this chapter, analyses of samples from AKU arthropathies were undertaken following our previous discovery of the extraordinary SCB and ACC phenotype and compared them with more common OA arthropathy samples (Taylor, 2011). In performing this study we were able to identify novel microanatomical structures in bone of patients with ochronotic arthropathy which may be the result of the abnormal loading in the tissues following changes in the load distribution across the joint because of aggressive remodelling of the SCB & ACC plate. These microanatomical structures were discovered using 3D SEM. This high depth of field technique, even when used at low magnification, allowed the identification and observation of numerous excrescences on free bone surfaces. Subsequently, conventional light microscopic histology and quantitative backscattered electron mode scanning electron microscopy (qBSE-SEM) both confirmed their presence in the calcified matrix. The number and type of excrescence were more difficult to distinguish by these latter imaging methods as they are limited either by the thickness of the specimens -  $\sim 5\mu\text{m}$  for light microscopy – or by the information depth of the method –  $\sim 0.5\mu\text{m}$  for 20kV qBSE-SEM.

Unexpectedly these structures were subsequently observed in 'ordinary' osteoarthritic samples that were being used as control, reference specimens for the investigation, and,

retrospectively, other archival OA samples used for BSE SEM studies. These structures add evidence to the literature that already describes the abnormal structure and function of tissues in joint arthropathy



## **7.2 RESULTS**

### **7.2.1. 3D topographical SEM imaging of AKU Bone**

3D topographical SEM imaging of the most severe ochronotic arthropathy sample revealed localised porotic bone within the femoral head. The more porotic regions were peripheral. In the centre of the sample, there was a greater amount of bone with fewer distinguishable trabeculae. The majority of mineralised matrix was present as large bone plates joined together by short trabeculae. Close examination of the trabecular plates and rods in the regions of high bone volume revealed the presence of numerous excrescences on the surface and frequently some distinct discontinuity with the established bone surface (Fig. 7.1-7.4).

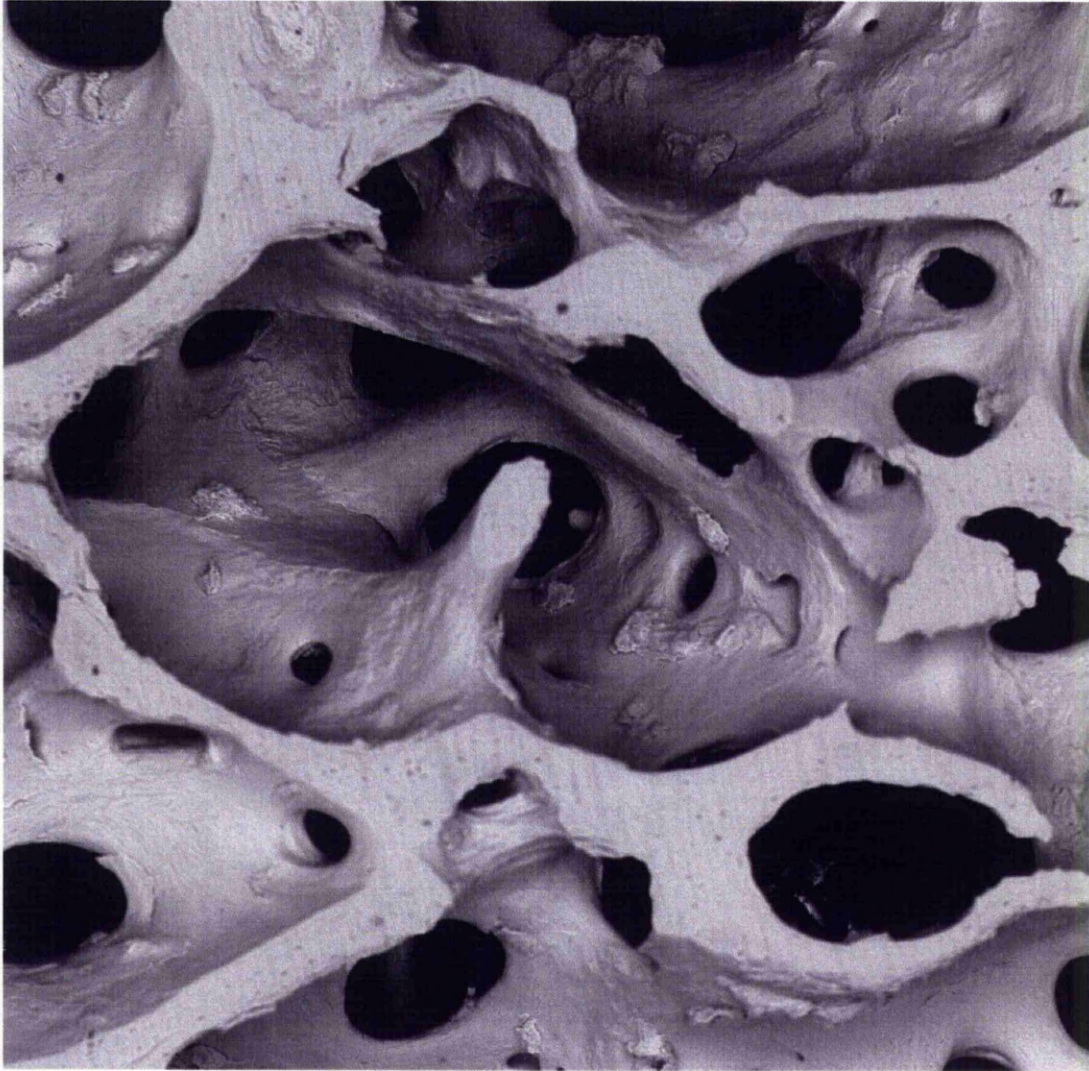


Figure 7.1: 20kV BSE 3D SEM images of carbon coated, macerated slice of femoral head from a 59 year old male who underwent a left total hip replacement for ochronotic osteoarthropathy. Numerous excrescences project from the otherwise smooth contour of the internal bone surfaces. Top centre shows an excrescence on pre-existing resting surface. Its surface is partly scalloped, suggesting osteoclastic resorption. Surface-osteocyte lacunae can also be seen in other parts of the excrescence. Image field is 2700 microns wide and high.



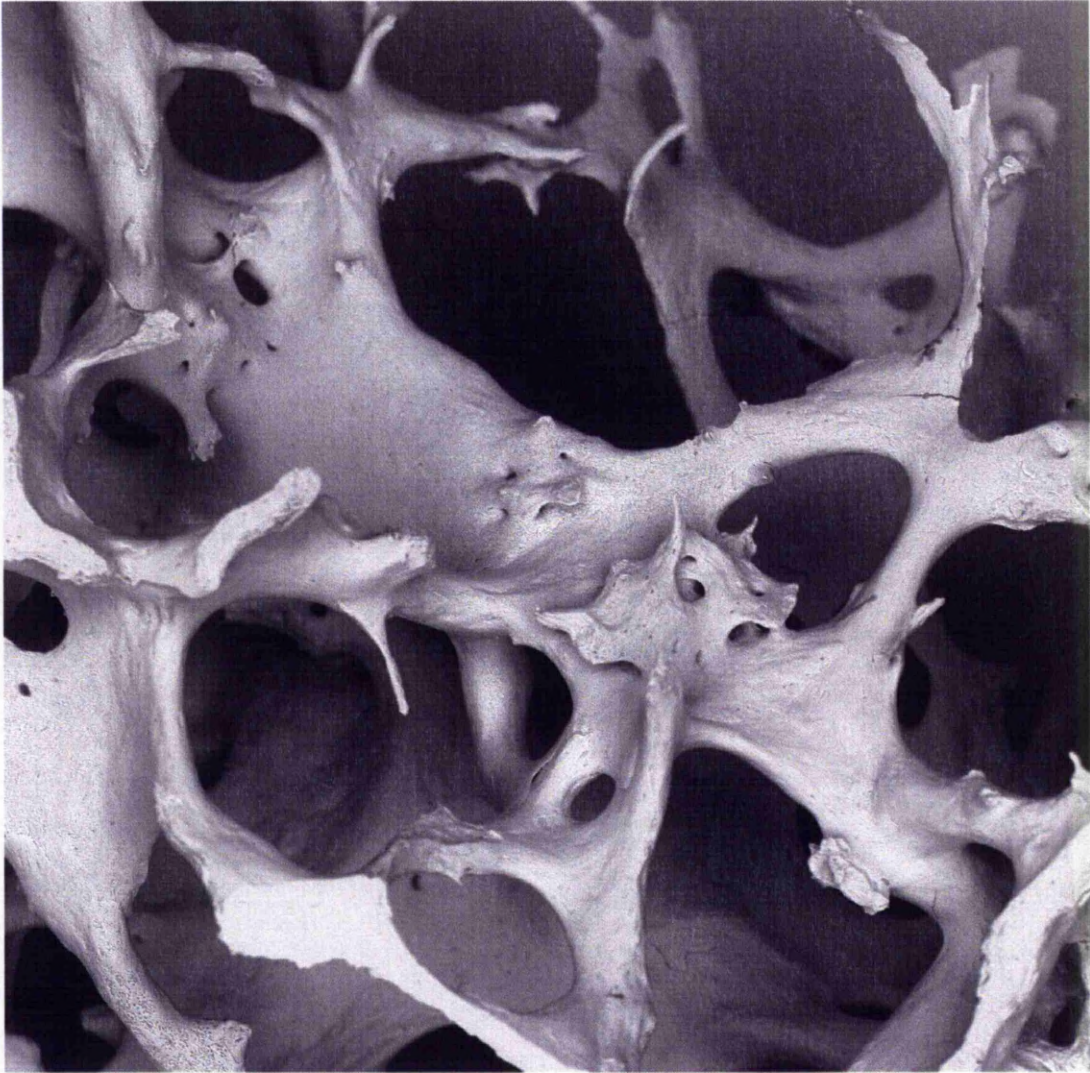


Figure 7.2: 20kV BSE 3D SEM images of carbon coated, macerated slice of femoral head from a 59 year old male who underwent a left total hip replacement for ochronotic osteoarthropathy. Numerous, many thin, free-ended (unloaded), resorbed trabeculae. Some have been partially resorbed, before new bone deposition over their surfaces (bottom right). Image field is 2700 microns wide and high.

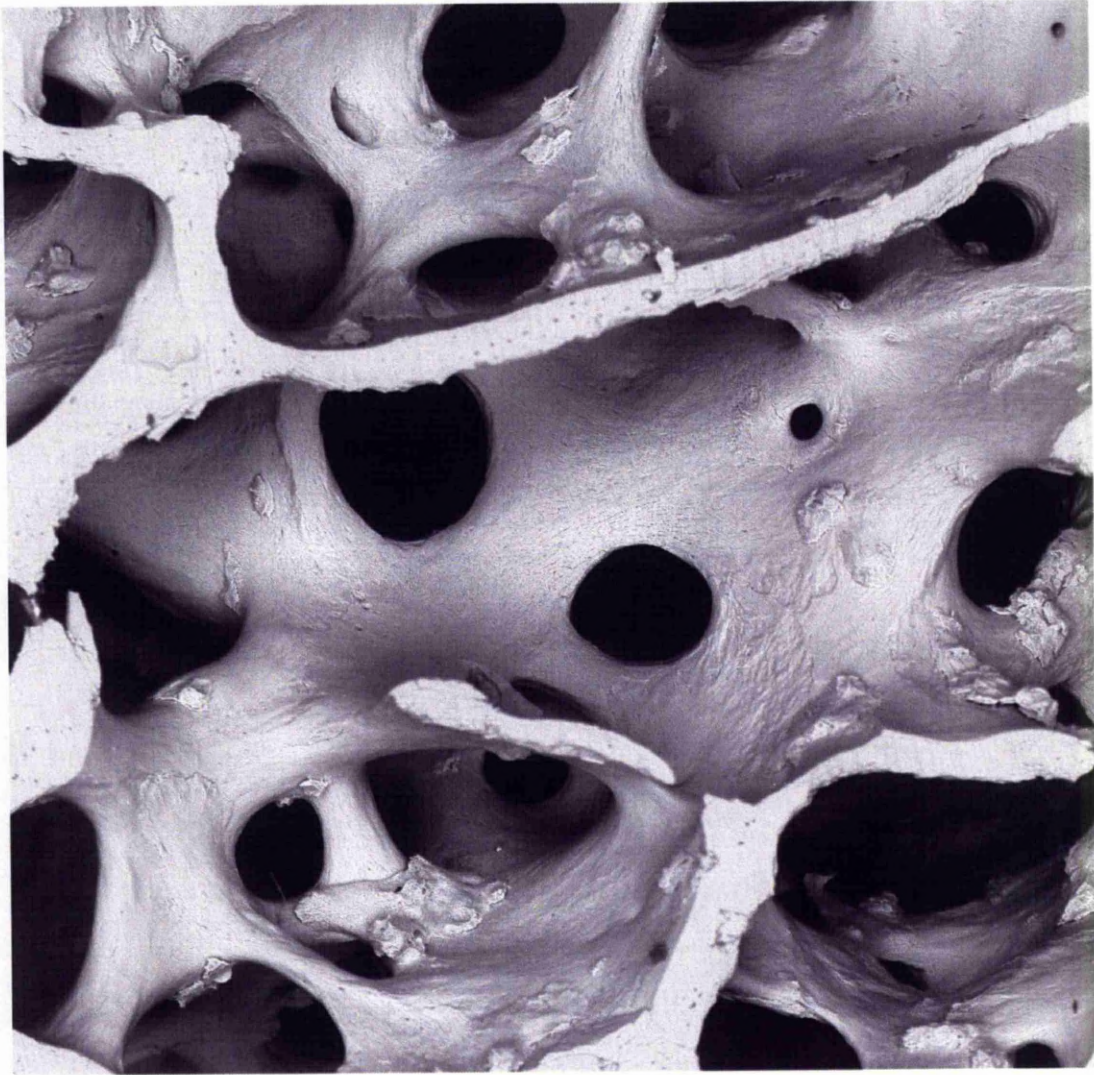


Figure 7.3: 20kV BSE 3D SEM images of carbon coated, macerated slice of femoral head from a 59 year old male who underwent a left total hip replacement for ochronotic osteoarthropathy. Another field of mostly plate-like trabeculae with numerous stucco projections from otherwise smooth surfaces. Image field is 2700 microns wide and high.



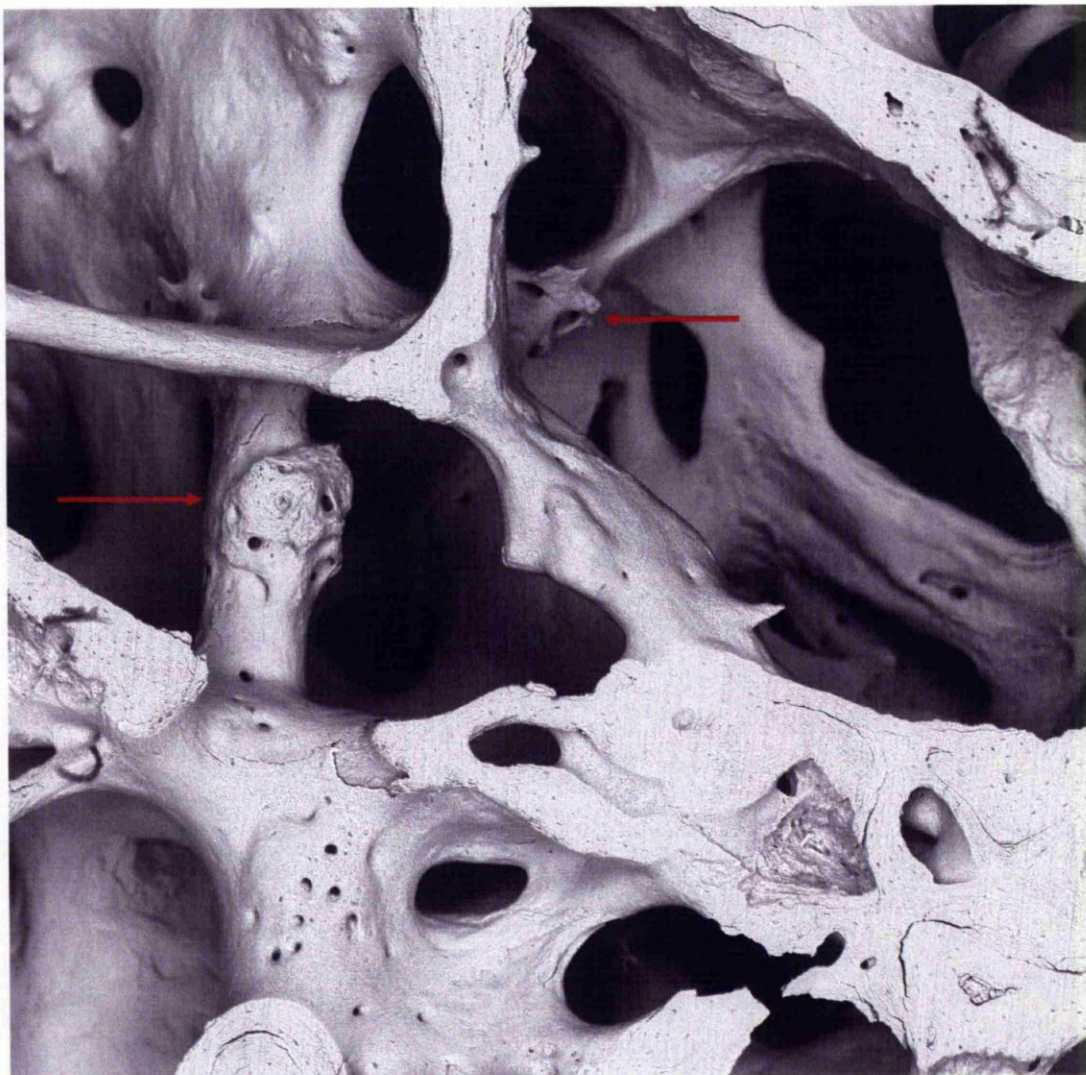


Figure 7.4: 20kV BSE 3D SEM images of carbon coated, macerated slice of femoral head from a 59 year old male who underwent a left total hip replacement for ochronotic osteoarthropathy. Large microcallus patches (arrows) formed from woven bone can be seen in the left hand side of the image. Several areas show incomplete integration of old and new bone packets. Also note incomplete, resorbed trabecular ends. Image field is 2700 microns wide and high.



There appeared to be various morphologies of excrescence. One very common type appears to have arisen from the incomplete resorption of something projecting above the general plane of the local bone surface, perhaps arising from partial removal of secondary or extra trabeculae, not part of the original stock of normally distributed trabeculae and which must have formed in prior marrow space. Extra trabeculae made of immature (woven) bone are a common accompaniment of osteoarthritis. These are characterised by deeply scalloped surfaces and rugged edges (Fig. 7.1 & 7.5). The resorption involved here is deeper and shows larger pits or scoops than those of normal resorption fields, an example of which is shown in Fig. 7.6.



Figure 7.5: 20kV BSE 3D SEM images of carbon coated, macerated slice of femoral head from a 59 year old male who underwent a left total hip replacement for ochronotic osteoarthropathy. A normal resorbed area is seen at left with shallow, skimming osteoclastic resorption: this 'packet' has been partly infilled with nearly completely mineralised bone; the scene is thus typical of normal resorption-formation coupling. This contrasts strongly with the rugged scalloped edges of the obvious 'stucco' excrescences. Image field is 900 microns wide and high.



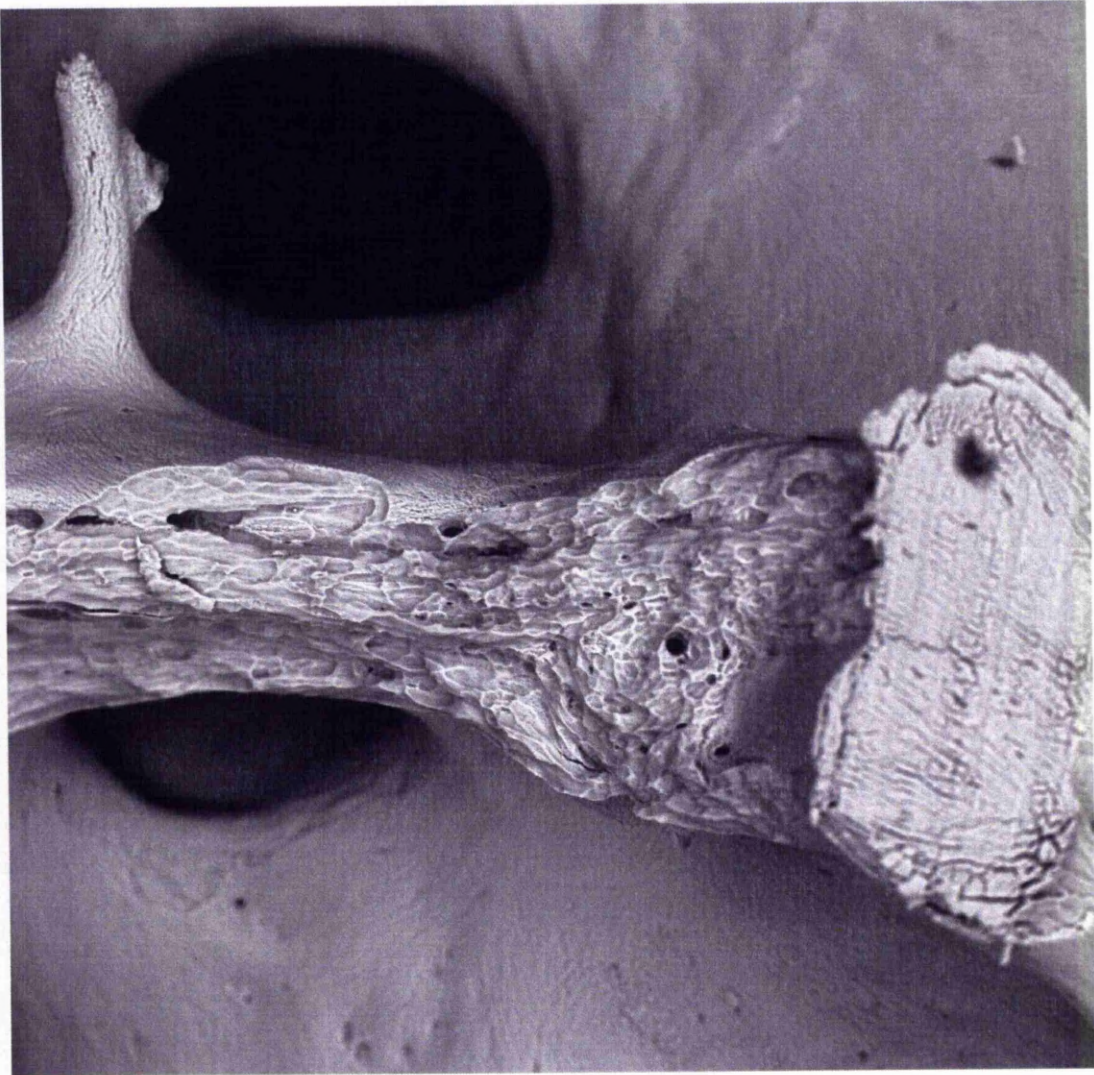


Figure 7.6: 20kV BSE 3D SEM images of carbon coated, macerated slice of femoral head from a 59 year old male who underwent a left total hip replacement for ochronotic osteoarthropathy. An area of normal, but unrepaired resorption on the side of a massive trabecula is seen at centre. Image field is 900 microns wide and high.



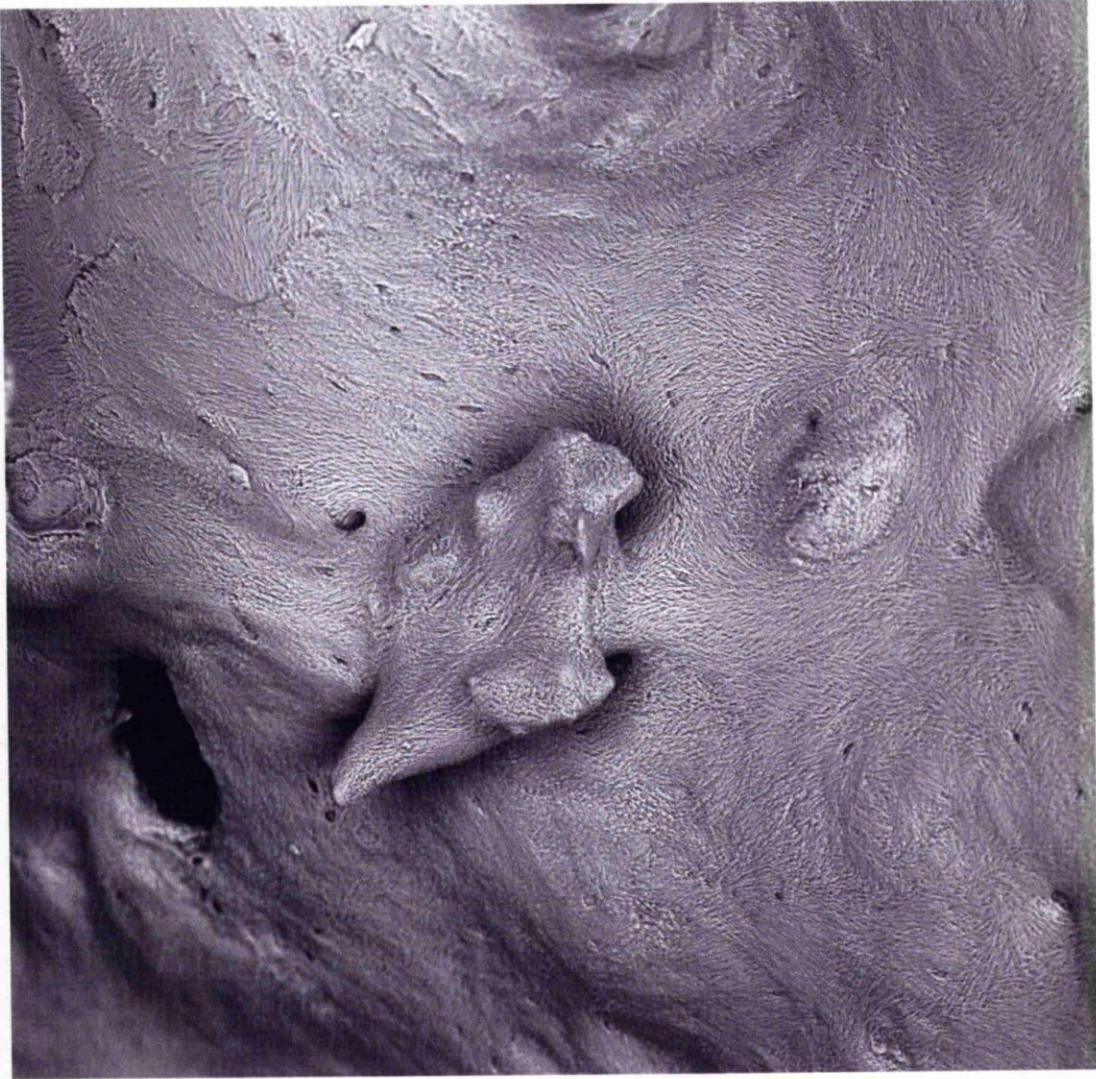


Figure 7.7: 20kV BSE 3D SEM images of carbon coated, macerated slice of femoral head from a 59 year old male who underwent a left total hip replacement for ochronotic osteoarthropathy. Excrescence just below centre resulted from incomplete resorption of prior trabeculae and is covered with nearly completely mineralised new bone matrix with continuous collagen fibre bundle profiles in this superficially anorganic, peroxide treated sample (Boyde, 1972). Image field is 900 microns wide and high.





Figure 7.8: 20kV BSE 3D SEM images of carbon coated, macerated slice of femoral head from a 59 year old male (AKU3) who underwent a left total hip replacement for ochronotic osteoarthropathy. Higher magnification detail of an immature bone patch seen in Fig 7.4. This microcallus patch is typical of those found in other ageing human bone samples, including in osteoporosis. Image field is 900 microns wide and high.



The second appearance of excrescence is similar to the first but they have been smoothed over by new bone deposition (Fig. 7.7). Neither of these types resemble the common type of microcallus patch (another form of excrescence but which is not consider novel) found in older human trabecular bone, and which was also found in this study, an example of which is shown in Fig. 7.8, which is a higher magnification of part of the field of view shown in Fig. 7.4.

A third appearance merges with the others, but more resembles coarse stucco and seems to have arisen where resting surfaces have been focally reactivated. These appear as random patches on the bone surface (Fig. 7.1 & 7.3). These deposits are frequently poorly attached to the prior trabecular wall in our macerated SEM samples, as demonstrated by clearly observable discontinuities between the excrescences and the otherwise continuous trabecular surfaces.

Analyses other pathological and normal bone have not yielded similar structures to date. (Li, 1999, Boyde 2003 & Boyde,2003).

### 7.2.2 Histology of AKU bone

Histological observations of the bone in ochronotic samples revealed multiple excrescences throughout the tissue, although the low section thickness makes it difficult to distinguish between types (Fig. 7.9 & 7.12). Examination of AKU histological sections using autofluorescence revealed differences in the fluorescence of the established bone matrix and excrescences which were attached to their surface (Fig. 7.13).

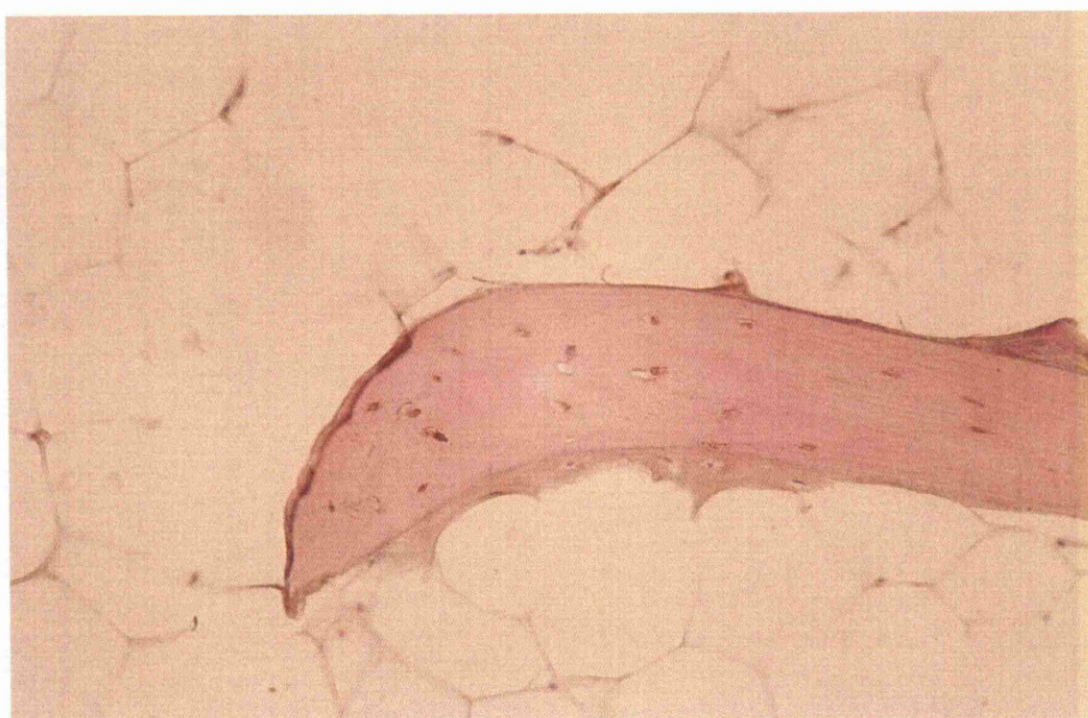


Figure 7.9: *Light microscopy of decalcified paraffin-embedded sections demonstrating excrescences on bone surface from a 59yr old male patient (AKU3) who underwent hip replacement surgery for ochronotic osteoarthropathy. H&E stained, in transmitted light, showing excrescences on both surfaces of a trabecula.*

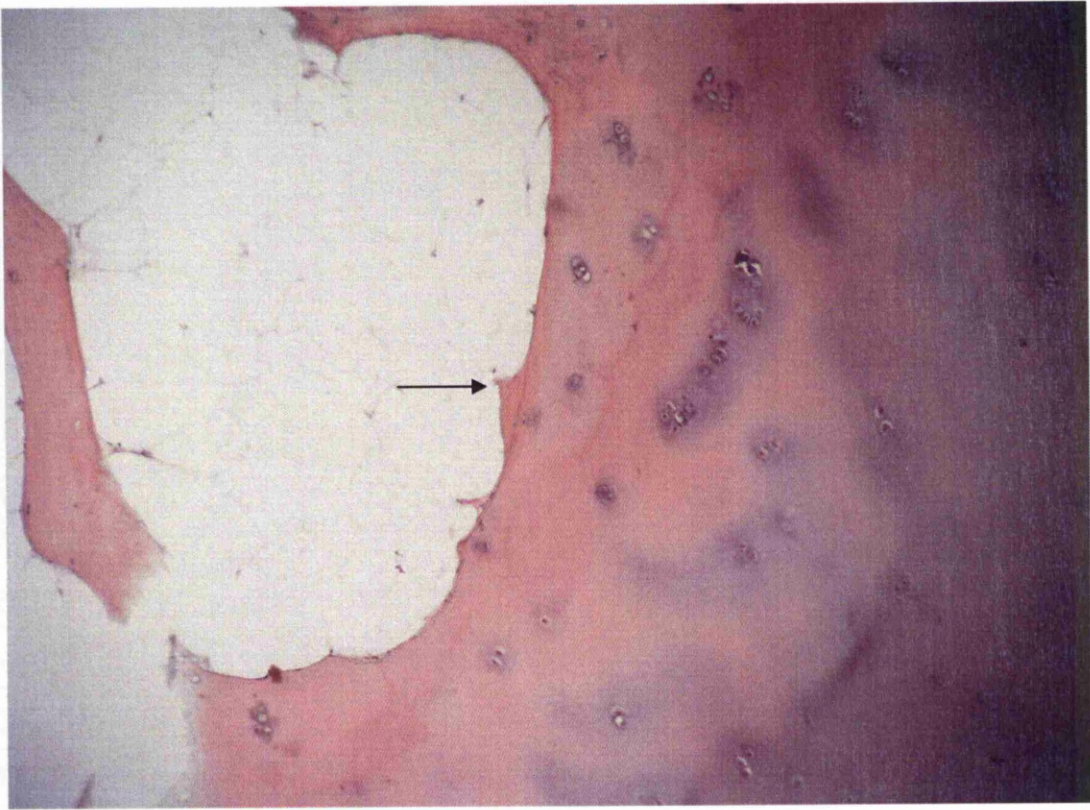


Figure 7.10: *Light microscopy of decalcified paraffin-embedded sections demonstrating excrescences on bone surface from the femoral condyle of a 46yr of male (AKU9) who underwent knee replacement surgery for ochronotic osteoarthropathy. H&E stained, in transmitted light, showing excrescence on the marrow surface of a thin subchondral plate, beneath the articular cartilage.*



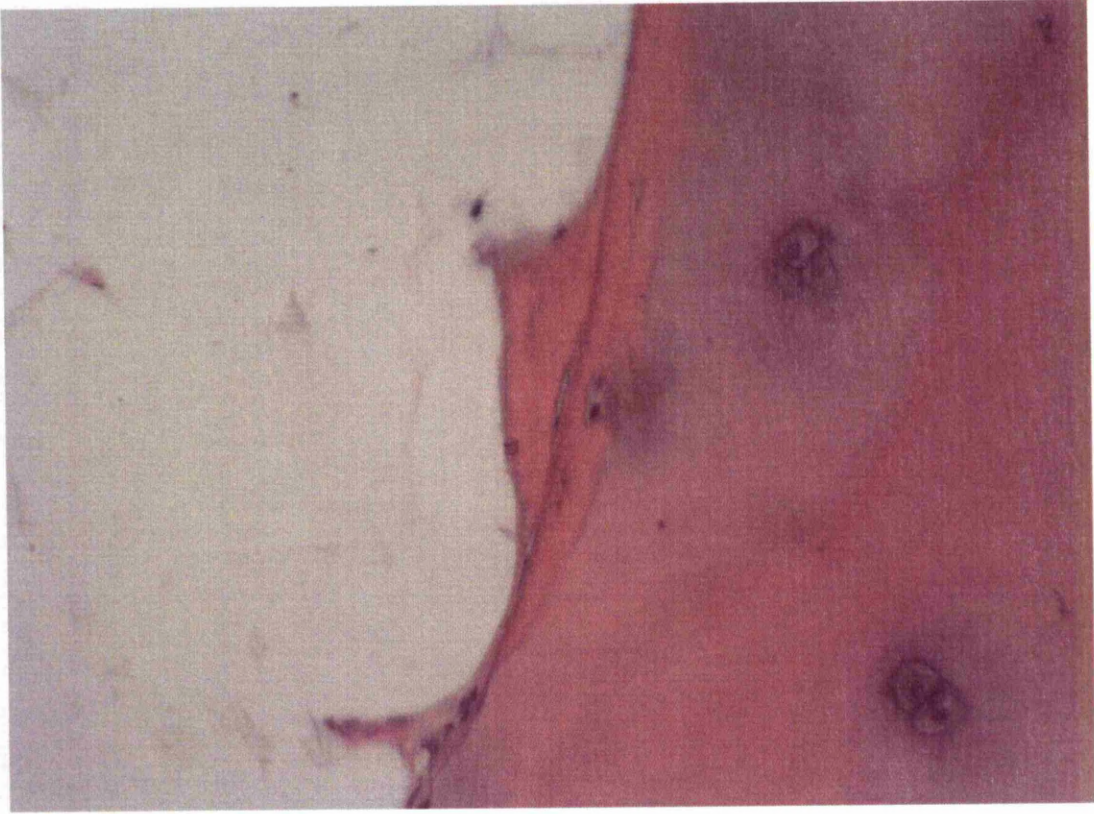


Figure 7.11: *Higher power light microscopy of decalcified paraffin-embedded sections demonstrating excrescences on bone surface from the femoral condyle of a 46yr old male (AKU9) who underwent knee replacement surgery for ochronotic osteoarthropathy. H&E stained, in transmitted light, showing excrescence on the marrow surface of a thin subchondral plate, beneath the articular cartilage. Note the incomplete incorporation into the thin subchondral bone plate.*

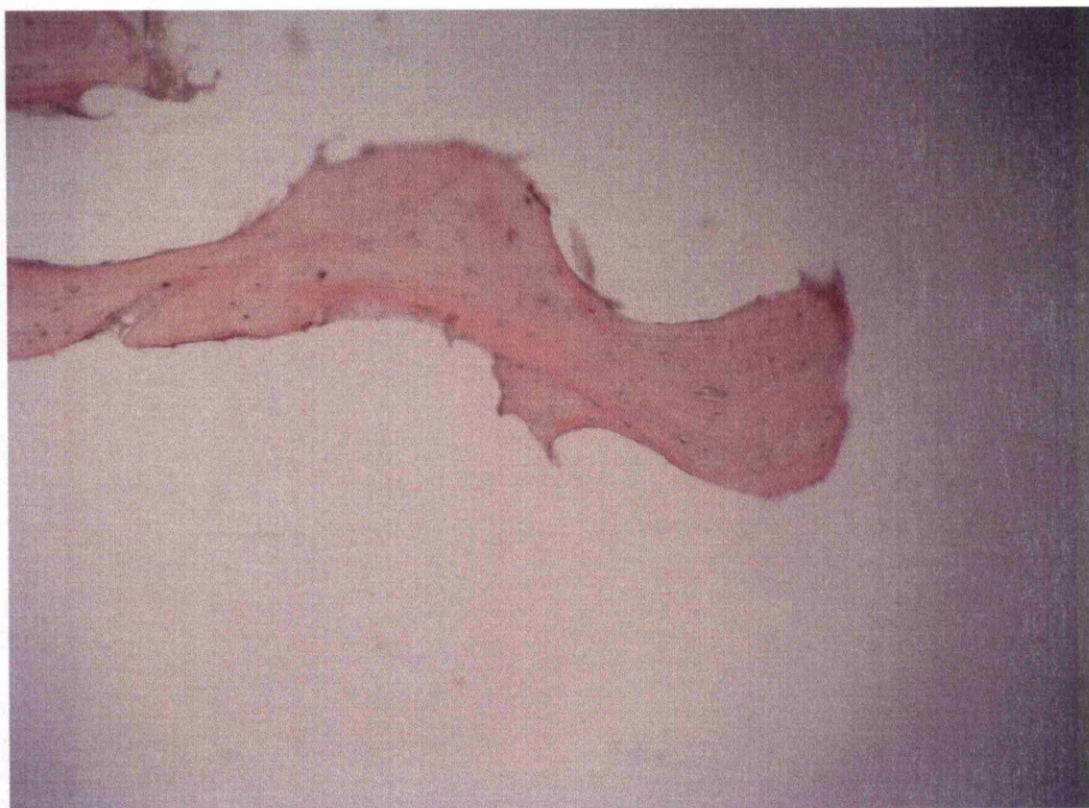


Figure 7.12: *Light microscopy of decalcified paraffin-embedded sections demonstrating excrescences on bone surface from the femoral condyle of a 58yr old female (AKU10) who underwent knee replacement surgery for ochronotic osteoarthropathy. H&E stained, in transmitted light, showing an excrescence on the trabecular surface.*



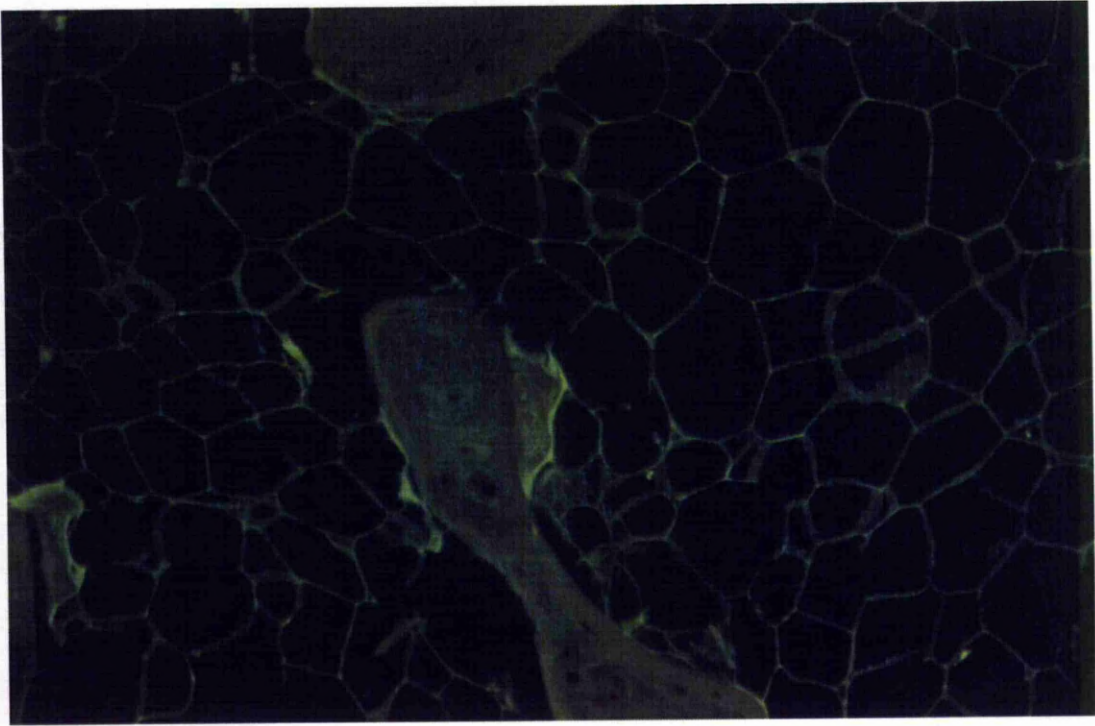


Figure 7.13: *Epifluorescence of an unstained section under blue excitation, showing the difference in fluorescence of the established matrix and the excrescence from a 59yr old male (AKU3) patient who underwent hip replacement surgery for ochronotic osteoarthropathy.*

### 7.2.3 qBSE - SEM imaging of AKU bone

qBSE - SEM imaging of AKU bone was performed to examine the bone quality of the AKU samples. Overall, mineralisation densities in trabeculae were within the normal range. Some of the trabecular surfaces showed surface abnormalities consistent with the 3D topographical images. Obvious excrescences showed increased mineralisation density (higher qBSE grey levels) than the underlying normal mineralised bone architecture (Fig 7.14 & 7.15). A few excrescences display preparative cracks at their attachment surfaces with the trabeculae, i.e., they were less well integrated with the existing bone. Other regions where normal new bone packets which formed over non-resorbed surfaces may also show artefactual detachment during sample preparation for SEM, as shown in Fig. 7.15. In Fig. 7.14 trabeculae show normal structure and range of mineral density. Excrescences (11 in the field of view) can be seen on the trabecular surfaces. The bulk of the trabeculae exhibit normal density range, but the excrescences show hypermineralisation when compared to the trabeculae.

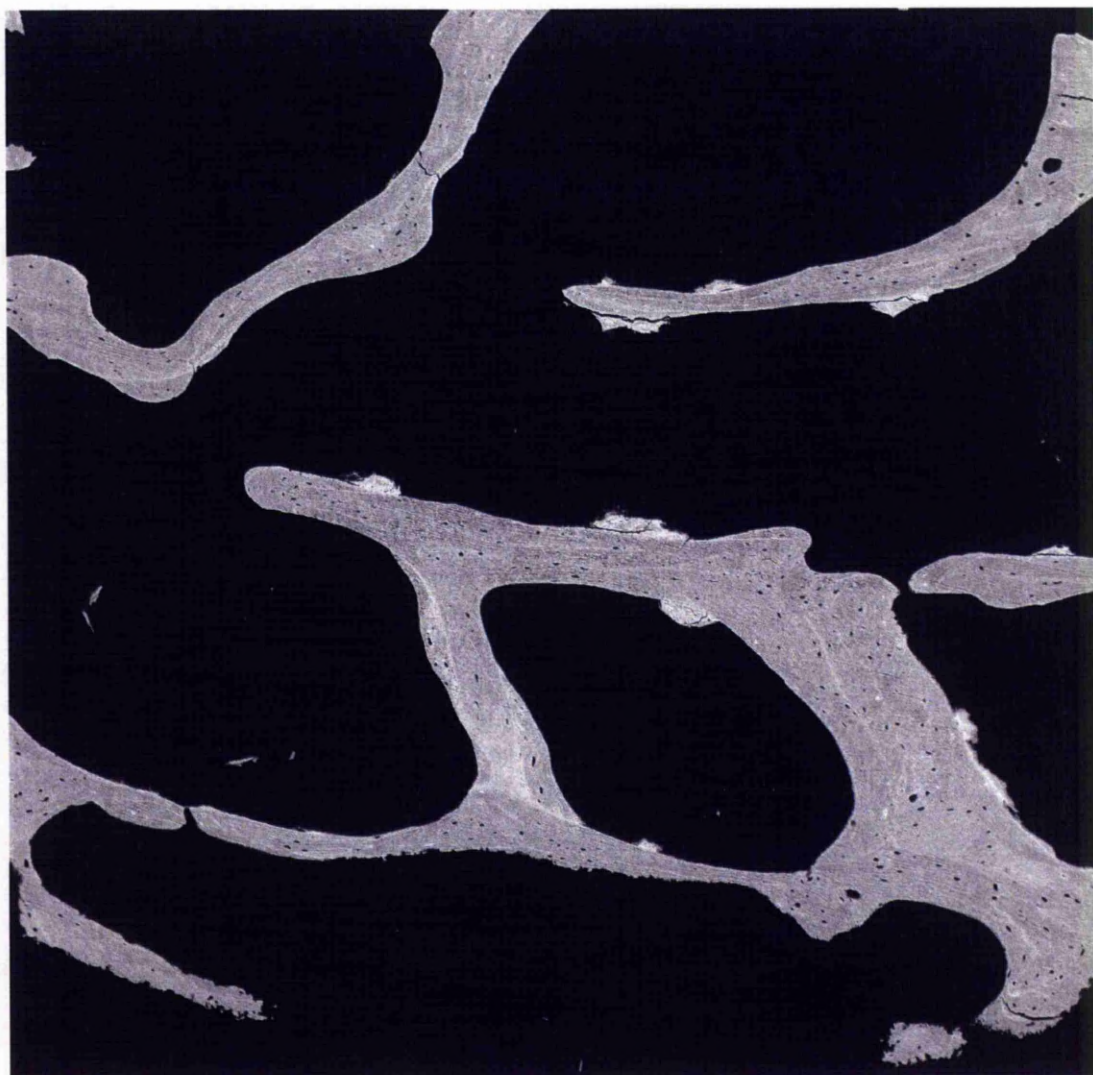
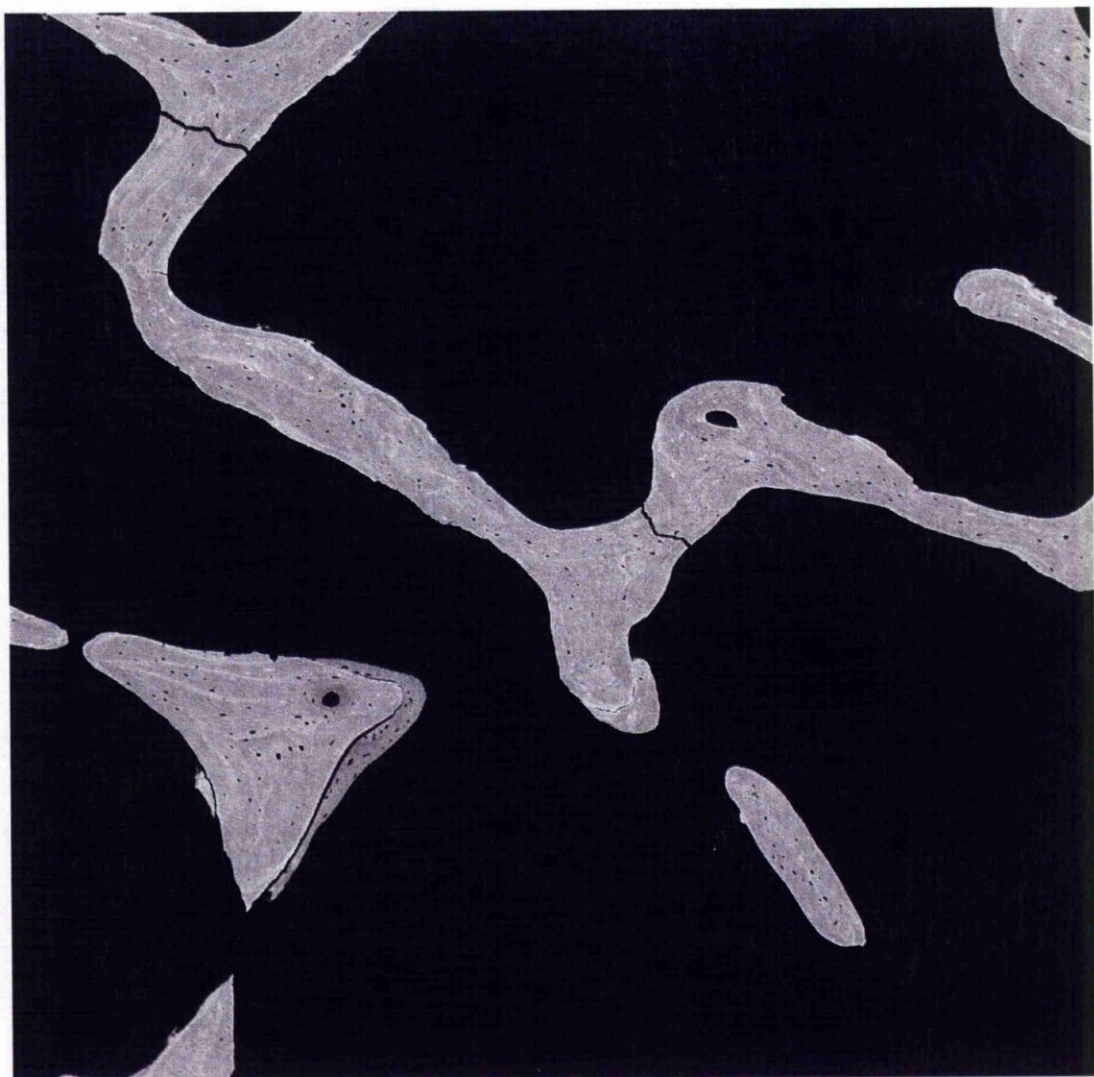




Figure 7.14: 20kV qBSE-SEM images of polished and carbon coated PMMA embedded slice of femoral head from same 59 year old ochronosis case: image fields are 2700 microns high and wide. Mineralisation density was determined by reference to halogenated dimethacrylate standards. For explanation, see table in inset. Grey levels were adjusted such that the value from the monobrominated standard was adjusted to zero and that for the monoiodinated standard to 255 (as detailed in Boyde, 1999 and Boyde, 2005).







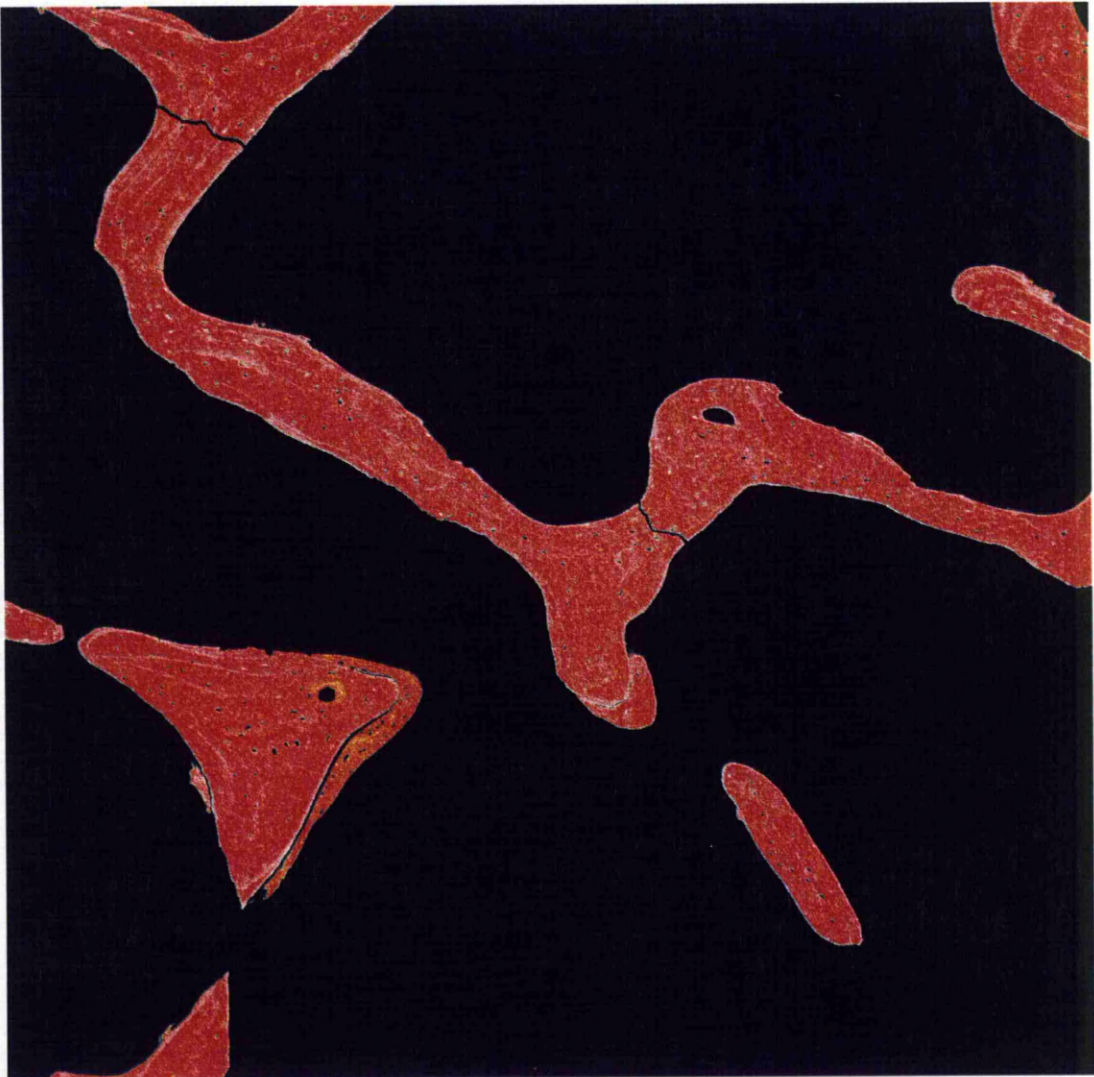


Figure 7.15: 20kV qBSE-SEM images of polished and carbon coated PMMA embedded slice of femoral head from same 59 year old ochronosis case: image fields are 2700 microns high and wide. Mineralisation density was determined by reference to halogenated dimethacrylate standards. For explanation, see table in inset. Grey levels were adjusted such that the value from the monobrominated standard was adjusted to zero and that for the monoiodinated standard to 255 (as detailed in Boyde, 1999 & Boyde, 2005). Trabeculae show normal architecture, with plane of poor integration

*between pre-existing unresorbed bone and overlying newly formed bone at lower left. Excrescence on left of this latter trabecula is also not well integrated and also not deposited on a resorbed surface.*7.2.4. 3D topographical SEM imaging of the osteoarthritic arthropathy samples

Examination of the osteoarthritic arthropathy samples used as reference material, with all the methods used – 3D- SEM (Fig. 7.16 & 7.17) light microscopy of sections (Fig. 7.18-7.20), and qBSE SEM (not figured) – showed similar excrescences (Figs. 7.16-7.20). These were present in the different forms observed in the ochronotic samples. 3D SEM also showed that there was some poor integration of the excrescences with the pre-existing bone matrix surface.

In histology, the excrescences observed were numerous “peak like” structures projecting from the surface of the trabeculae and displaying a different colour to the mineralised bone matrix when stained with H&E (Fig. 7.18-7.20). At the contact surface between the existing trabeculae and the attached structure there was a distinct joint line, also the marrow space periphery of the structures displayed rough edges, both features suggesting that integration between the excrescences and trabeculae was either not complete or occurred in an aberrant fashion.

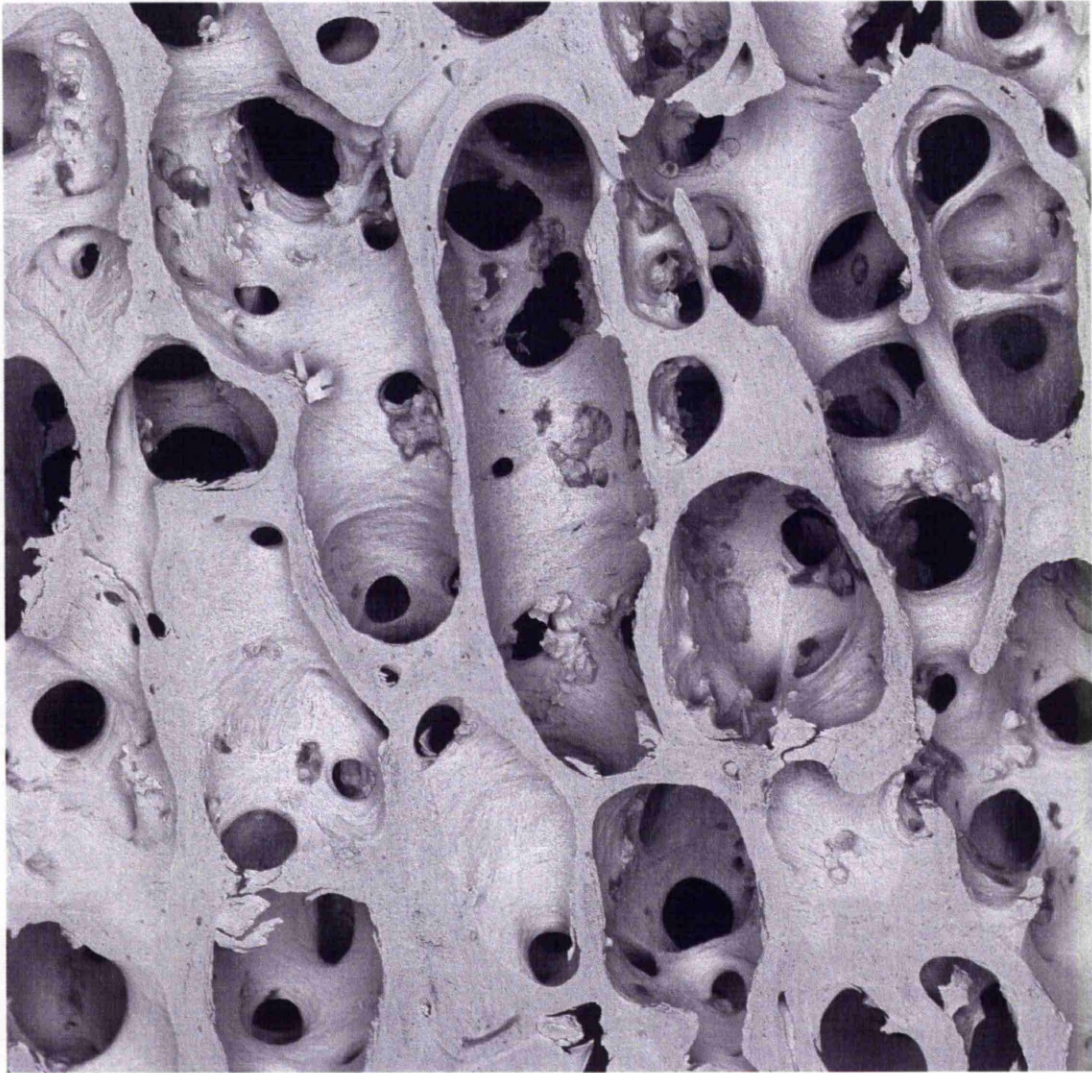


Figure 7.16: 20kV BSE 3D SEM images of carbon coated, macerated slice of medial femoral condyle from 51 year old female who underwent unicompartmental knee replacement for osteoarthritis. Numerous excrescences can be seen on the trabeculae, predominantly with rugged edges and scalloped surfaces. Some appear darker than the surrounding bone matrix, indicative of a lower degree of mineralisation because more recently formed. Field width and height is 4050 microns.



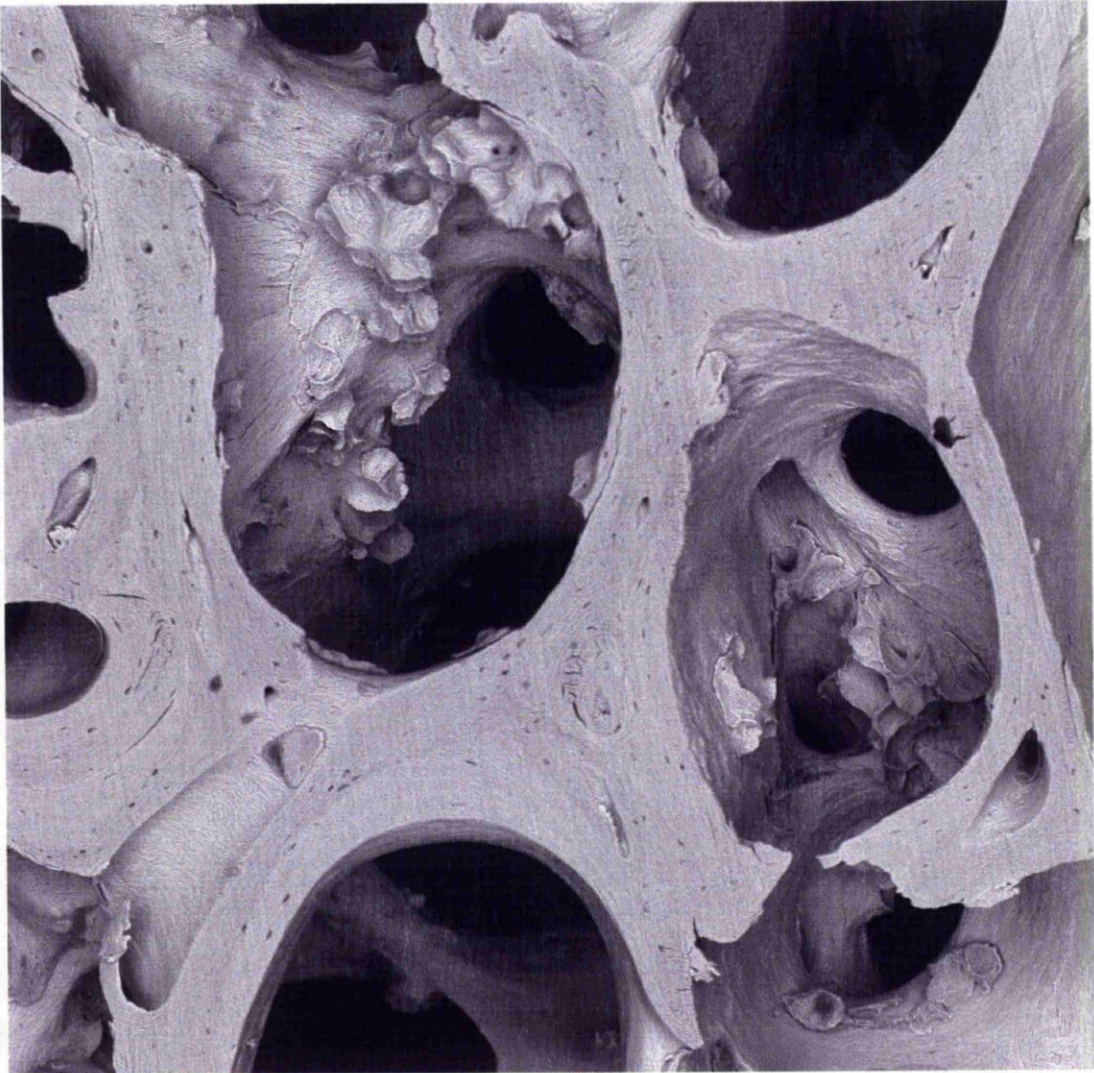


Figure 7.17: 20kV BSE 3D SEM images of carbon coated, macerated slice of medial femoral condyle from 51 year old female who underwent unicompartmental knee replacement for osteoarthritis. Large excrescences on free bone surfaces with multiple deeply indented surfaces and intervening rugged edges can be seen. The peripheries of some of these conglomerates show a line of demarcation where they have not been well integrated with the pre-existing surfaces. Field width and height are 1780 microns.





Figure 7.18: *Low power photomicrograph of a H& E stained decalcified paraffin-embedded section from the medial femoral condyle of a 51 year old female knee OA case who underwent unicompartmental knee replacement for OA.*



Figure 7.19: *Low power photomicrograph of an excrescence located on a trabeculae from medial femoral condyle from 74 year old male who underwent a total knee replacement for osteoarthritis.*



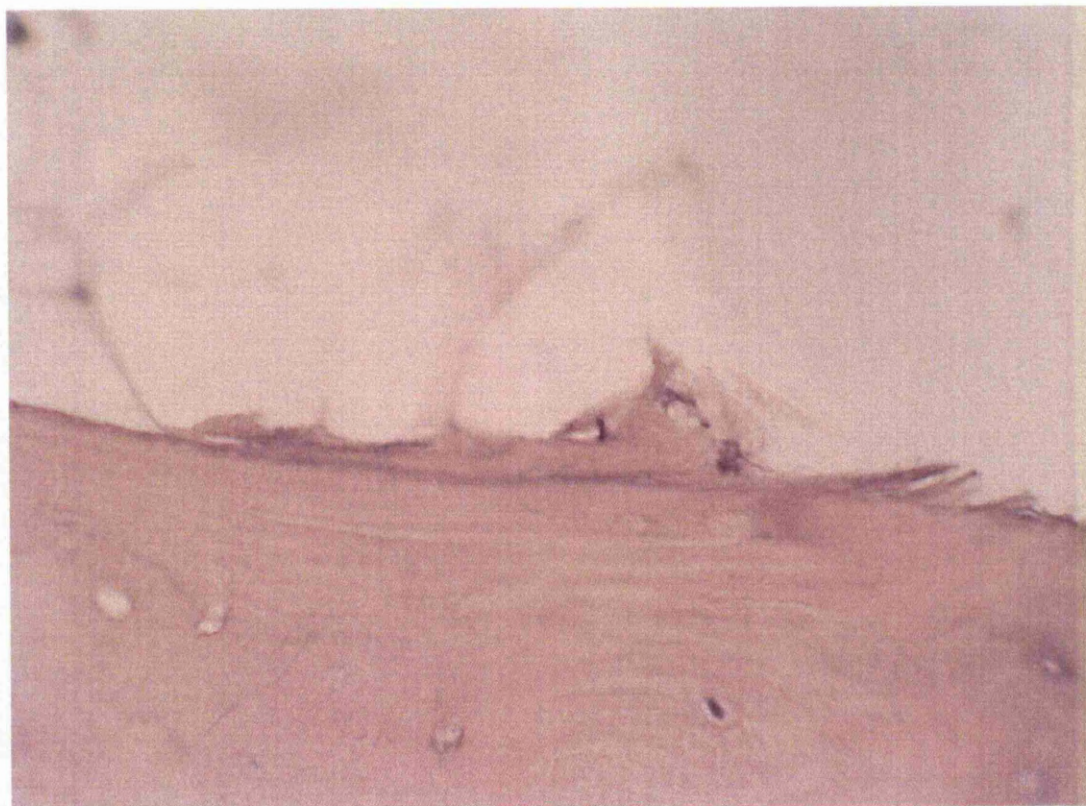


Figure 7.20: *A high power photomicrograph of the excrescence from the previous figure showing its presence on the trabecular surface. At least two cells can be seen as part of the excrescence body. There also appears to be a relationship with the adipose matrix in the marrow space.*

### **7.3 DISCUSSION**

This chapter reports the discovery of novel microanatomical structures in bone from patients with AKU osteoarthropathy, which have been termed trabecular excrescences. It has recently demonstrated that the subchondral bone and calcified cartilage plates in AKU undergo extreme remodelling; giving them a unique phenotype (Taylor, 2011) and chapter 5 in this thesis. Investigation of the bone architecture revealed the presence of novel excrescences on the bone surface, originally detected by SEM analysis and subsequently confirmed using histological techniques.

Following on from this initial discovery, OA samples were examined as a control, these structures were discovered in some, but not all of the OA samples examined. To date, they have been observed in all the AKU material that have been studied (12/12), but only a proportion of OA (7/10). Their initial discovery in AKU, resulted in the theory that the presence of these structures may be in part related to the presence of the HGA or HGA pigment in the joint tissues of AKU patients, but the detection of these excrescences in the OA samples suggests that these structures arise due to aberrant osteoblast/osteoclast signalling, possibly brought on by abnormal loading on the joint tissues following alterations in the normal biomechanical interactions related to disease. It is important to consider that the highly abnormal phenotype in AKU joint tissues appears to be at least in part a result of aberrant loading due to the presence of ochronotic pigment altering the stiffness of cartilage (Taylor, 2011). The presence of these excrescences within some common OA samples provides further evidence for the role of abnormal loading across the joint in OA patients as significant in the onset and progression of OA (Griffin, 2005).



The relationship between bone and cartilage in the progression of joint failure has been well investigated, and it is generally accepted that there are key roles for both in both the commencement and the progression of joint degeneration, particularly in OA (Burr, 2004). It is clear that the basic description of changes involved in joint degeneration are not limited to bone and cartilage, but are more appropriately attributed to highly specialised sub-divisions of these tissues which are related to their homeostatic and biomechanical functions.

The detection of these 3 types of excrescence, which may or may not all be interrelated, may be indicative of altered phenotype of cells and the abnormal homeostasis and signalling in these tissues. One type of excrescence arises from incomplete resorption of branching trabeculae which do not appear to be part and parcel of the 'normal', pre-existing trabecular architecture. It is common in OA for marrow spaces to be filled with immature 'woven' bone which some might describe as 'micro' callus, but the term callus should not be taken to imply that the tissue is formed in response to overt fracture. Similar obliteration of marrow space occurs in the densification of normal bone in response to heavy impact exercise with no evidence of any sign of trabecular microfracture (Boyde, 2005). Modelling of this excess bone tissue to restore the homeostatic mechanical loading balance might then result in this appearance.

However, these structures appear to be closely related to the another type of excrescence, in which short, branched trabeculae that had been subjected to partial osteoclastic action have been smoothed over by the deposition of new layers of bone by osteoblasts. The deposition of new matrix on these structures leads to smooth partial trabeculae projecting into the marrow space. The functional contribution of these partial trabeculae must be

severely questioned given that without connections at both ends, they could not provide any form of structural support in biomechanical function.

The type of excrescence which appears as coarse stucco represents stuck on spots on resting surfaces that have been focally reactivated. In turn, their surface morphology appears very frequently also to be altered by subsequent resorption. The coupling between bone resorption and formation is supposedly tightly regulated in the normal mature young adult, such that bone is only removed if there is going to be new bone to replace it. Osteoblasts normally arrive at the sites of resorption recently vacated by osteoclasts (Parfitt, 2000). However, this coupling phenomenon does not exist in the growing and drifting skeleton, and is less tight in ageing when trabecular modelling occurs. It can also be severely unbalanced in pathological states to cause bone loss (osteoporosis) or deposition (sclerosis). The deposition of new bone on the surface of existing trabeculae without osteoclastic resorption suggests that such coupling does not exist in this case.

Whilst the tissues examined in this study are from two different diseases, they both display similar structures on the trabecular network. The advanced osteoarthropathy of AKU provides an unprecedented opportunity to investigate regional unloading and factors that might be involved in this process. The initial discovery working on AKU samples, where the novel microanatomical structures which were grouped as excrescences were identified easily on internal surfaces. The follow up observations of OA samples as controls for this study and the catalogue of OA samples that the authors have observed previously, demonstrated that these structures are present, but are not as

obvious or widespread. This may suggest that whatever mechanisms are involved in their formation are more severe in the pathology of AKU.

In summary, through meticulous examination using a combination of light microscopy and SEM, identification of novel microanatomical structures in bone has been demonstrated. These were first identified in the osteoarthropathy of AKU, where they are abundant, and subsequently in OA where they proved more difficult to find. Their size and distribution would make these excrescences difficult to find using other imaging modalities, including microCT. Much further investigation is required to determine their development and functional significance and whether they are present in other pathological conditions. Interestingly the subsequent histological examination revealed that adipocytes exactly fitted the contours of the bone surfaces (Fig 7.18-7.20). A role for adipocytes as bone lining cells has been suggested previously (Boyde, 2006), but there is no literature proposing a role for adipocytes in templating or moulding the surface of bone. Immunohistochemistry shows that there is collagen VI in these excrescences (Unpublished observations, Taylor 2010). These results suggest that the deposition of the bone matrix within these mineralised excrescences is at least templated and modulated by adipocytes. However, the absence of osteoblasts from the forming surfaces raises the question of whether the matrix which is subsequently mineralised is partially synthesised by the adipocytes. Furthermore, it provides unequivocal evidence that adipocytes rather than inactive osteoblasts are the *de facto* lining cells on some bone surfaces. It is well recognised that adipocytes and osteoblasts can be derived from the same mesenchymal stem cells under the influence of different transcription factors. Furthermore there is

evidence of transdifferentiation between the cell types. However, this is the first report of an intimate role for adipocytes in osteogenesis.



**8. Investigation into the deposition of ochronotic pigment in submandibular tissues**

## **8.1 INTRODUCTION**

Whilst deposition of pigment in cartilage is well documented (O'Brien, 1963) deposition of pigment is also seen at non-cartilaginous sites (Helliwell, 2008). Although these presentations do not manifest uniformly in all patients, understanding the factors promoting pigment deposition in these less common places may improve the understanding of the pigmentation process as a whole. There is a clear role for pH in the pigment formation process, demonstrated by Boedecker, and black colouration of alkaptonuric urine under alkaline conditions in the presence of oxygen (cited by O'Brien). (O'Brien, 1963).

## **8.2. CASE HISTORY**

A 47 year old male was diagnosed with AKU in 2007. Later, he presented with swelling of the submandibular salivary gland and an associated lymph node, which became worse after eating. Ultrasound examination of the gland revealed numerous stones. The right submandibular gland and associated lymph node were excised. Macroscopically, no obvious ochronotic pigmentation was noted. Numerous ochronotic "marble-like" stones were removed at the time of surgery. These were observed by the surgeon but not retained. This chapter describes for the first time the presence of ochronotic pigment in acinar cells of the submandibular gland of an alkaptonuric patient.

### **8.3 RESULTS**

#### **8.3.1 Macroscopic examination of submandibular tissues**

Macroscopic examination of the submandibular gland and lymph node blocks and slices did not show any unusual pigmentation, consistent with that usually observed in joint tissues; calculi were noted in the submandibular gland (arrows).(Figs. 8.1-8.4).

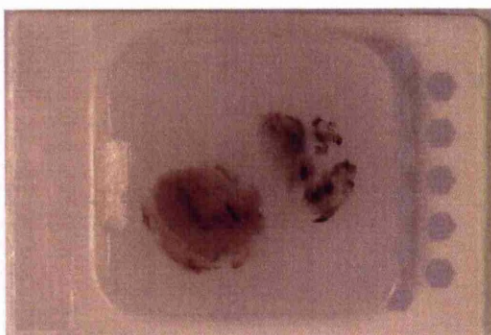


**Figure 8.1:-** *Photograph showing AKU7A1 block (lymph node) embedded in paraffin wax, with no obvious signs of ochronosis.*



**Figure 8.2:-** *photograph showing AKU7B1 block (submandibular gland) embedded in paraffin wax, with no obvious signs of ochronosis. A calculus can be seen within the gland (arrow).*



**Figure 8.3:-** Photograph showing AKU7B2 block (submandibular gland) embedded in paraffin wax, with no obvious signs of ochronosis. Calculi can clearly be seen located within the gland (arrows).



**Figure 8.4:-** Photograph showing AKU7B3 block (submandibular gland) embedded in paraffin wax, with no obvious signs of ochronosis. A calculus can clearly be seen within the gland.



### **8.3.2 Microscopic examination of submandibular tissue**

Microscopic examination of the submandibular gland showed mild chronic sialadenitis, with no evidence of tissue destruction. Examination of extracellular connective tissue around the vessels and ducts in the gland did not display any ochronotic pigment. A calculus was present in the lumen of a lobar duct. H&E staining of the calculus revealed calcium (Fig. 8.5) and addition of 1% HCl resulted in its dissolution.

Examination of secretory acini displayed differences across the gland (Fig. 8.6). It was noticeable that the duct lumen of certain acini displayed dark granular pigmentation, which appeared to fill the lumen of some acini. Closer examination revealed the presence of pigment within the cytoplasm at the apical surface of the cells in the pigmented regions. Acinar cells displayed morphologically normal nuclei with no signs of apoptosis or necrosis despite pigment in the cytoplasm. The cells lining the salivary ducts showed no pigmentation. Microscopic examination of the lymph node showed no pigmentation in the connective tissues or macrophages.

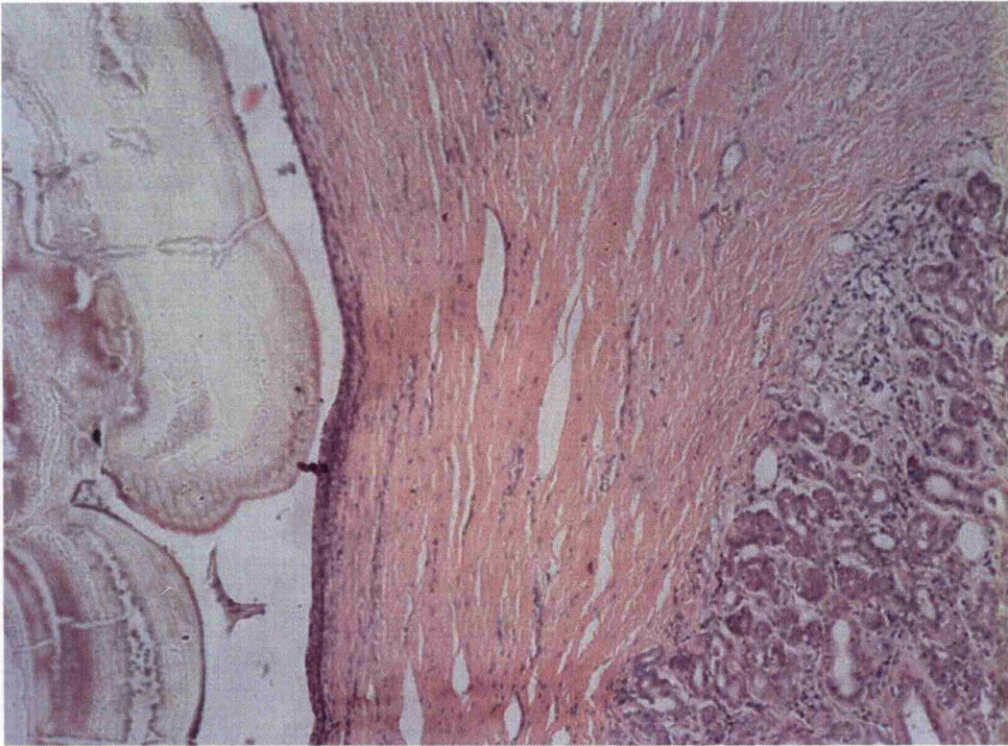


**Figure 8.5:-** Photomicrograph showing the remnants of a large calculus displaying calcium deposits along with other associated ochronotic deposits around the periphery. H&E

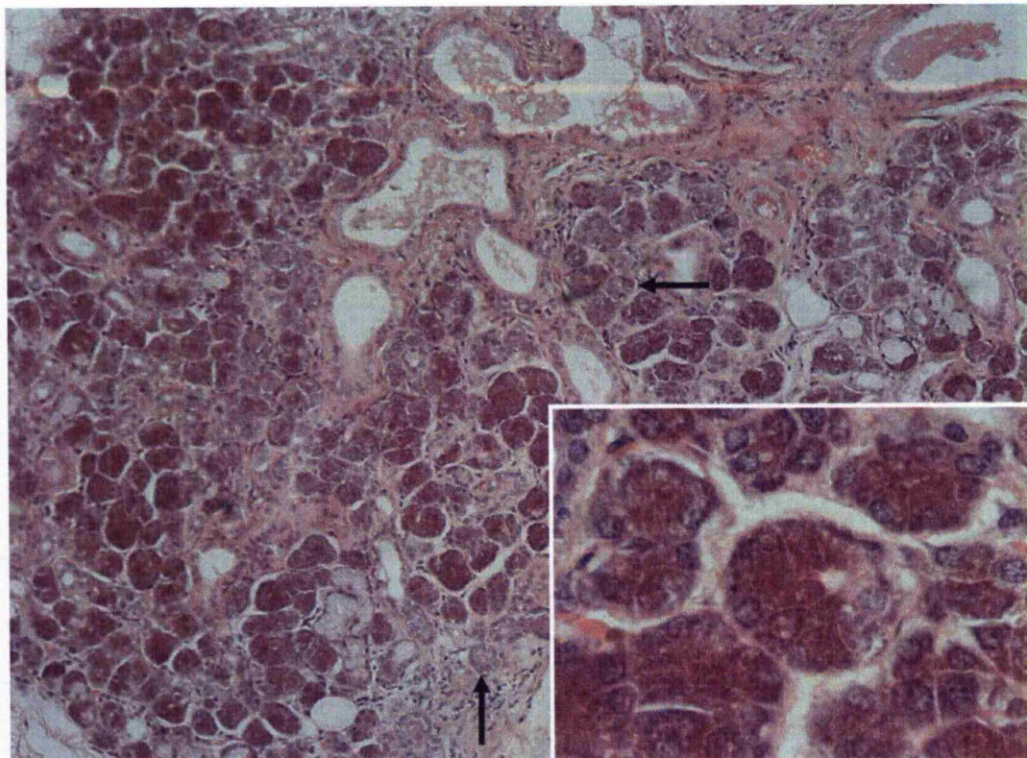


**Figure 8.6:-** Serous acini of the submandibular gland show variable amounts of dark pigmentation (arrows denote normal looking acini). Insert shows pigmentation in the apical parts of the serous cells at higher magnification. H&E

#### **8.4 DISCUSSION**

This is the first report of the presence of ochronotic pigment in the acinar cells and duct lumina of the submandibular gland in a patient with AKU. HGA is a small highly water-soluble molecule that does not accumulate in the body in health. In AKU the kidneys excrete large quantities of HGA into the urine, and, in alkaline conditions, the HGA undergoes oxidation to black pigment. HGA is present in tissues of the body because of its small molecular size and high solubility.

HGA is a small highly water soluble molecule (mw = 168) that does not accumulate in the body in health due to repaired metabolism in the liver and kidneys. The kidneys in AKU excrete

large quantities of HGA into the urine and, in alkaline conditions; the HGA undergoes oxidation to a black pigment. HGA is present in tissues of the body due to its small molecular size and high solubility.

Saliva is a clear, slightly acidic mucoserous exocrine secretion that is composed of 99% water and has a normal pH of between 6-7; during low or peak flow this pH can range from 5.3-7.8 (Humphrey, 2001). The saliva present in the oral cavity is the product of a process which sees the initial secretion in the serous acini modified along its path to the mouth. The secretion contains a mixture of ions including  $\text{Ca}_2^+$ ,  $\text{Na}^+$ ,  $\text{K}^+$ ,  $\text{HCO}_3^-$  and  $\text{Cl}^-$ . Once in the striated ducts, saliva undergoes modifications altering its composition and pH. The ducts have low permeability to water causing the saliva to become more hypotonic (Bridges, 1981). The saliva produced by the acinar cells is more alkaline than the final product in the mouth and as such may be sufficiently alkaline to promote HGA polymerisation in a similar fashion to that seen in alkalinised urine.

Ochronotic pigment has been reported in calculi in other systems, most commonly in the kidney, prostate gland and glands in the prostatic urethra of male alkaptonuric individuals. Analysis of these calculi has shown calcium compounds including oxalate, phosphate and carbonate, along with a substituted calcium compound probably associated with the pigment (Krizek, 1971).

The presence of the pigment within the salivary acinar cells suggests that some cells or parts of cells may promote HGA polymerisation. The absence of pigment in cells and lumina of the



striated ducts suggests the saliva has been modified to an extent that it no longer promotes oxidation of HGA or that pigmented secretions are moved along fast enough not to accumulate or be obvious microscopically. Salivary gland calculi affect 1.2% of general adult population; 80% occurring in the submandibular gland. Calculi are usually found in the excretory ducts. (Ledesma-Montes, 2007) The opportunity to study the calculi composition in this patient was not possible, but staining indicated presence of calcium as well as ochronotic-associated deposits.

Pigment accumulates in the cytoplasm of chondrocytes in alkaptonuric joints but the process(es) leading to pigmentation are uncertain (Helliwell, 2008). Pigmentation in chondrocytes could arise from within the cell, by pH-linked oxidation of HGA, as seen in the salivary acinar cells in our patient or by phagocytosis of pigment from the extracellular environment in a phagocytic manner. It is known that chondrocytes can phagocytose material in their extracellular environment (Castillo, 2004). Absence of extracellular pigmentation around the acinar cells in our case suggests the favoured method for pigmentation would be an intra-cellular mechanism linked to diffusion of HGA into cells, where changing pH in the cytoplasm or particular properties of secretory products of the cell promote polymerisation. There is currently no information on how much HGA is present in oral saliva, although it is assumed to be similar to that found in other body fluids. However, prostatic secretory products undergo darkening when left to stand, and secretions from sebaceous glands in the skin presumably contain HGA as they can stain clothing (Krizek, 1971, Turiansky, 2001).

In this case it is unclear whether pigment deposition in acinar cells may have preceded, resulted from, or be unrelated to calculus formation. Given the incidence of calculus formation in submandibular tissues in the general population it is probable that calculus formation in this case was not caused by alkaptonuria and that acinar cell pigmentation may be unrelated to calcification in other parts of the gland. The effect of HGA on the submandibular acinar cells has not been documented; in our case the cells show no adverse signs due to the presence of HGA pigment.

Ochronotic pigmentation in less commonly examined areas of the body, such as submandibular tissues, may provide insights into the mechanisms of pigment formation and deposition. It is possible that intracellular HGA polymerisation occurs before secretion and binding to extracellular connective tissue fibres, although the process that could lead to this is unknown. Evidence supports association of HGA oxidised product with collagen in the absence of cells (Milch, 1961). There may be separate intracellular and extracellular mechanisms mediating ochronotic pigmentation that overlap in joint tissues. Here I present evidence to support the probable involvement of cells in the formation of HGA pigment, in the absence of collagen or other extracellular matrix components.

**9. Ochronosis in a mediastinal mass**

## **9.1 INTRODUCTION**

As previously seen in Chapter 8, ochronosis in tissues without a collagenous scaffold has been described. Furthermore this case, in which deposition is observed in the submandibular gland, has shown association between the ochronotic pigment and calcium compounds. This chapter describes a further novel presentation of ochronotic pigmentation and the possible association between ochronotic pigment and calcium compounds.

## **9.2 CASE HISTORY**

A 51 year old female with AKU attended the AKU clinical evaluation unit in Liverpool and assessed by whole body MR scanning. The MR scan of the thorax revealed a 9cm diameter, multicystic, partly calcified mass in the anterior mediastinum (Fig. 9.1). Surgical access to the anterior mediastinum was through a median sternotomy. Ochronotic pigmentation was not seen on any of the surfaces exposed during access to the mediastinum. The mass was located posterior to the manubrium and there were inflammatory adhesions between the mass and the posterior table of the sternum, the mediastinal pleura bilaterally (including the left phrenic nerve and the right lung), the pericardium and the innominate (left brachiocephalic) vein. The mass was resected en bloc with the pericardium, mediastinal pleura and part of the right upper lobe of lung. The patient made an uneventful recovery and was discharged home after 5 days. The specimens were photographed immediately following removal and then fixed in 10% phosphate buffered formol saline. Tissues were processed routinely for paraffin embedding and 5µm sections were cut and stained with haematoxylin and eosin.



### **9.3 RESULTS**

#### **9.3.1 Macroscopic examination of Mediastinal tissues**

A cystic mass measuring 9.5 x 7 x 2.5 cm was excised. Ochronosis was clearly seen macroscopically on the excised mass (Fig. 9.2). The external surface showed indurations and haemorrhage. Dissection showed a unilocular cyst with calcification in the walls. The cyst was full of yellow acellular material. The cut surfaces and internal lining showed ochronosis.

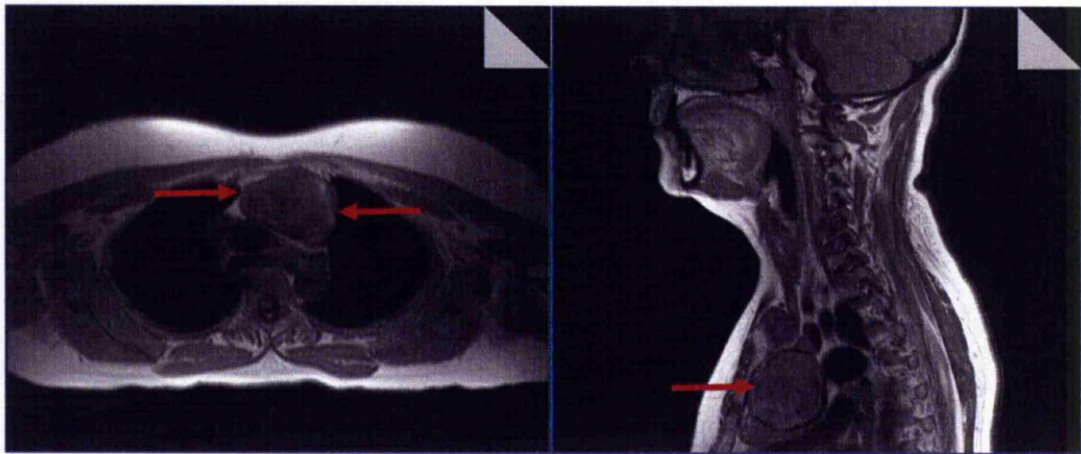


**Figure 9.1:-** MRI scans of the thorax. Sagittal and axial T1 weighted images demonstrate a large anterior mediastinal mass of cystic appearance in close relation to the great vessels.

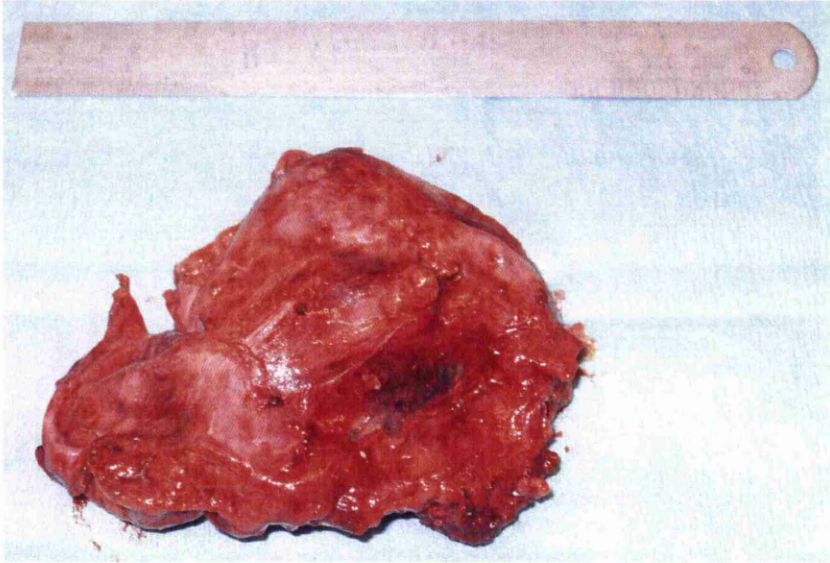


**Figure 9.2.:-** *Macroscopic appearance of excised mass with showing regions of dense ochronosis.*

### **9.3.2 Microscopic examination of Mediastinal tissues**

Examination of the tissues revealed that no cyst lining is seen. The cyst lining was replaced by histiocytes. Most of the histiocytes are mononuclear and multinucleate in nature, some of which contained ochronotic pigmentation. Also present in the wall is patchy inflammation and haemosiderin deposition. A foreign body giant cell reaction is also seen. In this specimen no benign immature or malignant epithelial tumour is seen. This is most likely a second pathology of an old benign cyst. Microscopic examination also revealed that the fibrous wall of the cyst showed patchy lymphocytic infiltration and variably dense ochronotic pigmentation in some areas. In these focal regions of pigmentation there were extracellular granules of ochronotic pigment associated with the collagen fibres. In some instances these fibres were completely encrusted by the granular pigment (Figs. 9.3 & 9.4). In the regions of pigmentation there were numerous fibroblasts

which showed dense intracellular pigmentation. The cytoplasm was in some cells completely full of ochronotic pigment, with numerous distinct individual granules in a single cell (Fig. 9.5). There are regions of tissues and cells which display no ochronosis. This was being interpreted as ochronosis and in keeping with the history of alkaptonuria in this patient. In this specimen very focally in the background a rim of lymphoid tissue is seen.



**Figure 9.3:-** *Photomicrograph of mediastinal tissues with ochronosis seen in the extracellular matrix.*



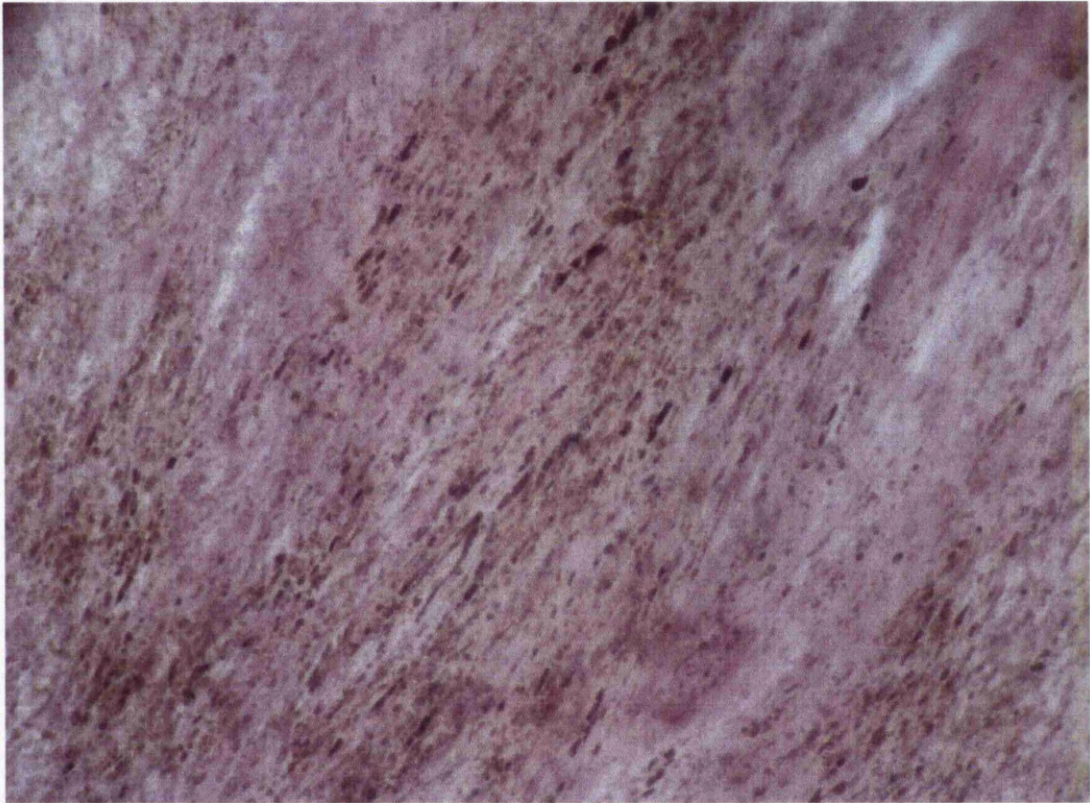


**Figure 9.4:-** *Photomicrograph of mediastinal tissues showing numerous pigment granules amongst and encrusting the collagen fibres of the extracellular matrix.*



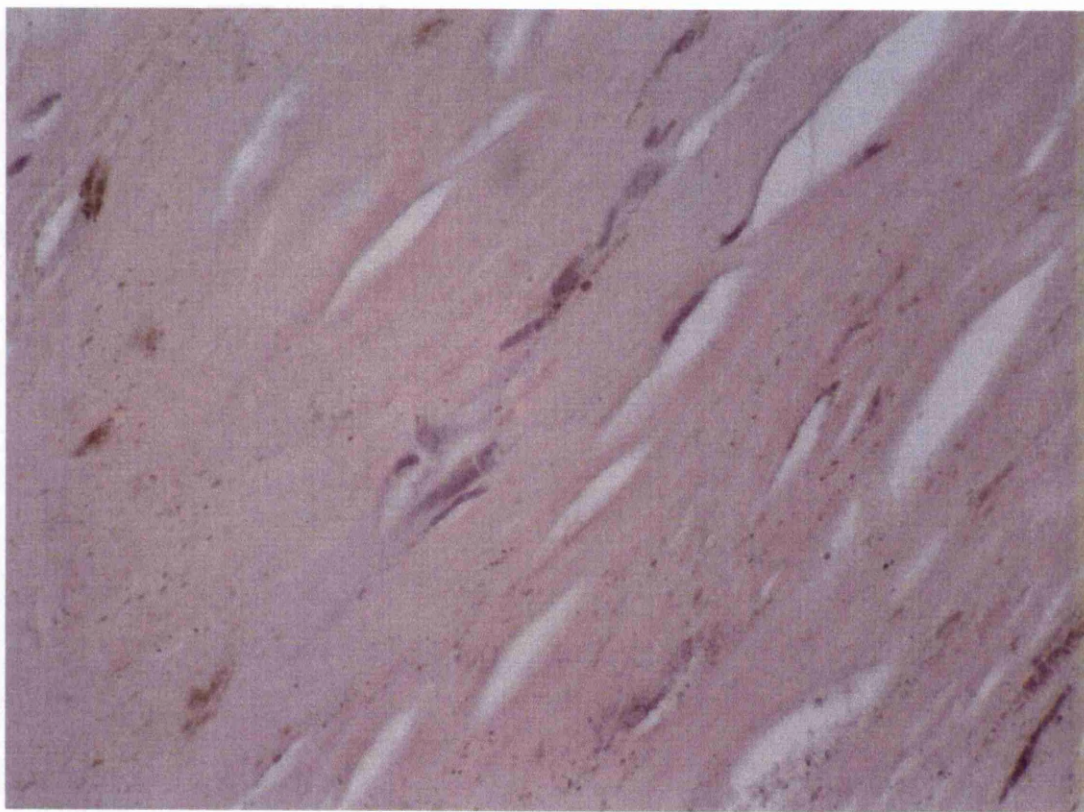


**Figure 9.5:-** *Photomicrograph showing intracellular pigmentation of fibroblasts and granules of extracellular ochronotic pigment.*

#### **9.4 DISCUSSION**

This is the first report of ochronosis associated with a mediastinal cyst, or any form of cyst, in a patient with alkaptonuria. It has been described previously that HGA, the small water soluble molecule which undergoes polymerisation to deposit as an ochre pigment, is assumed to be present in all tissues in the body, even with efficient renal excretion of the molecule (Taylor, 2010). Local tissue factors must promote the deposition of pigment in specific tissues. Mediastinal cysts are usually benign and are uncommon in the general population. Cysts arising in the anterior mediastinum are most commonly of thymic

origin or mature cystic teratomas (Takeda, 2003). Although there are no particular features to indicate the nature of the cyst in this patient, the presence of ochronotic pigment in the cyst wall but not in other mediastinal tissues suggests that inflammation and fibrosis in the cyst wall have promoted pigment deposition.

The presentation of 'non-uniform' ochronosis in patients with AKU may illuminate pathological factors involved in mediating deposition of ochronotic pigment and provide clues to the pathogenesis of pigment deposition in the tissues that are more commonly affected by ochronosis, such as the articular cartilages of the weight bearing joints and the cardiac valves (Helliwell, 2008). The two distinctly different types of pigment were observed in the mediastinal mass from this patient are similar to those seen in collagenous ligamentous capsular tissue from the joint of a patient with AKU, as reported in Chapter 4 (Taylor, 2010). This suggests an overlap, whereby similar pathological changes are occurring, in the deposition process between the different sites and the potential for elucidating changes in the collagenous matrix that may influence pigment deposition. Mediastinal pigmentation has not been described in autopsy tissues of patients with AKU (Helliwell, 2008). It has been suggested that cyst formation in other tissues may be associated with an increase in oxidative stresses and reduced antioxidant enzyme protection (Maser, 2002). As cystic structures are induced by increased oxidative stresses in other species (Murgia, 2004), a local increase in oxidative stress in the cystic tissues of this patient may have provided suitable conditions to promote pigmentation. It has been shown recently that there is a significant effect on the protein synthesis, cell organisation, defence and stress responses when cells are subject to HGA (Braconi, 2010).

Furthermore, chondrocytes cultured in HGA which are subject to antioxidants show decreased apoptosis, increased growth and partial restoration of proteoglycan release, all of which are caused by the presence of HGA (Tinti, 2010).

External scar tissues have not been shown to pigment, although scar tissue within cartilaginous structures displays ochronosis (Helliwell, 2008). The inflammatory response as part of scar tissue formation is interesting in AKU, as the presence of pigment itself does not seem to elicit a widespread inflammatory response in synovial tissue except as a foreign body type of reaction to cartilaginous debris (Mannoni, 2004). Several potential mechanisms may be involved. Inflammatory cells may secrete factors or alter the local physiological conditions and promote pigmentation. Secondly, the maturity and structure of the collagenous matrix may play a role in the preferential deposition of pigment around collagen bundles. Thirdly, the presence of proteoglycans and glycosaminoglycans in immature scar tissue may create conditions similar to those seen in articular cartilage in which pigment deposition is favoured (Clark, 1985). This would replicate the conditions in which pigmentation is seen in ageing joint tissues in AKU patients. The detection of calcified deposits within the mass and the presence of ochronotic pigmentation suggest that the polymeric HGA is not a homogenous mix of HGA polymer but can also recruit/encompass other molecules. It has been shown previously that HGA may associate with calcium compounds; Chapter 8 (Taylor, 2010). Calcification is often seen in mediastinal cysts and it may be that the calcification is in some way important for pigment deposition in these tissues. The interest of the pathological association of pigment with calcium is that it is assumed that collagen fibres

in the normal bone matrix are protected from pigmentation in AKU because of the calcification process. This is the first report of ochronosis in a mediastinal cyst of a patient with alkaptonuria. The possible mechanisms that may contribute to the pigmentation in these tissues may inform the pathogenesis of ochronosis at other sites.



## **10. General Discussion**

It is over 100 years since Archibald Garrod used AKU to prove the ‘one gene, one enzyme’ theory, recognising that there was a recessive inheritance and coined the term ‘inborn error of metabolism’ (Garrod, 1902 & Garrod, 1908). Whilst there have been significant advances in understanding the genetics of the disease such as the cloning and mapping of the HGD gene (Fernández-Cañón, 1996 & Granadino, 1997), there has been limited progress in understanding the intermediary steps that see HGA converted to the pigmented polymer which causes ochronotic osteoarthropathy. This thesis represents a body of work which presents novel data into some of these intermediate steps and the opportunity for novel therapeutic interventions. Because of the rarity of AKU, it is unusual rare to be able to study many specimens in a single project/investigation. The unique opportunity for study of patient tissues and models allows for new observations to be made. In this work it has been able to compare and contrast the presentation in joints from within a patient and across the AKU population, from a macroscopic to the ultrastructural level.

The observations in Chapter 3 represent the largest description of a series of alkaptonuric joint specimens undertaken. The number of specimens studied represents over 15% of the identified AKU population within the UK; 78 patients (Ranganath, 2011), although there is no doubt that other ‘unidentified’ patients exist in the population. When compared with studies into more common diseases such as arthritis; the percentage of observed samples from the known population in this study far outnumbered that for the study of more common diseases. The striking observation of non-uniform deposition of ochronotic pigment across the cartilages demonstrates that the widespread presence of HGA within

these tissues for many years appears not to be the limiting factor in pigment deposition, which has been suggested previously in Chapter 8 of this Thesis (Taylor, 2010). The observation of non-uniform and bi-lateral differences in presentation of pigmentation from knees within a patient suggests that the presence of HGA alone is not the seldom factor in dictating location of pigment (AKU10 & AKU19, Figs. 3.12 & 3.17 respectively). Also, given that the knees are not presenting at the same time and with the same severity and progression of ochronosis is further confirmation that intrinsic and extrinsic factors in and on the joint are somehow involved in influencing regions of matrix to pigment over others. Observations of unilateral joints from within a patient show that pigmentation is not uniform and the time of degeneration of the joints is not identical presenting further evidence that HGA alone is not the sole cause. The short time (5 months) between the hip and knee degeneration is interesting and it would be valuable for overall disease progression to determine if the rapid degeneration of the later was in part related to the arthropathy and subsequent replacement of the former.

Observations of the hip samples demonstrate that the most superior regions on the femoral head appear to be most severely affected. The absence of cartilage from these regions suggests that pigmentation in these areas of cartilage results in the articulation between hip and acetabulum causes cartilage from these areas to become dislodged. Given that the with any movement of the hip the area around the fovea is the most frequently articulated area with any movement, compared with the inferior parts of the femoral head which would only articulate at certain ranges of motion, this would make sense that any pigmentation in this area would be more detrimental than to the areas

which did not show as abundant pigmentation. Observations of the two pigmented surfaces; femoral and acetabular, can be seen in Fig. 3.13.

The observations of the knees show a high variability in the presence of pigment, with no uniform observations on the tibial or femoral components. The high degree of variability may in part be related to the differences in gait across the human population, which raises the question of what repeated loading, or perhaps specifically; repeated traumatic loading may have in causing certain areas to pigment. Whilst it is exciting to speculate a role for loading on these abnormal tissues, it cannot be ignored that abnormal loading may induce pathological changes in these originally normal tissues? Further analysis using finite element analysis (FEA) modeling may be able to answer this question, but this analysis is outside the remit of this thesis. Observations of predominantly non-pigmented osteophytes on the cartilage of these tissues suggest that newly formed cartilage is usually resistant to ochronosis. It can be speculated that pigmentation in cartilage may occur over a number of years as either HGA needs to reach a local concentration threshold to pigment, as seen in pure HGA cultures, or there are protective mechanisms *in vivo* that may cease to function or become less effective with the ageing or introduction of other pathological processes in tissues. This is confirmed by the observations of histological and ultrastructural pigmentation of matrix fibres in osteosarcoma (Tinti, 2010) and chondrosarcoma cultures in HGA (Taylor, 2007) and as seen in chapter 4 of this thesis. It has been shown at lower concentrations of HGA that pigmentation still occurs in a number of days, rather than the years it appears to take *in vivo* (Taylor, 2007 & Tinti, 2010). The role of pathological processes in pigmentation is



also described in Chapters 8 & 9, particularly in relation to pigmentation in the mediastinal mass.

This cohort of patient samples and their ages at replacement confirm the widely held suggestion that ochronotic osteoarthropathy is of rapid and early onset (Maxwell, 2005). The total average age for replacement across our samples was >10 years younger than those which have been observed for the national mean for hip and knee replacements. The non-uniform presentation of ochronosis at the macroscopic level is mirrored at the histological and ultrastructural level. Examination of collagen fibres in both the cartilage and capsule of patient tissues shows association with the pigment. It is of note that even in the most pigmented ochronotic regions of tissue examined, when examined ultrastructurally not all fibres present with ochronosis on them (Fig. 4.13). A gradient of pigmentation was seen across a few hundred nanometres within capsular tissues. A similar phenomenon was not apparent in the cartilage. The presentation in cartilage on collagen fibres was much more severe, with larger deposits seen and appearing to incorporate other matrix components, such as proteoglycan, which has been described previously (Mohr, 1980). In the tightly packed collagen in the capsular tissues pigment was seen on the fibre surface in longitudinal section, numerous granule and shards of pigment could be seen on one fibre. The observation of small granules on a single fibre is a novel observation and represents the earliest observed deposition of ochronotic pigment seen in alkaptonuric tissues. These appear related to larger more shardlike deposits on neighbouring collagen fibres (Fig. 4.14). It has been proposed that the ochronotic pigment deposition on collagen fibres may occur in a manner analogous to the mineralisation of bone collagen (Taylor, 2011). The process of mineralisation in bone

might actually prevent the deposition of pigment associated with collagen fibres in bone. This is in part supported by the observation of ochronotic pigment deposition in cultures of osteosarcoma cell lines that are cultured in  $3.3 \times 10^{-4}$  M HGA. Even though the osteosarcoma cells used represent different maturities of osteoblasts; the cells and the matrix they synthesise are widely used in the study of bone. These cultures do undergo mineralisation with the addition of an exogenous phosphate donor in the form of beta-glycerophosphate (McQuillan, 1995). In future this may provide a useful tool to investigate the protective mechanism of mineralisation of collagen by adding beta-glycerophosphate to SaOS-2 cultures for 40 days, sufficient time to allow mineralisation and then add HGA to examine for association of pigment with *in vitro* cultures. Analysis of bone specimens reveals that there is no pigment associated with the collagen fibres in human AKU bone matrix. From the analysis of other non-mineralising type I collagen fibres, such as seen in the capsular ligament and spinal ligament, shows clear association of type I collagen with ochronotic pigment.

Consistent with histological examination, ultrastructural examination of cells revealed intracellular ochronotic deposits. These in some cases appeared similar to the earliest deposits associated with the collagen fibres in the ligamentous capsule. The deposits seen in cells ultrastructurally will have been undetectable using histological techniques, which suggest that those detectable by histology are advanced. The cellular involvement in pigmentation is clear when intracellular pigmentation is seen in cells which have little or no collagenous matrices associated with them, such as the pigmentation seen in the acinar cells in Chapter 8 (Fig. 8.6).

The ultrastructural analysis of the *in vitro* cultures in this thesis represents the first observations of pigment deposition in *in vitro* cultures by TEM. The *in vitro* model used and examined in this thesis will prove invaluable in gaining an insight into the pigmentation process. This is emphasised even more given that based on the results in chapter 5, where pigmented cartilage matrix appears impervious to enzymatic degradation (Fig 5.4 & 5.5). This stresses that any therapeutic intervention needs to be targeted at the point prior to, or as close as possible to the earliest detection of pigmentation, before significant pigment can alter the biochemical and mechanical properties of cartilage sufficiently to cause observable pathology.

The results in chapter 5 demonstrate a novel advance in the understanding of the progression of ochronotic osteoarthropathy and may provide useful for understanding more common arthropathies in the wider population. The early histological observations seen in Fig. 5.8 show the earliest observed commencement of ochronosis. This is seen in the calcified cartilage, associated with individual cells and their matrices. Across examination of other tissues, pigment was never seen at the articular surfaces without it also being present in proximity to the subchondral boundary. This suggests that whatever factors have a role in the pigmentation process are associated with the cells in the calcified cartilage region in these tissues. In Chapter 5 it has been described that subchondral bone and calcified cartilage are important in the pathology of OA. Calcified cartilage has often been neglected in the study of joint degeneration in OA, but it is clearly the tissue through which loads are distributed from the hyaline articular cartilage to the underlying subchondral bone (Ferguson, 2003). The observations in Chapter 5

show a novel subchondral phenotype, with complete resorption of the subchondral and calcified cartilage plates. There are, however, many reports highlighting a role for subchondral bone in the pathogenesis of OA (Karsdal, 2008). It has been suggested that the structural integrity of articular cartilage is reliant on normal subchondral bone turnover, intact chondrocyte function and normal biomechanical stresses (Karsdal, 2008, Felson, 2004, Hayami, 2004). AKU has already been documented as mimicking or causing premature OA (Bálint, 2000, Lagier, 2006). This demonstrates that AKU may, in part, be useful for studying OA, given the extreme phenotype that it demonstrates. Perhaps in this instance the ochronotic pigment that is deposited may be a marker of tissue damage. Studies are underway to examine the deposition of HGA pigment in osteoarthritic tissues. The subchondral phenotype observed in the advanced ochronotic samples suggest that bisphosphonates may be worthy of reconsideration as a therapeutic strategy, although they would not directly prevent ochronotic pigment deposition, they may prolong the life of the joint, particularly if they are timed prior to any significant pigmentation of the overlying cartilage.

The observation of novel microanatomical structures; excrescences in both AKU and OA samples provides further evidence that the exceptional phenotype observed in AKU may be an extreme OA phenotype. The overlap of the presence of these structures in both sample sets suggests that any pathogenic mechanism(s) that are involved in the deposition of these abnormal structures may be present in both disorders. This indicates that the formation of these structures is not related to the presence of HGA in the tissues of AKU patients. One similarity in the two tissues is the abnormal loading that is present



across these tissues. The mineralised tissues underlying the pigmented cartilage are probably subject to regional unloading which results in focal removal of the subchondral plate. The spread of pigmentation results in a wider unloading phenomenon. It is also possible that following resorption of the mineralised material from beneath the ochronotic cartilage as seen in Figs. 5.5 – 5.7, that should deposition of new bone be induced that it is not possible for the osteoclasts to prepare a surface for the new bone to be deposited on, given that the pigmented cartilage matrix appears impervious to degradation. It appears that the subchondral phenotype in AKU is at the opposite end of the spectrum to that seen in OA, but as described above, thickening of the subchondral bone plate would be difficult to achieve if there is little or no subchondral bone or calcified cartilage to anchor new tissues to following removal due unloading of the bone in response to the pigmentation of the overlying cartilage. Within these samples it is interesting to observed trabeculae which are incompletely formed. Without a middle meeting point these structures offer no structural significance, although they may still maintain their homoeostatic function as a calcium store.

It is not possible to offer evidence to demonstrate why the excrescences are caused but further work is underway in order to determine the formation and functional significance of these structures. There is the possibility that these structures also form in the non-pathological ageing process whereby natural alterations and slow down in the body result in the formation of these structures. The relationship with adipocytes on these structures is also extremely interesting and warrants further investigation. The role of these cells as

bone lining cells has been suggested previously and the involvement of adipocytes in matrix templating and formation is interesting observation.

The observation of the first detection of ochronosis in a mouse model is a highly significant feature of this thesis. The understanding of many diseases and their pathogenesis has been vastly increased by the use of murine models. It was originally believed that mice do not demonstrate ochronosis, even with efficient urinary excretion of HGA. Whilst HGD  $-/-$  mice do excrete high levels of HGA in their urine, they do not appear to suffer from any of the adult symptoms seen in humans. Numerous hypotheses have been suggested as a reason for this, including life span, endogenous production of ASC and differences in the biomechanics of the joint. These hypotheses appear not to be completely true given that the observations in chapter 6 demonstrate pigmentation in FAH $-/-$ , HGD  $+/-$  animals. The observations in these animals raise interesting questions about what factors in these animals are promoting deposition in the kidneys and joint tissues. Given the macroscopic observations in the kidneys and the histological deposition in the knees and kidneys there must be factors that are promoting deposition in these tissues, which are not present in the HGD  $-/-$  mice. The kidneys and the cells of these mice are subject to abnormal stresses from the presence of succinylacetone in tissues that have not reverted to the alkaptonuric phenotype. This compound has carcinogenic and mutagenic properties and the focal stresses may be in part contributory to the deposition of ochronotic pigment in the renal tissues of these animals. It may also be that this model is a complex way of inducing renal failure, the results of which are contributory to induce pigmentation in these animals. In humans pigmentation has been observed in kidney stones from patients with AKU (Melis, 1994), although there is no

evidence to describe pigmentation associated with renal cells or their matrices. In the FAH<sup>-/-</sup>, HGD <sup>+/-</sup> mouse, it maybe that the absence of the FAH enzyme and the subsequent succinylacetone build up affects the renal performance, causing promotion of deposition of ochronotic pigment in these tissues. This may be similar to the changes seen in ageing in human kidneys. This is demonstrated in part by the observations of renal insufficiency in a patient with AKU, whose renal function was 1/3<sup>rd</sup> that of his siblings, resulting in an elevated plasma HGA level compared to his alkaptonuric siblings (Introne, 2002).

In these mice with ochronosis, the observations of pigmentation in the joints is a highly relevant observation into understanding the pathogenesis of the disorder and will prove valuable in screening therapeutic agents. Whilst these animals did not show full depth cartilage pigmentation, synonymous with that seen in advanced ochronosis in humans, they do show identical initiation of pigmentation, which would be the ideal time to target treatment(s) to preventing further deposition. This model would be useful to observe what, if any, other pathological changes in the joints of these animals maybe inducing pigmentation in and around certain cells and if the instigators are the same as those seen in the human condition.

The novel observations of chapters 8 & 9 show previously unpublished presentations of ochronosis in tissues of patients with AKU. The rarity of the disease means that the opportunity to observe these tissues from patients with AKU is uncommon. The deposition in the cells of the submandibular gland and the possible association with the

calculus is very interesting and suggests that the ochronotic pigment that is deposited in patient tissues is not a homogenous compound, but is able to recruit other proteins or molecules, or is in fact itself recruited to deposit in these areas. The importance of calcium in the deposition in these tissues warrants further investigation.

Both the cases in chapters 8 & 9 reinforce the question of the role of inflammation and underlying pathology in the deposition of ochronotic pigment in certain tissues. Both cases showed inflammation, and it may be the role of inflammatory cells and their secretions that in part are responsible for inducing pigmentation in these tissues. Interestingly, particularly in chapter 8, the tissues observed showed no notable deposition associated with the collagen fibres in the matrix, supporting the theory that pigmentation occurs in cells prior to matrix, or at the very least can occur independently of pigmentation in the matrix.

In summary these studies reported here provide novel findings which represent advancements in the understanding of the process of ochronosis and subsequent arthropathy in AKU. Whilst they do not complete the picture of what is happening in the disorder, they provide more evidence and knowledge for which new therapeutic strategies for treating this rare condition could be targeted.

### References

- Ahmad S, Teckman JH, Lueder GT. Corneal opacities associated with NTBC treatment. *Am J Ophthalmol.* 2002 Aug;134(2):266-8.
- Albrecht, H. Ueber Ochronose. *Ztschr. Heilk.*, 23: 366, 1902.
- Alexopoulos LG, Williams GM, Upton ML, Setton LA, Guilak F. Osteoarthritic changes in the biphasic mechanical properties of the chondrocyte pericellular matrix in articular cartilage. *J Biomech.* 2005 Mar;38(3):509-17.
- Aliberti G, Pulignano I, Schiappoli S, Minisola S, Romagnoli E, Proietta M. Bone metabolism in ochronotic patients. *J Intern Med* 2003 254, 296–300.
- Aliberti G, Pulignano I, Pisani D, Rocchietti March M, Del Porto F, Proietta M. Bisphosphonate treatment in ochronotic osteoporotic patients. *Clin Rheumatol* 2007 May;26(5):729-35.
- Andriacchi TP, Koo S, Scanlan SF. Gait mechanics influence healthy cartilage morphology and osteoarthritis of the knee. *J Bone Joint Surg Am* 2009; Feb;91 Suppl 1:95-101.
- Anikster Y, Nyhan WL, Gahl WA. (1998) NTBC and Alkaptonuria. *Am. J. Hum. Genet.* 63:920–921.
- Araki K, Sudo A, Hasegawa M, Uchida A. Devastating ochronotic arthropathy with successful bilateral hip and knee arthroplasties. *J Clin Rheumatol.* 2009 Apr;15(3):138-40.
- Arkill KP, Winlove CP. Solute transport in the deep and calcified zones of articular cartilage. *Osteoarthritis Cartilage* 2008; 16, 708-14.



Balaban B, Taskaynatan M, Yasar E, Tan K, Kalyon T. Ochronotic spondyloarthropathy: spinal involvement resembling ankylosing spondylitis. Clin Rheumatol. 2006 Jul;25(4):598-601.

Bálint G, Szebenyi B. Hereditary disorders mimicking and/or causing premature osteoarthritis. Baillieres Best Pract Res Clin Rheumatol 2000 Jun;14(2):219-50.

Bancroft JD, Stevens A, eds., Theory and practice of histological techniques. 4th edition. London, UK: Churchill Livingstone, 1996:253

Ben Rayana N, Chahed N, Khoctali S, Ghorbel M, Hamdi R, Rouis M, Bouajina I, Hamida FB. [Ocular ochronosis. A case report]. J Fr Ophtalmol. 2008 Jun;31(6 Pt 1):624.

Bernheim F, Bernheim MLC. The metabolism of tyramine, L-tyrosine and phenol by rat tissues *in vitro*. J. Biol. Chem. 1944 153: 369-373.

Blivaiss BB, Rosenberg EF, Kutuzov H, Stoner R. Experimental ochronosis. Induction in rats by long-term feeding with L-tyrosine. Arch Pathol. 1966 Jul;82(1):45-53.

Boedeker, C. Ueber das Alcapton; ein neuer Beitrag zur Frage: Welche Stoffe des Harns können Kupferreduktion bewirken? Ztschr. rat. Med., 7: 130, 1859.

Boedeker, C. Das Alkapton; ein Beitrag zur Frage: Welche Stoffe des Harns können aus einer alkalischen Kupferoxydlosüng Kupferoxydul reduceiren? Ann. Chem. Pharmacol., 117: 98, 1861.

Bondurant RE, Henry JB. Pathogenesis of ochronosis in experimental alkaptonuria in the white rat. Lab Invest. 1965 Jan;14:62-9.

Bonewald LF, Johnson ML. Osteocytes, mechanosensing and Wnt signaling. Bone. 2008 Apr;42(4):606-15.

Bory C, Boulieu R, Chantin C, Mathieu M. Homogentisic acid determined in biological fluids by HPLC. *Clin Chem*. 1989 Feb;35(2):321-2.

Bory C, Boulieu R, Chantin C, Mathieu M. Diagnosis of alcaptonuria: rapid analysis of homogentisic acid by HPLC. *Clin Chim Acta*. 1990 Jul;189(1):7-11.

Bowles WH. Protection against minocycline pigment formation by ascorbic acid (vitamin C). *J Esthet Dent*. 1998;10(4):182-6.

Boyde A. Scanning electron microscope studies of bone. In: Bourne GH (ed.) *The Biochemistry and Physiology of Bone*, 2nd ed., 1972; vol. 1. Academic Press, New York, NY, USA, pp.259-310.

Boyde A, Travers R, Glorieux FH, Jones SJ. The mineralisation density of iliac crest bone from children with osteogenesis imperfecta. *Calcif Tissue Int* 1999; 64:185-190.

Boyde A. The real response of bone to exercise. *J Anat*. 2003 Aug;203(2):173-89.

Boyde A. Improved digital SEM of cancellous bone: scanning direction of detection, through focus for in-focus and sample orientation. *J Anat*. 2003 Feb;202(2):183-94.

Boyde A, Firth EC. Musculoskeletal responses of 2-year-old Thoroughbred horses to early training. 8. Quantitative back-scattered electron scanning electron microscopy and confocal fluorescence microscopy of the epiphysis of the third metacarpal bone. *N Z Vet J*. 2005 Apr;53(2):123-32.

Boyde A. Three dimensional micro-anatomy of bone, with special reference to the mandible. *J Oral Biosci (Japan)*. 2006 48 Suppl 57-59.

Braconi D, Laschi M, Amato L, Bernardini G, Millucci L, Marcolongo R, Cavallo G, Spreafico A, Santucci A. Evaluation of anti-oxidant treatments in an in vitro model of alkaptonuric ochronosis. *Rheumatology (Oxford)*. 2010 Oct;49(10):1975-83.

Braconi D Laschi M, Taylor AM, Bernardini G, Spreafico A, Tinti L, et al. Proteomic and redox-proteomic evaluation of homogentisic acid and ascorbic acid effects on human articular chondrocytes. *J Cell Biochem* 2010 Nov 1;111(4):922-32.

Bridges RB. Salivary glands and saliva. In Roth GI, Calmes R. eds. *Oral biology*. St Louis: CV Mosby Company 1981:196-236.

Burr DB, Anatomy and physiology of the mineralized tissues: Role in the pathogenesis of osteoarthritis. *Osteoarthritis and Cartilage*. 2004; 12: S20–S30.

Butany J W, Naseemuddin A, Moshkowitz Y, Nair V. Ochronosis and Aortic Valve Stenosis. *J Card Surg* 2006; 21: 182-184.

Carrier DA, Harris CM. Bilateral hip and bilateral knee joint arthroplasties in a patient with ochronotic arthropathy. *Orthop Rev* 1990 19:1005–1009.

Castillo EC, Kourí JB. A new role for chondrocytes as non-professional phagocytes. An in vitro study. *Microsc Res Tech* 2004;64:269-278.

Catterall JB, Barr D, Bolognesi M, Zura RD, Kraus VB. Post-translational aging of proteins in osteoarthritic cartilage and synovial fluid as measured by isomerized aspartate. *Arthritis Res Ther* 2009;11(2):R55.

Chua SY, Chang HC. Bilateral spontaneous rupture of the quadriceps tendon as an initial presentation of alkaptonuria--a case report. *Knee*. 2006 Oct;13(5):408-10.

Crandall DI, Halikis DN. Homogentisic acid oxidase. I. Distribution in animal tissue and relation to tyrosine metabolism in rat kidney. *J Biol Chem*. 1954 Jun;208(2):629-38.

Culliford DJ, Maskell J, Beard DJ, Murray DW, Price AJ, Arden NK. Temporal trends in hip and knee replacement in the United Kingdom: 1991 to 2006. *J Bone Joint Surg Br.* 2010 Jan;92(1):130-5.

de Haas V, Carbasius Weber EC, de Klerk JBC, Bakker HD, Smit GPA, Huijbers WAR, Duran M, Poll-The BT. The success of dietary protein restriction in alkaptonuria patients is age-dependent. *J. Inher. Metab. Dis.* 1998 (8): 791-8.

Demir S. Alkaptonuric ochronosis: a case with multiple joint replacement arthroplasties.

*Clin Rheumatol.* 2003 Dec;22(6):437-9.

Di Franco M, Coari G, Bonucci E. A morphological study of bone and articular cartilage in ochronosis. *Virchows Arch.* 2000 Jan;436(1):74-81.

Di Lullo GA, Sweeney SM, Korkko J, Ala-Kokko L, San Antonio JD. Mapping the ligand-binding sites and disease-associated mutations on the most abundant protein in the human, type I collagen. *J Biol Chem.* 2002 Feb 8;277(6):4223-31.

Felson DT, Neogi T, Osteoarthritis: Is It a Disease of Cartilage or of Bone? *Arthritis Rheum* 2004 50, (2), 341–344.

Felson DT. Arthroscopy as a treatment for knee osteoarthritis. *Best Pract Res Clin Rheumatol.* 2010 Feb;24(1):47-50.

Ferguson VL, Bushby AJ, Boyde A, Nanomechanical properties and mineral concentration in articular calcified cartilage and subchondral bone. *J Anat* 2003 203, 191–202.

Fernandes RJ, Harkey MA, Weis M, Askew JW, Eyre DR. The post-translational phenotype of collagen synthesized by SAOS-2 osteosarcoma cells. *Bone.* 2007 May;40(5):1343-51.

Fernandez Canon JM, Penalva MA. Fungal metabolic model for human type I hereditary tyrosinaemia. *Proc. Natl. Acad. Sci. USA.* 1995; 92: 9132-9136.

Fernández-Cañón JM, Granadino B, Beltrán-Valero de Bernabé D, Renedo M, Fernández-Ruiz E, Peñalva MA, Rodríguez de Córdoba S. The molecular basis of alkaptonuria. *Nat Genet.* 1996 Sep;14(1):19-24.

Ffolkes LV, Brull D, Krywawych S, Hayward M, Hughes SE. Aortic stenosis in cardiovascular ochronosis. *J Clin Pathol.* 2007 Jan;60(1):92-3.

Filippou G, Frediani B, Selvi E, Bertoldi I, Galeazzi M. Tendon involvement in patients with ochronosis: an ultrasonographic study. *Ann Rheum Dis.* 2008 Dec;67(12):1785-6.

Fisher AA, Davis MW. Alkaptonuric ochronosis with aortic valve and joint replacements and femoral fracture: a case report and literature review. *Clin Med Res.* 2004 Nov;2(4):209-15.

Forslind K, Wollheim FA, Akesson B, Rydholm U. Alkaptonuria and ochronosis in three siblings. Ascorbic acid treatment monitored by urinary HGA excretion. *Clin Exp Rheumatol.* 1988 Jul-Sep;6(3):289-92.

Foster M. Non-enzymatic oxidation of tyrosine and DOPA. *Proc Natl Acad Sci U S A.* 1950; 36: 606-11.

Friderich, H. Nikolowski W. Endogene Ochronose. *Arch. Dermat. u. Syph.,* 192: 273, 1951.

Frost HM. Dynamics of bone remodelling. In: Frost HM (ed.) *Bone biodynamics*, 1964. Little Brown, Boston, USA. pp. 315-333.



Frost HM. A new direction for osteoporosis research: A review and proposal. *Bone*. 1991;12(6):429-37.

Fuchs RK, Allen MR, Ruppel ME, Diab T, Phipps RJ, Miller LM, Burr DB. In situ examination of the time-course for secondary mineralization of Haversian bone using synchrotron Fourier transform infrared microspectroscopy. *Matrix Biol*. 2008 Jan;27(1):34-41.

Gaines JJ. A comparative scanning electron microscopic and light microscopic study of the synovium in Ochronosis. *Am J Clin Pathol* 1987 Jun; 87 (6): 762-65.

Gaines JJ Jr. The pathology of alkaptonuric ochronosis. *Hum Pathol*. 1989 Jan;20(1):40-6.

Galdston M. Steele JM, Dobriner K. Alcaptonuria and ochronosis; with a report of three patients and metabolic studies in two. *Am. J. Med*. 1952; 13; 432–452.

Garrod AE. The incidence of alkaptonuria. A study in chemical individuality. *Lancet*. 1902; 160(4137): 1616–1620.

Garrod AE, Hele TS. The uniformity of the homogentisic acid excretion in alkaptonuria. *J Physiol*. 1905; Dec 19;33(3):198-205.

Garrod A.E. The Croonian lectures on inborn errors of metabolism, lecture II: alkaptonuria. *Lancet*. 1908; 2: 73–79.

Gehrig A, Schmidt SR, Müller CR, Srsen S, Srsnova K, Kress W. Molecular defects in alkaptonuria. *Cytogenet Cell Genet*. 1997; 76:14–16.

Gelse K, Söder S, Eger W, Diemtar T, Aigner T. Osteophyte development--molecular characterization of differentiation stages. *Osteoarthritis Cartilage*. 2003 Feb;11(2):141-8.

Granadino B, Beltrán-Valero de Bernabé D, Fernández-Cañón JM, Peñalva MA, Rodríguez

de Córdoba S. The human homogentisate 1,2-dioxygenase (HGO) gene. *Genomics*. 1997 Jul 15;43(2):115-22.

Greenberg GL, Boyde A. Convenient and controllable direct-view 3D imaging in conventional optical microscopes: approaches via illumination and inspection. *Proc Roy Microsc Soc* 1997; 32/2: 87-100.

Goldring MB, Human chondrocyte cell cultures as a model of cartilage specific gene regulation. In: Picot, J (Ed.). *Human cell culture protocols*. 2<sup>nd</sup> ed., 2005. Humana Press, Totowa, New Jersey, USA.

Goldring MB, Goldring SR. Osteoarthritis. *J Cell Physiol* 2007; 213:626-634.

Goldring MB, Marcu KB. Cartilage homeostasis in health and rheumatic diseases. *Arthritis Res Ther*. 2009;11(3):224.

Granadino B, Beltrán-Valero de Bernabé D, Fernández-Cañón JM, Peñalva MA, Rodríguez de Córdoba S. The human homogentisate 1,2-dioxygenase (HGO) gene. *Genomics*. 1997 Jul 15;43(2):115-22.

Goldring MB, Otero M, Tsuchimochi K, Ijiri K, Li Y. Defining the roles of inflammatory and anabolic cytokines in cartilage metabolism. *Ann Rheum Dis*. 2008 Dec;67 Suppl 3:iii75-82.

Goldring SR. Pathogenesis of bone and cartilage destruction in rheumatoid arthritis. *Rheumatology* 2003 May;42 Suppl 2:ii11-6.

Goldsmith, L A. Cutaneous changes in errors of amino acid metabolism: Alkaptonuria. In: Fitzpatrick T, Arthur E, Wolff K, Irwin F, Frank A. ed. *Dermatology in general medicine*. 4th Ed. New York: McGraw Hill, 1993: 1841-1845.

Gordon MK, Hahn RA. Collagens. *Cell Tissue Res*. 2010 Jan;339(1):247-57.

Granadino B, Beltrán-Valero de Bernabé D, Fernández-Cañón JM, Peñalva MA, Rodríguez de Córdoba S. The human homogentisate 1,2-dioxygenase (HGO) gene. *Genomics*. 1997 Jul 15;43(2):115-22.

Gray C, Boyde A, Jones SJ. Topographically induced bone formation in vitro: implications for bone implants and bone grafts. *Bone*. 1996;18(2):115-23.

Griffin TM, Guilak F. The role of mechanical loading in the onset and progression of osteoarthritis. *Exerc Sport Sci Rev*. 2005 ;33(4):195-200.

Grompe M, Lindstedt S, al-Dhalimy M, Kennaway NG, Papaconstantinou J, Torres-Ramos CA, Ou CN, Finegold M. Pharmacological correction of neonatal lethal hepatic dysfunction in a murine model of hereditary tyrosinaemia type I. *Nat Genet*. 1995 Aug;10(4):453-60.

Hayami T, Pickarski M, Wesolowski GA, McLane J, Bone A, Destefano J, et al. The Role of Subchondral Bone Remodeling in Osteoarthritis: Reduction of Cartilage Degeneration and Prevention of Osteophyte Formation by Alendronate in the Rat Anterior Cruciate Ligament Transection Model. *Arthritis Rheum* 2004 50, (4), 1193–1206.

Hayami T, Pickarski M, Zhuo Y, Wesolowski GA, Rodan GA, Duong le T. Characterization of articular cartilage and subchondral bone changes in the rat anterior cruciate ligament transection and meniscectomized models of osteoarthritis. *Bone*. 2006 Feb;38(2):234-243.

Helliwell TR, Gallagher JA, Ranganath L. Alkaptonuria--a review of surgical and autopsy pathology. *Histopathology*. 2008 Nov;53(5):503-12.

Hill PA. Bone remodelling. *Br J Orthod*. 1998; 25(2):101-7.

Hoch, DH, Grodzinsky AJ, Koob TJ, Albert ML, Eyre DR. Early changes in material properties of rabbit articular cartilage after meniscectomy. *J Orthop Res*. 1983;1(1):4-12.

Humphrey SP, Williamson RT. A review of saliva: Normal composition, flow, and function J Prosthet Dent; 2001;85:162-169.

Hunter DJ, Gerstenfeld L, Bishop G, Davis AD, Mason ZD, Einhorn TA, et al. Bone marrow lesions from osteoarthritis knees are characterized by sclerotic bone that is less well mineralized. Arthritis Res Ther. 2009;11(1):R11.

Intema F, Hazewinkel HA, Gouwens D, Bijlsma JW, Weinans H, Lafeber FP, et al. In early OA, thinning of the subchondral plate is directly related to cartilage damage: results from a canine ACLT-meniscectomy model. Osteoarthritis Cartilage. 2010 May;18(5):691-8.

Intema F, Sniekers YH, Weinans H, Vianen ME, Yocum SA, Zuurmond AM, et al. Similarities and discrepancies in subchondral bone structure in two differently induced canine models of osteoarthritis. J Bone Miner Res. 2010 Jul;25(7):1650-7.

Introne WJ, Kayser MA, Gahl WA. 2003. Alkaptonuria. In: Gene Reviews. Pagon RA, Bird TC, Dolan CR, et al., editors. Seattle, WA.

Introne WJ, Phornphutkul C, Bernardini I, McLaughlin K, Fitzpatrick D, Gahl WA. Exacerbation of the ochronosis of alkaptonuria due to renal insufficiency and improvement after renal transplantation. Mol Genet Metab 2002; Sep-Oct;77(1-2):136-42.

Janocha S, Wolz W, Srsen S, Srsnova K, Montagutelli X, Guénet JL, Grimm T, Kress W, Müller CR. The human gene for alkaptonuria (AKU) maps to chromosome 3q. Genomics. 1994 Jan 1;19(1):5-8.

Jayasinghe JA, Jones SJ, Boyde A. Scanning electron microscopy of human lumbar vertebral trabecular bone surfaces. Virchows Arch A Pathol Anat Histopathol. 1993;422(1):25-34.

Jayasinghe JA, Jones SJ, Boyde A. Three-dimensional photographic study of cancellous bone in human fourth lumbar vertebral bodies. *Anat Embryol (Berl)*. 1994;189(3):259-74.

Johnson EH, Miller RL. Alkaptonuria in a cynomolgus monkey (*Macaca fascicularis*). *J Med Primatol*. 1993 Sep-Oct;22(7-8):428-30.

Kadler KE, Hill A, Canty-Laird EG. Collagen fibrillogenesis: fibronectin, integrins, and minor collagens as organizers and nucleators. *Curr Opin Cell Biol*. 2008 Oct;20(5):495-501.

Kamoun P, Coude M, Forest M, Montagutelli X, Guenet JL. Ascorbic acid and alkaptonuria. *Eur J Pediatr*. 1992 Feb;151(2):149.

Karsdal MA, Leeming DJ, Dam EB, Henriksen K, Alexandersen P, Pastoureau P, et al. Should subchondral bone turnover be targeted when treating osteoarthritis? *Osteoarthritis Cartilage* 2008 16, 638-646.

Keeling ME, McClure HM, Kibler RF. Alkaptonuria in an orangutan (*Pongo pygmaeus*). *Am J Phys Anthropol*. 1973 Mar;38(2):435-8.

Kefeli M, Tomak Y, Can B, Bariş S. [Arthroplasty for the treatment of joint degeneration caused by ochronosis in two cases] *Acta Orthop Traumatol Turc*. 2008 Mar-Apr;42(2):139-44.

Keller J, Macaulay W, Nercessian OA, Jaffe IA. New developments in ochronosis: review of the literature. *Rheumatol Int* (2005) 25: 81–85.

Knox, W. E. and Edwards, S. W. (1955) Homogentisate oxidase of liver. *J. Biol. Chem.* 216, 479–487.



Kobak AC, Oder G, Kobak S, Argin M, Inal V. Ochronotic arthropathy: disappearance of alkaptonuria after liver transplantation for hepatitis B-related cirrhosis. *J Clin Rheumatol* 2005; Dec;11 (6):323-5.

Kraus VB. Rare osteoarthritis: Ochronosis, Kashin-Beck disease and Meleni joint disease. In Hochberg MC, Smolen SJ, Weinblatt ME, Weisman MH, (eds.) *Rheumatology*. 5th ed., 2011. Mosby, Philadelphia, PA, USA. pp 1825-1837.

Krizek, V. Urolithiasis and Prostatolithiasis in Alcaptonuria with Ochronosis. *Int Urol Nephrol* 1971;3:245-250.

Kutty M K, Iqbal Q M, Teh E C. Ochronotic arthropathy. An electron microscopic study with a view on pathogenesis. *Arch Pathol* 1974; 98: 55--57.

Kwan Tat S, Lajeunesse D, Pelletier JP, Martel-Pelletier J. Targeting subchondral bone for treating osteoarthritis: what is the evidence? *Best Pract Res Clin Rheumatol*. 2010 Feb;24(1):51-70.

La Du BN, Zannoni VG, Laster L, Seegmiller JE. The nature of the defect in tyrosine metabolism in alcaptonuria. *J Biol Chem*. 1958 Jan;230(1):251-60.

La Du BN. Alcaptonuria. In: *The Metabolic Basis of Inherited Disease Vol II*. 1989 CR Scriver, AL Beaudet, WS Sly, D Valle (eds.) (New York: McGraw-Hill), pp 775–790

Lagier R, Steiger U. Hip arthropathy in ochronosis: anatomical and radiological study. *Skeletal Radiol*. 1980 Apr;5(2):91-8.

Lagier R, Baud C A, Lacotte D Cunningham T. Rapidly progressive osteoarthrosis of ochronotic origin. *Am J Clin Pathol* 1988; 90: 95-102.

Lagier R. Ochronotic arthropathy, an approach to osteoarthritis bone remodelling. *Rheumatol Int* 2006 Apr;26(6):561-4.

Ledesma-Montes C, Garcés-Ortíz M, Reyes-Gasga J, Salcido-García JF, Hernández-Flores F. Scanning Electron Micrographic Features of a Giant Submandibular Sialolith. *Ultrastruct Pathol* 2007;31:385-391.

Levine M. New concepts in the biology and biochemistry of ascorbic acid. *N Engl J Med*. 1986 Apr 3;314(14):892-902.

Lewis JH, Alcaptonuria in a rabbit. *J Biol Chem*. 1926; 70: 659.

Li B, Marshall D, Roe M, Aspden RM. The electron microscope appearance of the subchondral bone plate in the human femoral head in osteoarthritis and osteoporosis. *J Anat*. 1999 Jul;195 ( Pt 1):101-10.

Lichtenstein, L. Kaplan L. Hereditary ochronosis: pathologic changes observed in two necropsied cases. *Am. J. Path.* 1954 30: 99-125.

Lindeman RD, Tobin J, Shock NW. Longitudinal studies on the rate of decline in renal function with age. *J Am Geriatr Soc*. 1985 Apr;33(4):278-85.

Lindstedt S, Holme E, Lock EA, Hjalmarson O, Strandvik B. Treatment of hereditary tyrosinaemia type I by inhibition of 4-hydroxyphenylpyruvate dioxygenase. *Lancet*. 1992 340:813–817.

Liu W, Prayson RA. Dura mater involvement in ochronosis (alkaptonuria). *Arch Pathol Lab Med*. 2001 Jul;125(7):961-3.

Lonsdale D. Why I left orthodox medicine. Healing for the 21st century. Hampton Roads Publishing Company. Charlottesville, VA. 1994 38.

Lorenzini S, Mannoni A, Selvi E. Alkaptonuria. *N Engl J Med*. 2003 348:1408.

Lustberg TJ, Schulman JD, Seegmiller JE. Decreased binding of <sup>14</sup>C-homogentisic acid induced by ascorbic acid in connective tissue of rats with experimental alcaptonuria. *Nature*. 1970 Nov 21;228(5273):770-1.

Manning K, Fernández-Cañón JM, Montagutelli X, Grompe M. Identification of the mutation in the alkaptonuria mouse model. *Mutations in brief* no. 216. Online. *Hum Mutat*. 1999;13(2):171.

Manning K, Al-Dhalimy M, Finegold M, Grompe M. In vivo suppressor mutations correct a murine model of hereditary tyrosinemia type I. *Proc Natl Acad Sci U S A*. 1999 Oct 12;96(21):11928-33.

Manoj Kumar RV, Rajasekaran S. Spontaneous tendon ruptures in alkaptonuria. *J Bone Joint Surg Br*. 2003 Aug;85(6):883-6.

Martel-Pelletier J, Boileau C, Pelletier JP, Roughley PJ. Cartilage in normal and osteoarthritis conditions. *Best Pract Res Clin Rheumatol*. 2008 Apr;22(2):351-84.

Martin JP Jr, Batkoff B. Homogentisic acid autoxidation and oxygen radical generation: implications for the etiology of alkaptonuric arthritis. *Free Radic Biol Med*. 1987;3(4):241-50.

Mayatepek E, Kallas K, Anninos A, Müller E. Effects of ascorbic acid and low-protein diet in alkaptonuria. *Eur J Pediatr*. 1998 Oct;157(10):867-8.

Maxwell D. Alkaptonuria and photography: a patient's urine tells the story. *CMAJ*. 2005 Apr 12;172(8):1002-3.

McQuillan DJ, Richardson MD, Bateman JF. Matrix deposition by a calcifying human osteogenic sarcoma cell line (SAOS-2). *Bone*. 1995 Apr;16(4):415-26.

Melis M, Onori P, Aliberti G, Vecchi E, Gaudio E. Ochronotic arthropathy: structural and ultrastructural features. *Ultrastruct Pathol*. 1994 Sep-Oct;18(5):467-71.

Meyer EG, Baumer TG, Slade JM, Smith WE, Haut RC. Tibiofemoral contact pressures and osteochondral microtrauma during anterior cruciate ligament rupture due to excessive compressive loading and internal torque of the human knee. *Am J Sports Med*. 2008 Oct;36(10):1966-77.

Milch RA. Studies of alcaptonuria: binding of homogentisic acid solutions to hide powder collagen. *Proc Soc Exp Biol Med* 1961;106:68-70.

Mitchell G A, Grompe M, Lambert M, Tanguay R M. In: *The Metabolic Basis of Inherited Disease*. Scriver C R, Beaudet A L, Sly W, Valle D, editors. Vol. 1. New York: McGraw-Hill; 1999. pp. 1077-1106.

Mohr W, Wessinghage D, Lenschow E. Ultrastructure of hyaline cartilage and articular capsule tissue in alkaptonuric ochronosis. *Z Rheumatol*. 1980 Mar-Apr;39(3-4):55-73.

Montagutelli X, Lalouette A, Coudé M, Kamoun P, Forest M, Guénet JL. aku, a mutation of the mouse homologous to human alkaptonuria, maps to chromosome 16. *Genomics*. 1994 Jan 1;19(1):9-11.

Moran TJ, Yunis EJ. Studies on ochronosis. 2. Effects of injection of homogentisic acid and ochronotic pigment in experimental animals. *Am J Pathol*. 1962 Mar;40:359-69.

Morava E, Kosztolányi G, Engelke UF, Wevers RA. Reversal of clinical symptoms and radiographic abnormalities with protein restriction and ascorbic acid in alkaptonuria. *Ann Clin Biochem.* 2003 Jan;40(Pt 1):108-11.

Müller CR, Fregin A, Srsen S, Srsnova K, Halliger-Keller B, Felbor U, Seemanova E, Kress W. Allelic heterogeneity of alkaptonuria in Central Europe. *Eur J Hum Genet.* 1999 7:645–651

Noll WW, Glass DD. Causes of dark urine. *JAMA.* 1980 Jun 20;243(23):2398.

O'Brien WM, La Du BN, Bunim JJ. Biochemical, Pathologic and Clinical Aspects of Alcaptonuria, Ochronosis and Ochronotic Arthropathy. Review of World Literature (1584-1962). *Am J Med.* 1963; 34: 813-838.

Orzincolo C, Castaldi G, Scutellari PN, Cicognani P, Bariani L, Feggi L. [Ochronotic arthropathy in alkaptonuria. Radiological manifestations and physiopathological signs]. *Radiol Med.* 1988 May;75(5):476-81.

Osler W. Ochronosis: the pigmentation of cartilages, sclerotics, and skin in alkaptonuria. *Lancet*; 1904, 1: 10.

Parambil JG, Daniels CE, Zehr KJ, Utz JP. Alkaptonuria diagnosed by flexible bronchoscopy. *Chest.* 2005 Nov;128(5):3678-80.

Parfitt AM. The coupling of bone formation to bone resorption: a critical analysis of the concept and of its relevance to the pathogenesis of osteoporosis. *Metab Bone Dis Relat Res.* 1982;4(1):1-6.

Parfitt AM. The mechanism of coupling: a role for the vasculature. *Bone.* 2000 Apr;26(4):319-23.



Peker E, Yonden Z, Sogut S. From darkening urine to early diagnosis of alkaptonuria. *Indian J Dermatol Venereol Leprol*. 2008 Nov-Dec;74(6):700.

Pelletier JP, Raynauld JP, Berthiaume MJ, Abram F, Choquette D, Haraoui B, et al. Risk factors associated with the loss of cartilage volume on weight-bearing areas in knee osteoarthritis patients assessed by quantitative magnetic resonance imaging: a longitudinal study. *Arthritis Res Ther* 2007; 9(4):R74.

Perry MB, Suwannarat P, Furst GP, Gahl WA, Gerber LH. Musculoskeletal findings and disability in alkaptonuria. *J Rheumatol*. 2006 Nov;33(11):2280-5.

Phornphutkul C, Introne WJ, Perry MB, Bernardini I, Murphey MD, Fitzpatrick DL, Anderson PD, Huizing M, Anikster Y, Gerber LH, Gahl WA. Natural history of alkaptonuria. *N Engl J Med*. 2002 Dec 26;347(26):2111-21.

Phornphutkul C, Introne WJ, Gahl WA. *N Eng J Med*. 2003 Apr 348;14.

Pollak MR, Chou YH, Cerda JJ, Steinmann B, La Du BN, Seidman JG, Seidman CE. Homozygosity mapping of the gene for alkaptonuria to chromosome 3q2. *Nat Genet*. 1993 Oct;5(2):201-4.

Prockop DJ, Fertala A. Inhibition of the self-assembly of collagen I into fibrils with synthetic peptides. Demonstration that assembly is driven by specific binding sites on the monomers. *J Biol Chem*. 1998 Jun 19;273(25):15598-604.

Reginato A J, Schumacher R, Martinez V A. Ochronotic arthropathy with calcium pyrophosphate crystal deposition. A light and electron microscopy study. *Arthritis Rheum* 1973; 16: 705-714.

Romero P, Wagg J, Green ML, Kaiser D, Krummenacker M, Karp PD. Computational prediction of human metabolic pathways from the complete human genome. *Genome Biol.* 2005;6(1):R2.

Rose GK. Ochronosis. *Br J Surg.* 1957 Mar;44(187):481-2.

Russell RGG. Pathogenesis of osteoporosis. In: Hochberg MC, Silman AJ, Smolen SJ, Weinblatt ME, Weisman MH, (eds.) *Rheumatology*, 3rd ed., 2003. Mosby, New York, NY, USA. pp.2075-2147.

Sahin G, Milcan A, Bağış S, Köktürk A, Pata C, Erdoğan C. A case of ochronosis: upper extremity involvement. *Rheumatol Int.* 2001 21: 78-80

Schenck, J. Urine nigra in sanis quibusdam. In: *Observationes Medicae*, lib. III, p. 558. Frankfort, 1609.

Schulz A, Ort O, Beyer P, Kleinig H. SC-0051, a 2- benzoyl-cyclohexane-1,3-dione bleaching herbicide, is a potent inhibitor of the enzyme p-hydroxyphenylpyruvate dioxygenase. *FEBS Lett.* 1993 318:162–166

Scriver CR. Garrod's Croonian Lectures (1908) and the charter 'Inborn Errors of Metabolism': Albinism, alkaptonuria, cystinuria, and pentosuria at age 100 in 2008. *J Inherit Metab Dis* 2008; 31:580–598.

Scriver CR, Beaudet AL, Valle D, Sly WS. 2001. Alkaptonuria. In: Scriver CR, Beaudet AL, Valle D, Sly WS, editors. *The metabolic and molecular basis of inherited disease*. New York: McGraw-Hill. 2109–2123.

Scribonius G. A. *De Inspectione Urinarum*, p. 50. Lemgo, Germany, 1584.

Sealock RR, Gladstone M, Steele JM. Administration of ascorbic acid to an alkaptonuric patient. *Proc Soc Exp Biol Med* 1940; 44:580-3.

Seegmiller JE, Zannoni VG, Laster L, La Du BN. An enzymatic spectrophotometric method for the determination of homogentisic acid in plasma and urine. *J Biol Chem.* 1961 Mar;236:774-7.

Seradge H. Ochronotic stenosing flexor tenosynovitis--case report. *J Hand Surg Am.* 1981 Jul;6(4):359-60.

Shimizu I, Hamada T, Khalpey Z, Miyanishi K, Hara T. Ochronotic arthropathy: pathological evidence of acute destruction of the hip joint. *Clin Rheumatol.* 2007 Jul;26(7):1189-91.

Slawson M. Thirty-three drugs that discolor urine and/or stools. *RN.* 1980 Jan;43(1):40-1.

Srsen S, Vondráček J, Srsnová K, Svác J. Analysis of the life span of alkaptonuric patients. *Cas Lek Cesk.* 1985 Oct 18;124(41-42):1288-91.

Spencer JM, Gibbons CL, Sharp RJ, Carr AJ, Athanasou NA. Arthroplasty for ochronotic arthritis: no failure of 11 replacements in 3 patients followed 6-12 years. *Acta Orthop Scand.* 2004; Jun;75(3):355-8.

Stanbury, J. B. Alcaptonuria. In: *The Metabolic Basis of Inherited Disease*. eds. Wyngaarden, JB, Fredrickson DS. 1978 4th ed. New York: McGraw-Hill; 268-282.

Stevens A. Pigments and minerals. In: Bancroft J D, Stevens A. ed. *Theory and practice of histological techniques*. 1982 2nd Ed. New York: Churchill Livingstone, 252.

Sutor DJ, Wooley SE, Krízek V. The composition of calculi from patients with alcaptonuria. *Br J Urol.* 1970 Aug;42(4):386-8.

Suwannarat P, O'Brien K, Perry MB, Sebring N, Bernardini I, Kaiser-Kupfer MI, Rubin BI, Tsilou E, Gerber LH, Gahl WA. Use of nitisinone in patients with alkaptonuria. *Metabolism*. 2005 Jun;54(6):719-28.

Suzuki Y, Oda K, Yoshikawa Y, Maeda Y, Suzuki T. A novel therapeutic trial of homogentisic aciduria in a murine model of alkaptonuria. *J Hum Genet*. 1999;44(2):79-84.

Taylor AM, An investigation into the binding of homogentisic acid to the extracellular matrix in cultures of human chondrocytes and osteosarcoma cells. Undergraduate dissertation, University of Liverpool. 2007.

Taylor, AM, Wlodarski B, Prior IA, Wilson PJM, Jarvis JC, Ranganath LR, Gallagher JA. Ultrastructural examination of tissue in a patient with alkaptonuric arthropathy reveals a distinct pattern of binding of ochronotic pigment. *Rheumatology*. 2010; 49: 1412-1414.

Taylor AM, Wilson PJM, Ingrams DR, Helliwell TR, Gallagher JA, Ranganath LR. Calculi and intracellular ochronosis in the submandibular tissues from a patient with alkaptonuria. *J Clin Pathol* 2010; Feb;63(2):186-8.

Taylor AM. Observations of collagen VI association with excrescences. 2010

Taylor AM, Boyde A, Wilson PJM, Jarvis JC, Davidson JS, Hunt JA, Ranganath LR, Gallagher JA. The role of calcified cartilage and subchondral bone in the initiation and progression of ochronotic arthropathy in alkaptonuria. *Arthritis and Rheumatism*. 2011; Under revision.

Tinti L, Spreafico A, Braconi D, Millucci L, Bernardini G, Chellini F, Cavallo G, Selvi E, Galeazzi M, Marcolongo R, Gallagher JA, Santucci A. Evaluation of antioxidant drugs for

the treatment of ochronotic alkaptonuria in an in vitro human cell model. *J Cell Physiol.* 2010 Oct;225(1):84-91.

Tinti L, Taylor AM, Santucci A, Wlodarski B, Wilson PJ, Jarvis JC, Fraser WD, Davidson JS, Ranganath LR, Gallagher JA. Development of an in vitro model to investigate joint ochronosis in alkaptonuria. *Rheumatology(Oxford).* 2011 Feb;50(2):271-7.

Titus GP, Mueller HA, Burgner J, Rodriguez De Cordoba S, Penalva MA, Timm DE. Crystal structure of human homogentisate dioxygenase. *Nat Struct Biol.* 2000;7:542–546.

Turiansky GW, Levin SW. Bluish patches on the ears and axillae with dark urine: ochronosis and alkaptonuria. *Int J Dermatol* 2001;40:333-335.

Vilboux T, Kayser M, Introne W, Suwannarat P, Bernardini I, Fischer R, O'Brien K, Kleta R, Huizing M, Gahl WA. Mutation spectrum of homogentisic acid oxidase (HGD) in alkaptonuria. *Hum Mutat.* 2009 Dec;30(12):1611-9.

Virchow, R. Ein Fall von allgemeiner Ochronose der Knorpel und knorpelähnlichen Theile. *Arch. path. Anat.* 1866; 37: 212-219.

Watkins SP, Benley H, Shulman NR. 1970. Alkaptonuria in a chimpanzee. In: Goldsmith EI, Moor-Jankowski J, editors. 2nd Conference on Experimental Medicine and Surgery in Primates, New York, NY, September 1969. *Medical Primatology* 1970. Basel: Karger. p 297–298

Wolff JA, Barshop B, Nyhan WL, Leslie J, Seegmiller JE, Gruber H, Garst M, Winter S, Michals K, Matalon R. Effects of ascorbic acid in alkaptonuria: alterations in benzoquinone acetic acid and an ontogenic effect in infancy. *Pediatr Res.* 1989 Aug;26(2):140-4.



Wolkow M, Baumann E. Ueber das Wesen der Alkaptonurie. Hoppe-Seyler Ztschr. Physiol. Chem. 1891 15: 228.

Yamaguchi S, Koda N, Ohashi T. Diagnosis of alkaptonuria by NMR urinalysis: rapid qualitative and quantitative analysis of homogentisic acid. Tohoku J Exp Med. 1986 Oct;150(2):227-8.

Zannoni VG, Lomtevas N, Goldfinger S. Oxidation of homogentisic acid to ochronotic pigment in connective tissue. Biochim Biophys Acta. 1969 Feb 18;177(1):94-105.

Zatkova A, de Bernabé DB, Poláková H, Zvarík M, Feráková E, Bosák V, Ferák V, Kádasi L, de Córdoba SR. High Frequency of Alkaptonuria in Slovakia: Evidence for the Appearance of Multiple Mutations in HGO Involving Different Mutational Hot Spots. Am. J. Hum. Genet. 2000 67:1333–1339.

Zatkova A, Polakova H, Micutkova L, Zvarik M, Bosak V, Ferakova E, Matusek J, Ferak V, Kadasi L. Novel mutations in homogentisate-1,2-dioxygenase gene identified in Slovak patients with alkaptonuria. J Med Genet 2000 37: 539–542.

### Appendix A: Publications

**Taylor AM**, Batchelor TJP, Adams VL, Helliwell TR, Gallagher JA, Ranganath LR.

Ochronosis and calcification in the mediastinal mass of a patient with alkaptonuria. J Clin Pathol. In press. 2011.

Ranganath L, **Taylor AM**, Shenkin A, Fraser WD, Jarvis J, Gallagher JA, Sireau N. Identification of alkaptonuria in the general population: a United Kingdom experience describing the challenges, possible solutions and persistent barriers. J Inherit Metab Dis. 2011 Feb 11. [Epub ahead of print]

Tinti L, **Taylor AM**, Santucci A, Wlodarski B, Wilson PJ, Jarvis JC, Fraser WD, Davidson JS, Ranganath LR, Gallagher JA. Development of an in vitro model to investigate joint ochronosis in alkaptonuria. Rheumatology (Oxford). 2011 Feb;50(2):271-7.

Braconi D, Laschi M, **Taylor AM**, Bernardini G, Spreafico A, Tinti L, Gallagher JA, Santucci A. Proteomic and redox-proteomic evaluation of homogentisic acid and ascorbic acid effects on human articular chondrocytes. J Cell Biochem. 2010 Nov 1;111(4):922-32.

**Taylor AM**, Boyde A, Davidson JS, Jarvis JC, Ranganath LR, Gallagher JA. Identification of novel microanatomical structures in bone from a patient with alkaptonuria. JBMR 2010 Suppl.

**Taylor AM**, Boyde A, Wlodarski B, Davidson JS, Wilson PJM, Jarvis JC, Ranganath LR, Gallagher JA. Elucidating the mechanism of the osteoarthropathy in alkaptonuria: lessons for osteoarthritis. *Osteoarthritis cartilage*. Oct 2010, Suppl. 2 S116-S117.

**Taylor AM**, Preston A, Paulk NK, Grompe M, Keenan C, Ranganath LR, Jarvis JC, Gallagher JA. Identification of joint ochronosis in a mouse model of alkaptonuria. *Osteoarthritis cartilage*. Oct 2010, Suppl. 2. S54

**Taylor AM**, Wlodarski B, Wilson PJM, Jarvis JC, Ranganath LR, Boyde A, Gallagher JA. Deposition of ochronotic pigment in articular cartilage in alkaptonuria is initiated near the tidemark and progresses to the articular surface. *Calcif Tissue Int*. 2010

**Taylor AM**, Wlodarski B, Prior IA, Wilson PJ, Jarvis JC, Ranganath LR, Gallagher JA. Ultrastructural examination of tissue in a patient with alkaptonuric arthropathy reveals a distinct pattern of binding of ochronotic pigment. *Rheumatology (Oxford)*. 2010 Jul;49(7):1412-4.

**Taylor AM**, Wilson PJ, Ingrams DR, Helliwell TR, Gallagher JA, Ranganath LR. Calculi and intracellular ochronosis in the submandibular tissues from a patient with alkaptonuria. *J Clin Pathol*. 2010 Feb;63(2):186-8.

**Taylor AM**, Fraser WD, Wilson PJM, Ranganath LR, Gallagher JA. Ultrastructural analysis of collagen in the arthropathy of alkaptonuria in vivo and in vitro. *Osteoarthritis Cartilage*. Sept 2009, Vol. 17, Suppl. 1 S244.

**Taylor AM**, Fraser WD, Wilson PJM, Ranganath LR, Gallagher JA. Ultrastructural studies on the binding of ochronotic pigment to collagen fibres in cartilage and bone in vivo and in vitro. *Calcif Tissue Int*. 2009, 85:187.

**Taylor AM**, Wilson PJM, Fraser WD, Ranganath LR, Gallagher JA. Studies on the deposition of ochronotic pigment in alkaptonuria reveal tyrosine metabolism in human chondrocytes. *JBMR*. 2008; 23 (Suppl. 1), S414.

**Taylor AM**, Prior IA, Wlodarski BW, Wilson PJM, Fraser WD, Ranganath LR, Gallagher JA. Ultrastructural examination of collagen from alkaptonuric tissue provides clues to pathogenesis of ochronosis. *Calcif Tissue Int*. 2008; 83: (Suppl. 1), 33.

**Taylor AM**, Prior IA, Wilson PJM, Fraser WD, Ranganath LR, Gallagher JA. High resolution electron microscopy identifies distinctive binding of ochronotic pigment to collagen fibres in alkaptonuria. *Calcif Tissue Int*. 2008; 82: (Suppl. 1), S93.